

# **A Study of Type-3 Copper Proteins from Arthropods**

**By**

**Sharon Baird**

Submitted to:

The Faculty of Natural Sciences

University of Stirling

September 2007

For the degree of

Doctor of Philosophy

This research was conducted in the School of Biological and Environmental Sciences,  
University of Stirling, Stirling, UK.

## **ACKNOWLEDGEMENTS**

Firstly I would like to dedicate this thesis to my now husband, Craig McFadyen, who has helped keep me connected with the real world over the past few years, and has always been there with a reassuring hug in times of need! I also wish to dedicate this thesis to my mum and dad for their financial support and pride and belief in my ability.

This research was funded by the University of Stirling. My primary supervision was provided by Dr Jacqueline Nairn whose knowledge of an array of biological and biophysical techniques helped me tremendously in undertaking this research. Many thanks also to Jacqueline for never failing to find the time amongst her hectic schedule to sit down and discuss my work and make sure I kept on track. Secondary supervision was provided by Dr Kenneth Wilson (University of Lancaster, formerly University of Stirling).

The biophysical research would have been much less fruitful without the invaluable guidance and thoughts from my many collaborators: Thomas Jess, Dr Sharon Kelly and Professor Nicholas Price of the BBSRC funded Circular Dichroism Facility, University of Glasgow, Margaret Nutley and Professor Alan Cooper of the BBSRC/EPSCMicrocalorimetry Service, University of Glasgow, who obtained and interpreted the ITC data and Dr Elmar Jaenicke and Professor Heinz Decker of the Institute of Molecular Biophysics, University of Mainz, Germany.

Further thanks extend to: Dr Peter Dominy of the University of Glasgow for guiding the ICP OES experimental design, Professor Thorsten Burmester of the Institute of Zoology, University of Mainz, Germany for assistance with oligomeric primer design, Dr Michael Wyman for his useful input on various aspects of the the molecular biology based research, Mary Everhart and Dr. Michael Kanost of the Department of Biochemistry, Kansas State University for generously providing the *Manduca sexta* prophenoloxidase cDNA clones, Beatrice Lanzrein of the Institute of Cell Biology, University of Berne, Switzerland for kindly gifting two *Spodoptera littoralis* cDNA libraries and Dr Kenneth Wilson and Susan Williamson for providing live *Spodoptera littoralis* specimens and training in bleeding of larvae.

## **STATEMENT OF ORIGINALITY**

I hereby confirm that the work contained within is original and written by the undersigned, and that all research material has been duly referenced and cited.

.....

Sharon Baird

September 2007

## ABSTRACT

Arthropod hemocyanin and phenoloxidase are members of a group of proteins called the Type-3 copper oxygen-binding proteins, both possessing a highly conserved oxygen-binding site containing two copper atoms each coordinated by three histidine residues (Decker and Tuczec, 2000). Despite similarities in their active site, these proteins have very different physiological functions. Phenoloxidase possesses both tyrosinase and *o*-diphenoloxidase activity, and is predominantly involved in reactions which protect insects from infection (Kopáček et al., 1995). Hemocyanin is a large multi-subunit protein with a primary function as a respiratory protein, reversibly binding and transporting molecular O<sub>2</sub> (Decker and Rimke, 1998; Decker and Tuczec, 2000).

Recently, it has been demonstrated *in vitro* that arthropod hemocyanin possesses an inducible phenoloxidase activity when incubated with denaturants, detergents, phospholipids or proteolytic enzymes. This activity appears to be restricted to only a few subunit types, and it has been hypothesised that it may be accompanied by conformational change which opens the active site increasing access for larger phenolic substrates (Decker and Jaenicke, 2004; Decker et al., 2001; Decker and Tuczec, 2000). This possibly suggests a dual role of hemocyanin in arthropods.

The presented thesis deals with two distinct aims. The first was to isolate and sequence a phenoloxidase gene from the insect *Spodoptera littoralis* (Egyptian Cottonleaf Worm). Despite efforts, progress was hindered by a number of experimental problems which are outlined within the relevant chapters. The second aim was to characterise the mode of SDS induced phenoloxidase activity in arthropod hemocyanin from the ancient chelicerates *Limulus polyphemus* (horseshoe crab) and *Eurypelma californicum* (tarantula) and the more modern chelicerate *Pandinus imperator* (scorpion), using a number of biophysical techniques. The results indicated that the SDS induced phenoloxidase activity is associated with localised tertiary and secondary conformational changes in hemocyanin, most likely in the vicinity of the dicopper centre, thus enhancing access for larger phenolic substrates. Experiments indicate that copper remains associated with the protein during these structural changes; however the nature of the association is unclear. SDS concentrations approximating the CMC appeared critical in causing the necessary structural changes required for a significant increase in the detectable phenoloxidase activity to be exhibited.

## ABBREVIATIONS

|             |  |
|-------------|--|
| $\beta$ GRP | $\beta$ – glucan recognition protein                     |
| CD          | Circular dichroism                                       |
| CMC         | Critical micelle concentration                           |
| CPC         | Cetyl pyridium chloride                                  |
| Cu          | Copper   |
| ddNTP       | Dideoxy nucleoside triphosphate                          |
| DDP         | Density dependant prophylaxis                            |
| DLS         | Dynamic light scattering                                 |
| DOPA        | Dihydroxyphenylalanine                                   |
| EtBr        | Ethidium bromide   |
| EuryHc      | <i>Eurypelma californicum</i> hemocyanin                 |
| Hc          | Hemocyanin   |
| ICP OES     | Inductively coupled plasma optical emission spectroscopy |
| IL-1        | Interleukin-1  |
| ITC         | Isothermal titration calorimetry                         |
| LimHc       | <i>Limulus polyphemus</i> hemocyanin                     |
| LPS         | Lipopolysaccharide                                       |
| MAP kinase  | Mitogen activated protein kinase                         |
| NADA        | N – acetyldopamine                                       |
| NBAD        | N – $\beta$ - alanyldopamine                             |
| NBDG        | n – nonyl – $\beta$ – D - glucopyranoside                |
| PanHc       | <i>Pandinus imperator</i> hemocyanin                     |
| PAP         | Prophenoloxidase activating proteinase                   |
| PC          | Phosphatidylcholine                                      |
| PE          | Phosphatidylethanolamine                                 |
| PGRP        | Peptidoglycan recognition protein                        |
| Phe         | Phenylalanine  |
| PO          | Phenoloxidase  |
| PPAE        | Prophenoloxidase activating enzyme                       |
| PPO         | Prophenoloxidase   |
| PRP         | Pattern recognition protein                              |
| SDS         | Sodium dodecyl sulphate                                  |
| SPH         | Serine protein homologue                                 |
| SUV         | Small unilamellar vesicle                                |
| TBE         | Tris borate EDTA   |
| Trp         | Tryptophan   |
| Tyr         | Tyrosine   |

## TABLE OF CONTENTS

|                                       |             |
|---------------------------------------|-------------|
| <b>Acknowledgements</b> .....         | <b>I</b>    |
| <b>Statement of Originality</b> ..... | <b>III</b>  |
| <b>Abstract</b> .....                 | <b>IV</b>   |
| <b>Abbreviations</b> .....            | <b>V</b>    |
| <b>Table of Contents</b> .....        | <b>VI</b>   |
| <b>List of Figures</b> .....          | <b>XI</b>   |
| <b>List of Tables</b> .....           | <b>XXVI</b> |

|   |           |
|---|-----------|
| <b>Chapter 1 : Thesis Overview</b> .....  | <b>1</b>  |
| <b>1.1 Insect phenoloxidase</b> .....   | <b>1</b>  |
| <b>1.2 Arthropod hemocyanin</b> .....   | <b>2</b>  |
| <b>1.3 Research Objectives</b> .....  | <b>3</b>  |
| <b>Chapter 2 : Phenoloxidase in Insect Immunity – A Review of the Literature</b> .....    | <b>5</b>  |
| <b>2.1 Introduction to Insect Immunity</b> .....  | <b>5</b>  |
| <b>2.2 Insect Phenoloxidase</b> .....   | <b>8</b>  |
| 2.2.1 Phenoloxidase Types and their Functions.....  | 9         |
| 2.2.2 Site of Synthesis of Phenoloxidase.....   | 10        |
| 2.2.3 Structural Features of Phenoloxidase.....   | 10        |
| <b>2.3 Phenoloxidase is a Type-3 Copper Protein Similar to Arthropod Hemocyanin</b> ..... | <b>15</b> |
| <b>2.4 The Prophenoloxidase Activation Cascade</b> .....                                  | <b>20</b> |
| 2.4.1 Introduction.....   | 20        |
| 2.4.2 Pattern Recognition Proteins.....   | 23        |
| 2.4.3 PPAE Activation and its Activation of Phenoloxidase.....                            | 25        |
| <b>2.5 Physiological Roles of Active Phenoloxidase in Insects</b> .....                   | <b>29</b> |
| 2.5.1 Melanisation – Melanotic Encapsulation and Wound Healing.....                       | 29        |
| 2.5.2 Sclerotisation.....   | 31        |
| <b>2.6 Control of Phenoloxidase Activity <i>in vivo</i></b> .....                         | <b>34</b> |
| 2.6.1 Introduction.....   | 34        |
| 2.6.2 Metabolon Formation.....  | 36        |
| 2.6.3 Hemocyte Surface Phenoloxidase.....   | 37        |

|  |   |           |
|--|---|-----------|
| 2.7  | <b>Phenoloxidase as an Indicator of Immune Function in the<br/>Lepidoptera.....</b>                       | <b>39</b> |
| <b>Chapter 3 : Sequencing and analysis of a putative 600 bp <i>Spodoptera<br/>littoralis</i> phenoloxidase gene fragment .....</b> |   |           |
| <b>3.1</b>   | <b>Introduction .....</b>   | <b>43</b> |
| <b>3.2</b>   | <b>Methods .....</b>  | <b>47</b> |
| 3.2.1  | Preparation of purified plasmid containing the 600 bp insert.....   | 47        |
| 3.2.2  | PCR amplification of the 600 bp DNA fragment. ....  | 48        |
| 3.2.3  | Gel slice clean-up of the amplified 600 bp DNA fragment. ....   | 49        |
| 3.2.4  | Sequencing the 600 bp DNA fragment.....   | 49        |
| 3.2.5  | Sequence analysis. ....   | 51        |
| <b>3.3</b>   | <b>Results .....</b>  | <b>51</b> |
| 3.3.1  | Successful PCR Amplification and Gel Slice Clean-up of the 600 bp<br>Plasmid Insert. ....                 | 51        |
| 3.3.2  | Analysis of the 600 bp DNA fragment sequence.....   | 53        |
| <b>3.4</b>   | <b>Discussion.....</b>  | <b>58</b> |
| <b>Chapter 4 : Screening for a Prophenoloxidase Gene in a <i>Spodoptera<br/>littoralis</i> cDNA library.....</b>                   |   |           |
| <b>4.1</b>   | <b>Introduction .....</b>   | <b>62</b> |
| <b>4.2</b>   | <b>Methods .....</b>  | <b>65</b> |
| 4.2.1  | Polymerase chain reaction and Southern blotting.....  | 65        |
| 4.2.1.1  | Primer design. ....   | 65        |
| 4.2.1.2  | Generating stocks of the plasmid vector containing a clone of the<br>Manduca sexta PPO1 or PPO2 gene..... | 65        |
| 4.2.1.3  | Gradient PCR.....   | 66        |
| 4.2.1.4  | Southern blotting via the capillary method.....   | 67        |
| 4.2.2  | DIG-labelled probe membrane hybridisation. ....   | 69        |
| 4.2.2.1  | DIG-labelled phenoloxidase DNA probe synthesis.....   | 69        |
| 4.2.2.2  | Dot blot preparation.....   | 70        |
| 4.2.2.3  | Hybridisation of nylon membranes with DIG-labelled PPO1 DNA<br>probe. ....                                | 71        |
| 4.2.2.4  | Post hybridisation washes.....  | 72        |
| 4.2.2.5  | Incubating probe hybridized membranes with an Anti-DIG-Alkaline<br>phosphatase antibody.....              | 73        |
| 4.2.2.6  | Detection of membrane bound DIG-labelled DNA probe.....   | 73        |
| 4.2.3  | Screening a <i>Spodoptera littoralis</i> cDNA library for a prophenoloxidase<br>cDNA.....                 | 74        |
| 4.2.3.1  | Preparation of E. coli Y1090 viable working and glycerol stocks. ....                                     | 74        |
| 4.2.3.2  | cDNA library titration.....   | 75        |
| 4.2.3.3  | Plaque lifts for screening. ....  | 77        |
| 4.2.3.4  | DIG-labelled PPO1 DNA probe hybridisation of cDNA library plaque<br>lifts. ....                           | 79        |
| 4.2.4  | Restriction digest of <i>Spodoptera littoralis</i> genomic DNA. ....                                      | 79        |
| 4.2.4.1  | Restriction digest. ....  | 79        |
| 4.2.4.2  | Southern blotting via the capillary method.....   | 80        |

|   |  |            |
|---|--|------------|
| 4.2.4.3   | DIG-labeled PPO1 DNA probe hybridisation of restriction digest membrane.....   | 81         |
| 4.2.5   | Comparing the sensitivity of DIG-labelled PPO1 and DIG-labelled PPO2 DNA probes.....   | 81         |
| <b>4.3</b>  | <b>Results .....</b>   | <b>82</b>  |
| 4.3.1   | Gradient PCRs using degenerate primers generated numerous products of varying size.....  | 82         |
| 4.3.2   | DIG-labelled PPO1 probe hybridisation to membrane bound PCR product DNA could not conclusively identify any prophenoloxidase DNA.....        | 97         |
| 4.3.3   | cDNA library screening and genomic DNA digests, initially suggest <i>Spodoptera littoralis</i> does not contain a prophenoloxidase gene..... | 104        |
| 4.3.4   | Neither DIG-labelled probe is suitably sensitive or specific enough for its intended use.....  | 108        |
| <b>4.4</b>  | <b>Discussion.....</b>   | <b>112</b> |
| 4.4.1   | PPO gene transcription may be inhibited in Braconid wasp parasitised Lepidoptera larvae.....   | 112        |
| 4.4.2   | The cDNA library may have been synthesised from a low PPO transcript copy number or degraded RNA source.....                                 | 114        |
| 4.4.3   | No PPO DNA could be identified due to the low sensitivity and high non-specificity of the DIG-labelled probe.....                            | 115        |
| 4.4.4   | Summary of conclusions.....  | 116        |
| <b>Chapter 5 : Steps towards isolating a Prophenoloxidase Gene from <i>Spodoptera littoralis</i> hemocytes.....</b> |  |            |
| <b>5.1</b>  | <b>Introduction .....</b>  | <b>117</b> |
| <b>5.2</b>  | <b>Methods .....</b>   | <b>119</b> |
| 5.2.1   | <i>Spodoptera littoralis</i> larvae culture.....   | 119        |
| 5.2.2   | Hemolymph collection and isolation of hemocytes.....   | 119        |
| 5.2.3   | Total RNA isolation from hemocytes.....  | 120        |
| <b>5.3</b>  | <b>Results .....</b>   | <b>122</b> |
| 5.3.1   | Larvae culture.....  | 122        |
| 5.3.2   | Total RNA isolation.....   | 125        |
| <b>5.4</b>  | <b>Discussion.....</b>   | <b>128</b> |
| 5.4.1   | Solitary larvae display variation in their level of cuticular melanisation.....  | 129        |
| 5.4.2   | Slowed development, cannibalism and hemolymph melanisation in gregarious <i>Spodoptera littoralis</i> larvae.....                            | 130        |
| 5.4.3   | RNA degradation.....   | 132        |
| <b>Chapter 6 : Arthropod Hemocyanin – An introduction to structure and function. ....</b>                           |  |            |
| <b>6.1</b>  | <b>Introduction .....</b>  | <b>133</b> |
| <b>6.2</b>  | <b>A History of the Studies of Hemocyanin .....</b>  | <b>135</b> |
| <b>6.3</b>  | <b>The Structure of Hemocyanin.....</b>  | <b>137</b> |
| 6.3.1   | Quaternary Structure.....  | 137        |
| 6.3.2   | Tertiary Structure.....  | 140        |
| 6.3.3   | Active Site Structure.....   | 142        |
| 6.3.4   | Ion Binding Sites.....   | 146        |

|  |  |            |
|--|--|------------|
| 6.3.5  | Primary Structure.....   | 148        |
| <b>6.4</b>   | <b>Arthropod Hemocyanin – a multifunctional protein? .....</b>   | <b>148</b> |
| 6.4.1  | Site of Hemocyanin Synthesis .....   | 148        |
| 6.4.2  | Primary Function – Oxygen Transporter .....  | 150        |
| 6.4.3  | Secondary Function – Defensive Protein.....  | 151        |
| <b>Chapter 7 : Biophysical Characterisation of the Mode of Activation of</b> |  |            |
| <b>Phenoloxidase Activity in Arthropod Hemocyanin .....</b>                  |  |            |
| <b>7.1</b>   | <b>Introduction .....</b>  | <b>156</b> |
| 7.1.1  | Overview.....  | 156        |
| 7.1.2  | Current Knowledge of the Activation of Arthropod Hemocyanin<br>Phenoloxidase Activity.....                                     | 157        |
| 7.1.3  | Hypotheses on the Structural Changes Required to Elicit Phenoloxidase<br>Activity in Arthropod Hemocyanin.....                 | 159        |
| <b>7.2</b>   | <b>Methods .....</b>   | <b>160</b> |
| 7.2.1  | Phenoloxidase Activity Assays.....   | 160        |
| 7.2.2  | Isothermal Titration Calorimetry.....  | 162        |
| 7.2.3  | Circular Dichroism Spectroscopy.....   | 163        |
| 7.2.4  | Fluorescence Spectroscopy.....   | 163        |
| 7.2.5  | Dynamic Light Scattering.....  | 164        |
| 7.2.6  | Absorbance Spectroscopy.....   | 165        |
| 7.2.7  | Inductively Coupled Plasma Optical Emission Spectroscopy.....  | 166        |
| 7.2.8  | Phospholipid and Small Unilamellar Vesicle Preparation.....  | 167        |
| <b>7.3</b>   | <b>Results .....</b>   | <b>167</b> |
| 7.3.1  | SDS Induced Phenoloxidase Activity of Arthropod Hemocyanins.....   | 167        |
| 7.3.2  | The Binding of SDS to Arthropod Hemocyanin.....  | 170        |
| 7.3.3  | The Effect of SDS on Arthropod Hemocyanin Secondary Structure. ....  | 176        |
| 7.3.4  | The Effect of SDS on Arthropod Hemocyanin Tertiary and Quaternary<br>Structure.....  | 181        |
| 7.3.4.1  | Intrinsic Tryptophan Fluorescence.....   | 181        |
| 7.3.4.2  | Aromatic Amino Acid Near UV Circular Dichroism Spectra.....  | 188        |
| 7.3.4.3  | Dynamic Light Scattering.....  | 194        |
| 7.3.5  | The Effect of SDS on the Arthropod Hemocyanin Type-III Dicopper<br>Centre.....   | 197        |
| 7.3.5.1  | Absorption spectra.....  | 197        |
| 7.3.5.2  | Type-3 Copper Centre Near UV Circular Dichroism Spectra.....   | 201        |
| 7.3.5.3  | Fluorescence Spectra at 330nm Excitation.....  | 202        |
| 7.3.5.4  | ICP OES.....   | 206        |
| 7.3.6  | Correlation of Data from PO Activity Assays and Fluorescence and Far<br>UV Circular Dichroism Spectroscopy.....                | 208        |
| 7.3.7  | The Effect of Non-ionic Detergents on the Secondary and Tertiary<br>Structure of Limulus polyphemus Hemocyanin Subunit II..... | 210        |
| 7.3.8  | Reversibility of the Effects of SDS on Arthropod Hemocyanin.....   | 213        |
| 7.3.9  | The Effect of Phospholipids and Liposomes on Arthropod Hemocyanin.<br>.....  | 218        |
| <b>7.4</b>   | <b>Discussion.....</b>   | <b>225</b> |
| 7.4.1  | Introduction.....  | 225        |

|   |  |            |
|---|--|------------|
| 7.4.2   | The SDS Induced PO Activity of Arthropod Hemocyanin Suggests Enzyme-Micelle Interaction. ....  | 225        |
| 7.4.3   | The Interaction Between SDS and Arthropod Hemocyanin Demonstrates Very Complex Thermodynamics. ....  | 228        |
| 7.4.4   | SDS Causes Significant Structural Changes in Arthropod Hemocyanin, Particularly in the Region of the Dicopper centre. ....   | 231        |
| 7.4.4.1   | Changes in Arthropod Hemocyanin Quaternary Structure. ....   | 231        |
| 7.4.4.2   | Changes in Arthropod Hemocyanin Tertiary Structure. ....   | 232        |
| 7.4.4.3   | Changes in Arthropod Hemocyanin Secondary Structure. ....  | 237        |
| 7.4.4.4   | Changes in the Arthropod Hemocyanin Type-3 Dicopper centre. ....   | 238        |
| 7.4.5   | SDS Induced Arthropod Hemocyanin Phenoloxidase Activity and the Associated Structural Changes Appear to Vary in their Reversibility. ..                                | 241        |
| 7.4.6   | Lipids/Liposomes and physiological relevance of SDS induced PO activity .....  | 242        |
| 7.4.7   | Summary and Conclusions .....  | 247        |
| <b>Chapter 8 : Summary of Research Findings and Future Work .....</b> |  | <b>253</b> |
| 8.1   | <b>Summary of Chapters 3, 4 and 5 – Attempts to Isolate a Phenoloxidase Gene from Larvae of the Egyptian Cotton Leafworm, <i>Spodoptera littoralis</i>. ....</b>       | <b>253</b> |
| 8.2   | <b>Summary of Chapter 7 – Biophysical Characterisation of the Mode of SDS Induced Arthropod Hemocyanin Phenoloxidase Activity. .</b>                                   | <b>256</b> |
| 8.3   | <b>Research into the Structure and Function of Type-3 Copper Proteins has Medical, Industrial and Agricultural Importance. ....</b>                                    | <b>260</b> |
| <b>Chapter 9 : Appendices.....</b>                                    |  | <b>265</b> |
| 9.1   | <b>Appendix A – Primers and binding-site map. ....</b>   | <b>265</b> |
| 9.2   | <b>Appendix B - Raw nucleotide sequence of a putative 600 bp prophenoloxidase DNA fragment as deduced in forward and reverse direction for clones 2a and 10a. ....</b> | <b>267</b> |
| 9.3   | <b>Appendix C – Integrity checks of total RNA, isolated from <i>S. littoralis</i> hemocytes. ....</b>  | <b>269</b> |
| 9.4   | <b>Appendix D – Complete activity plot of SDS induced arthropod hemocyanin phenoloxidase activity. ....</b>  | <b>270</b> |
| 9.5   | <b>Appendix E – ITC data of SDS binding to arthropod hemocyanin, analysed in terms of a single binding site model. ....</b>  | <b>271</b> |
| <b>Bibliography .....</b>   |  | <b>273</b> |

## LIST OF FIGURES

- Figure 1: Research study species, which were the source of the cDNA library, genomic DNA or total RNA (Panel A: *Spodoptera littoralis* (Egyptian Cotton Leafworm) larva), or the purified hemocyanins (Panel B: *Limulus polyphemus* (North Atlantic Horseshoe Crab); Panel C: *Pandinus imperator* (Emperor Scorpion); Panel D: *Eurypelma californicum* (North American Tarantula)) \_\_\_\_\_ 4
- Figure 2: Phagocytosis of fluorescently labelled yeast by hemocytes from the insect *Manduca sexta*. Phase-contrast (left) and fluoresced hemocytes containing multiple engulfed yeast cells are indicated by arrows (Yu, Accessed: 2003.). \_\_\_\_\_ 7
- Figure 3: Multiple alignment of amino acid sequences of PPO polypeptides from six insect species. These are *Bombyx mori* PPO1 (BmoriPPO1), *Galleria mellonella* PPO (GmellonPPO), *Sarcophaga bullata* PPO1 (SbullPPO1), *Tenebrio molitor* PPO5 (TmolitPPO5), *Hyphantria cunea* PPO2 (HcuneaPPO2), and *Spodoptera litura* PPO (SlituraPPO). The NCBI Genbank accession numbers for these sequences are NM\_001043870, AF336289, AF161260, AB020738, AF020391 and AY703825 respectively. The two copper-binding sites are singly underlined and labelled, and the 3 conserved histidines in each are highlighted with ‘Δ’. The conserved RF and REE cleavage sites are marked with ‘^’, the conserved thiol-ester motif is double underlined ‘=’ and the conserved C-terminal site is underlined with ‘~’. (Multiple alignment constructed using MULTALIN (pbil) available via the ExPASy online Proteomics Server and the NCBI PubMed nucleotide databank).\_ 12
- Figure 4: Dioxygen bridges the two copper atoms of the *Limulus polyphemus* hemocyanin Type-3 copper oxygen-binding site in a side-on configuration. Due to the identity between the copper-binding site sequences of insect prophenoloxidase and arthropod hemocyanin, it is likely this arrangement exists in phenoloxidase during the incorporation of oxygen into phenolic compounds (taken and adapted from (Decker and Terwilliger, 2000)). \_\_\_\_\_ 16
- Figure 5: Multiple alignment of amino acid sequences of the CuA (top) and CuB binding sites of prophenoloxidase from three insect species, *Bombyx mori* PPO1 (B.moriPPO1), *Anopheles gambiae* PPO4 (A.gambPPO4) and *Galleria mellonella* PPO (G.melloPPO), and hemocyanin subunit II from *Limulus polyphemus* (L.polyHcII). The NCBI accession numbers for these sequences are NM\_001043870, AJ010193, AF336289 and AM260213 respectively. CuA and CuB binding sites are singly underlined and labelled, and the conserved coordinating histidines are highlighted by ‘Δ’. Alignment constructed as in Figure 3. \_\_\_\_\_ 17
- Figure 6: The dicopper oxygen-binding site from subunit II of *Limulus polyphemus* hemocyanin. CuA and CuB and their coordinating histidines are labelled. Image generated using file 1LLA from the protein data bank (PDB) and Pymol molecular graphics software. \_\_\_\_\_ 18

- Figure 7: Proposed overview of the insect prophenoloxidase (PPO) activation cascade. Polysaccharides present at the surface of micro-organisms and other compounds released upon self-tissue damage, are bound by pattern recognition proteins (PRPs) in the insect soft body. It has been hypothesised that binding of PRP and elicitor causes a conformational change in the PRP allowing its interaction with the first protease of the PPO cascade, perhaps resulting in its auto-activation. Subsequent activation of a cascade of proteases culminates in the activation of phenoloxidase (PO). PO is activated from PPO by the prophenoloxidase activating enzyme (PPAE) which may or may not, depending on species, require to be associated with one or more serine protease homologues (SPHs) to perform this function efficiently. ‘n’ represents an unknown number of proenzymes/active proteases. Adapted from (Cerenius and Söderhäll, 2004). \_\_\_\_\_ 22
- Figure 8: Proteolytic cleavage of PPO by PPAE at the conserved arginine-phenylalanine (RF) activation site. PPAE cleaves the bond at the carbonyl side of the arginine in both subunits of PPO, converting it to its active form – PO. Removal of this N-terminal segment causes a reduction in the molecular mass of PPO by approximately 6 kDa (Müller et al., 1999; Kawabata et al., 1995). \_\_\_\_\_ 28
- Figure 9: Steps of the melanin synthetic pathway in insects. Phenoloxidase hydroxylates tyrosine to dopa and immediately oxidises the dopa to dopaquinone. Dopaquinone then non-enzymatically transforms into dopachrome which is converted to 5,6-dihydroxyindole. Further oxidation and polymerization steps result in the formation of melanin pigment (adapted from (Blois, 1978)). \_\_\_\_\_ 30
- Figure 10: Mechanism for sclerotisation of the insect cuticle. The lettered arrows represent a reaction catalysed by phenoloxidase (A), quinone isomerase (B) or quinone methide isomerase (C). D highlights non-enzymatic reactions (Sugumaran et al., 2000b). Quinones rapidly form adducts with the amino acids present in cuticular structural proteins, which ensures the hardening process. Quinone methides also perform this chemical process, but due to their more reactive nature, they also form adducts with the side chain hydroxyl groups of chitin polymer in the cuticle. Quinone methide imine amides go one step further and can perform this function whilst also acting as the cross-linking agents necessary for complete hardening of the newly ecdysed cuticle (Sugumaran, 2002). \_\_\_\_\_ 33
- Figure 11: Density-dependant phase polyphenism is a form of phenotypic plasticity displayed by some species of larval Lepidoptera. Shown above is the high density (top) and low density forms of the larvae of the moth species *Spodoptera exempta*. Cuticular melanisation, a characteristic of the high density form, results in a distinctive blackening of the insects cuticle (Wilson et al., 2001). \_\_\_\_\_ 41
- Figure 12: Multiple alignment of amino acid sequences of the four known full length *Spodoptera* PPO polypeptides. These are *Spodoptera frugiperda* PPO2 (SfrugiPPO2 – DG289582), *Spodoptera litura* PPO (SlituraPPO – AY703825), *Spodoptera exigua* PPO (SexiguaPPO – EF684939) and *Spodoptera frugiperda* PPO1 (SfrugiPPO1 – DG289581). The eight digit letter and number codes in brackets are the NCBI accession numbers for each respective sequence. The two copper-binding sites are singly underlined and labelled, and the 3 conserved histidines in each are

highlighted with ‘Δ’. The conserved RF and REE cleavage sites are marked with ‘^’, the conserved thiol-ester motif is double underlined ‘=’ and the conserved C-terminal site is underlined with ‘~’. (Multiple alignment constructed using MULTALIN (pbil) available via the ExPASy online Proteomics Server and the NCBI PubMed nucleotide databank). \_\_\_\_\_ 45

Figure 13: pDrive Cloning Vector Map. The 600 bp DNA fragment isolated by Dr Jacqueline Nairn (unpublished data 2003) was cloned into this plasmid between the EcoR1 restriction sites before transformation into competent NM552 bacterial cells. \_\_\_\_\_ 48

Figure 14: Panel A: Amplification of the 600 bp plasmid insert. The 600 bp insert was successfully amplified by PCR from clones 2a, 10a and 10b. The reaction to amplify clone 2b was unsuccessful and shows a staining pattern characteristic of unincorporated primers and dNTPs. Panel B: Gel extraction and ‘clean-up’ of the amplified 600bp DNA fragment from each clone. The lanes in the gel shown were loaded with 5µl of the amplified and purified 600 bp DNA fragments from clones 10b, 10a and 2a, to ensure the extraction and clean-up steps were successful. The lanes marked ‘M’ contain PCR markers. \_\_\_\_\_ 52

Figure 15: Finalised nucleotide sequence of the 600 bp DNA fragment from clone 10a, produced in a sequencing reaction containing the M13 reverse primer. The sequence was finalised by comparison of the raw outputted sequence with its corresponding original sequence trace and any necessary changes then made. The sequence was also clipped at both the N- and C-termini to remove undefined (N) nucleotides from the sequence. The highlighted portion indicates the only stretch of sequence which, when subjected to a blastn search, showed identity with the lowest Expect value to another prophenoloxidase gene sequence. The lower the Expect value the less likely that the similarities are random. \_\_\_\_\_ 53

Figure 16: Amino acid sequence alignment of the red underlined (RU) sequence in Table 3 and the known sequences of the *D. melanogaster* Ect3 (beta galactosidase) and *A. aegypti* beta-galactosidase genes (UniProtKB/TrEMBL Accession numbers Q9VGE7 and Q17CH4 respectively). The alignment has been truncated to show only amino acids 181 – 300, as this is the region within which the RU sequence aligns with the known sequences. The RU sequence shares 40-50% identity with the two known sequences, which in turn is the range of identity shared between the full length sequences of known insect beta-galactosidases. \_\_\_\_\_ 57

Figure 17: Structure of the *Anopheles gambiae* prophenoloxidase 1 gene (AgPPO1). The gene spans 10 kb and is composed of five exons (I – V, blue rectangles) separated by introns i, ii, iii and iv (solid black horizontal lines). The lengths depicted are simply for illustrative purposes and are not to scale. Diagram has been adapted from that shown in (Ahmed et al., 1999). \_\_\_\_\_ 58

Figure 18: The life cycle of a bracoviridae polydnavirus (PDV). During parasitisation of Lepidoptera larvae by Braconid parasitoid wasps, PDVs are injected into the host hemocoel along with the egg, venom and ovarian proteins. These function to inhibit normal cellular and humoral immune responses thus protecting the wasp egg and

allowing development of the wasp larvae in the hemocoel. Taken from (Shelby and Webb, 1999). \_\_\_\_\_ 63

Figure 19: Apparatus used for Southern blotting of nylon membranes by the capillary method. To allow full transfer of DNA from the gel to the nylon membrane the apparatus was left at room temperature for 12 – 16 hours. \_\_\_\_\_ 68

Figure 20: Amplification of actin cDNA from *Spodoptera littoralis* L5p and XL6 cDNA libraries. A DNA fragment of approximately 400 bp was generated across the full temperature gradient indicated, although the product band was approximately 50-fold brighter when the L5p library was the template DNA. This suggested that the L5p library was more viable and thus more suitable for use in PCR reactions aimed at amplifying a phenoloxidase cDNA. Two further repeat reactions produced the same results. \_\_\_\_\_ 83

Figure 21: Determining the suitability of various degenerate primer pair combinations for the amplification of an *S. littoralis* PPO DNA fragment. Each lane shows products formed in PCR reactions which contained the *M. sexta* PPO1 clone as the template DNA and one pair of degenerate primers. Lanes marked 'M' contained PCR markers with sizes as detailed in the top right image. Primer combinations and expected fragment size (in brackets), as determined from the known sequence of the *M. sexta* PPO1 clone, were as follows: Lane 1 – MsextaPPO1-F and MsextaPPO1-R (1155 bp); Lane 2 – CuA4-F and CuB2-R (606 bp); Lane 3 – CuA4-F and MIELD-R (969 bp); Lane 4 – CuA4-F and Cys2-R (1131 bp); Lane 5 – CuA4-F and Cterm-R (1317 bp); Lane 6 – GELF-F and CuB2-R (534 bp); Lane 7 – GELF-F and MIELD-R (897 bp); Lane 8 – GELF-F and Cys2-R (1059 bp); Lane 9 – GELF-F and Cterm-R (1245 bp); Lane 10 – CuB2-F and MIELD-R (387 bp); Lane 11 – CuB2-F and Cys2-R (549 bp); Lane 12 – CuB2-F and Cterm-R (735 bp); Lane 13 – CuA4-F and Cys-R (1131 bp); Lane 14 – GELF-F and Cys-R (1065 bp); Lane 15 – CuB2-F and Cys-R (555 bp); Lane 16 – CuA-F and Cterm-R (1317 bp); Lane 17 – CuA2-F and Cterm-R (1317 bp); Lane 18 – CuA3-F and Cterm-R (1317 bp). Control PCR reactions were performed to ensure primers could not generate products alone. Lanes C1 – C11 contained only CuA4-F, CuB2-R, MIELD-R, Cys2-R, Cterm-R, GELF-F, CuB2-F, CuA-F, CuA2-F, CuA3-F or Cys-R respectively. Reactions containing no template DNA generated no products (data not shown).\_ 85

Figure 22: PCR reaction products selected for Southern blotting and subsequent membrane probing. All reactions used the *Spodoptera littoralis* L5p cDNA library as the template DNA. The reaction products in each numbered lane are the result of the following primer pair combinations (reaction annealing temperature and expected product size are shown in brackets): Lane 2 – CuA4-F and Cterm-R (45°C, 1341 bp); Lane 4 – CuA4-F and Cterm-R (49.4°C, 1341 bp). PCR marker sizes in Lane M are indicated to the left. Each PCR reaction used a 2.5°C/sec annealing touchdown ramp to increase primer annealing specificity. Southern blotting of this gel and subsequent membrane manipulation resulted in the membrane found in Panel A, Figure 32. \_\_\_\_\_ 89

Figure 23: PCR reaction products selected for Southern blotting and subsequent membrane probing. All reactions used the *Spodoptera littoralis* L5p cDNA library

as the template DNA. The reaction products in each numbered lane are the result of the following primer pair combinations (reaction annealing temperature and expected product size are shown in brackets): Lane 1 – CuA4-F and Cterm-R (55°C, 1341 bp); Lane 2 – GELF-F and Cys2-R (55°C, 1044 bp); Lane 3 – GELF-F and Cys2-R (59.4°C, 1044 bp) Lane 4 - CuA-F and Cys-R (40°C, 1155 bp); Lane 5 – CuA-F and MIELD-R (40°C, 987 bp); Lane 6 – 1 µl of a 1:10 dilution of the *M. sexta* clone plasmid; Lane 7 – 5µl of a 1:10 dilution of the *M. sexta* clone plasmid. PCR marker sizes in Lane M are indicated to the left. Each PCR reaction used a 2.5°C/sec annealing touchdown ramp to increase primer annealing specificity. Southern blotting of this gel and subsequent membrane manipulation resulted in the membrane found in Panel B, Figure 32. \_\_\_\_\_ 90

Figure 24: PCR reaction products selected for Southern blotting and subsequent membrane probing. All reactions used the *Spodoptera littoralis* L5p cDNA library as the template DNA. The reaction products in each numbered lane are the result of the following primer pair combinations (reaction annealing temperature and expected product size are shown in brackets): Lane 1 – CuA-F and Cys-R (40°C, 1155 bp); Lane 2 – CuA-F and Cys-R (44.4°C, 1155 bp); Lane 3 – CuA-F and Cys-R (50°C, 1155 bp); Lane 4 – CuA-F and MIELD-R (40°C, 987 bp); Lane 5 – CuA-F and MIELD-R (44.4°C, 987 bp); Lane 6 – CuA-F and MIELD-R (50°C, 987 bp). PCR marker sizes in Lane M are indicated to the left. Each PCR reaction used a 2.5°C/sec annealing touchdown ramp to increase primer annealing specificity. Southern blotting of this gel and subsequent membrane manipulation resulted in the membrane found in Panel A, Figure 33. \_\_\_\_\_ 91

Figure 25: PCR reaction products selected for Southern blotting and subsequent membrane probing. All reactions used the *Spodoptera littoralis* L5p cDNA library as the template DNA. The reaction products in each numbered lane are the result of the following primer pair combinations (reaction annealing temperature and expected product size are shown in brackets): Lane 1 – CuA2-F and CuB2-R (40°C, 606 bp); Lane 2 – CuA2 and CuB2-R (44.4°C, 606 bp); Lane 3 – CuA2-F and CuB2-R (50°C, 606 bp); Lane 4 – CuA2-F and MIELD-R (40°C, 987 bp); Lane 5 – CuA2-F and CuB2-R (44.4°C, 987 bp) Lane 6 – CuA2-F and MIELD-R (50°C, 987 bp). PCR marker sizes in Lane M are indicated to the left. Each PCR reaction used a 2.5°C/sec annealing touchdown ramp to increase primer annealing specificity. Southern blotting of this gel and subsequent membrane manipulation resulted in the membrane found in Panel B, Figure 33. \_\_\_\_\_ 92

Figure 26: PCR reaction products selected for Southern blotting and subsequent membrane probing. All reactions used the *Spodoptera littoralis* L5p cDNA library as the template DNA. The reaction products in each numbered lane are the result of the following primer pair combinations (reaction annealing temperature and expected product size are shown in brackets): Lane 1 – GELF-F and Cys-R (55°C, 1044 bp); Lane 2 – CuA4-F and Cterm-R (49.4°C, 1341 bp) and Lane 3 – contains 1 µl of a 1:10 dilution of the *M. sexta* PPO1 clone plasmid as a control for subsequent hybridisation steps. PCR marker sizes in Lane M are indicated to the left. Each PCR reaction used a 2.5°C/sec annealing touchdown ramp to increase primer annealing

specificity. Southern blotting of this gel and subsequent membrane manipulation resulted in the membrane found in Panel C, Figure 33. \_\_\_\_\_ 93

Figure 27: PCR reaction products selected for Southern blotting and subsequent membrane probing. All reactions used the *Spodoptera littoralis* L5p cDNA library as the template DNA. The reaction products in each numbered lane are the result of the following primer pair combinations (reaction annealing temperature and expected product size are shown in brackets): Lane 1 – CuA-F and MIELD-R (40°C, 987 bp); Lane 2 – CuA-F and MIELD-R (44.4°C, 987 bp); Lane 3 – CuA2-F and CuB2-R (40°C, 606 bp); Lane 4 – CuA2-F and CuB2-R (50°C, 606 bp); Lane 5 – CuA2-F and MIELD-R (40°C, 987 bp); Lane 6 – CuA2-F and MIELD-R (50°C, 987 bp); and Lane 7 – contains 1 µl of a 1:10 dilution of the *M. sexta* PPO1 clone plasmid as a control for subsequent hybridisation steps. PCR marker sizes in Lane M are indicated to the left. Each PCR reaction used a 2.5°C/sec annealing touchdown ramp to increase primer annealing specificity. Southern blotting of this gel and subsequent membrane manipulation resulted in the membrane found in Panel A, Figure 34. \_\_\_\_\_ 94

Figure 28: PCR reaction products selected for Southern blotting and subsequent membrane probing. All reactions used the *Spodoptera littoralis* L5p cDNA library as the template DNA. The reaction products in each numbered lane are the result of the following primer pair combinations (reaction annealing temperature and expected product size are shown in brackets): Lane 1 – GELF-F and Cys-R (55°C, 1044 bp); Lane 2 – CuA4-F and Cterm-R (49.4°C, 1341 bp); Lane 3 – CuA4-F and Cterm-R (45°C, 1341 bp); Lane 4 – GELF-F and Cys2-R (55°C, 1044 bp); Lane 5 – GELF-F and Cys2-R (60.9°C, 1044 bp); Lane 6 – CuA-F and Cys-R (40°C, 1155 bp); and Lane 7 – CuA-F and Cys-R (50°C, 1155 bp). PCR marker sizes in Lane M are indicated to the left. Each PCR reaction used a 2.5°C/sec annealing touchdown ramp to increase primer annealing specificity. Southern blotting of this gel and subsequent membrane manipulation resulted in the membrane found in Panel B, Figure 34. \_\_\_\_\_ 95

Figure 29: PCR reaction products selected for Southern blotting and subsequent membrane probing. All reactions used the *Spodoptera littoralis* L5p cDNA library as the template DNA. The reaction products in each numbered lane are the result of the following primer pair combinations (reaction annealing temperature and expected product size are shown in brackets): Lane 1 – MsextaPPO1-F and MsextaPPO1-R (35°C, 1158 bp); Lane 2 – MsextaPPO1-F and MsextaPPO1-R (40.6°C, 1158 bp); Lane 3 – MsextaPPO2-F and MsextaPPO2-R (35°C, 1179 bp); Lane 4 – MsextaPPO2-F and MsextaPPO2-R (45°C, 1179 bp). PCR marker sizes in Lane M are indicated to the left. Each PCR reaction used a 1°C/sec annealing touchdown ramp to increase primer annealing specificity. Southern blotting of this gel and subsequent membrane manipulation resulted in the membrane found in Figure 35. \_\_\_\_\_ 96

Figure 30: DIG-labelled heterologous prophenoloxidase probe synthesis. The successful incorporation of DIG-11-UTP into amplified *M. sexta* PPO1 and PPO2 clones during PCR is determined by electrophoresis. The resulting DIG-labelled PPO1 and PPO2 probes (Lanes 1 and 3 respectively) show an apparent increase in their base

pair size compared to the corresponding non-labelling reactions (Lanes 2 and 4 respectively). \_\_\_\_\_ 98

Figure 31: DIG-labelled PPO-1 probe hybridised dot blot spotted with a series of dilutions of the *M. sexta* PPO1 clone plasmid. This method provides a control to test the sensitivity of the DIG-labelled PPO1 probe, and also to determine whether the NBT/BCIP colourimetric detection method is suitable. 2 µl of each of the dilutions of the *M. sexta* PPO1 clone plasmid was spotted onto the membrane as detailed. \_ 98

Figure 32: DIG-labelled PPO1 probe hybridized membranes. Membranes were subjected to 60°C hybridisation and low and moderate stringency washes prior to Anti-DIG-AP antibody incubation and BCIP/NBT colorimetric detection protocols. Membranes A and B contain bound DNA transferred by Southern blotting from the gels shown in Figure 22 and Figure 23 respectively. \_\_\_\_\_ 100

Figure 33: DIG-labelled PPO1 probe hybridized membranes. Membranes were subjected to a 65°C hybridisation step and low and moderate stringency washes prior to Anti-DIG-AP antibody incubation and BCIP/NBT colorimetric detection protocols. Membranes A, B and C contain bound DNA transferred by Southern blotting from the gels shown in Figure 24, Figure 25 and Figure 26 respectively. \_\_\_\_\_ 101

Figure 34: DIG-labelled PPO1 probe hybridized membranes. Membranes were subjected to a 65°C hybridisation step and low and high stringency washes prior to Anti-DIG-AP antibody incubation and BCIP/NBT colorimetric detection protocols. Membranes A and B contain bound DNA transferred by Southern blotting from the gels shown in Figure 27 and Figure 28 respectively. \_\_\_\_\_ 102

Figure 35: DIG-labelled PPO1 probe hybridized membrane. Membranes were subjected to a 65°C hybridisation step and low and high stringency washes prior to Anti-DIG-AP antibody incubation and BCIP/NBT colorimetric detection protocols. Membrane contains bound DNA transferred by Southern blotting from the gel shown in Figure 29. \_\_\_\_\_ 103

Figure 36: Plaque lift membranes from a screen of the *S. littoralis* L5p cDNA library. Plaque lifts were conducted on each of six plates in duplicate. All were hybridised with the DIG-labelled PPO1 probe at 65°C and washed under low and moderate stringency conditions. The duplicate membranes above are representative of all the membrane pairs resulting from screening of the cDNA library. They show no small dots of staining representing DIG-labelled PPO1 probe binding, suggesting perhaps that the cDNA library was of poor quality and therefore did not contain any representative PPO cDNA or that *S. littoralis* does not contain a PPO gene. \_\_\_\_ 105

Figure 37: Check of *S. littoralis* genomic DNA integrity. Genomic DNA was isolated from *S. littoralis* hemocytes by Nairn (2003, unpublished work). Prior to its use in restriction digest reactions, 4µl of each DNA sample (1A, 2A and 2B) was electrophoresed on a 0.8% agarose 1X TBE 0.2 µg/ml EtBr gel to check its integrity. Lane 'M' contains the 1kb DNA ladder markers (New England BioLabs Cat# N32325). The resulting gel shows that each sample had remained intact during storage, but DNA sample 1A has a higher yield. \_\_\_\_\_ 105

Figure 38: DIG-labelled PPO1 probe incubated nylon membranes generated by Southern blotting of agarose gels containing the separated products of a series of *S. littoralis* genomic DNA restriction digest reactions. Membranes A and B were generated by repeats of the methods. Membranes were hybridised at 65°C and washed using low and high stringency wash conditions. The lane contents are as follows: EcoR1 digest products (Lane 1), HindIII digest products (Lane 2), EcoR1/HindIII digest products (Lane 3), non-digested *S. littoralis* hemocyte genomic DNA (Lane 4), and the *M. sexta* PPO1 clone plasmid from which the DIG-labelled probe used was synthesised (Lane 7). DIG-PPO1 probe binding could only be detected in that lane (Lane 7) which contained the *M. sexta* clone PPO1 plasmid DNA – the template DNA of the probe. Binding of the DIG-PPO1 probe to the marker DNA is visible in Lane M of membrane A (circled). \_\_\_\_\_ 107

Figure 39: Probing of duplicate membranes with the DIG-PPO1 or DIG-PPO2 DNA probe to determine which was the more sensitive and specific in the recognition and binding of a PPO sequence heterologous to its own. Replica membranes A and B contain PCR markers (Lane 1), products of a PCR reaction amplifying the *M. sexta* PPO1 clone using CuA3-F and Cys-R primers (Lane 3) and products of a PCR reaction amplifying the *M. sexta* PPO2 clone using CuA3-F and Cys-R primers (Lane 5). In replica membranes C and D the lane contents are 1 – PCR markers, 2 – products of a PCR reaction amplifying the *M. sexta* PPO1 clone using *M. sexta* PPO1-specific forward and reverse primers, 3 – products of a PCR reaction amplifying the *M. sexta* PPO2 clone using *M. sexta* PPO2-specific forward and reverse primers, 4 – a 1:10 dilution of the *M. sexta* PPO1 clone, and 5 – a 1:10 dilution of the *M. sexta* PPO2 clone. All four membranes were hybridised at 65°C and washed under low and moderate stringency washes. Ultimately the DIG-PPO2 probe was the most sensitive of the two probes however neither probe demonstrated any specificity solely for PPO DNA, evidenced by their binding to marker and non-specific PCR product DNA bands \_\_\_\_\_ 110

Figure 40: Probing of duplicate membranes using the DIG-PPO2 probe at 68°C hybridisation and using low and high stringency washes. Probing and bound probe detection methods were also identical. Lane contents of membranes A and B above are as described in Figure 39 for membranes A and B respectively. The conditions used here included a higher hybridisation temperature and higher wash stringency than was used in probing of the membranes in Figure 39, in an attempt to eliminate binding of the DIG-PPO2 probe to marker DNA and other non-PPO DNA PCR products. Unfortunately these efforts failed to reduce the non-specificity of the DIG-PPO2 probe, and as is evident, probe binding to markers and other DNA bands remains an issue even under these higher stringency conditions. \_\_\_\_\_ 111

Figure 41: *Spodoptera littoralis* larvae display a characteristic known as density dependant phase polyphenism. Individuals reared in high density populations have darker cuticles and head capsules due to enhanced cuticular melanisation (left), compared to those reared in low density populations, which are usually pale brown/green with pale brown head capsules. Scale shown is in centimetres. \_\_\_\_ 118

Figure 42: A photographic record of the growth phases of solitary *Spodoptera littoralis* larva over a 14 day period. By day 14/15 larvae were ready for bleeding (3 – 4 cm

length), and depending on health, were bled once each day for two days. The scale shown is in centimetres. \_\_\_\_\_ 123

Figure 43: *Spodoptera littoralis* larvae reared under conditions designed to recreate high density population, had slower development rates and smaller larval size than those reared in solitary conditions. A typical example of a high population density (*gregaria* phase) culture pot from this experiment is shown above, and illustrates the great difference in size between individuals by the age of 14 days. Whilst the larva nearest the scale bar is of expected size, that to the centre left is equivalent in size to that of a 10 day old larva. 1 in 4 fatalities occurred in gregarious larvae and many of the surviving gregarious larvae had melanised hemolymph indicative of active PO. The fatalities were generally among the smaller larvae and appeared to be a result of cannibalistic behaviour. The scale shown is in centimetres. \_\_\_\_\_ 124

Figure 44: Total RNA integrity check. The sample in Panel A was the most successful of five RNA isolation attempts. The sample was separated in a native 1% agarose gel. In panel B, examples of fully degraded and intact total RNA samples are shown in a 1.5 % denaturing agarose gel (Taken from (Ambion, Accessed: 2006.)). These illustrate that the 28S and 18S ribosomal RNA (rRNA) bands in panel A are not as sharp and clear as is desirable, although they can still be identified. The sample is therefore too degraded to provide a reliable source of mRNAs for synthesis of a complete *S. littoralis* hemocyte first strand cDNA mix. \_\_\_\_\_ 127

Figure 45: Quaternary structures of the 4x6-meric hemocyanin subunits from *Limulus polyphemus* (Panel A) and *Eurypelma californicum* (Panel B). The subunits shown in red are those known to possess phenoloxidase activity. The complete native *L. polyphemus* hemocyanin is composed of two superimposed 4 x 6-mers (Adapted from (Decker et al., 2001)). \_\_\_\_\_ 139

Figure 46: Tertiary structure of subunit II of *Limulus polyphemus* hemocyanin. The three domains are coloured green (domain I), cyan (domain II) and magenta (domain III). CuA and CuB are shown as orange spheres. Image generated using PDB file 1LLA and Pymol molecular graphics software. \_\_\_\_\_ 141

Figure 47: The binuclear copper site of *Limulus polyphemus* hemocyanin subunit II. CuA and CuB (orange) and their coordinating His (shown in stick format) are highlighted. View shown is perpendicular to the Cu-Cu axis. Image produced as in Figure 46. \_\_\_\_\_ 143

Figure 48: Active site of *Limulus polyphemus* subunit II hemocyanin showing the orientation of the 'placeholder' amino acid, phenylalanine-49 (magenta coloured residue shown in stick format in domain I), in the entrance to the dicopper centre. Domains are highlighted in green (domain I), cyan (domain II) and magenta (domain III). Copper ions are shown as orange spheres and their coordinating histidine residues in yellow stick format. Note the differing domain location of the dicopper centre and Phe-49 residue. Image produced as in Figure 46. \_\_\_\_\_ 145

Figure 49: Ion binding sites in *Limulus polyphemus* hemocyanin subunit II. The chloride ion (blue sphere) binding site is positioned at the interface of domain I (green) and II (cyan), whilst the putative calcium ion (purple sphere) binding site is located at the

subunit surface near two flexible regions of domain III (magenta). Both chloride and calcium ions are known to be important effectors of cooperative oxygen binding by the *L. polyphemus* hemocyanin complex (Sullivan et al., 1974; Hazes et al., 1993). The copper ions of the dicopper centre are represented by orange spheres at the core of domain II. Image produced as in Figure 46. \_\_\_\_\_ 146

Figure 50: Phenoloxidase catalyses a two-step reaction which incorporates molecular oxygen into phenolic molecules at its dicopper centre. Crustacean Hcs are thought only to possess *o*-diphenoloxidase activity (only one exception has been found), whilst chelicerate hemocyanins have been shown to exhibit both tyrosinase and *o*-diphenoloxidase activity (Decker and Jaenicke, 2004). \_\_\_\_\_ 152

Figure 51: Induced phenoloxidase activity of hemocyanin from *Limulus polyphemus*, *Pandinus imperator* and *Eurypelma californicum*. Typical assays included 2 mM dopamine hydrochloride plus hemocyanin (concentrations in legend) in 1 ml of 100 mM sodium phosphate buffer, pH 7.5. Phenoloxidase activity (expressed in units where 1 unit = formation of 1  $\mu$ mol of dopachrome per minute) was initiated by the addition of SDS, and after 5 minutes, followed by monitoring an increase in absorbance at 475 nm resulting from the formation of dopachrome and its derivatives. Inset provides clearer detail of the region of the main plot contained within the red box, and shows PO activity expressed as a percentage of the maximum activity achieved by each hemocyanin. A full version of the inset plot including data for SDS up to 40 mM can be found in Section 9.4 – Appendix D. 169

Figure 52: ITC data for binding of SDS to *Limulus polyphemus* hemocyanin. Upper trace in top panel shows a control in which SDS was injected into buffer alone to determine the CMC of SDS in 100 mM sodium phosphate buffer, pH 7.5, and also to correct for heat of dilution of the ligand. Lower trace in upper panel presents the data for injection of 30 mM SDS (0.15 mM per injection) into  $0.77 \pm 0.015$  mg/ml (10  $\mu$ M) *L. polyphemus* hemocyanin monomers (equivalent to 210 nM of the 8 x 6-meric unit). The lower panel shows the calculated binding isotherm (integrated heat data), corresponding to the lower trace in the upper panel, and the best-fitted curve of the data. The calorimetry data shown were analysed by nonlinear regression in terms of a sequential binding site model using the MicroCal ORIGIN software package. \_\_\_\_\_ 171

Figure 53: ITC data for binding of SDS to *Pandinus imperator* hemocyanin. Upper trace in top panel shows a control in which SDS was injected into buffer alone to determine the CMC of SDS in 100 mM sodium phosphate buffer, pH 7.5, and also to correct for heat of dilution of the ligand. Lower trace in upper panel presents the data for injection of 30mM SDS (0.15 mM per injection) into  $0.77 \pm 0.015$  mg/ml (10  $\mu$ M) *P. imperator* hemocyanin monomers (equivalent to 420 nM of the 4 x 6-meric unit). The lower panel shows the calculated binding isotherm (integrated heat data), corresponding to the lower trace in the upper panel, and the best-fitted curve of the data. The calorimetry data shown were analysed by nonlinear regression in terms of a sequential binding site model using the MicroCal ORIGIN software package. \_\_\_\_\_ 172

- Figure 54: ITC data for binding of SDS to *Eurypelma californicum* hemocyanin. Upper trace shows the control in which SDS was injected into buffer alone to determine the CMC of SDS in 100 mM sodium phosphate buffer, pH 7.5, and also to correct for heat of dilution of the ligand. Lower trace presents the data for injection of 75mM (0.375 mM per injection) SDS into  $0.77 \pm 0.015$  mg/ml (10  $\mu$ M) *E. californicum* hemocyanin monomers (equivalent to 420 nM of the 4 x 6-meric unit). As is evident from this lower trace, no heat changes occurred as a result of SDS injection into the protein, therefore no data was available for analysis. \_\_\_\_\_ 173
- Figure 55: Determination of the critical micelle concentration of SDS in 100 mM TrisHCl pH 7.5 buffer, which was used in ICP OES experiments. The trace shows data for the injection of 20 mM SDS (0.1 mM per injection) into 100 mM TrisHCl pH 7.5 buffer alone. \_\_\_\_\_ 174
- Figure 56: Far UV CD spectra of 0.3 mg/ml *Limulus polyphemus* hemocyanin following 5 minute incubations with SDS across the range 0 – 3.5 mM. \_\_\_\_\_ 177
- Figure 57: Far UV CD spectra of 0.3 mg/ml *Pandinus imperator* hemocyanin following 5 minute incubations in SDS across the range 0 – 2.0 mM. \_\_\_\_\_ 178
- Figure 58: Far UV CD spectra of 0.3 mg/ml *Eurypelma californicum* hemocyanin in the absence of SDS and following a 5 minute and 16 hour incubation in 5.0 mM SDS. \_\_\_\_\_ 179
- Figure 59: Fluorescence emission spectra of 0.1 mg/ml *Limulus polyphemus* hemocyanin in 100 mM sodium phosphate buffer pH 7.5, excited at 290 nm, following 5 minutes incubation in SDS across the range 0 – 2.7 mM. \_\_\_\_\_ 182
- Figure 60: Fluorescence emission spectra of 0.1 mg/ml *Pandinus imperator* hemocyanin in 100 mM sodium phosphate buffer pH 7.5, excited at 290 nm, following 5 minutes incubation in SDS across the range 0 – 2.0 mM. \_\_\_\_\_ 183
- Figure 61: Fluorescence emission spectra of 0.1 mg/ml *Eurypelma californicum* hemocyanin in 100 mM sodium phosphate buffer pH 7.5, excited at 290nm, in the absence of SDS and following 5 minutes or 16 hours incubation in 5.0 mM SDS. 184
- Figure 62: Fluorescence emission spectra of 2  $\mu$ M *N*-acetyl tryptophan amide in 100 mM sodium phosphate buffer pH 7.5 at 290nm, in the absence of SDS and following 5 minutes incubation in 2.7 mM SDS. \_\_\_\_\_ 187
- Figure 63: Near UV circular dichroism spectra of 0.3 mg/ml *Eurypelma californicum* hemocyanin in 100 mM sodium phosphate buffer pH 7.5, in the absence of SDS and following either 5 minutes or 16 hours incubation in 5.0 mM SDS. Molecular ellipticity at 260 - 305 nm is associated with the microenvironment of protein aromatic residues. The 340 nm peak is a characteristic near UV signal of the Type-3 copper centre. \_\_\_\_\_ 189
- Figure 64: Near UV circular dichroism spectra of 0.3 mg/ml *Limulus polyphemus* hemocyanin in 100 mM sodium phosphate buffer pH 7.5 following 5 minutes incubation in SDS across the range 0 – 3.5 mM. Molecular ellipticity between 260 - 305 nm is associated with the microenvironment of protein aromatic residues. The 340 nm peak is a characteristic near UV signal of the Type-3 copper centre. \_\_\_\_ 190

- Figure 65: Near UV circular dichroism spectra of 0.3 mg/ml *Pandinus imperator* hemocyanin in 100 mM sodium phosphate buffer pH 7.5 following 5 minutes incubation in SDS across the range 0 – 2.0 mM. Molecular ellipticity at 260 - 305 nm is associated with the microenvironment of protein aromatic residues. The 340 nm peak is a characteristic near UV signal of the Type-3 copper centre. \_\_\_\_\_ 191
- Figure 66: Near UV circular dichroism spectra of 0.3, 0.6 and 0.9 mg/ml *Limulus polyphemus* hemocyanin in 100 mM sodium phosphate buffer pH 7.5 following 5 minutes incubation is SDS at 0, 1.4 and 3.5 mM. Molecular ellipticity at 260 - 305 nm is associated with the microenvironment of protein aromatic residues. The 340 nm peak is a characteristic near UV signal of the Type-3 copper centre. The spectra indicate that protein concentration had no effect on the circular dichroism spectra at the wavelengths and SDS concentrations concerned. \_\_\_\_\_ 193
- Figure 67: Determination of the stability of *Pandinus imperator* and *Eurypelma californicum* hemocyanin upon incubation with sub-micellar and micellar concentrations of SDS. Dynamic light scattering was used to monitor changes in particle size (diameter) over 24 hours, of 1 mg/ml hemocyanin samples in 100 mM sodium phosphate buffer pH 7.5, incubated with 0.5 mM SDS, 2.0 mM (*P. imperator* Hc only) or 5.0 mM (*E. californicum* Hc only) SDS. \_\_\_\_\_ 195
- Figure 68: Determination of SDS critical micelle concentration (CMC) in 100 mM sodium phosphate buffer pH 7.5. Dynamic light scattering was used to record changes in particle size (diameter and width) of SDS when present at increasing concentrations in this buffer. The results show that the CMC of SDS in this buffer lies between 1.00 and 1.05 mM. \_\_\_\_\_ 196
- Figure 69: Absorbance spectra of 0.3 mg/ml *Limulus polyphemus* hemocyanin in 100 mM sodium phosphate buffer pH 7.5 following 5 minutes incubation in SDS across the range 0 – 2.7 mM. \_\_\_\_\_ 198
- Figure 70: Absorption spectra of 0.3 mg/ml *Pandinus imperator* hemocyanin in 100 mM sodium phosphate buffer pH 7.5 following 5 minutes incubation in SDS across the range 0 – 2.0 mM. \_\_\_\_\_ 199
- Figure 71: Absorption spectra of 0.3 mg/ml *Eurypelma californicum* hemocyanin in 100 mM sodium phosphate buffer pH 7.5 following 5 minutes incubation in SDS across the range 0 – 10 mM. \_\_\_\_\_ 199
- Figure 72: Absorption spectra of 0.3 mg/ml *Eurypelma californicum* hemocyanin in 100 mM sodium phosphate buffer pH 7.5 following 5 minutes or 16 hours incubation in the absence or presence of 5.2 mM SDS. \_\_\_\_\_ 200
- Figure 73: Fluorescence spectra of 0.1 mg/ml *Limulus polyphemus* hemocyanin in 100 mM sodium phosphate buffer pH 7.5 excited at 330 nm following 5 minutes incubation with 0 – 2.7 mM SDS. \_\_\_\_\_ 203
- Figure 74: Fluorescence spectra of 0.1 mg/ml *Pandinus imperator* hemocyanin in 100 mM sodium phosphate buffer pH 7.5 excited at 330 nm following 5 minutes incubation with 0 or 2 mM SDS. \_\_\_\_\_ 204

- Figure 75: Fluorescence spectra of 0.1 mg/ml *Eurypelma californicum* hemocyanin in 100 mM sodium phosphate buffer pH 7.5 excited at 330 nm following 5 minutes or 16 hours incubation with 5 mM SDS. \_\_\_\_\_ 204
- Figure 76: Relationship between the phenoloxidase activity data, far UV circular dichroism spectroscopic data and tryptophan fluorescence data of *L. polyphemus* and *P. imperator* hemocyanin following incubation with submicellar and micellar concentrations of SDS. *E. californicum* hemocyanin data was not included due to a lack of any spectroscopic change in this hemocyanin over the 5 minute time period during which most data was collected. The percentage of maximum activity and the percentage of total structural change remaining are plotted against increasing SDS concentration. For both hemocyanin types, phenoloxidase activity was correlated with the far UV circular dichroism measurements made at 207 nm and the tryptophan fluorescence measurements made at  $\lambda_{\text{max}}$ . \_\_\_\_\_ 209
- Figure 77: Far UV circular dichroism spectra (top panel) of *Limulus polyphemus* hemocyanin subunit II in 100 mM sodium phosphate buffer, pH 7.5 (green) and following 5 minutes incubation in the presence of 2.7 mM SDS (maroon) or 2.7 mM NBDG (dark blue). \_\_\_\_\_ 211
- Figure 78: Near UV circular dichroism spectra (top panel) of *Limulus polyphemus* hemocyanin subunit II in 100 mM sodium phosphate buffer, pH 7.5 (green) and following 5 minutes incubation in the presence of 2.7 mM SDS (maroon) or 2.7 mM NBDG (dark blue). \_\_\_\_\_ 212
- Figure 79: Near UV CD spectra of 0.9 mg/ml *Limulus polyphemus* hemocyanin in 100 mM sodium phosphate buffer, pH 7.5, before and after 5 minutes incubation with 1.1 mM SDS, then 5 minutes after the solution was diluted by a third to bring the SDS concentration to below CMC (0.36 mM), subsequently also diluting the hemocyanin to 0.3 mg/ml. \_\_\_\_\_ 215
- Figure 80: Near UV CD spectra of 0.9 mg/ml *Pandinus imperator* hemocyanin in 100 mM sodium phosphate buffer, pH 7.5 before and after 5 minutes incubation with 1.1 mM SDS, then also 5 minutes after the solution was diluted by a third to bring the SDS concentration to below CMC (0.36 mM), subsequently also diluting the hemocyanin to 0.3 mg/ml. \_\_\_\_\_ 216
- Figure 81: Far UV CD spectra of 0.3 mg/ml *Limulus polyphemus* hemocyanin in 100 mM sodium phosphate buffer, pH 7.5, before and after 5 minutes incubation with 1.1 mM SDS then once SDS was diluted out to 0.36 mM, below CMC. \_\_\_\_\_ 217
- Figure 82: Fluorescence spectra of 0.1 mg/ml *Limulus polyphemus* hemocyanin in 100 mM sodium phosphate buffer, pH 7.5 following 5 minutes incubation with a 50:50 mixture of the phospholipids phosphatidylethanolamine and phosphatidylcholine at final concentrations between 0 and 4 mM as indicated in the legend. \_\_\_\_\_ 219
- Figure 83: Fluorescence spectra of 0.1 mg/ml *Pandinus imperator* hemocyanin in 100 mM sodium phosphate buffer, pH 7.5 following 5 minutes incubation with a 50:50 mixture of the phospholipids phosphatidylethanolamine and phosphatidylcholine at final concentrations between 0 and 4 mM as indicated in the legend. \_\_\_\_\_ 220

- Figure 84: Fluorescence spectra of 0.1 mg/ml *Limulus polyphemus* hemocyanin in 100 mM sodium phosphate buffer, pH 7.5 following 5 minutes incubation with 0, 0.5 or 1.0 mM small unilamellar vesicles, composed of a 50:50 ratio of the phospholipids phosphatidylethanolamine and phosphatidylcholine. \_\_\_\_\_ 221
- Figure 85: Fluorescence spectra of 0.1 mg/ml *Pandinus imperator* hemocyanin in 100 mM sodium phosphate buffer, pH 7.5 following 5 minutes incubation with 0, 0.5 or 1.0 mM small unilamellar vesicles, composed of a 50:50 ratio of the phospholipids phosphatidylethanolamine and phosphatidylcholine. \_\_\_\_\_ 222
- Figure 86: Schematic binding isotherm of protein-surfactant interactions. In general, the isotherm of the binding of ionic surfactants to proteins displays four characteristic regions (with increasing surfactant concentration): (I) specific binding, (II) non-cooperative binding, (III) cooperative binding, and (IV) saturation. Taken from Valstar, 2000. \_\_\_\_\_ 230
- Figure 87: Location of the eight tryptophan residues (yellow) in *Limulus polyphemus* subunit II. One tryptophan (Trp65) is located in domain I (green) and two (Trp538 and 563) in domain III (magenta) whilst the remaining five (Trp174, 176, 184, 326 and 363) are located at the copper A and B binding sites of the dicopper centre in domain II (cyan). Copper ions are shown as orange spheres. Image generated using PDB file 1LLA and Pymol molecular graphics software. \_\_\_\_\_ 234
- Figure 88: Structure of the phospholipids phosphatidylethanolamine and phosphatidylcholine (adapted from Avanti Polar Lipids, Accessed: 2007.) and the detergent sodium dodecyl sulphate (SDS) (Key Centre for Polymer Colloids, Accessed: 2007.). ‘R’ represents the fatty acid side chains of the phospholipids which can range in length and may be either saturated or unsaturated. \_\_\_\_\_ 244
- Figure 89: Primer binding-site map. Each of the degenerate primers detailed in Table 11, which were designed specifically for the amplification of a phenoloxidase sequence, are represented as labelled black rectangles positioned next to the DNA strand they are designed to anneal to. Arrows associated with each indicate the direction of strand extension once each primer has annealed to its designed sequence. The numerical values alongside each primers given name indicate the amino acids of the template PPO DNA to which the primers are designed to anneal, as estimated from the amino acid sequence alignment in Figure 3, Chapter 2. \_\_\_\_\_ 266
- Figure 90: Isolated *Spodoptera littoralis* hemocyte total RNA integrity check. The samples shown in Panels A - D were the 2<sup>nd</sup> – 5<sup>th</sup> total RNA isolation attempts made, respectively, in Chapter 5. The samples were separated in a native 1% agarose gel. These images illustrate that the 28S and 18S ribosomal RNA (rRNA) bands are not sharp and clear as is desirable (see Figure 44 Panel B in Chapter 5), and in fact cannot be identified in most of the samples. These total RNA samples were therefore too degraded to provide a reliable source of mRNAs for synthesis of a complete *S. littoralis* hemocyte first strand cDNA mix. \_\_\_\_\_ 269
- Figure 91: Induced phenoloxidase activity of hemocyanin from *Limulus polyphemus*, *Pandinus imperator* and *Eurypelma californicum*. Typical assays included 2 mM dopamine hydrochloride plus hemocyanin (concentrations in legend) in 1 ml of 100

mM sodium phosphate buffer, pH 7.5. Phenoloxidase activity (expressed as a percentage of the maximum activity achieved by each hemocyanin) was initiated by the addition of SDS, and after 5 minutes, followed by monitoring an increase in absorbance at 475 nm resulting from the formation of dopachrome and its derivatives. This plot is the complete version of the inset plot in Figure 51, Chapter 7

---

270

Figure 92: ITC data for binding of SDS to *Limulus polyphemus* hemocyanin. Upper trace in top panel shows a control in which SDS was injected into buffer alone to determine the CMC of SDS in 100 mM sodium phosphate buffer, pH 7.5, and also to correct for heat of dilution of the ligand. Lower trace in upper panel presents the data for injection of 30 mM SDS (0.15 mM per injection) into  $0.77 \pm 0.015$  mg/ml (10  $\mu$ M) *L. polyphemus* hemocyanin monomers (equivalent to 210 nM of the 8 x 6-meric unit). The lower panel shows the calculated binding isotherm (integrated heat data), corresponding to the lower trace in the upper panel, and the best-fitted curve of the data. The calorimetry data shown were analysed by nonlinear regression in terms of a single binding site model using the MicroCal ORIGIN software package.

---

271

Figure 93: ITC data for binding of SDS to *Pandinus imperator* hemocyanin. Upper trace in top panel shows a control in which SDS was injected into buffer alone to determine the CMC of SDS in 100 mM sodium phosphate buffer, pH 7.5, and also to correct for heat of dilution of the ligand. Lower trace in upper panel presents the data for injection of 30mM SDS (0.15 mM per injection) into  $0.77 \pm 0.015$  mg/ml (10  $\mu$ M) *P. imperator* hemocyanin monomers (equivalent to 420 nM of the 4 x 6-meric unit). The lower panel shows the calculated binding isotherm (integrated heat data), corresponding to the lower trace in the upper panel, and the best-fitted curve of the data. The calorimetry data shown were analysed by nonlinear regression in terms of a single binding site model using the MicroCal ORIGIN software package.

---

272

## LIST OF TABLES

- Table 1: Pattern recognition proteins found in the hemolymph of the tobacco hornworm, *Manduca sexta*. A level of redundancy is displayed in the binding specificities of these PRPs, with some recognising more than one microbial polysaccharide (constructed using data from (Yu et al., 2002)). \_\_\_\_\_ 24
- Table 2: Examples of the mechanisms insects utilise for the control of phenoloxidase activity. Such mechanisms function to regulate production of cytotoxic quinones that are by-products of the reactions catalysed by phenoloxidase (Sugumaran, 2001). \_\_\_\_\_ 35
- Table 3: The nucleotide sequence of the 600 bp DNA fragment from clone 10a was translated in all six reading frames to its corresponding amino acid sequence. The translation was conducted using the 'Translate' tool available online via the ExPASy proteomics server. Compact output format is shown where '#' represents a stop codon. The sequence highlighted in yellow indicates the only region out of all six of the reading frames that showed identity/similarity to phenoloxidases from other arthropod species. The red underlined sequence is that which generated the hit with the lowest E value and contained a putative glycosyl hydrolase domain, characteristic of beta-galactosidase enzymes. The double underlined amino acids have the sequence of the forward (5'3' Frame 3) and reverse (5'3' Frame 2) primers and represent those parts of the sequence from which strand extension was initiated. \_\_\_\_\_ 56
- Table 4: Primer pairs categorized according to the DNA products formed during PCRs in which each primer pair was used to amplify a particular stretch of a *M. sexta* PPO clone. Those which were successful in the amplification of a DNA fragment of the expected size, as well as those generating non-specific products in addition to this expected fragment, were utilized as primer pairs in subsequent rounds of PCR designed to amplify a PPO gene fragment from an *S. littoralis* L5p cDNA library. The number in brackets alongside each primer pair indicates the lane number in Figure 21 which illustrates the products formed. \_\_\_\_\_ 86
- Table 5: Examples of proteins containing the Type-3 copper centre, and their location, activity and function within biological systems. Phenoloxidase (Ashida and Brey, 1997; Decker and Tuzcek, 2000; Sugumaran et al., 2000b; Sugumaran and Nellaiappan, 2000), tyrosinase (Sugumaran et al., 2000a; Decker and Jaenicke, 2004) and catecholoxidase (Greving et al., ) possess the Type-3 copper centre only, whereas ceruloplasmin (Maltais et al., 2003) and laccase (Garcia-Pineda et al., 2004; Santagostini et al., 2004) also contain the Type-2 copper centre. \_\_\_\_\_ 134
- Table 6: Percentage change in secondary structure content of each hemocyanin following incubation in SDS as detailed within the table. Secondary structure predictions were conducted on DICHROWEB, using SELCON 3 and reference set 3. \_\_\_\_\_ 180

- Table 7: Upon excitation at 290 nm, the tryptophan fluorescence peak wavelength of *Limulus polyphemus* and *Pandinus imperator* hemocyanin in 100 mM sodium phosphate buffer pH 7.5, exhibits a blue-shift in the presence of increasing concentrations of SDS. *Eurypelma californicum* hemocyanin on the other hand exhibits a red-shift after 5 minutes incubation. Following 16 hours incubation however, the latter displays a blue shift in the tryptophan fluorescence peak wavelength. \_\_\_\_\_ 186
- Table 8: ICP-OES analysis of *Limulus polyphemus* hemocyanin in the absence and presence of SDS. Hemocyanin in 100 mM sodium phosphate buffer, pH 7.5, was incubated with no SDS, sub-micellar or micellar concentrations of SDS, then applied to a NAP-5 desalting column equilibrated with respective concentrations of SDS. Protein peak and wash eluant were pooled separately and diluted 5-fold in 5% nitric acid prior to ICP-OES analysis. The ‘Expected’ copper concentrations shown were calculated for the diluted samples, and on the basis that both copper ions remained associated with each hemocyanin subunit upon incubation with SDS. Protein concentration was determined from UV absorbance measurements at 280nm using a value of 1.39 for a 1 mg/ml *L. polyphemus* hemocyanin solution, which in turn contained 1.7 mg/L Cu<sup>2+</sup>. The negative values of the ‘Actual’ wash eluant are due to the copper concentrations being lower than those in the 0 µg/L standard used for calibration of the ICP-OES equipment. Effectively there was no Cu in these washes. \_\_\_\_\_ 207
- Table 9: Upon excitation at 290 nm, the emission fluorescence peak of *Limulus polyphemus* and *Pandinus imperator* hemocyanin exhibits a blue-shift in the presence of increasing concentrations of SUVs. \_\_\_\_\_ 224
- Table 10: Upon excitation at 290 nm, the emission fluorescence peak of *Limulus polyphemus* and *Pandinus imperator* hemocyanin exhibits a blue-shift in the presence of increasing concentrations of phospholipids. \_\_\_\_\_ 224
- Table 11: Primers designed specifically for the amplification of an insect phenoloxidase sequence. Primers CuA’03-F and PO2-R were previously designed by Nairn 2002 (unpublished data) and used to amplify the putative PPO 600 bp gene fragment analysed in Chapter 3. All others were utilized during PCR protocols performed in the presented research of Chapter 4. The given name of each primer is shown along with the details of its nucleotide and amino acid sequence, and the amino acid sequence position it anneals to, as established from the alignment of six different arthropod PPO sequences found in Figure 3, Chapter 2. \_\_\_\_\_ 265

## **Chapter 1 : Thesis Overview**

Proteins containing a binuclear copper centre, in which each copper ion is coordinated by three histidine residues, belong to a group known as the Type-3 copper proteins. Examples from this group include the mammalian tyrosinases and plant catecholoxidases. Those of interest and relevance to the subsequently presented research, however, are the insect phenoloxidases and arthropod hemocyanins, which each contain a single Type-3 copper centre per protein subunit.

### **1.1 Insect phenoloxidase**

Under normal *in vivo* conditions, insect phenoloxidase (PO) exists as a zymogen known as prophenoloxidase (PPO). Upon wounding or immune challenge, PPO is converted to its active form for the catalysis of defence reactions which generate compounds which afford the insect protection from infection. PO is also important developmentally, as products of its catalysis are responsible for hardening of the insect cuticle following each moult. The mechanism of PPO activation is poorly understood, although a number of components of the so called PPO cascade have been characterised more recently. Further discussions of these points are presented in Chapter 2.

To date, the complete sequence of approximately 55 PPOs from a number of insect species have been submitted to the global database. However no sequence for a *Spodoptera littoralis* PPO has been elucidated despite published research demonstrating the presence of PO activity in the hemolymph of the larvae of this Lepidopteran species. *Spodoptera littoralis*, more commonly known as the Egyptian Cotton Leafworm, is an

economically important crop pest in many regions of Africa and Asia, the larvae of which are responsible for the destruction of entire crop harvests. Research aimed at unravelling the mechanisms by which these and other pest insects protect themselves from disease and environmental damage may well provide new opportunities for the development of species specific pest control. Structural and functional characterisation of the molecules involved in these mechanisms, one of which is PO, will be the first step towards this goal.

## **1.2 Arthropod hemocyanin**

Arthropod hemocyanin (Hc) is a very large respiratory protein found in chelicerates, crustaceans, and more recently an insect model. The three dimensional structure of the dicopper centre of Hc is virtually super imposable with that of another Type-3 copper protein, catecholoxidase, and therefore it is hypothesised that all Type-3 copper proteins share this dicopper centre structure. The focus of the current research is the existence of a mechanism which, when triggered *in vitro*, elicits an intrinsic PO-like enzymatic activity in hemocyanin. This potential dual-functionality of Hc is very unusual. It has been known for some years that the anionic detergent sodium dodecyl sulphate (SDS), can induce PO-type activity in arthropod Hc. Structural analyses have suggested that the presence of SDS causes a conformational change which opens the entrance to the dicopper centre of the Hc subunits, allowing larger phenolic substrates to enter. However, until now there have been no published results from experiments designed to characterise these SDS induced conformational changes in arthropod Hc. Discussions focusing on the structure and function of arthropod hemocyanin, as well as what was known of the effect of SDS to date, are presented in Chapter 6.

### 1.3 Research Objectives

The presented research was based on two core objectives, the first of which was aimed at isolating, sequencing and characterising a PPO gene, from larvae of the insect crop pest *S. littoralis* (Figure 1 Panel A). A range of molecular techniques were used in experiments designed to address this aim, the results of which are presented in Chapter 3, Chapter 4 and Chapter 5. The second objective was to conduct a biophysical characterisation study of the mechanism of SDS induced PO activity in hemocyanin from the chelicerates (Phylum Arthropoda) *Limulus polyphemus*, *Pandinus imperator* and *Eurypelma californicum* (Figure 1, Panels B, C and D respectively). Some preliminary experiments were also conducted in attempts to determine a possible *in vivo* explanation for the effect that SDS has on Hc. The data and discussions for these experiments are presented in Chapter 7. The final chapter (Chapter 8) of this thesis draws together the main points established from the research and suggests possibilities for future work, as well as highlighting the importance of continuing to research the structure and function of Type-3 copper proteins.

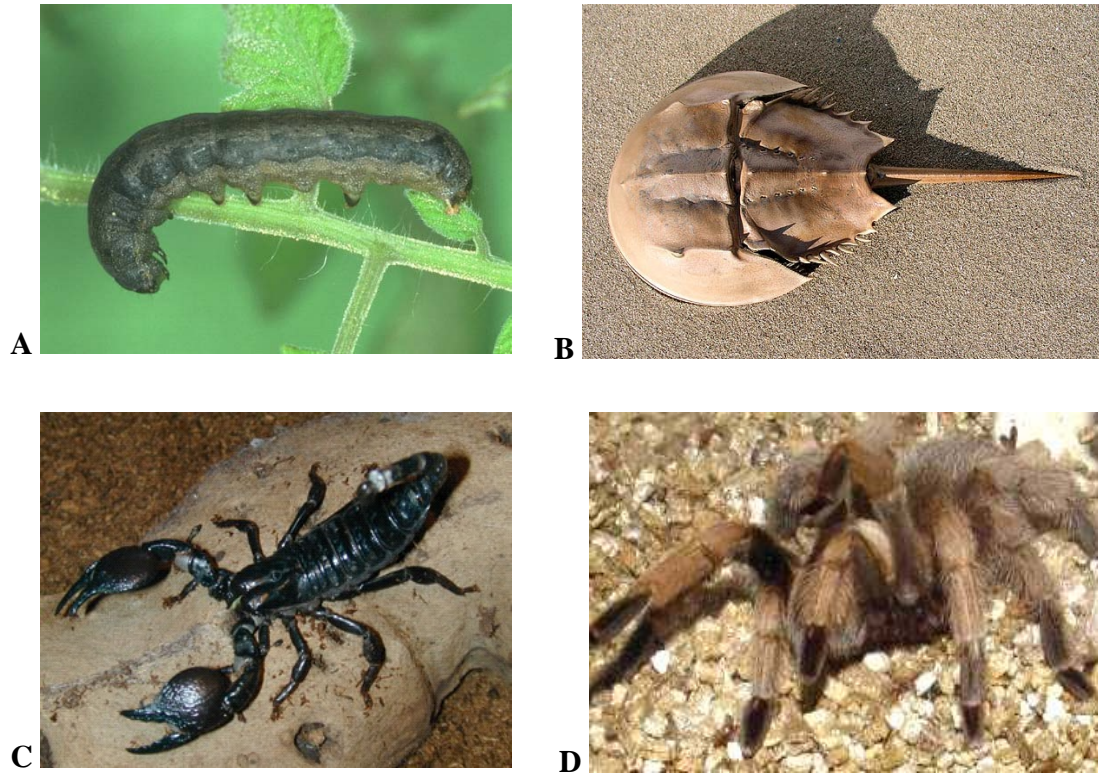


Figure 1: Research study species, which were the source of the cDNA library, genomic DNA or total RNA (Panel A: *Spodoptera littoralis* (Egyptian Cotton Leafworm) larva), or the purified hemocyanins (Panel B: *Limulus polyphemus* (North Atlantic Horseshoe Crab); Panel C: *Pandinus imperator* (Emperor Scorpion); Panel D: *Eurypelma californicum* (North American Tarantula))

## **Chapter 2 : Phenoloxidase in Insect Immunity – A Review of the Literature**

### **2.1 Introduction to Insect Immunity**

Insects (Phylum: Arthropoda; Class: Insecta) are extraordinary animals that have adapted and evolved to inhabit almost every environment on earth (Söderhall and Cerenius, 1998), including deserts and the Antarctic. Only in the oceans are insects less commonly found (Weeden et al., Accessed: 2003.). This success is believed to depend to a large extent on their defence systems against, and very efficient means of recognising, various potentially harmful micro-organisms and parasites, as many insects live in environments where micro-organisms are thriving (Söderhall and Cerenius, 1998).

An insects' first line of defence against invading organisms is afforded by a hard chitinous armour-like exoskeleton known as the cuticle (Sugumaran, 2001; Asano and Ashida, 2001a). The cuticle is a matrix of protein and carbohydrate secreted from an underlying monolayer of epidermal cells that features the body plan of the insect, covering its entire surface including respiratory trachea, reproductive ducts and anterior and posterior portions of the digestive tract (Asano and Ashida, 2001a; Asano and Ashida, 2001b; Ashida and Brey, 1995). Once considered inert, a view now changing dramatically with the demonstration of its active participation in defence reactions against invading pathogens (Asano and Ashida, 2001a), the cuticle provides a physical barrier between the internal tissues of the insect and the external environment (Ashida and Brey, 1995), protecting the animal from both physical damage and pathogenic attack (Ottaviani, 2005). If the cuticle is circumvented, organisms entering the

soft body of an insect face a highly effective arsenal of cellular (non-targeted) and humoral (targeted) immune defence reactions (Sugumaran, 2001), which have evolved the capacity to discriminate between self and non-self (Ottaviani, 2005; Richman and Kafatos, 1995). Insects do contain proteins with immunoglobulin domains (Söderhäll and Cerenius, 1998), but lack true antibodies (immunoglobulins) and other complicated proteins found in vertebrates, and as such lack an adaptive (or aquired) immune system (Sugumaran, 2001; Müller et al., 1999). They therefore have to rely solely on these cellular and humoral innate immune systems (Müller et al., 1999; Söderhäll and Cerenius, 1998). Despite their segregation into two different groups, there is evidence that the cellular and humoral components of the insect immune response in fact function cooperatively in the destruction and clearing of pathogenic micro-organisms from the insect body (Park et al., 2005; Lavine and Strand, 2002).

Cellular defence reactions are hemocyte mediated responses which include phagocytosis, trapping of bacteria by nodule formation, and encapsulation of larger objects such as parasitoid eggs. In Lepidoptera, most of these cellular responses involve two hemocyte types: granular cells and plasmatocytes (Lavine and Strand, 2002). Phagocytosis, illustrated in Figure 2, is a function performed by hemocytes found circulating the insect soft body. These cells act to efficiently eliminate smaller pathogenic micro-organisms such as bacteria, and also to 'clean up' self dead cells and tissue debris from the hemolymph (Ling and Yu, 2005). Aggregations of bacteria are bound by multiple hemocytes during nodule formation whilst larger parasitic organisms entering the soft body are usually destroyed by encapsulation. Both response types result in the formation of overlapping layers of hemocytes which

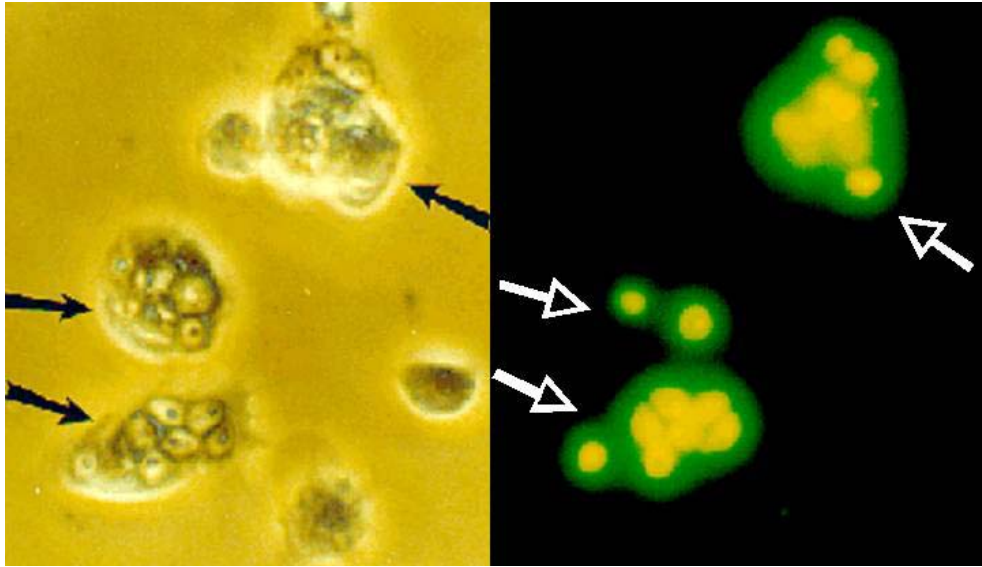


Figure 2: Phagocytosis of fluorescently labelled yeast by hemocytes from the insect *Manduca sexta*. Phase-contrast (left) and fluoresced hemocytes containing multiple engulfed yeast cells are indicated by arrows (Yu, Accessed: 2003.).

surround the target. In some species encapsulation is accompanied by melanisation (Ling and Yu, 2005; Lavine and Strand, 2002) and so the process was subsequently termed melanotic encapsulation, details of which are discussed in Sections 2.2 and 2.5.1. In such instances, oenocytoid hemocytes are likely to be involved as these cells contain the precursors of the melanisation reaction (Lavine and Strand, 2002).

An important factor in insect humoral immunity is the rapid expression of a broad spectrum of potent antimicrobial peptides in response to infection and injury (Yu et al., 2003). These peptides have unique structural properties which enable them to permeate and disrupt target membranes such as those of bacterial and fungal pathogens (Schmidt et al., 2005). Phenoloxidase and its activation pathway are also key elements of the insect humoral immune response (Park et al., 2005; Lee et al., 1999), and discussions on this topic form the remaining sections of this review.

## **2.2 Insect Phenoloxidase**

Despite all that is known about its biological functions, and the sequencing of approximately 55 of its gene sequences from various insect species by 2006, the molecular mechanism and regulation of phenoloxidase (PO) are not well understood because of a lack of any known structure (Decker and Rimke, 1998). This is primarily due to studies being hampered by POs instability, ‘stickiness’, loss of activity during purification, insolubility, inactivation during reaction (Hall et al., 1995a) and spontaneous activation during collection of hemolymph through integumental incisions (Ashida and Brey, 1997). These problems have been overcome by studying the pro-form of the enzyme, prophenoloxidase (PPO). More recently an insect PPO has been expressed in an *E. coli* system which has inducible catalytic activity

(Rajagopal et al., 2005), offering the opportunity to study various aspects of PO activation and improve our understanding of this poorly studied area of insect biology.

### **2.2.1 Phenoloxidase Types and their Functions**

PO is present throughout the life stages of insects (Sugumaran and Nellaiappan, 2000), and circulates throughout the insect body (Sugumaran et al., 2000a). It is found, mostly in hemolymph but also in the cuticle (Kawabata et al., 1995; Fujimoto et al., 1995), as a soluble inactive pro-form or zymogen known as prophenoloxidase (PPO) (Chosa et al., 1997), which is activated as the need arises (Sugumaran, 1998a; Sugumaran and Nellaiappan, 2000). Four types of PO - wound, granular, hemolymph and a laccase-type PO - are present in most insects (Ashida and Brey, 1997) and are named according to their functions. Wound PO (also referred to as cuticular or injury PO), granular PO and laccase-type PO are all located in the cuticle. Hemolymph PO, as the name suggests, is found in the hemocoel (Asano and Ashida, 2001a). Wound PO appears to become activated at sites of cuticular damage, acting to seal off the injury and generate cytotoxic quinones to destroy opportunistic micro-organisms (Asano and Ashida, 2001a) – a mechanism detailed further in Section 2.5.1. Granular PO is involved in pigmentation of the insect body wall (Ashida and Brey, 1997), developing colour patterns by synthesising melanin during the course of normal development (Asano and Ashida, 2001a). PO granules are formed in the epidermal cells and transported to the cuticle in response to a hormonal signal, demonstrating that the enzymatic activity of granular PO is under hormonal control (Ashida and Brey, 1997). Laccase-type PO is important in sclerotisation of newly formed cuticle (Section 2.5.2), and would also appear to be under hormonal control with laccase activity becoming detectable in the cuticle soon after each moulting cycle (Ashida and Brey, 1997). And finally, hemolymph PO, on which most PO

studies have been carried out in the past 10-15 years (Ashida and Brey, 1997), is that responsible for synthesising melanin during the melanisation reaction.

### **2.2.2 Site of Synthesis of Phenoloxidase**

In Lepidopteran insects, all four types of PPO are synthesised constitutively by specialized types of hemocytes called oenocytoids (Müller et al., 1999). However the specific hemocyte type involved can vary amongst arthropods; for example crystal cells and granular cells are responsible for the bulk of PPO synthesis in the fruit fly and crustaceans respectively (Cerenius and Söderhäll, 2004). Studies of hemocytes and epidermal cells at the protein and RNA levels have demonstrated that although PPO protein is present in both hemolymph and cuticle, PPO mRNA can be localised only in hemocytes (Ashida and Brey, 1995; Asano and Ashida, 2001b). Further to this, immunofluorescence labelling of isolated *Manduca sexta* hemocytes detects PPO protein only in oenocytoids (Jiang et al., 1997b). These findings imply all types of PPO are synthesised in oenocytoids and released into the plasma. If destined for the cuticle, PPO will perhaps undergo a post-translational modification and be transported into the epidermal cells for storage until its activity is required (Ashida and Brey, 1997; Söderhäll and Cerenius, 1998; Ashida and Brey, 1995).

### **2.2.3 Structural Features of Phenoloxidase**

PPO preferentially exists as a heterodimer (Asano and Ashida, 2001b), although, depending on ionic strength, it can monomerise or polymerise into multi-subunit molecules (Chase et al., 2000; Jiang et al., 1997b). Each PPO type can also exist in different forms, or isoenzymes, depending on their constituent subunits (Asano and Ashida, 2001a). Hemolymph PPO from the silkworm, *Bombyx mori*, for example, exists in two forms named

PPO-HS and PPO-HF, distinguishable by differences in their mobility in native PAGE. One of the two subunits from each isoenzyme is identical, but the other is different in five amino acids (Asano and Ashida, 2001b).

Each PPO polypeptide (monomer) has a molecular weight between 70 - 90 kDa and contains approximately 685 amino acids, depending on the species from which it originates (Söderhäll and Cerenius, 1998; Sugumaran, 2002; Fujimoto et al., 1995; Jiang et al., 1997a; Jiang et al., 1997b). Amino acid sequence similarity amongst the PPOs of different insect species ranges from 40 to 80% (Hall et al., 1995a). An alignment of a number of insect PPOs (Figure 3) indicates most contain a conserved C-terminal thiol-ester bridge motif (Jiang et al., 1997b), a conserved C-terminal site (Sugumaran, 2002) whose role is unknown, and an N-terminal RF (arginine-phenylalanine) cleavage site for activation (Müller et al., 1999). A second potential cleavage site, with the conserved sequence REE has also been identified further downstream of the RF site (Müller et al., 1999). The amino acid sequences of the two copper binding sites (named CuA and CuB) in each PPO monomer are also conserved amongst insect species, although CuA appears more conserved than CuB (Fujimoto et al., 1995).

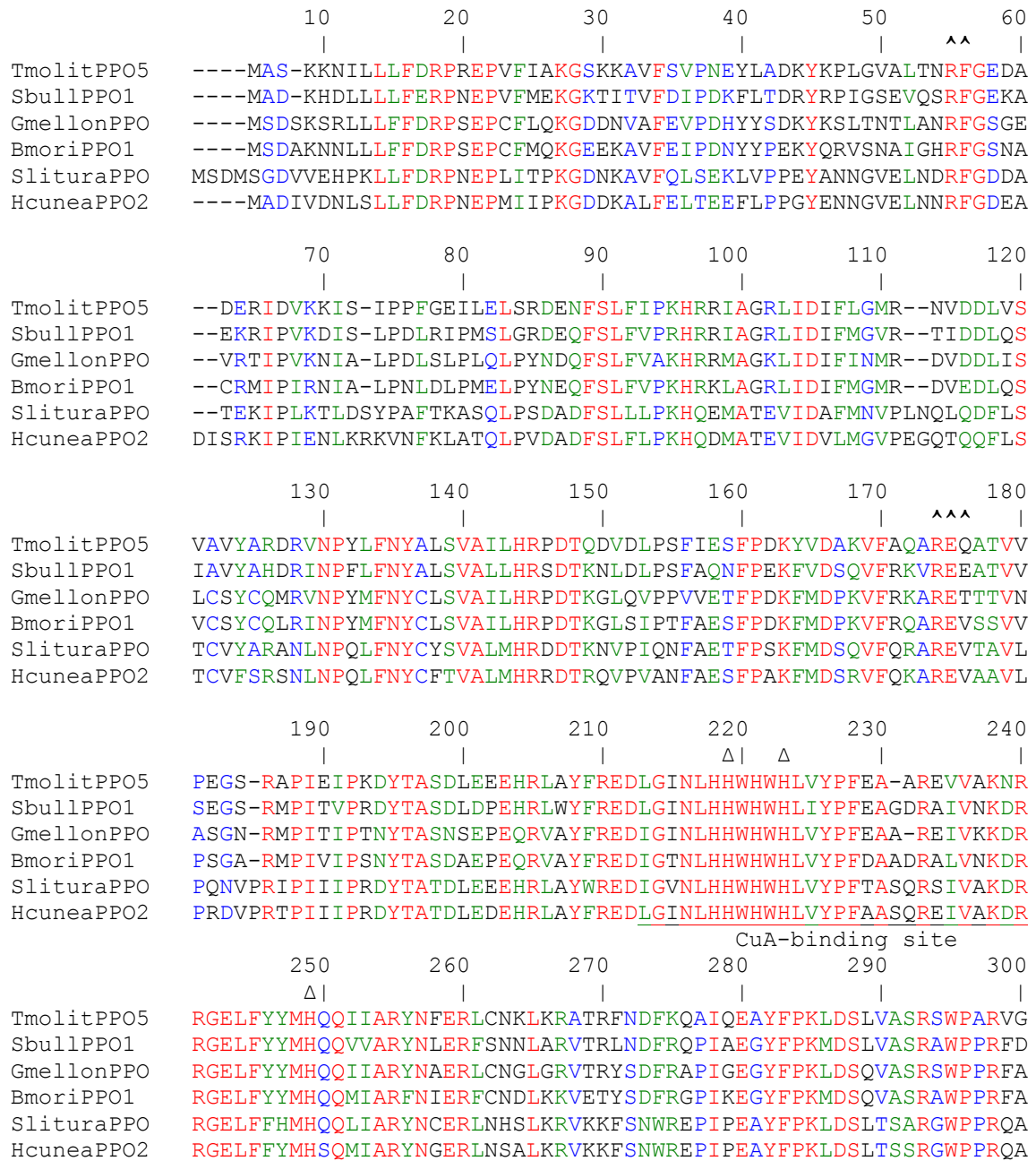


Figure 3: Multiple alignment of amino acid sequences of PPO polypeptides from six insect species. These are *Bombyx mori* PPO1 (BmoriPPO1), *Galleria mellonella* PPO (GmellonPPO), *Sarcophaga bullata* PPO1 (SbullPPO1), *Tenebrio molitor* PPO5 (TmolitPPO5), *Hyphantria cunea* PPO2 (HcuneaPPO2), and *Spodoptera litura* PPO (SlituraPPO). The NCBI Genbank accession numbers for these sequences are NM\_001043870, AF336289, AF161260, AB020738, AF020391 and AY703825 respectively. The two copper-binding sites are singly underlined and labelled, and the 3 conserved histidines in each are highlighted with 'Δ'. The conserved RF and REE cleavage sites are marked with '^', the conserved thiol-ester motif is double underlined '=' and the conserved C-terminal site is underlined with '~'. (Multiple alignment constructed using MULTALIN (pbil) available via the ExpASY online Proteomics Server and the NCBI PubMed nucleotide databank).

|            |   |     |                  |     |     |     |  |
|------------|---|-----|------------------|-----|-----|-----|--|
|            | 310   | 320 | 330              | 340 | 350 | 360 |  |
| TmolitPP05 | NQRLKDLNREVDQIKQDVDDLKRWSDRIYAAIHQGSATDERGRKIELTENEGIDILGNMI          |     |                  |     |     |     |  |
| SbullPP01  | NTKLSDLNRELDQINLDIADLERWRDRIFEAIHQGFVVDESGNRVPLDEQRGIDILGNIL          |     |                  |     |     |     |  |
| GmellonPPO | NTVIRDIDRPVNEIKIDVFQLETWDRFLQAIENMSVMLPNGRQLPLDEETGIDVLGNLM           |     |                  |     |     |     |  |
| Bmoripp01  | GTTIRDLDRPVDQIRSDVSELETWRDRFLQAIENMSVMLPNGRQLPLDEETGIDVLGNLM          |     |                  |     |     |     |  |
| SlituraPPO | NMYWQDLNRPVDGLNITINDMERWRRNVEEAI STGRVTKADGSSAELD----IDTLGNML         |     |                  |     |     |     |  |
| HcuneaPPO2 | NMTWQDLNRPVDGLLVITIDMERWRRNIEEAI STGRVTTADGRTIDLD----IDILGNMM         |     |                  |     |     |     |  |
|            | 370   | 380 | 390              | 400 | 410 | 420 |  |
|            |   | Δ   | Δ                |     |     | Δ   |  |
| TmolitPP05 | ESSILSPNRFTFYGDMHNMGHVFISYVHDPDHRHLESFGVMGDSATAMRDPFYRWHYSYID         |     |                  |     |     |     |  |
| SbullPP01  | ESSITSVNRSLYGDLHNMGHVFISYAHPDHRHLESFGVMGDSATAMRDPVFYRWHAFVD           |     |                  |     |     |     |  |
| GmellonPPO | ESSILSLNRGYGDLHNMGHVFIAYSHDPDHRHLEEYFGVMGDSATAMRDPVFYRWHAYID          |     |                  |     |     |     |  |
| Bmoripp01  | ESSIISRNRPHYGDLHNMGHVFISYSHDPDHRHLEQFGVMGDSATAMRDPVFYRWHAYID          |     |                  |     |     |     |  |
| SlituraPPO | EASILSPNRELYGSIHNNHGSFAAYMHDPTHRYLESFGVIAD EATTMRDPFFYRWHAWID         |     |                  |     |     |     |  |
| HcuneaPPO2 | EASILSPNRELYGSIHNNHGSFSAYMHDLQHRYLESFSVIAD EATTMRDPFFYRWHAYID         |     |                  |     |     |     |  |
|            |   |     | CuB-binding site |     |     |     |  |
|            | 430   | 440 | 450              | 460 | 470 | 480 |  |
| TmolitPP05 | DIFQEYKAT--LPRYTENQLNFPQVTVSKVEVQVQGG SANTLNTFWQQSDVDM SRGMDFQ        |     |                  |     |     |     |  |
| SbullPP01  | DMFQEHKTR--LTSYTLPLQLQYDGITIGGIQVASDGG RPNVLS TFWQQSDVDLSRGMDFV       |     |                  |     |     |     |  |
| GmellonPPO | DIFNLYKSK--LTPYGDSQLDYPGIRVSSISVE-GPAGANRFATQWQQSLVELSQGLDFT          |     |                  |     |     |     |  |
| Bmoripp01  | DIFHLYKYK--LTPYGNDRLDFPNIRVSSVSIE-GGGTPNTLNTLWEQSTVDLGRGMDFT          |     |                  |     |     |     |  |
| SlituraPPO | DTCQRHKESAYVRPYTRSELENPGVQVTSVSVETAGGQPN T LNTFWMSSDVDLSKGLDFS        |     |                  |     |     |     |  |
| HcuneaPPO2 | <u>DTFQRHKESPYVRPYTRSELENPGVRLT</u> SI AIESSNNQMNTLNTFWMSSDVDLSRGLDFS |     |                  |     |     |     |  |
|            | 490   | 500 | 510              | 520 | 530 | 540 |  |
| TmolitPP05 | PRGSVFRFTHLQHQPFTYKITVKNSSNGNRKGTCRIF IAPKLD ERGNPWLYRDQKNMFV         |     |                  |     |     |     |  |
| SbullPP01  | PRGNV FARFTHLQHTPFTYTINVNNSSGAQRFGTVRI FLGPKT DERGQPMLLSDQRLLMI       |     |                  |     |     |     |  |
| GmellonPPO | PRGSVLAKFTHLQHEEFTYVIEVNN TSGQSKMGTFRVFMAPKT DERGQPLAFEDQRRLMI        |     |                  |     |     |     |  |
| Bmoripp01  | PRGSVLARFTHLQHDEYNYVVEVNN TGGSSVMGMFRIF IAPT VDES GKPF SFDEQRKLM I    |     |                  |     |     |     |  |
| SlituraPPO | DRGAVYARFTYLNNRPFYVININN-TGSARRTTVRI FMAPKFDERNLWVSLADQRKMFI          |     |                  |     |     |     |  |
| HcuneaPPO2 | ERRPVYARFTHLNHTPFRYVIKVNNTGSARRTTVRI F IAPKFDERNLTWALADQRKMFI         |     |                  |     |     |     |  |
|            | 550   | 560 | 570              | 580 | 590 | 600 |  |
| TmolitPP05 | ELDKFTVNLKQGQNNITRASSQSSVTIPFERTFRNLDLNR PQGG-EELAQFNFCGCGWTQ         |     |                  |     |     |     |  |
| SbullPP01  | ELDKFVVALNPGQNTIRRRSTDSSVTIPFERTFRNLDANRPAAGSAEELEFNFCGCGWPQ          |     |                  |     |     |     |  |
| GmellonPPO | ELDKFTRGLKPGNNTIRQRSLDSSVTIPFERTFRNQANRPGDPGSATAAEFDFCGCGWPH          |     |                  |     |     |     |  |
| Bmoripp01  | ELDKFSQGVKPGNNTIRRKSIDSSVTIPYERTFRNQADRPADPGTAGAAEFDFCGCGWPH          |     |                  |     |     |     |  |
| SlituraPPO | EMDRFVQPLNAGQNTITRNSTDSSVTIPFEQTFRDLSPQGS DPRRTSLAEFNFCGCGWPQ         |     |                  |     |     |     |  |
| HcuneaPPO2 | EMDIFVTPLNAGENTITRLSTQSSVTIPFEQTFRDLSPQSGDPRRTNLAAFNFCGCGWPQ          |     |                  |     |     |     |  |

Figure 3: Continued

```

          610      620      630      640      650      660
          |        |        |        |        |        |
TmolitPPO5  HMLIPKGTPEGMPQCLFVMISNYEDDKVNQSTEG--VCNDAGSYCGIKDKLYPDRRSMGY
SbullPPO1  HMLIPKGLPEGMRCELFVMISNYEDDRVDQQLVG--ACSDAASFCGVRDRLYPDRRPMGY
GmellonPPO HMLIPKGTEQGYPVVLYVMVSDNNADKIEQDTVG--ACNDAASYCGLRDRKYPDKRHMGF
BmoripPO1  HMLVPKGTTQGYPMVLFVMVSNWNDDRVEQDLVG--LCNDAASYCGIRDRKYPDRRAMGF
SlituraPPO HMLVPKGTEAGAAYQLFVMLSNYDLSVDQPGGNQLSCVEASSFCGLKDKKYPDRRSMGF
HcuneaPPO2 HMLVPKGNEAGVTYQFFVMLSNYELDRIEESSNVQSNCVEASSFCGLRDRKYPDRRAMGF
==                                               ~~~~~~

          670      680      690      700
          |        |        |        |
TmolitPPO5  PFDRMPRNGVDTLQQFLTSNMRVQDVTIKFTNRTVVRPKSRN-----
SbullPPO1  PFDRLPRAGADRLVN-----
GmellonPPO PFDRRS--EARNLTDFLKPNMATRDCTIKFTDAIREGTQRQ-----
BmoripPO1  PFDRPAP-AATTLSDFLRPNMAVRDCIVRFTDGTRQRGQGG-----
SlituraPPO PFDRPSS-IATNIEDFILPNMALQDITIRLSNVVEQNPRNPPSAV--
HcuneaPPO2 PFDRPST-TAANIEDFILPNMGLQDITIRLRNETIPNPRNPVTQTPO
~~~~~

```

Figure 3: Continued

Interestingly insect PPO polypeptides lack the hydrophobic N-terminal signal sequence required for secretion, and this has raised a debate over how PPO, synthesised in hemocytes, arises in the hemolymph plasma (Ashida and Brey, 1997). Earlier discussion (Section 2.2.2) pointed out that PPO is synthesised in particular subsets of hemocytes depending on species, with the oenocytoid hemocytes being responsible in Lepidoptera insects. Ultra-structurally, oenocytes are non-typical in that they are almost entirely composed of ribosomes and mitochondria, with no evident rough endoplasmic reticulum. Therefore it is now generally assumed that the cell membranes of oenocytoid hemocytes, rupture to release PPO, although there is no experimental evidence to prove this (Ashida and Brey, 1997; Cerenius and Söderhäll, 2004; Kawabata et al., 1995).

### **2.3 Phenoloxidase is a Type-3 Copper Protein Similar to Arthropod Hemocyanin**

PO is a bi-functional enzyme possessing both tyrosinase (EC 1.14.18.1) and *o*-diphenoloxidase (EC 1.10.3.1) activity (Hall et al., 1995a; Jiang et al., 1997a), catalysing the incorporation of oxygen from molecular O<sub>2</sub> (Solomon et al., 1996) into phenolic molecules, in a two step reaction (Decker and Terwilliger, 2000) that generates reactive quinonoid compounds: firstly the *ortho*-hydroxylation of monophenols into *o*-diphenols and secondly the oxidation of *o*-diphenols into *o*-quinones (Ashida and Brey, 1997) (Kawabata et al., 1995).

These functions are attributed to PPOs oxygen-binding binuclear dicopper active site, which contains two copper atoms (CuA and CuB) each coordinated by three histidine residues; this is known as a Type-3 copper centre (Decker and Tucek, 2000). The peptide sequences of each copper binding site have been found to be similar, not only amongst those insect PPOs so far sequenced, but also with the dicopper centers of arthropod hemocyanin (Hc) (Ashida and Brey, 1997), another Type-3 copper oxygen-binding protein. It has been hypothesised, therefore, that during catalysis molecular oxygen bridges the two copper atoms in PO in a side-on configuration as in arthropod Hc (Figure 4).

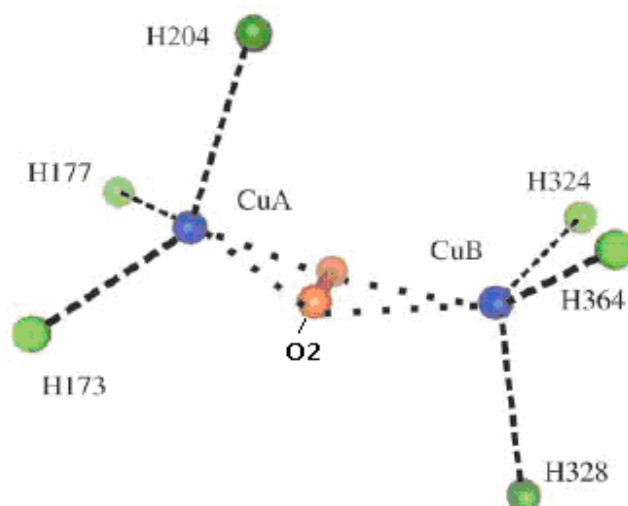


Figure 4: Dioxygen bridges the two copper atoms of the *Limulus polyphemus* hemocyanin Type-3 copper oxygen-binding site in a side-on configuration. Due to the identity between the copper-binding site sequences of insect prophenoloxidase and arthropod hemocyanin, it is likely this arrangement exists in phenoloxidase during the incorporation of oxygen into phenolic compounds (taken and adapted from (Decker and Terwilliger, 2000)).

The sequence alignment in Figure 5 demonstrates identities and similarities between the residues of the Hc and PPO copper binding sites and highlights the perfect alignment of the copper-coordinating histidine residues which are conserved throughout. Nevertheless, it should be noted that full length sequence similarity between PO and Hc is < 30%

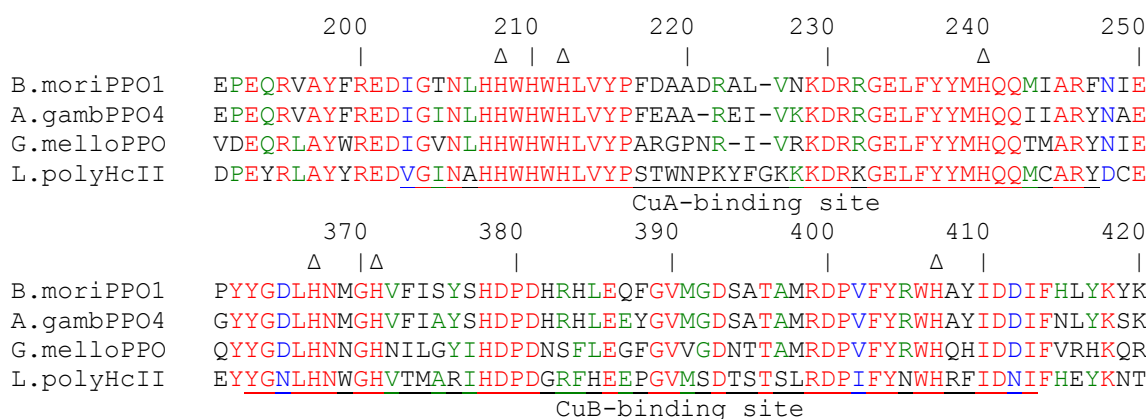


Figure 5: Multiple alignment of amino acid sequences of the CuA (top) and CuB binding sites of prophenoloxidase from three insect species, *Bombyx mori* PPO1 (B.moriPPO1), *Anopheles gambiae* PPO4 (A.gambPPO4) and *Galleria mellonella* PPO (G.melloPPO), and hemocyanin subunit II from *Limulus polyphemus* (L.polyHcII). The NCBI accession numbers for these sequences are NM\_001043870, AJ010193, AF336289 and AM260213 respectively. CuA and CuB binding sites are singly underlined and labelled, and the conserved coordinating histidines are highlighted by 'Δ'. Alignment constructed as in Figure 3.

(Decker, 2005). Arthropod PO and Hc also share several physico-chemical properties (Decker and Terwilliger, 2000) - both are extra-cellular proteins that exhibit PO activity after proteolysis or treatment with detergents, and both bind dioxygen at their dicopper centers (Decker et al., 2001; Nagai and Kawabata, 2000). As such, although the structure of an insect PPO has not yet been elucidated, its dicopper active site is probably similar to the dicopper center of the well characterised Hc from the ancient chelicerate *Limulus polyphemus*, (Atlantic horseshoe crab) (Figure 6) (Ashida and Brey, 1997; Decker and Terwilliger, 2000).

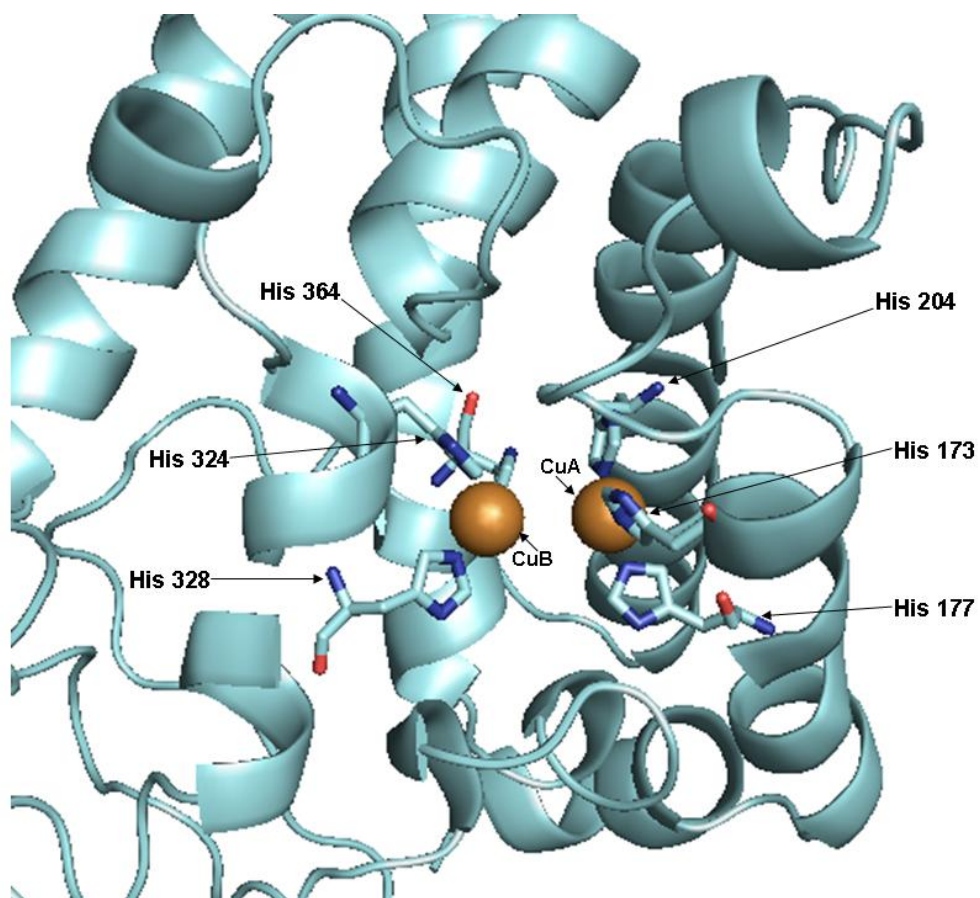


Figure 6: The dicopper oxygen-binding site from subunit II of *Limulus polyphemus* hemocyanin. CuA and CuB and their coordinating histidines are labelled. Image generated using file 1LLA from the protein data bank (PDB) and Pymol molecular graphics software.

These similarities suggest a common evolutionary ancestor for arthropod PPO and Hc. Hc is speculated to have evolved from an ancestral mono-copper protein by gene duplication and subsequent gene fusion. PPO is thought to have evolved from two separate mono-copper proteins by a single gene fusion step (Kawabata et al., 1995). This perhaps explains why there is greater sequence similarity between the CuB binding site, compared to the CuA binding site, of arthropod PPO and Hc (Ashida and Brey, 1997). Despite the similarities in dicopper center structure and activation of PPO activity, when one compares arthropod Hc with PPO, it becomes apparent that they are very different proteins in respect of size, quaternary structure, native physiological function and distribution among subphyla (Decker and Tucek, 2000; Decker and Terwilliger, 2000). Arthropod Hc is characterised by a very complex quaternary structure composed of multiple kidney-shaped subunit types, each with three domains, which form a basic hexamer (Decker and Terwilliger, 2000). These hexamers, depending on the species, can then form high molecular mass aggregates ranging from 1x6mers to 8x6mers (Decker and Terwilliger, 2000; Zlateva et al., 1996). PPO on the other hand most commonly occurs as a dimer of two subunit types, although it is known to form monomers, trimers or tetramers under specific conditions (Decker and Tucek, 2000; Chase et al., 2000). Under normal physiological conditions, Hc functions as an oxygen transport protein that can reversibly bind dioxygen without modifying it (Nagai and Kawabata, 2000) and has been found in crustaceans and chelicerates (Decker and Tucek, 2000), and more recently in an insect species, *Perla marginata* (Stonefly) (Lee et al., 2004). PPO however has been found only in crustaceans and insects (Decker and Tucek, 2000), and when active, utilises one of the oxygen atoms from the bound dioxygen to catalyse important immune defence reactions (Decker and Terwilliger, 2000).

In the absence of an insect PPO structure, the remarkable similarities between arthropod PPO and Hc justify the use of the structure of arthropod Hc as a model for experiments aimed at determining the secondary, tertiary and quaternary structure of PPO, understanding which regions of the PPO protein are important in the formation of multimers, and in site-directed mutagenesis studies designed to analyse PPO's catalytic and binding sites (Jiang et al., 1997b).

## **2.4 The Prophenoloxidase Activation Cascade**

### **2.4.1 Introduction.**

PPO can be activated directly, *in vitro*, by proteolytic cleavage of the proenzyme into its active form, or by adding specific detergents (the cationic detergent cetyl pyridinium chloride activates PPO most specifically (Sugumaran, 1998b)), phospholipids or fatty acids (Chosa et al., 1997; Sugumaran, 2002) which are thought to cause a conformational change in the proenzyme exposing the active site and eliciting PO activity without cleaving any peptide bond (Sugumaran, 1998b; Sugumaran, 2001). Phospholipid activation perhaps has physiological relevance, since during immune challenge the insect phospholipase pathway is also activated. This pathway is involved in triggering the immune response, but more importantly it generates phospholipids and lysophospholipids which may provide the insect with an alternative PPO activation mechanism (Sugumaran, 2002).

*In vivo* activation of PPO, generally referred to as the PPO activation cascade, is a system triggered by invasion of the insect's soft body by foreign organisms (Kopáček et al., 1995). The components of this cascade may already be present in the hemolymph or released from

hemocytes or the fat body when pathogens or parasites are encountered (Jiang et al., 2003). The only identified natural activator of PPO in insects is a trypsin-like serine protease known as the PPO activating enzyme (PPAE; sometimes referred to as PPO activating proteinase or PAP) (Jiang et al., 1997a; Chosa et al., 1997), which is itself present as a zymogen (proPPAE) (Ashida and Brey, 1997) secreted from hemocytes and activated by another as yet uncharacterised serine protease that also exists in a proform (Sugumaran, 2001). The little understood PPO cascade (a proposed outline is illustrated Figure 7) was thus named since the activation of subsequent serine protease zymogens following an initial trigger, culminates in activation of PPO.

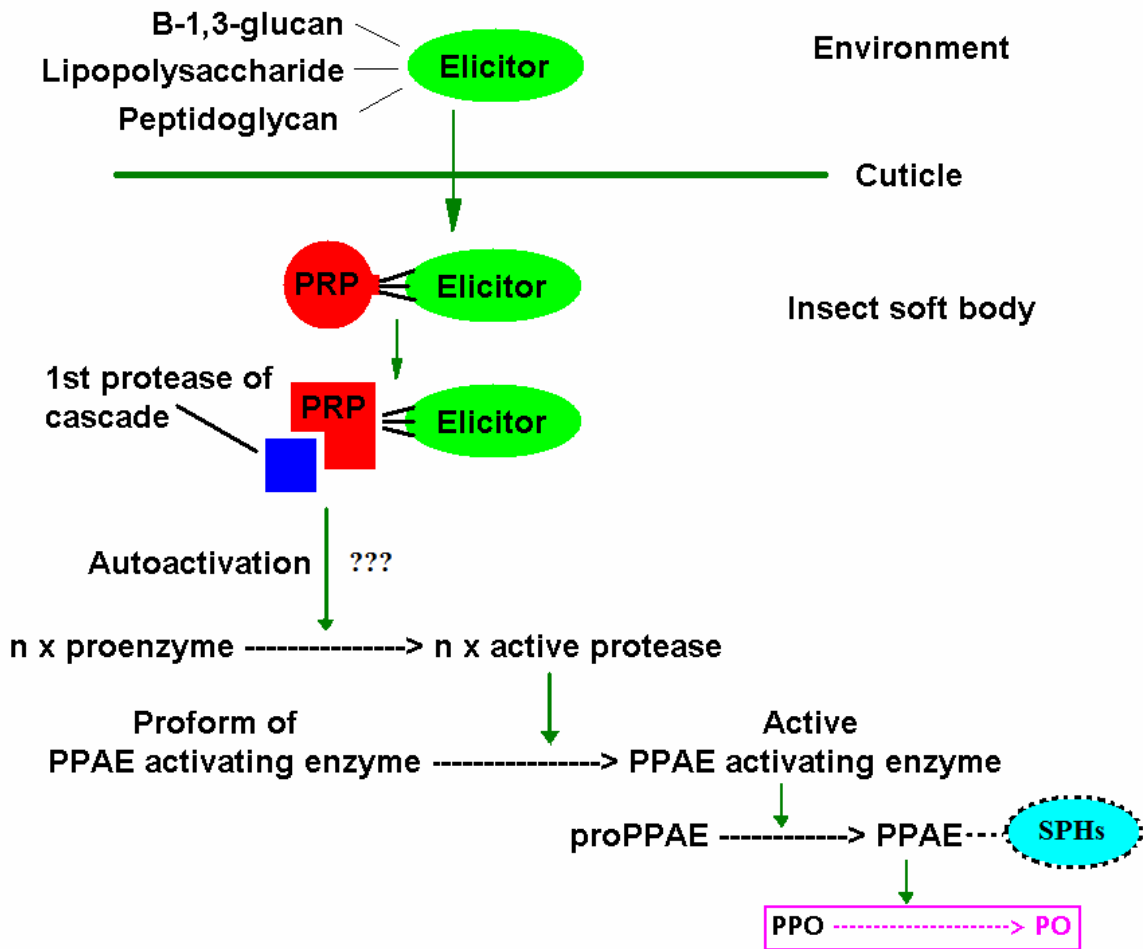


Figure 7: Proposed overview of the insect prophenoloxidase (PPO) activation cascade. Polysaccharides present at the surface of micro-organisms and other compounds released upon self-tissue damage, are bound by pattern recognition proteins (PRPs) in the insect soft body. It has been hypothesised that binding of PRP and elicitor causes a conformational change in the PRP allowing its interaction with the first protease of the PPO cascade, perhaps resulting in its auto-activation. Subsequent activation of a cascade of proteases culminates in the activation of phenoloxidase (PO). PO is activated from PPO by the prophenoloxidase activating enzyme (PPAAE) which may or may not, depending on species, require to be associated with one or more serine protease homologues (SPHs) to perform this function efficiently. 'n' represents an unknown number of proenzymes/active proteases. Adapted from (Cerenius and Söderhäll, 2004).

#### **2.4.2 Pattern Recognition Proteins.**

The most widely studied and understood elicitors of the PPO cascade are foreign pattern molecules such as  $\beta$ -1,3-glucan, peptidoglycan and lipopolysaccharide (LPS) (Kopáček and Sugumaran, 1998), which are cell wall components of fungi, Gram-positive bacteria and Gram-negative bacteria respectively (Park et al., 2005). One of the links between these elicitors and activation of the first protease in the cascade is the recognition of non-self molecules, termed pattern recognition. A group of proteins known as pattern recognition proteins (PRPs) perform this function (Figure 7) and can be either humoral or cellular in form (Yu et al., 2002). As insects lack true antibodies (acquired immune system), and these PRPs do not possess the specificity of antibodies, they function instead by recognising and binding to different classes of polysaccharides, such as those mentioned above, which are not found in the host (Yu et al., 2002). Humoral PRPs function as 'biosensors' to detect non-self molecular patterns (Ma and Kanost, 2000) and in their bound form relay the infection signal by binding to a surface protein of immune cells which will direct the appropriate immune responses (Söderhäll and Cerenius, 1998). Less is known of the cellular PRPs, although a search of the *Drosophila* genome database has revealed several genes with sequence similarity to humoral PRPs that possess transmembrane domains, suggesting they may be cellular PRPs. Nonetheless, they are understood to function similarly to humoral PRPs, except that they are found at cell surfaces and thus bind non-self molecules directly to immune-responsive cells (Lavine and Strand, 2002).

There are a number of humoral PRPs in insects, and each type recognizes and binds a particular class of polysaccharide. In the Silkworm, *Bombyx mori*, for example, only two

classes of polysaccharide have been identified which can initiate the PPO cascade,  $\beta$ -1,3-glucans and peptidoglycans (Ashida and Brey, 1997). PRPs that exist separately in the hemolymph have been shown to interact with either  $\beta$ -1,3-glucan or peptidoglycan, and were named  $\beta$ -1,3-glucan recognition protein ( $\beta$ GRP – 62 kDa) and peptidoglycan recognition protein (PGRP – 19 kDa) respectively (Ashida and Brey, 1997).  $\beta$ GRP and PGRP demonstrate high levels of specificity in *B. mori*, with activation of the PPO cascade observed only on  $\beta$ GRP binding with glucans possessing  $\beta$ -1,3-linkages or PGRP binding peptidoglycans with a glycan portion larger than two repeating units (Ashida and Brey, 1997). *Manduca sexta* (the Tobacco Hornworm), however, has been shown to possess four different classes of PRPs that are involved in immune responses. These are  $\beta$ GRP and PGRP as in *B. mori*, as well as hemolin and immulectins (C-type lectins) (Yu et al., 2002). An interesting point to note here is that the PRPs from *M. sexta* display a level of redundancy in their specificity i.e. they can recognize and bind more than one class of microbial polysaccharide (Table 1).

Table 1: Pattern recognition proteins found in the hemolymph of the tobacco hornworm, *Manduca sexta*. A level of redundancy is displayed in the binding specificities of these PRPs, with some recognising more than one microbial polysaccharide (constructed using data from (Yu et al., 2002)).

| Protein     | Molecular Mass (kDa) | Microbial Polysaccharide Recognised        |
|-------------|----------------------|--|
| $\beta$ GRP | 53/54                | $\beta$ -1,3-glucans and Lipoteichoic acid |
| PGRP        | 19                   | Peptidoglycan                              |
| Hemolin     | 48                   | LPS and lipoteichoic acid                  |
| Immulectins | 35/36                | LPS and other unidentified polysaccharides |

It must be emphasised that it is unlikely that insects possess an array of PRPs each tailored to recognise only a particular group of non-self molecular patterns. As a range of targets such as protozoans, nematodes, parasitoids and damaged self-tissues elicit similar immune responses,

it seems reasonable to assume that insect PRPs have redundancy in their binding properties, enabling them to recognise and bind a variety of molecules not normally found in the hemocoel (Lavine and Strand, 2002).

As yet it is not understood how the signal produced by the binding of PRPs to elicitors is transduced to trigger an immune response in insects. It is most likely, however, that there are a number of different signalling pathways, each of which induce a different type of immune response e.g. phagocytosis or melanin synthesis. It has been hypothesised that the bound polysaccharides cause a conformational change in the PRP allowing it to interact with the first protease of the PPO cascade, perhaps leading to its auto-activation (Yu et al., 2002). Suggestions from research of cell-mediated immunity in the Medfly, *Ceratitis capitata*, imply that the change in conformation of humoral or cellular PRPs in response to microbial infection causes induction of a mitogen activated protein (MAP) kinase pathway in hemocytes. The signal is thought to be transduced from elicitor-bound PRPs either directly, as in the case of cellular PRPs, or via binding of humoral PRPs to a hemocyte cell surface protein. The MAP kinase pathway is then thought to regulate subsequent immune responses. One example may be the regulation of PPAE secretion from hemocytes which is a prerequisite to the activation of PPO (Mavrouli et al., 2005; Foukas et al., 1998).

### **2.4.3 PPAE Activation and its Activation of Phenoloxidase.**

PPAE is a serine protease responsible for the activation of PO from its zymogen, and is the earliest component of the enzymatic PPO cascade to have had any characterisation studies performed so far. It is synthesized constitutively by circulating hemocytes, and its secretion, which is suggested to be regulated by a MAP kinase pathway, increases in response to the

presence of LPS or bacterial cells (Mavrouli et al., 2005; Foukas et al., 1998). It exists primarily as a zymogen, activated by another as yet uncharacterised serine protease by proteolysis at a conserved RI/KI site (Sugumaran, 2001). Very little is currently known of the exact number of proteases which may be involved in the PPO cascade (Yu et al., 2003).

Since 1998, PPAEs have been purified and cloned from *Bombyx mori*, *Holotrichia diomphalia*, *Pacifastacus leniusculus* and *Manduca sexta* (Zou et al., 2005). In fact, three *M. sexta* PPAEs have been purified, one of which, PAP-1 (PPO activating protease-1), has been found to be expressed constitutively in the insect fat body during all larval, pupal and adult phases, although to varying degrees. During periods of immune challenge, PAP-1 expression levels increase markedly in this tissue, as well as in hemocytes. However, PAP-1 mRNA is detectable during different stages, in differing quantities, in numerous tissue types including the trachea, nerve tissue, integument, hemocytes and midgut of the *M. sexta* larval and adult phases. These findings suggest that the PAP-1 gene (and possibly all other PPAE genes) is an immune-responsive gene, whilst perhaps also under hormonal control (Zou et al., 2005; Jiang et al., 2003).

All PPAEs belong to the clip-domain serine protease family, and proPPAE contains one or two amino-terminal clip-domains connected to a carboxyl-terminus catalytic serine protease domain (Sugumaran, 2001). It is postulated that the clip domain has a regulatory function or may control the interactions between PPAE and its substrate and/or other proteins (Jiang et al., 1998). ProPPAE has a molecular weight of 40 kDa which, after cleavage at its conserved RI/KI proteolytic activation site, is reduced to the 28 kDa PPAE active form (Sugumaran, 2001). PPAEs purified from *M. sexta* larvae have each been found to require two clip-domain

serine protease homologues (SPHs) in order to successfully activate PO, which in turn also require cleavage to elicit their intrinsic function (Wang and Jiang, 2004; Zou et al., 2005). SPHs are similar in structure to PPAEs with the exception that their catalytic domain active site contains a glycine residue in place of a serine (Jiang et al., 2003). PPAE associates with these SPHs, and also the C-type lectin immulectin-2, to form a ternary complex that hydrolyses the peptide bond at the carbonyl side of arginine-51 in the sequence –Asn-Arg-Phe-Gly- (conserved RF site) of both subunits of PPO (Müller et al., 1999). Immulectin-2 is in fact a pattern recognition protein, and its association with PPAE via the SPHs may act to ensure localised activation of PPO to sites of infection (Jiang et al., 2003) (Ling and Yu, 2005). Furthermore, the clip domain of the crayfish PPAE interacts with Gram-negative bacteria exerting an antibacterial function and also possibly acting to anchor the PPAE catalytic domain onto the bacterial surface where it will activate PPO, thus localising PO activity to the area it is required (Jiang et al., 2003). In the absence of its cofactor, *M. sexta* PPAE still cleaves PPO on the carbonyl side of Arg-51, however, the product is catalytically inactive. In contrast *B. mori* PPAE does not require such cofactors to activate PPO (Wang and Jiang, 2004).

Removal of the N-terminal segment at the conserved RF site converts inactive PPO to active PO with a concurrent reduction in the molecular mass of each polypeptide by about 6 kDa (Figure 8) (Kawabata et al., 1995). A second potential cleavage site, with the conserved sequence REE, has also been identified in PPO from a number of insect species (see alignment in Figure 3), suggesting that there may be more than one PPAE responsible for activating PPO (Müller et al., 1999). The action of PPAE thus activates the endogenous PO

activity of PPO, enabling this enzyme to participate in various physiologically important reactions.

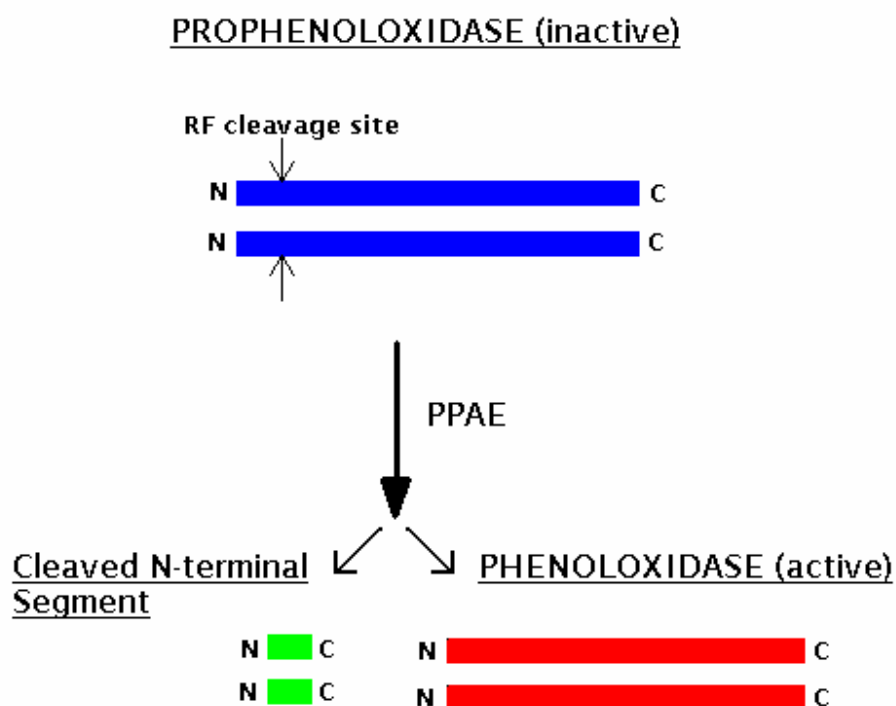


Figure 8: Proteolytic cleavage of PPO by PPAAE at the conserved arginine-phenylalanine (RF) activation site. PPAAE cleaves the bond at the carbonyl side of the arginine in both subunits of PPO, converting it to its active form – PO. Removal of this N-terminal segment causes a reduction in the molecular mass of PPO by approximately 6 kDa (Müller et al., 1999; Kawabata et al., 1995).

## **2.5 Physiological Roles of Active Phenoloxidase in Insects**

### **2.5.1 Melanisation – Melanotic Encapsulation and Wound Healing**

When a foreign organism which is too large to be phagocytosed, e.g. a nematode or parasitoid egg, enters the soft body of an insect, a process known as cellular melanotic encapsulation takes place (Sugumaran and Nellaiappan, 2000). Melanotic encapsulation is a well regulated, complex yet common immune response in insects (Richman and Kafatos, 1995). Rapid deposition of a layer of melanin pigment around the foreign body (Sugumaran et al., 2000b) occurs through the action of many plasma proteins, including those involved in pattern recognition and the phenoloxidase activation cascade (Section 2.4) (Ling and Yu, 2005). Also required is the coordinated effort of hemocytes to form a capsule in order that a physical barrier is erected between self and non-self (Ling and Yu, 2005; Sugumaran, 1998a; Sugumaran et al., 2000a). This is an effective means of arresting the growth of, and limiting the damage caused by, invading pathogens (Sugumaran and Nellaiappan, 2000).

Melanin is one of the most widely distributed and visible of the biological pigments, and is an important, insoluble, phenolic biopolymer found in the hair, feathers and skin of animals as well as in plants, fungi and some bacteria (Sugumaran et al., 2000a; Hall et al., 1995a; Decker et al., 2001). Most melanins appear to be mixed polymers based on indoles but also contain variable quantities of other pre-indolic products from earlier steps in its synthetic pathway, making many regions of the polymer unpredictable (Riley, 1997).

In insects, melanin synthesis (Figure 9) is initiated by the product of the PPO cascade - the activity of PO (Sugumaran and Nelliappan, 2000). During melanin synthesis, also called the melanisation reaction, PO hydroxylates the monophenolic compound tyrosine, to the diphenol dopa (3,4-dihydroxyphenylalanine) (Shiao et al., 2001), and oxidizes this dopa to dopaquinone (Lee and Anstee, 1995). Dopaquinone rapidly transforms non-enzymatically by cyclisation into dopachrome (Zou et al., 2005) which is subsequently acted upon by dopachrome isomerase (a second enzyme involved in the melanisation reaction) to produce 5,6-dihydroxyindoles. Further oxidation and polymerisation of these indoles produces melanin pigment (Sugumaran and Nelliappan, 2000; Zou et al., 2005). The reactive electrophilic quinone intermediates of the melanisation reaction are proposed to have deleterious effects on cellular macromolecules (Sugumaran et al., 2000a), and hence would be highly cytotoxic to foreign organisms possibly functioning to kill them (Jiang et al., 1997a).

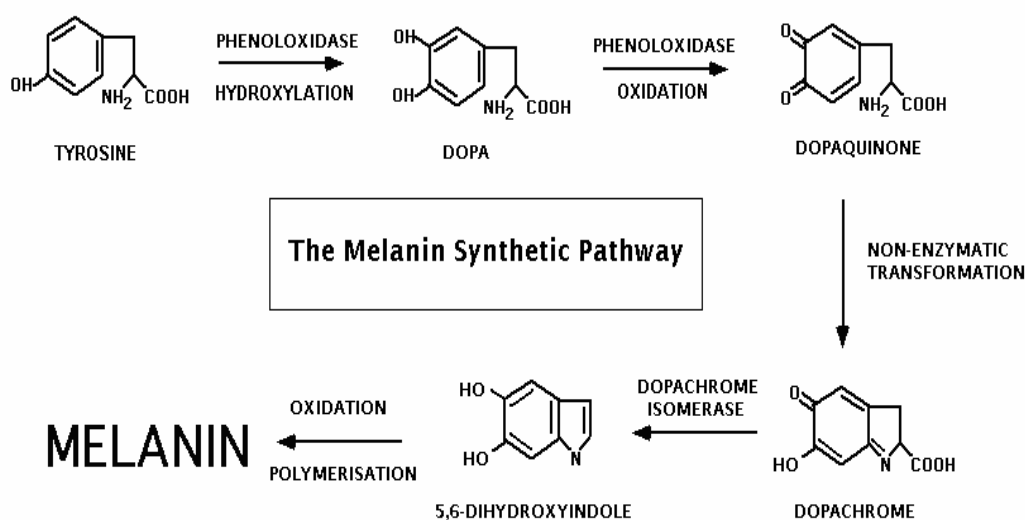


Figure 9: Steps of the melanin synthetic pathway in insects. Phenoloxidase hydroxylates tyrosine to dopa and immediately oxidises the dopa to dopaquinone. Dopaquinone then non-enzymatically transforms into dopachrome which is converted to 5,6-dihydroxyindole. Further oxidation and polymerization steps result in the formation of melanin pigment (adapted from (Blois, 1978)).

Whilst there is overwhelming evidence to support the importance of melanin in innate immunity, there is currently very little evidence to allow the role of melanin and its quinonoid precursors to be accurately defined (Nappi and Christensen, 2005). What is understood however, is that the cytotoxicity of the products of melanogenesis requires that the process must be well regulated, localised and target specific, to avoid fatal systemic damage to the host organism.

In a manner similar to melanotic encapsulation, wound healing in the insect cuticle requires active PO for the synthesis and subsequent mass deposition of melanin and its intermediates at the wound site. Along with hemolymph clotting and hemocyte aggregation (Lavine and Strand, 2002) this creates an impervious scab (Decker and Terwilliger, 2000) which prevents continuous loss of hemolymph and blocks the entry of opportunistically invading pathogens (Hall et al., 1995a). It was initially suggested that melanin and cytotoxic quinonoid compounds, generated as a result of the melanisation reaction, may act as a second line of defence at the wound site, killing any such opportunistic microorganisms (Sugumaran et al., 2000b; Sugumaran, 2001). However, since this time, investigations of clot formation in native and mutant forms of *Drosophila melanogaster* and *Galleria mellonella* larvae (Bidla et al., 2005) infer that the action of PO has no effect on bacterial survival at clotting wound sites, and may therefore function only to generate the cross-linking agents to solidify the clot and seal the wound.

### **2.5.2 Sclerotisation**

Due to the rigid nature of the insect exoskeleton, periodical shedding of old cuticle and development of a new larger cuticle is necessary to allow for normal growth and

development. Freshly formed cuticle is soft however, and leaves the insect exposed and vulnerable. In addition to its critical role in cellular melanotic encapsulation and wound healing, PO is also important in another physiologically crucial process in insects known as cuticular sclerotisation (Kopáček and Sugumaran, 1998). Sclerotisation of the cuticle is a vital process essential for the survival of all insects (Saul and Sugumaran, 1988), with arrest or even delay of this process having detrimental consequences (Sugumaran, 2002). The sclerotisation reaction (Figure 10) is responsible for hardening the newly ecdysed larval and adult cuticle, egg cases and pupal cases of most insects (Saul and Sugumaran, 1988). The catecholamine precursors of the sclerotisation reaction, N-acetyldopamine (NADA) and N- $\beta$ -alanyldopamine (NBAD), are stored in large amounts in the insect hemolymph. PO is important during cuticular hardening as it oxidises these precursor molecules into their corresponding quinones (Sugumaran et al., 2000b; Sugumaran, 2002).

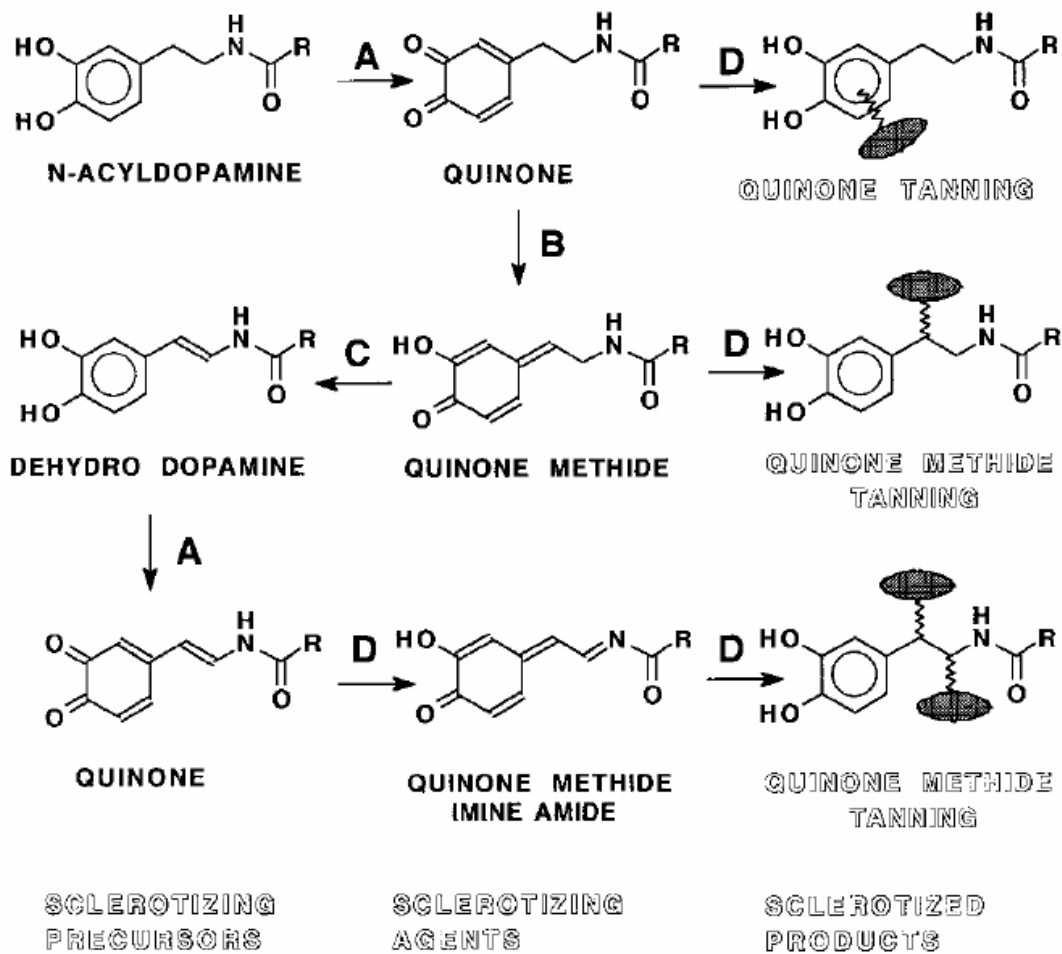


Figure 10: Mechanism for sclerotisation of the insect cuticle. The lettered arrows represent a reaction catalysed by phenoloxidase (A), quinone isomerase (B) or quinone methide isomerase (C). D highlights non-enzymatic reactions (Sugumaran et al., 2000b). Quinones rapidly form adducts with the amino acids present in cuticular structural proteins, which ensures the hardening process. Quinone methides also perform this chemical process, but due to their more reactive nature, they also form adducts with the side chain hydroxyl groups of chitin polymer in the cuticle. Quinone methide imine amides go one step further and can perform this function whilst also acting as the cross-linking agents necessary for complete hardening of the newly ecdysed cuticle (Sugumaran, 2002).

Quinones are either directly involved in quinone tanning (one of the mechanisms of cuticular hardening in insects (Chase et al., 2000)), or further metabolised by a second enzyme involved in the sclerotisation reaction, quinone isomerase, which converts long-lived N-acyldopamine quinones to short-lived quinone methides (Sugumaran et al., 2000b). Once again, these quinone methides either participate in a second mechanism of tanning, quinone methide sclerotisation (Chase et al., 2000), or serve as substrates for the third sclerotising enzyme - quinone methide isomerase (Hall et al., 1995a). Quinone methide isomerase synthesises 1,2-dehydro-N-acyldopamines. These are further oxidised by PO to ultimately generate quinone methide imine amides that serve as bifunctional cross-linking agents (Sugumaran et al., 2000b). The reactive quinones thus formed are necessary for adduct formation and the cross-linking of cuticular structural proteins and chitin rendering them insoluble (Kopáček and Sugumaran, 1998; Sugumaran, 2002; Sugumaran and Nellaiappan, 2000). The hard cuticle that results performs a number of functions including acting as a physical barrier to the environment whilst providing waterproofing, points of muscle attachment and sites of waste disposal (Sugumaran, 2002).

## **2.6 Control of Phenoloxidase Activity *in vivo***

### **2.6.1 Introduction**

It has already been established that active PO participates in steps of pathways, such as melanin synthesis, which generate cytotoxic quinonoid compounds, toxic not only to invading micro-organisms but also to the cells of the host insect i.e. self-cells (Sugumaran et al., 2000a; Yu et al., 2003). It thus seems that systemic activation of the PPO cascade would

be deleterious to the insect, so it is reasonable to assume factors/biochemical mechanisms are present in insects to regulate the activity of PO (Ashida and Brey, 1997). There are indeed numerous control mechanisms of the PPO cascade (Table 2) functioning either prior to, or following, the activation of PPO. Some of the control mechanisms utilised before activation of PPO, i.e. protease mediated activation of PPO and preservation of PO and its' activating

Table 2: Examples of the mechanisms insects utilise for the control of phenoloxidase activity. Such mechanisms function to regulate production of cytotoxic quinones that are by-products of the reactions catalysed by phenoloxidase (Sugumaran, 2001).

| Control Mechanisms of the PPO Cascade                             |   |
|---|---|
| Before PPO activation   | After PPO activation  |
| Preservation of the enzyme in its inactive proform (PPO).         | Protection of substrates against PO action.   |
| Protease mediated activation of PPO.                              | Self inactivation of PO.  |
| Preservation of PPAAE in its inactive proform (proPPAAE).         | Metabolon formation – multi-enzyme complexes with each enzyme catalysing steps in a particular reaction pathway             |
| Use of proteinase inhibitors to control the activating proteases. | Localisation of enzyme activity by<br>- complex formation with accessory proteins<br>and/or – aggregation/stickiness of PO. |
| Compartmentalisation of enzymes and substrates.                   | Use of specific PO inhibitors (Serpins).  |

enzyme, PPAAE, in an inactive form, were discussed earlier. Here, however, we will concentrate on two post-activation control mechanisms: the formation of multi-enzyme complexes known as metabolons and localisation of PO activity to the surfaces of hemocytes/pathogens during melanisation, via protein-protein interactions.

## 2.6.2 Metabolon Formation

Active PO appears to carry out multiple tasks, and in order to perform such diverse functions, this enzyme employs the unique strategy of forming specific complexes called metabolons (Sugumaran, 1998a). Metabolons are composed of enzymes that catalyse sequential metabolic transformations such as those in the melanotic and sclerotinogenic pathways (Sugumaran et al., 2000a). Investigations have identified three different PO complexes responsible for either cellular melanotic encapsulation, sclerotisation or melanogenic reactions in insects, and one thing common to all is lack of stoichiometry, i.e. the ratios of the different protein components in different complexes has yet to be established (Sugumaran, 1998a; Sugumaran et al., 2000b). The melanotic encapsulation metabolon or defence complex (400 kDa) is one which forms in the hemolymph only under non-sterile conditions, e.g. after infection by micro-organisms, and is composed of PO, PPO (2 – 3-fold more than PO), dopachrome isomerase (although not found in all defence complexes) and an interleukin-1-like molecule (IL-1) (Söderhäll and Cerenius, 1998; Sugumaran, 1998a). The interaction of IL-1 with PO seems to be specific to formation of the melanotic encapsulation metabolon as it does not associate with PO in any other known instance (Sugumaran, 1998a). The melanogenic metabolon is another high molecular weight complex localised to the insect cuticle and composed of PO and dopachrome isomerase (Sugumaran et al., 2000a). The component enzymes of this metabolon clearly demonstrate its functions to synthesise melanin, but whether it is involved in melanotic encapsulation, cuticular pigmentation or wound healing is not clear (Sugumaran, 1998a). Sclerotinogenic complexes (620-680 kDa) possess the activities of the three enzymes of the sclerotinogenic pathway: PO, quinone isomerase and quinone methide isomerase (Sugumaran et al., 2000b). They are evidently quite different

from the defence and melanogenic complexes, functioning to harden newly formed cuticle to reduce an insects susceptibility to microbial attack and dehydration (Sugumaran, 1998a).

Metabolon formation offers several advantages to insects and seems to be a physiologically significant process providing a unique way of attributing different properties to a single enzyme, in this case PO, allowing its use in a number of different biochemical reactions (Sugumaran et al., 2000b). PO metabolon formation allows better control of PO activity and the subsequently generated reactive intermediary quinones, which can be channelled and safely transformed into non-toxic compounds (Sugumaran et al., 2000a). It has also been found that complexed PO is remarkably stable in comparison to free PO, which is unstable and loses its activity rapidly after activation (Sugumaran et al., 2000b; Sugumaran et al., 2000a). It has been reported that PO complexed with quinone isomerase appears to be stabilised via an inhibitory effect on its activity by up to 50% (Sugumaran and Kanost, 1993). A final advantage is that when a biochemical is synthesised solely to be the substrate of the next enzyme in a pathway, e.g. as in the melanisation reaction, complex formation can prevent the loss/dilution of these substrates whilst raising their concentration in the vicinity of the next enzyme to achieve high metabolic turnover (Sugumaran et al., 2000b; Sugumaran et al., 2000a).

### **2.6.3 Hemocyte Surface Phenoloxidase**

It was noted earlier that PO is a 'sticky' protein in its active form, and is one of the reasons it has been so difficult to study. However, it is this adhesive nature that allows PO to bind to pathogenic organisms and cause their melanisation and destruction. This characteristic has

further advantages to the insect as a whole, as it allows the enzymatic activity to be restricted to the immediate vicinity of an infection.

Research by Ling and Yu, 2005, indicates that PO also adheres to the surface of self hemocytes, triggering theories that such hemocyte-surface PO may be the enzyme activity involved in melanisation during the cellular melanotic encapsulation response (Section 2.5.1). Ling and Yu (2005) addressed this theory by investigating which particular hemocyte types from *M. sexta* possess surface bound PPO/PO, and the roles such hemocyte surface PPO/PO have in cellular melanotic encapsulation. One of the conclusions of their study contradicted the well documented occurrence of active PO binding to foreign surfaces and hemocytes. Instead they found that in *M. sexta* larvae, it is the stable inactive pro-form of PO that binds to hemocyte surfaces. This was also described earlier by another group working on the Medfly, *C. capitata* who found surface PPO to be constitutively present on hemocytes (Mavrouli et al., 2005). PPO does not exhibit the adhesive properties of its active form and therefore binding of PPO to hemocytes must involve either its direct binding to surface receptors or the formation of protein complexes which would include other plasma proteins acting as accessory proteins. The pattern recognition protein immunelectin-2 is probably one such accessory protein which, as described in Section 2.4.3, associates with PPO and PPAE through its SPH cofactors, to facilitate PPO activation. Immuelectin-2 can bind to the surface of hemocytes as well as pathogenic organisms, so it seems plausible that such protein complexes could form to recruit hemolymph PPO to hemocyte surfaces for activation and involvement in the cellular melanotic encapsulation response. A further possibility is that once PO has been activated, the accessory proteins will dissociate and PO will complex with

the necessary enzymes to form the melanotic encapsulation and/or melanogenic metabolons as discussed in section 2.6.2.

Further results from the investigations conducted by Ling and Yu (2005) indicated that the only hemocyte types possessing surface bound PPO/PO were spherule cells and granulocytes, not oenocytoids which are the site of synthesis of PPO in insects. During cellular melanotic encapsulation, it is proposed that a monolayer of granulocytes possessing surface-bound PPO forms around the hemocyte capsule which is surrounding a pathogen. Activation of granulocyte surface PPO results in melanisation of the capsule. The nature of active PO dictates its tendency to aggregate with other active PO. Therefore active surface-bound PO recruits free hemolymph PO and further hemocyte surface PO causing systemic melanisation of the capsule.

Discussions here demonstrate that localising PO to sites of infection by interactions with accessory proteins provides another level of control over its activity. This, like metabolon formation, reduces the risk of systemic activation of PO during responses to immune challenge and any unwanted damage which would arise as a consequence. Instead the activity of the enzyme is limited to the immediate area of an infection where its function is required.

## **2.7 Phenoloxidase as an Indicator of Immune Function in the Lepidoptera**

PO has been demonstrated to be a good indicator of ability to cope with infection in Lepidopteran insects. Higher levels of PO activity are present in individuals which display

greater resistance to infection (Cotter and Wilson, 2002; Cotter et al., 2004). Resistance to pathogenic micro-organisms is a very costly system to maintain and express, so it is expected that insects invest in resistance only when required (Barnes and Siva-Jothy, 1999). The likelihood of an insect encountering a pathogen or parasite often increases with population density, and the transmission of disease is also usually density-dependant. One could predict, therefore, that insects living in high density (HD) populations will have invested more in resistance than those in low density (LD) populations (Reeson et al., 1998). This pattern is in fact the case with many species of Lepidoptera (Reeson et al., 1998).

In situations where population density fluctuates between generations, individuals must rely on a form of phenotypic plasticity known as density-dependant phase polyphenism or density-dependant prophylaxis (DDP), which allows them to match their phenotype to the surrounding environment (Wilson et al., 2001; Barnes and Siva-Jothy, 1999). Some species of larval Lepidoptera display this phenotypic plasticity, with HD and LD forms displaying differences in colour, behaviour and development time (Reeson et al., 1998). Dark cuticular pigmentation, for example, is a common characteristic of the HD form not displayed in the LD form (Reeson et al., 1998). The difference in colour is therefore very clear (Figure 11)



Figure 11: Density-dependant phase polyphenism is a form of phenotypic plasticity displayed by some species of larval Lepidoptera. Shown above is the high density (top) and low density forms of the larvae of the moth species *Spodoptera exempta*. Cuticular melanisation, a characteristic of the high density form, results in a distinctive blackening of the insects cuticle (Wilson et al., 2001).

enabling the two forms to be easily distinguished. Pigmentation, also referred to as cuticular melanisation, results from the synthesis and deposition of melanin and a number of quinonoid tanning agents generated during sclerotisation of the newly formed cuticle (Sugumaran, 2002). Melanisation and sclerotisation reactions are catalysed partly by the action of PO, an enzyme important in insect immune reactions, particularly during the encapsulation of foreign organisms in the hemolymph (as discussed in Sections 2.2 and 2.5.1) (Barnes and Siva-Jothy, 1999). This suggests that the cuticular melanisation occurring in individuals from HD populations may be a useful indicator of enhanced immune function/PO activity (Reeson et al., 1998; Cotter et al., 2004). Reeson et al (1998) have in fact demonstrated a positive correlation between resistance and both hemolymph PO activity and cuticular melanisation in *Spodoptera exempta* (African armyworm) larvae. They found that larvae reared in HD populations were more resistant to nuclear polyhedrosis virus (NPV), and had elevated PO activity and levels of cuticular melanisation when compared to larvae from LD populations.

This characteristic trait of *Spodoptera* species presents a controllable system which can be used to study the synthesis and activation of PO and forms the rationale of the research presented in Chapter 3, Chapter 4 and Chapter 5. If the activity of PO is influenced by organism population density then perhaps the control occurs at the level of transcription. It was thus hypothesised that variations in transcription levels between the different PO genes would arise as a consequence of population density. This project was designed with the aim of sequencing the first PO gene from larvae of the Egyptian Cotton Leafworm, *Spodoptera littoralis*, before using this sequence to screen for further PO genes. By rearing *S. littoralis* larvae under LD and HD conditions, it was hoped that any effect population density had on the transcription of the different PO genes identified in this species could be established. Unfortunately, despite efforts to isolate the first PO gene from *S. littoralis*, none could be identified. Nonetheless, the following three chapters detail the attempts made and discuss possible explanations for the outcome.

## **Chapter 3 : Sequencing and analysis of a putative 600 bp *Spodoptera littoralis* phenoloxidase gene fragment .**

### **3.1 Introduction**

By 2006 the complete or partial sequence of 55 different prophenoloxidase (PPO) genes from a number of insect species had been characterised. Indeed some of these sequences represent different PPO genes from the same source species. For example, *Bombyx mori* and *Manduca sexta* (Order: Lepidoptera) each have two PPO genes, whilst *Armigeres subalbatus* and *Anopheles gambiae* (Order: Diptera) have four and nine, respectively. This implies that perhaps all insect species possess more than one gene coding for phenoloxidase (PO) enzymes. Whilst the reason for having more than one PPO gene is not currently understood, studies using *Anopheles gambiae* PPO 1 to 6 (Müller et al., 1999) have revealed that each PPO has a distinct temporal and spatial expression pattern arising during larval development. It has been suggested that each PPO may have a unique role to play throughout development or may be activated in response to specific triggers. As discussed in the literature review in Chapter 2, different PPO types perform different functions, such as wound healing and cuticle pigmentation, and it may be the case that each PPO type is encoded by a unique gene.

The species in this study is *Spodoptera littoralis* (Insecta: Lepidoptera: Noctuidae), more commonly known as the Egyptian Cotton Leafworm. The larval stage of this insect is one of the most destructive agricultural Lepidopteran pests within its subtropical and tropical range, which covers Africa, Asia and southern-most parts of Europe (DEFRA, Accessed: 2003.; Smith et al., 1997). Whilst four full length *Spodoptera* PPO sequences are known (Figure 12)

(NCBI Accession numbers DQ289581, DQ289581, EF684939 and AY703825), to date, no PPO sequence has been elucidated for *S. littoralis*. Prior to the onset of this research, a 600 bp stretch of DNA had been amplified and isolated from the genomic DNA of *S. littoralis* larval hemocytes by Dr. Jacqueline Nairn (2003 unpublished data). Subsequently, the aim of this research was to purify and sequence this DNA fragment, before subjecting the sequence to further analyses to determine whether it was in fact a fragment of a *S. littoralis* PPO gene.

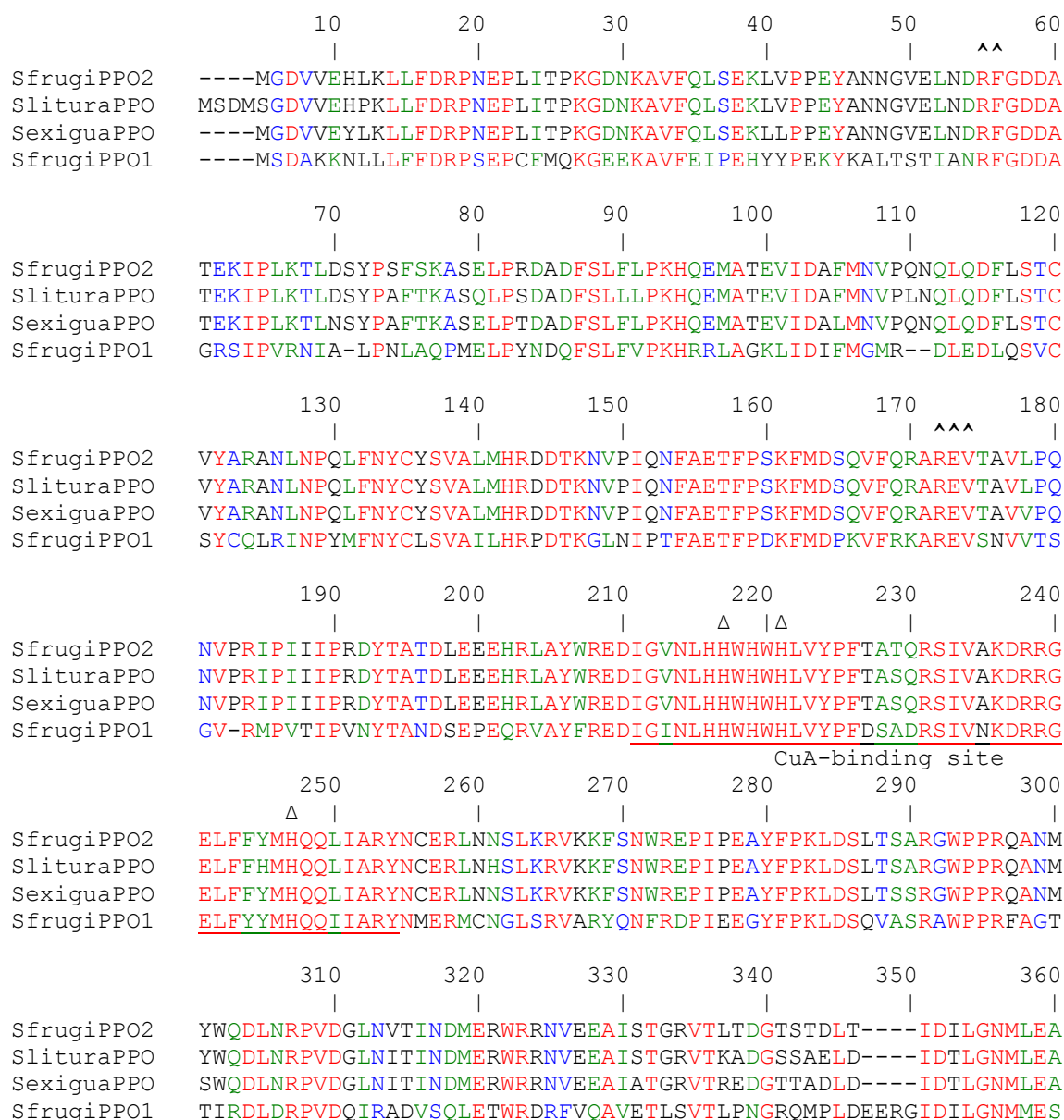


Figure 12: Multiple alignment of amino acid sequences of the four known full length *Spodoptera* PPO polypeptides. These are *Spodoptera frugiperda* PPO2 (SfrugiPPO2 – DG289582), *Spodoptera litura* PPO (SlituraPPO – AY703825), *Spodoptera exigua* PPO (SexiguaPPO – EF684939) and *Spodoptera frugiperda* PPO1 (SfrugiPPO1 – DG289581). The eight digit letter and number codes in brackets are the NCBI accession numbers for each respective sequence. The two copper-binding sites are singly underlined and labelled, and the 3 conserved histidines in each are highlighted with ‘Δ’. The conserved RF and REE cleavage sites are marked with ‘^’, the conserved thiol-ester motif is double underlined ‘=’ and the conserved C-terminal site is underlined with ‘~’. (Multiple alignment constructed using MULTALIN (pbil) available via the ExPASy online Proteomics Server and the NCBI PubMed nucleotide databank).

```

          370      380      390      400      410      420
          |  Δ  Δ  |      |      |      |      |  Δ  |
SfrugiPPO2  SILSPNRDLYGSIHNNGHSEFAAYMHDP THRYLESFGVI |ADEATTMRDPFFYRWHAWIDDT
SlituraPPO  SILSPNRELYGSIHNNGHSEFAAYMHDP THRYLESFGVI |ADEATTMRDPFFYRWHAWIDDT
SexiguaPPO  SILSPNRELYGSIHNNGHSEFSAYMHDP THRYLESFGVI |ADEATTMRDPFFFRWHAWIDDT
SfrugiPPO1  SIISPNRGYYGDLHNMGHVFISYSHDPDRHLEQFGVMGSATAMRDPVFYRWHSIDDL
                                     CuB-binding site
          430      440      450      460      470      480
          |      |      |      |      |      |
SfrugiPPO2  CQRHKESQYVRPYTRSELENPGVQVTSIAVETAGGQPNTLNTFWMSSDVDLSKGLDFSDR
SlituraPPO  CQRHKESAYVRPYTRSELENPGVQVTSVSVETAGGQPNTLNTFWMSSDVDLSKGLDFSDR
SexiguaPPO  CQKHKESPYVRPYTRSELENPGVQVTSVSVETPGGQPNTLNSTFWMSSDVDLSRGLDFSDR
SfrugiPPO1  FQLYKVK--LTPYGDDKLDFPGVRVSSVSLEGAAGR-NTLGTFWELSTVDLGRGLDFTPR

          490      500      510      520      530      540
          |      |      |      |      |      |
SfrugiPPO2  GAVYARFTHLNNRAFRYVIKVNNT-GSARRTTVRIFMAPKFDERNLVWSLADQRKMFIEM
SlituraPPO  GAVYARFTYLNNRPFRYVININNT-GSARRTTVRIFMAPKFDERNLVWSLADQRKMFIEM
SexiguaPPO  GPVYARFTHLNNRPFRYVINVNNT-GSARRTTVRIFIAPKYDERNLVWSLADQRKMFIEM
SfrugiPPO1  GSVLARFTHLQHQDFNYVIEVNNTSGQSVMGTVRIFMAPVQDERGAPLSFDDQRSMIEL

          550      560      570      580      590      600
          |      |      |      |      |      |
SfrugiPPO2  DRFVHPLNAGENTITRSSTDSSVTIPFEQTFRDLSPQGSDPRRTSLAEFNFCGCGWPQHM
SlituraPPO  DRFVQPLNAGQNTITRNSTDSSVTIPFEQTFRDLSPQGSDPRRTSLAEFNFCGCGWPQHM
SexiguaPPO  DRFVQPLNAGQNTITRMSTQSSVTIPFEQTFRDLSVQGNDPRRTSLAEFNFCGCGWPQHM
SfrugiPPO1  DKFTAGLRPGNNTIRHRSVDSSVTIPYERTFRDQSARPGDPGSEEAAEFDFCGCGWPHH
                                                                    =====

          610      620      630      640      650      660
          |      |      |      |      |      |
SfrugiPPO2  LVPKGTEAGAAYQLFVMLSNYDLSDVQPDGTQLSCVEASSFCGLKDKKYPDRRAMGFPF
SlituraPPO  LVPKGTEAGAAYQLFVMLSNYDLSDVQPGGNQLSCVEASSFCGLKDKKYPDRRSMGFPF
SexiguaPPO  LVPKGTEAGAPYQLFVMLSNYDLSDVQPDGSQLSCVEASSFCGLKDKKYPDRRSMGFPF
SfrugiPPO1  LIAKGNQQGYPVVLFAMVSNWAEDRVEQDLVG--SCNDAASYCGIRDRKYPDRRAMGFPF
                                                                    ~~~~~~

          670      680      690      700
          |      |      |      |
SfrugiPPO2  DRPSSIATNIEDFILPNMALQDITIRLSNVVEPNPRNPPSTV
SlituraPPO  DRPSSIATNIEDFILPNMALQDITIRLSNVVEQNPRNPPSAV
SexiguaPPO  DRPSSTATNIEDFILPNMALQDITIRLSNVVEPNPRNPPSAV
SfrugiPPO1  DRPS-PAQSLTDFLRPNMAMQNCSIRFTDTTIPRQQR----
          ~~

```

Figure 12: Continued

## **3.2 Methods**

### **3.2.1 Preparation of purified plasmid containing the 600 bp insert.**

A 600 bp DNA fragment believed to be that of a PPO from *S. littoralis*, had been previously isolated by Dr Jacqueline Nairn from purified *S. littoralis* larval hemocyte genomic DNA, using primers designed to anneal to regions of the PPO gene which form the active site CuA (CuA'03-F) and CuB (PO2-R) binding sites (unpublished work). For details of these primers please refer to section 9.1 - Appendix A. The fragment had been subcloned into a pDrive cloning vector (Figure 13) and transformed into competent NM522 bacterial cells using the QIAGEN PCR Cloning Kit (Cat #231124). Successfully transformed colonies were selected by plating onto LBA/IPTG/X-Gal plates, 20 of which were picked for further culture and plasmid purification, using the protocol described in the QIAGEN QIAprep Miniprep Kit Handbook under the heading 'QIAprep Spin Miniprep Kit Protocol: Using a Centrifuge'. A series of clones resulted which contained the 600 bp DNA fragment as confirmed by performing EcoR1 digests of the purified plasmids and PCR amplification of the DNA fragment from each clone.

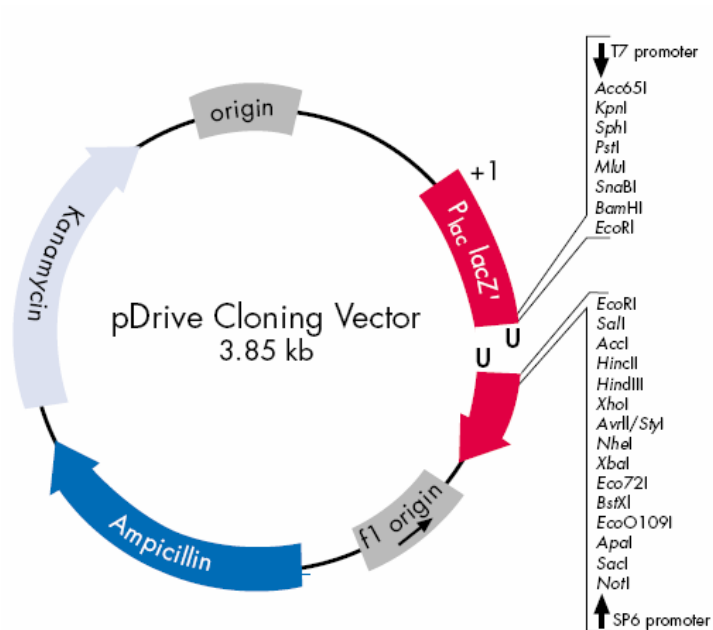


Figure 13: pDrive Cloning Vector Map. The 600 bp DNA fragment isolated by Dr Jacqueline Nairn (unpublished data 2003) was cloned into this plasmid between the EcoRI restriction sites before transformation into competent NM552 bacterial cells.

To generate purified stocks of the 600 bp clones labelled 2 and 10, a culture loop-full of the original transformed NM552 cells was mixed into two sterile glass universal tubes per clone ('a' and 'b'), each containing 5 ml of LB broth plus 50 µg/ml of ampicillin (LBamp). The tubes were sealed and the cells cultured overnight in a 37°C orbital incubator. 1 ml of each culture (2a, 2b, 10a and 10b) was transferred into a fresh 1.5 ml Eppendorf tube then centrifuged for 5 minutes at 13000 rpm to pellet the bacterial cells. The remaining supernatant was aspirated and discarded. The protocol followed for purifying the plasmids was the same as that detailed above using the QIAGEN QIAprep Miniprep Kit.

### 3.2.2 PCR amplification of the 600 bp DNA fragment.

Four 100 µl reactions containing final concentrations of the following reagents were prepared: 1 X Taq PCR Master Mix (QIAGEN Cat #201443), 25-fold dilution of the

template DNA (600 bp clone 2a, 2b, 10a or 10b from section 3.2.1) and 1.25  $\mu$ M M13 forward (5'-G-TAA-AAC-GAC-GGC-CAG-3') and reverse (5'-A-ACA-GCT-ATG-ACC-ATG-3') primers. Each reaction was subjected to the following PCR conditions: 2 minutes at 95°C followed by 30 cycles of: 30 seconds at 95°C, 45 seconds at 50°C and 45 seconds at 72°C. To each tube, 20  $\mu$ l of 6 X Type-II Loading Buffer was added before the PCR products were loaded onto a 1 X TBE, 1 % agarose, 0.2  $\mu$ g/ml EtBr gel. The PCR products were electrophoresed alongside PCR Markers (Sigma Cat #P-9577) at 50 V for 1.5 hours, and the DNA bands visualised by exposing the gel to UV light.

### **3.2.3 Gel slice clean-up of the amplified 600 bp DNA fragment.**

Extraction and purification of the 600 bp DNA fragment from the agarose gel resulting in Section 3.2.2, was conducted following the protocol described in the QIAGEN QIAquick Spin Handbook for the QIAquick Gel Extraction Kit (Cat #28304). Variations of the standard protocol used were as follows: the QIAquick column was allowed to stand for 5 minutes after the addition of Buffer PE before centrifugation, and in the final step, the DNA concentration was increased by adding 30  $\mu$ l of elution buffer to the QIAquick membrane, and allowing the column to stand for 5 minutes before centrifugation. To check the success of the clean-up process, a small aliquot of each extracted and purified DNA sample was run on a 1 X TBE 1 % agarose 0.2  $\mu$ g/ml EtBr gel.

### **3.2.4 Sequencing the 600 bp DNA fragment.**

Prior to sequencing, gel extracted PCR products were used in a second round of PCR to generate copies of the clone 600 bp DNA fragment with incorporated synthetic ddNTPs. Four 20  $\mu$ l reactions (two for each of the 600 bp clones 2a and 10a) were prepared using

reagents from the DYEnamic ET Terminator Cycle Sequencing Kit (Amersham Pharmacia Biotech Cat #US-81050). Each reaction contained 10 µl SDW, 1 µl of gel extracted and purified 2a or 10a 600 bp DNA fragment and 8 µl of sequencing reagent premix. One of each pair of reactions contained 1 µl of 5 µM M13 forward primer and the other 1 µl of 5 µM M13 reverse primer, which were added immediately prior to the reactions being placed in the thermocycler. PCR reaction conditions were 25 cycles of 20 seconds at 95°C, 15 seconds at 50°C and 1 minute at 60°C. An initial longer denaturing step was not required as extended periods at this temperature can prematurely inactivate the DNA polymerase and ultimately produce weak signals.

Immediately following the final cycle, the PCR reaction tubes were placed on ice. To each 20 µl reaction, 2 µl of 3 M sodium acetate, pH 5.2 and 50 µl of 95 % ice cold ethanol were added, before vortexing (Nickel Electro Ltd. WhirliMixer). This was left on ice for 5 minutes to allow the DNA to precipitate and then centrifuged at 13000 rpm for 20 minutes. The supernatant was carefully aspirated and the pellet washed in 190 µl of ice cold 70 % ethanol (or the maximum volume the reaction tube will hold). The tube was centrifuged for a further 5 minutes and the supernatant removed as before, ensuring that minimal ethanol was left. The tubes were placed in a pre-heated 60°C heating block (Techne Dri-Block DB.2D) for a maximum of 5 minutes, avoiding over-drying, and if any ethanol was still present the tubes were left open and on their side to air dry. Once all trace of ethanol had been removed, the tubes were placed back on ice and 2 µl of formamide loading buffer was added to each pellet ready for sequencing. The DNA was stored at -20°C until ready for sequencing. The samples were loaded into and analysed by an ABI 377 DNA sequencer, through a service operated by Stephen Powell of the Institute of Aquaculture, University of Stirling. The protocol used was

as described in literature accompanying the ABI 377 sequencer and DYEnamic ET Terminator Cycle Sequencing Kit.

### **3.2.5 Sequence analysis.**

DNA sequencing produced a raw nucleotide sequence and an original sequence trace for each sample. Prior to analysis, the raw nucleotide sequences were compared to their original sequence traces, and any discrepancies between the two were noted and confident changes made in the raw nucleotide sequence. The sequence used for further analysis was that which had the least discrepancies between its raw nucleotide sequence and sequence trace and also the least unidentified 'N' nucleotides in the main stretch of sequence. Following removal of the C- and N-terminal unidentified 'N' nucleotides, the sequence was submitted to a BLAST Nucleotide-Nucleotide search (blastn), using default search parameters, except the search and format options were limited to the Arthropoda. Subsequently, the nucleotide sequence was translated in all six reading frames to its corresponding amino acid sequence using the online ExPasy proteomics server DNA to protein 'Translate' tool. Each reading frame amino acid sequence was finally subjected to a Protein-Protein BLAST (blastp) search, using default search settings, once again limiting the search and format options to the Arthropoda.

## **3.3 Results**

### **3.3.1 Successful PCR Amplification and Gel Slice Clean-up of the 600 bp Plasmid Insert.**

PCR and gel extraction protocols were utilised to amplify and purify a cloned 600 bp DNA fragment, believed to be that of an *S. littoralis* PPO gene, from a pDrive cloning vector.

Duplicate PCRs for amplification of the 600 bp fragment from two different clones (labelled 2 and 10) produced three out of four successful reactions (Figure 14 – Panel A) – 2a, 10a and 10b. Following gel extraction and purification of the PCR products (Figure 14 – Panel B), only reactions 2a and 10a were selected for subsequent sequencing steps due to the apparent higher yield of DNA.

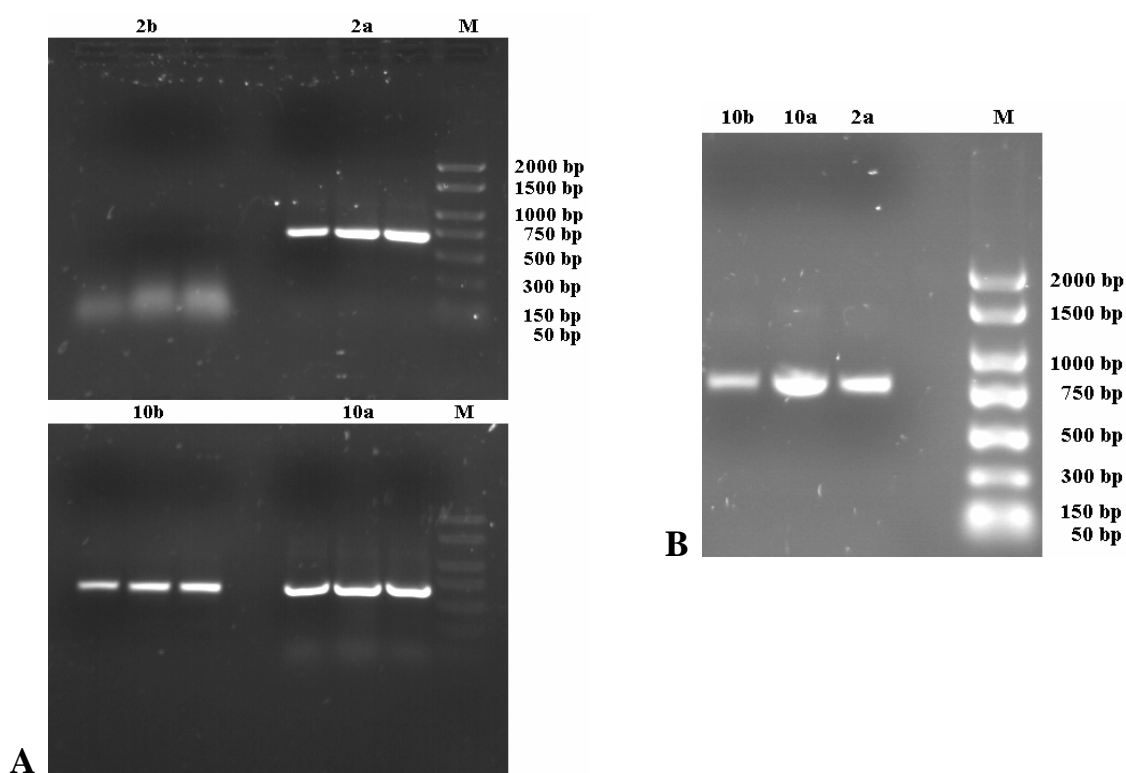


Figure 14: Panel A: Amplification of the 600 bp plasmid insert. The 600 bp insert was successfully amplified by PCR from clones 2a, 10a and 10b. The reaction to amplify clone 2b was unsuccessful and shows a staining pattern characteristic of unincorporated primers and dNTPs. Panel B: Gel extraction and 'clean-up' of the amplified 600bp DNA fragment from each clone. The lanes in the gel shown were loaded with 5µl of the amplified and purified 600 bp DNA fragments from clones 10b, 10a and 2a, to ensure the extraction and clean-up steps were successful. The lanes marked 'M' contain PCR markers.

### 3.3.2 Analysis of the 600 bp DNA fragment sequence.

The raw sequence of clones 2a and 10a in both the forward and reverse direction, as derived by the ABI 377 DNA sequencer, can be found in section 9.2 - Appendix B. Whilst all four reactions generated some stretch of sequence, the reverse reaction containing clone 10a produced the most reliable and complete sequence with the longest stretch of A, T, G or C nucleotides unbroken by 'N' which represents an undefined nucleotide. The final nucleotide sequence of clone 10a reverse is shown in Figure 15 with its N- and C-terminal 'N' nucleotides removed.

```
TTGAAACGCCACTTCAAATACGACTCACTGATAGTCCAAGCATCGGTGACCACGCATGCTGC
AGACGCGTTATCGTATCGGATCCAGAATTCGTGATTCACCACTGGCACTGGCACCTGGTCTG
CGCGTTCGGAGATAAAAGGCGTGATGTTATATGAGTGGTCTTATAACCAAAGCATTATATTT
ATTTAATTAATCACTTAATTGTCAAATCTGATTATAAGTGCTGTGAATGGGCCTTAAAATCT
TTGTTTGCTATCCAGGTAGAAAATGAGTACGGTAGCTATGGCAACAACATGAACTATCGAGT
CCAAGTCCGCAACATGCTGCAGAACCACGTCGGTACCAACGCTCTCCTCTACACTACTGACG
GGAATGCAATTTCTTTCTTCAGAAATGGTGCCGTTCTAACACTCTCATCACCATCGATTTT
GGTCCCCACTCAAGTCAGTATAATTTTTAATAATGTATTTACATAATTATGTAGACTTTTTT
CCCCAAAACCTAAATTATAATATAATACCTACCTTGGAGTCCTTCGGTGTTCATCGCCAAATC
TGAATTCGGTCGACAAAGCTTCTCGAAGCCCTAGCGCGCTTAA
```

Figure 15: Finalised nucleotide sequence of the 600 bp DNA fragment from clone 10a, produced in a sequencing reaction containing the M13 reverse primer. The sequence was finalised by comparison of the raw outputted sequence with its corresponding original sequence trace and any necessary changes then made. The sequence was also clipped at both the N- and C-termini to remove undefined (N) nucleotides from the sequence. The highlighted portion indicates the only stretch of sequence which, when subjected to a blastn search, showed identity with the lowest Expect value to another prophenoloxidase gene sequence. The lower the Expect value the less likely that the similarities are random.

To determine whether this nucleotide sequence shared any similarities with the PPO sequences from other insect species, a blastn search was conducted using default parameters

with the exception that the search and format options were limited to the Arthropoda. The search hit with the lowest Expect (E) value for a PPO was the *Tribolium castaneum* pro-phenol oxidase subunit 2 mRNA (E value = 0.006), where the lower the E value the less likely that the similarities are random and occurring by chance. The only region of identity however, was that highlighted in Figure 15. Whilst there was 100% identity across this stretch of sequence with *T. castaneum* PPO2, which forms part of the nucleotide sequence encoding the PPO Cu-A binding site, this was also the sequence of the forward primer used in the original gene amplification from genomic DNA. A number of different insect and crustacean PPO nucleotide sequences, as well as chelicerate hemocyanin sequences, were also hits resulting from this search with E values ranging from 0.023 for *Galleria mellonella* (Wax moth) PPO mRNA to 5.7 for *Armigeres subalbatus* (mosquito) PPO. Whilst these insect PPOs shared 100% identity to the putative PPO sequence, it should be noted that where search hits were arthropod PPOs or hemocyanins, the identity was limited only to the region highlighted in Figure 15. All also possessed similarly high E values indicating random similarities.

For further analysis, the amino acid sequence of the 600 bp DNA fragment was deduced, in all six reading frames, using the ‘Translate’ tool available via the online ExPasy proteomics server (Table 3). It was evident upon examination that all six reading frames had multiple stop codons randomly dispersed throughout the sequence. Despite this, each reading frame (stop codons removed) was submitted to a blastp search using default search and format options limited to the Arthropoda. Frame 3 translated in the 5’ 3’ direction was the only sequence to produce hits during the blastp search which were arthropod PPOs or hemocyanins. Again, as with the blastn search, the only region to generate hits which were

insect PPOs, was that with identity to the PPO CuA binding site of these proteins (shown highlighted in Table 3).

Table 3: The nucleotide sequence of the 600 bp DNA fragment from clone 10a was translated in all six reading frames to its corresponding amino acid sequence. The translation was conducted using the ‘Translate’ tool available online via the ExPASy proteomics server. Compact output format is shown where ‘#’ represents a stop codon. The sequence highlighted in yellow indicates the only region out of all six of the reading frames that showed identity/similarity to phenoloxidasases from other arthropod species. The red underlined sequence is that which generated the hit with the lowest E value, sharing 40% identity to its respective matched sequence, and contained a putative glycosyl hydrolase domain, characteristic of beta-galactosidase enzymes. The double underlined amino acids have the sequence of the forward (5’3’ Frame 3) and reverse (5’3’ Frame 2) primers and represent those parts of the sequence from which strand extension was initiated.

| Frame        | Amino Acid Sequence   |
|--------------|---|
| 5’3’ Frame 1 | L K R H F K Y D S L I V Q A S V T T H A A D A L S Y R I Q N<br>S # F T T G T G T W S A R S E I K G V M L Y E W S Y N Q S I<br>I F I # L I T # L S N L I I S A V N G P # N L C L L S R # K<br>M S T V A M A T T # T I E S K S A T C C R T T S V P T L S S<br>T L L T G M Q F L S S E M V P F L T L S S P S I L V P T Q V<br>S I I F N N V F T # L C R L F S P K L K L # Y N T Y L G V L<br>R C H R Q I # I R S T K L L E A L A R L                         |
| 5’3’ Frame 2 | # N A T S N T T H # # S K H R # P R M L Q T R Y R I G S R I<br>R D S P L A L A P G L R V R R # K A # C Y M S G L I T K A L<br>Y L F N # S L N C Q I # L # V L # M G L K I F V C Y P G R K<br># V R # L W Q Q H E L S S P S P Q H A A E P R R Y Q R S P L<br>H Y # R E C N F F L Q K W C R S # H S H H R F W S P L K S<br>V # F L I M Y L H N Y V D F F P Q N L N Y N I I P T <u>L E S F</u><br>G V I A K S E F G R Q S F S K P # R A #                    |
| 5’3’ Frame 3 | E T P L Q I R L T D S P S I G D H A C C R R V I V S D P E F<br>V <u>I H H W H W H L V</u> C A F G D K R R D V I # V V L # P K H Y<br>I Y L I N H L I V K S D Y K C E W A L K S <u>L F A I Q V E N</u><br><u>E Y G S Y G N N M N Y R V Q V R N M L Q N H V G T N A L L Y</u><br><u>T T D G N A I S F F R N G A V P N T L I T I D F G P H S S Q</u><br>Y N F # # C I Y I I M # T F F P K T # I I I # Y L P W S P S<br>V S S P N L N S V D K A S R S P S A L |
| 3’5’ Frame 1 | L S A L G L R E A L S T E F R F G D D T E G L Q G R Y Y I I<br>I # V L G K K V Y I I M # I H Y # K L Y # L E W G P K S M V<br>M R V L G T A P F L K K E I A F P S V V # R R A L V P T W F<br>C S M L R T W T R # F M L L P # L P Y S F S T W I A N K D F<br>K A H S Q H L # S D L T I K # L I K # I # C F G Y K T T H I<br>T S R L L S P N A Q T R C Q C Q W # I T N S G S D T I T R L<br>Q H A W S P M L G L S V S R I # S G V S                         |
| 3’5’ Frame 2 | # A R # G F E K L C R P N S D L A M T P K D S K V G I I L #<br>F K F W G K K S T # L C K Y I I K N Y T D L S G D Q N R W #<br># E C # E R H H F # S K C L H S Y R Q # C R G E R W Y R R G S<br>A A C C G L G L D S R C C C H S Y R T H F L P G # Q T K I L<br>R P I H S T Y N Q I # Q L S D # L N K Y N A L V I R P L I #<br>H H A F Y L R T R R P G A S A S G E S R I L D P I R # R V C<br>S M R G H R C L D Y Q # V V F E V A F Q                       |
| 3’5’ Frame 3 | K R A R A S R S F V D R I Q I W R # H R R T P R # V L Y Y N<br>L S F G E K S L H N Y V N T L L K I I L T # V G T K I D G D<br>E S V R N G T I S E E R N C I P V S S V E E S V G T D V V L<br>Q H V A D L D S I V H V V A I A T V L I F Y L D S K Q R F #<br>G P F T A L I I R F D N # V I N # I N I M L W L # D H S Y N<br>I T P F I S E R A D Q V P V P V V N H E F W I R Y D N A S A<br>A C V V T D A W T I S E S Y L K W R F                           |

However, a hit also generated from Frame 3 translated in the 5' to 3' direction, which had a very low E value of  $4e^{-10}$ , was that of the Ect3 gene (beta-galactosidase) from *Apis melliferis* (Honey bee), which shared ~40% identity to the red underlined (RU) sequence in Figure 15. A number of the other hits from this frame with similarly low E values and higher percentage identities were also insect beta-galactosidases (*Drosophila melanogaster* and *Aedes aegypti*). Furthermore this RU sequence was predicted to contain a putative glycosyl hydrolase domain, characteristic of the beta-galactosidases. To illustrate the similarities, the RU sequence was aligned with the known sequences of the *D. melanogaster* Ect3 (beta-galactosidase) and *A. aegypti* beta-galactosidase genes (Figure 16). The 67 amino acid RU sequence was found to align with amino acids 192 – 261 of the known beta-galactosidases.

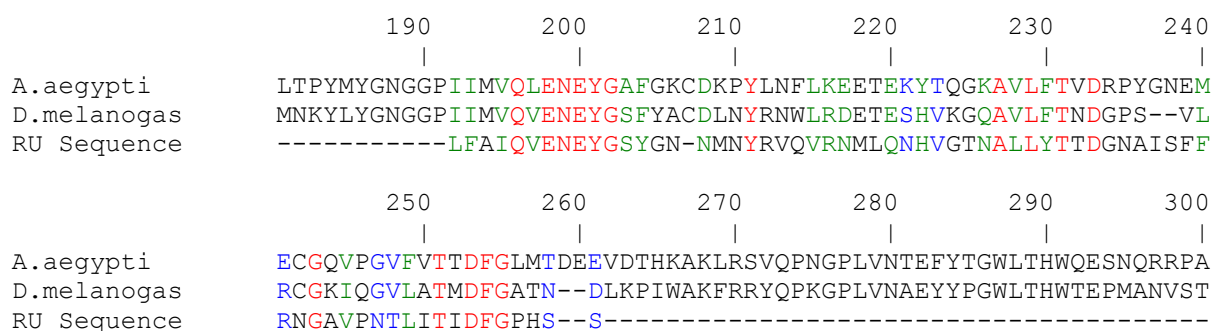


Figure 16: Amino acid sequence alignment of the red underlined (RU) sequence in Table 3 and the known sequences of the *D. melanogaster* Ect3 (beta galactosidase) and *A. aegypti* beta-galactosidase genes (UniProtKB/TrEMBL Accession numbers Q9VGE7 and Q17CH4 respectively). The alignment has been truncated to show only amino acids 181 – 300, as this is the region within which the RU sequence aligns with the known sequences. The RU sequence shares 40-50% identity with the two known sequences, which in turn is the range of identity shared between the full length sequences of known insect beta-galactosidases.

In a bid to establish a reason for the amplification of a beta-galactosidase gene sequence rather than a PPO sequence, alignments were performed using the same alignment tool and known beta-galactosidase sequences as above, but instead of the RU sequence, either the CuA'03-F or PO2-R primer sequence (see section 9.1 – Appendix A) was included in the alignment (primers used by Nairn, 2003 unpublished data, for the amplification of a PPO gene from *S. littoralis* larval hemocyte genomic DNA). However, neither primer demonstrated any confident alignment within the predicted region of the two known beta-galactosidase genes.

### 3.4 Discussion

Earlier work by Nairn (2003, unpublished work) generated a series of clones containing a 600 bp DNA fragment, amplified from *S. littoralis* larval hemocyte genomic DNA using PPO specific primers. Using genomic DNA as a template in PCR has an inherent complication due to the presence of introns and the problem of crossing them during the extension phase of PCR. Only one PPO gene structure is available, and is that of the African malarial mosquito, *Anopheles gambiae* (Ahmed et al., 1999). This gene is composed of five exons and four introns as shown in Figure 17. The five exons are labelled I, II, III, IV and V, and span 447, 683, 440, 197 and 670 base pairs respectively. The length of each intron



Figure 17: Structure of the *Anopheles gambiae* prophenoloxidase 1 gene (AgPPO1). The gene spans 10 kb and is composed of five exons (I – V, blue rectangles) separated by introns i, ii, iii and iv (solid black horizontal lines). The lengths depicted are simply for illustrative purposes and are not to scale. Diagram has been adapted from that shown in (Ahmed et al., 1999).

also varies (i - 2831 bp, ii - 74 bp, iii - 2175 bp and iv - 101 bp). The highly conserved characteristic CuA and CuB binding sites are located within exons II and III respectively and the forward and reverse primers used during amplification of the 600 bp DNA fragment from *S. littoralis* genomic DNA were based on these regions of the PPO gene sequence. Assuming a similar structure for all insect PPO genes, the expected length of the amplified fragment when using this primer combination was approximately 600 bp; this includes the length of intron ii (74 bp). In this case, the problem of crossing introns was expected to be minimal as the intron was short requiring minimal strand extension. Ultimately, the length of the DNA fragment expected was in fact that which resulted in the original PCR.

Sequencing and subsequent analysis of the 600bp stretch of DNA led to the conclusion, however, that the fragment was not that of a PPO. This conclusion was based on a lack of substantial similarity between the deduced nucleotide sequence of the 600 bp fragment and that of known PPO genes. Despite one small stretch of the DNA fragment having a striking resemblance to the CuA site of insect PPO and arthropod Hc, it seemed the sequence shared greater similarity to the insect beta-galactosidase gene.

Amplification of this particular non-PPO stretch of DNA was perhaps as a result of non-specific priming of the primers (designed to amplify a PPO gene from genomic DNA) to the source genomic DNA. The forward primer had the nucleotide sequence 5'-CAC-CAC-TGG-CAC-TGG-CAC-CT(AGCT)-GT(AGC)-TAC-CC-3' (HHWHWHLVYP), and the reverse primer 5'-GGC-GAT-GAC-ACC-GAA-(AG)GA-CTC-CAG-GTA-3' (YLESFGVIA), which are regions of the PPO CuA and CuB binding sites, respectively, and are highly conserved amongst arthropod PPOs. Further investigation, using the *A. aegypti* beta-galactosidase and

*D. melanogaster* Ect3 gene sequences, failed to reveal any short stretch of these sequences which could potentially have been a site recognised and bound by the primers. However, as genomic DNA was used as the template there is the possibility that they annealed to intron regions of a beta-galactosidase gene, subsequently amplifying the region coding for the putative glycosyl hydrolase domain.

The possibility that the amplified stretch of DNA could have been a pseudogene was also considered. Pseudogenes are stretches of genomic DNA with a similar sequence to that of known functional genes. They arise via retrotransposition or duplication, but as a result of mutations, they are considered functionally inactive. Typical modifications which affect functionality involve insertion of stop codons and alterations to other regulatory elements. The presence of numerous stop codons in the currently analysed 600 bp DNA fragment became apparent upon translation of the nucleotide sequence, with all six reading frames containing multiple methionine residues (Table 3). It may be proposed therefore that the isolated DNA fragment was an insect  $\beta$ -galactosidase pseudogene, or perhaps even a PO or another copper binding protein pseudogene with a different function.

Despite unsuccessful attempts to amplify a stretch of PPO DNA, the primers and experimental design utilised were appropriate for their purpose. Performing an alignment of a number of arthropod PPO sequences, see Figure 3, Chapter 2, demonstrates that the sequence regions on which the forward and reverse primers were designed, are conserved both within and between species. To further emphasise the validity of the primer design, amplification of a PPO gene from other insect species such as *Apis mellifera* (Lourenco et al., 2005), *Sarcophaga bullata* (Chase et al., 2000) and *Anopheles gambiae* (Müller et al., 1999) has

been achieved successfully using forward primers with a similar sequence to the CuA'03-F primer used here. Subsequently there were no reasons to assume that the primers utilised would not be suitable for their intended purpose.

## **Chapter 4 : Screening for a Prophenoloxidase Gene in a *Spodoptera littoralis* cDNA library.**

### **4.1 Introduction**

During earlier work (Chapter 3) to sequence a PPO gene fragment, it became apparent that the isolated fragment was in fact not that of a PPO gene, but rather a stretch of DNA which appeared to have some similarity to a region of an insect beta - galactosidase. In the following chapter, a different approach was adopted. This method made use of a *Spodoptera littoralis* cDNA library and a number of molecular techniques, ultimately aiming to identify and isolate a PPO cDNA.

The cDNA libraries (gifted by Beatrice Lanzrein, University of Berne, Switzerland), L5p and XL6, were generated from homogenised whole *S. littoralis* larvae, parasitized by either non-irradiated (L5p) or X-ray irradiated (XL6) female Braconid parasitoid wasps, of the species *Chelonus inanitus* (Johner and Lanzrein, 2002). Endoparasitoids are parasites which infect and develop within the bodies of host insects, and therefore must be able to protect themselves from the hosts' natural defence systems. Successful parasitisation thus requires host immune depression and developmental arrest to protect the wasp egg/larva and divert host nutrients for the support of wasp development (Bae and Kim, 2004). Larval endoparasitic wasps, such as *C. inanitus*, possess host immune system avoidance mechanisms which exist in the form of venoms, ovarian proteins and polydnaviruses (PDVs), injected into the host at parasitisation (Bae and Kim, 2004). Polydnaviruses (PDVs) are a group of viruses which have formed an endosymbiotic relationship with some parasitic

ichneumonid and braconid wasps (Lavine and Beckage, 1995). The two PDV groups – the ichnoviridae or the bracoviridae – show morphological differences in packaging of their viral DNA, and use different mechanisms to disable host immune and development systems (Lavine and Beckage, 1995). The PDV genome (both the proviral DNA segments integrated into the wasp genome and the circular extra-chromosomal viral segments) is replicated and packaged into virions solely within the calyx cells of the female wasps' reproductive tract (Doucet and Cusson, 1996; Lavine and Beckage, 1995). The process of budding from (ichnoviruses), or cell lysis of (bracoviruses), calyx cells, allows accumulation of mature PDVs to a high concentration in the ovarian calyx lumen (Lavine and Beckage, 1995). These are subsequently introduced into the host Lepidoptera egg/larva during oviposition, along with the wasp egg, venom and ovarian proteins (Shelby and Webb, 1999) (Figure 18). At this

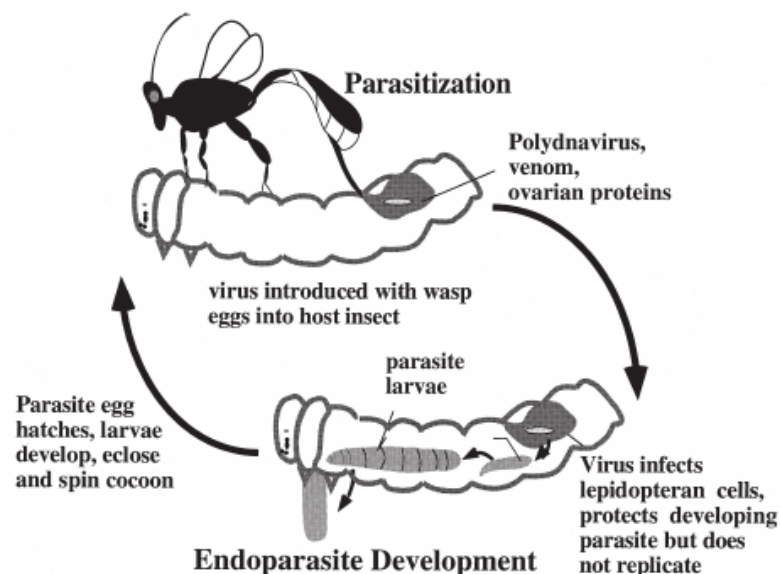


Figure 18: The life cycle of a bracoviridae polydnavirus (PDV). During parasitisation of Lepidoptera larvae by Braconid parasitoid wasps, PDVs are injected into the host hemocoel along with the egg, venom and ovarian proteins. These function to inhibit normal cellular and humoral immune responses thus protecting the wasp egg and allowing development of the wasp larvae in the hemocoel. Taken from (Shelby and Webb, 1999).

time, no evidence exists for PDV replication within host Lepidopteran larvae. PDV DNA is, however, actively transcribed within the host. Along with venom components and ovarian proteins, the PDV genome encoded proteins rapidly cause an array of alterations and disruptions to the host immune and physiological systems (Lavine and Beckage, 1995). Examples include a reduction in growth, developmental arrest, altered metabolism, inhibition of encapsulation, inhibition of antimicrobial peptide synthesis and elimination of hemolymph melanisation (Shelby et al., 1998; Doucet and Cusson, 1996; Bae and Kim, 2004; Lavine and Beckage, 1995). Ultimately these effects on the host facilitate the uninterrupted development of the wasp eggs and larvae.

Research has suggested that microbially immune challenged insects display greater levels of detectable PPO mRNA transcripts and hemolymph PO activity (Rajagopal et al., 2005). Conversely, host larvae parasitized by parasitoid wasps show evidence of greatly reduced hemolymph PO activity, predominantly due to the presence of PDVs, and enhanced by the presence of venom (Bae and Kim, 2004; Doucet and Cusson, 1996; Zhang et al., 2004). PDVs are believed to function at the post-transcriptional/translational step of gene expression, a common mechanism utilised by other viruses to regulate cell physiology. Such translational regulation of insect host immune response and development-associated proteins was previously demonstrated during the parasitisation of *Heliothis virescens* (Lepidoptera: Noctuidae) by the ichneumonid wasp *Campoletis sonorensis* (Shelby et al., 1998). PDV post-transcriptional control was found to be responsible for reducing the levels of three storage proteins, juvenile hormone esterase and lysozyme present in the hemolymph.

It therefore seemed likely that whilst the PO activity of parasitized larvae was limited, PPO gene transcripts would still be abundant in the parasitized individuals used for synthesis of the L5p and XL6 cDNA libraries. These cDNA libraries presented potential for isolating an *S. littoralis* PPO gene.

## **4.2 Methods**

### **4.2.1 Polymerase chain reaction and Southern blotting.**

#### **4.2.1.1 Primer design.**

A range of forward and reverse degenerate primers were designed for the amplification of a *S. littoralis* PPO cDNA. The amino acid sequences of highly conserved regions of arthropod PPOs were identified, and the subsequent nucleotide sequence was determined with reference to the *S. littoralis* codon usage table (available online at [www.kazusa.or.jp/codon/](http://www.kazusa.or.jp/codon/)). Primers were synthesised by MWG at a scale of 0.01  $\mu$ mol and purified by HPSF. Section 9.1 - Appendix A lists all primers designed and used throughout this research. Nucleotide and amino acid sequences are provided along with an indication of their location on the PPO gene sequence.

#### **4.2.1.2 Generating stocks of the plasmid vector containing a clone of the *Manduca sexta* PPO1 or PPO2 gene.**

Lyophilised cDNA clones of *Manduca sexta* PPO1 and PPO2 genes were kindly gifted from Michael Kanost and Mary Everhart of Kansas State University, Manhattan, USA. These cDNAs had been cloned using EcoR1 and Xho2 (5' – 3') and packaged into the pBluescript cloning vector. To re-suspend the clones, 100  $\mu$ l of TE buffer was added to each and

centrifuged for 1 minute at 13000 rpm then stored on ice. 300 µl of competent *E. coli* NM552 cells in 0.1 M calcium chloride was transferred into eight sterile culture tubes. To the first four aliquots of competent cells, 0 (control), 1, 10 or 50 µl of clone plasmid PPO1 was added, and to the second four aliquots, the same volumes of clone plasmid PPO2. All tubes were swirled gently to ensure even dispersion of the plasmids and left on ice for 1 hour. The cells were heat shocked in a 42°C water bath for 2 minutes before 5 ml of sterile LB broth was added and the culture placed in an orbital incubator at 37°C for 1 hour. The cells were centrifuged for 10 minutes at 4°C and 2100 rpm and the pellet re-suspended in 60 µl of sterile LB broth. For each dilution of each clone, two volumes (10 and 50 µl) were transferred onto separate 90 mm round 50 µg/ml ampicillin LB agar plates. The plates were inverted and incubated overnight at 37°C.

Approximate colony counts were conducted on each overnight plate. Plates with counts of 100 - 400 colonies were chosen for colony picking. Colonies selected were preferably those with smaller satellite colonies, and were ejected into 5 ml of 50 µg/ml ampicillin sterile LB broth. Following an overnight incubation in an orbital incubator at 37°C, 1 ml of each culture was transferred into each of two fresh 1.5 ml Eppendorf tubes then centrifuged for 5 minutes at 13000 rpm to pellet the bacterial cells. From this point, the protocol for purifying plasmids was exactly as described in the QIAGEN QIAprep Miniprep Handbook under the heading 'QIAprep Spin Miniprep Kit Protocol: Using a Centrifuge'.

#### **4.2.1.3 Gradient PCR.**

PCR reactions were prepared with the following final concentrations of components: 1X PCR buffer (1.5 mM MgCl<sub>2</sub>), 2.5 U Taq DNA Polymerase (both from QIAGEN Cat

#201205), 200  $\mu$ M dNTPs, 1  $\mu$ M forward and reverse primers and template DNA (plasmid DNA (Section 4.2.1.2) or cDNA library (details in Sections 4.1 and 4.2.3.2)). Final reaction volumes were made up with sterile distilled water. Reactions were vortexed briefly and centrifuged at 6500 rpm for 1 minute at 4°C. Utilising separately provided components for the PCR reactions turned out to be the most efficient method, although during earlier attempts, either Taq PCR Master Mix (QIAGEN Cat #201443) or HotStarTaq PCR Master Mix (QIAGEN Cat #203443) was used, at a final concentration of 1X, which contain PCR buffer, Taq polymerase and dNTP components.

Each PCR reaction was typically performed over a 10°C gradient of annealing temperatures (which generally included a temperature 10°C lower than the  $T_m$  values of the primer pairs). Reaction conditions were as follows: 95°C for 2 minutes, followed by 30 cycles of 95°C for 30 seconds, selected temperature gradient for 45 seconds and 72°C for 1 minute. The rate of temperature change between the denaturing and annealing step (the touchdown ramp) varied between reactions, at either 5°C, 2.5°C or 1°C/second. A small aliquot of each PCR product was separated by electrophoresis in a 1X TBE, 1 % agarose, 0.2  $\mu$ g/ml EtBr gel and visualized under UV light. The reaction generating the most intense, correctly sized product band was designated as having the optimal annealing temperature. If any combination of template DNA and primer pairs produced a product band of the expected size at a particular temperature, these reaction products were run on a second gel for Southern blotting.

#### **4.2.1.4 Southern blotting via the capillary method**

Each gel to be blotted was trimmed to the minimum possible size leaving the wells intact. A corner was cut away to record gel orientation for comparison to the resulting blot. If the gel

contained genomic DNA where large fragments were to be transferred to a membrane (such as genomic DNA restriction digest products), the gel was soaked for 10 minutes in 200 ml of depurination buffer (0.125 M HCl). When small DNA fragments and plasmids were involved, this step was not necessary. The gel was soaked in denaturation buffer (1.5 M NaCl and 0.5 M NaOH) for 30 minutes, then neutralization buffer (for alkaline transfer of DNA to nylon membranes - 1.5 M NaCl, 0.5 M Tris, pH 7.5) for a further 15 minutes. The gel was equilibrated in 10X SSC (20X SSC = 3.0 M NaCl and 0.3 M sodium citrate) for 5 minutes, prior to assembly of the blotting apparatus shown in Figure 19.

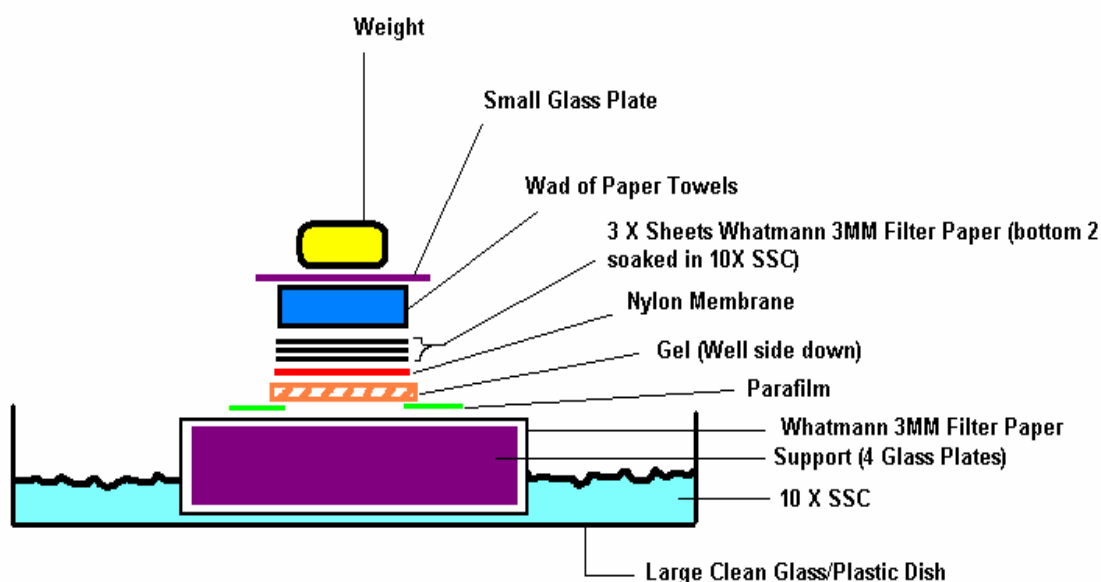


Figure 19: Apparatus used for Southern blotting of nylon membranes by the capillary method. To allow full transfer of DNA from the gel to the nylon membrane the apparatus was left at room temperature for 12 – 16 hours.

Following overnight transfer of DNA to the membrane, the apparatus was dismantled. On the non-DNA-side of the nylon membrane, the position of each well was marked using a lead pencil, and the corner which corresponds to the cut corner of the gel was cut away. The membrane was placed DNA-side up between two sheets of Whatmann 3MM paper until dry,

and the DNA was fixed by exposing the membrane to UV light for 1 minute. The blot was transferred into 2X SSC, washed for 3 minutes and dried as above.

To ensure that complete DNA transfer from gel to membrane had occurred, the blotted gel was submerged in 20 ml of 1X TBE buffer with 20  $\mu$ l of 15 mg/ml EtBr for 10 minutes. This would stain any DNA remaining within the gel. A lack of any visible DNA bands was used as an indicator that all DNA had been successfully transferred to the membrane.

## **4.2.2 DIG-labelled probe membrane hybridisation.**

### **4.2.2.1 DIG-labelled phenoloxidase DNA probe synthesis.**

Two forward and two reverse primers were specifically designed to anneal to clones of the *Manduca sexta* PPO1 and PPO2 genes in the plasmid vector pBluescript, purified in Section 4.2.1.2. Primers were synthesised by MWG at a scale of 0.01  $\mu$ mol and purified by HPSF. They were named MsextaPPO1-F, MsextaPPO1-R, MsextaPPO2-F and MsextaPPO2-R (See section 9.1 - Appendix A for sequences). Prior to the DIG-labelling step, gradient PCR reactions using separate reaction components were conducted as in Section 4.2.1.2 to establish the optimal annealing temperature for these primer pairs.

DIG-labelling of PCR products requires reactions that contain DIG – 11- UTP in place of some TTP. Therefore two reactions were set up for each PPO gene – one standard and one DIG-labelling reaction – containing the following final concentrations of each component: 1 X PCR buffer (1.5 mM MgCl<sub>2</sub>), 2.5 U/reaction Taq polymerase, 0.5 ng/ $\mu$ l template *Manduca sexta* PPO1 or PPO2 clone plasmid, 1  $\mu$ M of the respective clones' specific forward and

reverse primers, and 200  $\mu\text{M}$  ATP, GTP and CTP. The standard reaction contained 200  $\mu\text{M}$  TTP whereas the DIG-labelling reaction contained 130  $\mu\text{M}$  TTP and 70  $\mu\text{M}$  DIG -11-UTP. Reactions were prepared to their final volumes with sterile distilled water. PCR reaction conditions were: 2 minutes at 95°C, followed by 30 cycles at 95°C for 30 seconds, 55°C for 45 seconds and 72°C for 1 minute. A small aliquot of each reaction was loaded onto a 1X TBE, 1% agarose, 0.2  $\mu\text{g/ml}$  EtBr gel, and the products separated by electrophoresis and visualised under exposure to UV light. Successfully labelled products were observed to have slower electrophoretic mobility than the native products, and were named DIG-PPO1 and DIG-PPO2 according to the *M. sexta* PPO clone from which they were derived.

#### **4.2.2.2 Dot blot preparation.**

A series of 10-fold dilutions of the *M. sexta* PPO1 clone plasmid DNA was prepared in sterile distilled water, covering the range 20 ng – 2  $\mu\text{g}$ . The samples were heated to 95°C then chilled immediately on ice. 1  $\mu\text{l}$  of each dilution was transferred to a fresh Eppendorf tube on ice, and 1  $\mu\text{l}$  of 20X SSC mixed gently into each. Using a lead pencil, five 8 mm diameter circles were drawn at regular intervals along the length of a strip of positively charged nylon membrane (Roche Cat# 1 417 240). Each circle was labelled with the DNA concentration to be spotted into it. The membrane was soaked in 2X SSC firstly by floating it on the solution surface for a few seconds then submerging it completely for 2 minutes. The membrane was dried on a sheet of Whatmann 3MM filter paper for 20 minutes. Each 2  $\mu\text{l}$  sample of the plasmid DNA dilutions prepared above was spotted into the centre of its relevant circle on the membrane. Between each spot the membrane was allowed to dry for 30 seconds. The membrane was soaked in denaturing buffer (1.5 M NaCl and 0.5 M NaOH) for 5 minutes by transferring it DNA-side up, onto a block of Whatmann 3MM filter paper soaked in the

solution. The membrane was then transferred to a second block of filter paper soaked in neutralizing buffer (1.5 M NaCl, 0.5 M Tris, pH 7.5) for another 5 minutes. The membrane was dried for 20 minutes, DNA-side up between two sheets of filter paper, before being exposed to UV light for 2-3 minutes to fix the DNA.

#### **4.2.2.3 Hybridisation of nylon membranes with DIG-labelled PPO1 DNA probe.**

Dry DNA-bound membranes were re-wetted in 70 ml of 2X SSC for 5 minutes and transferred DNA-side up into a hybridisation tube. 5 ml of hybridisation solution (6X SSC, 1 % Blocking reagent, 0.1 % Sarkosyl, 0.02 % SDS) per membrane was added to the hybridisation tube(s), which were sealed tightly and placed in a rotating hybridisation chamber pre-warmed to the desired hybridisation temperature (between 60 - 68°C). 3 hours were allowed for pre-hybridisation of the membranes.

The pre-hybridisation solution was discarded. A further 5 ml per membrane of fresh hybridisation solution was added to each tube which was placed back into the hybridisation oven to re-warm to the desired hybridisation temperature. Meanwhile, the DIG-labelled probe generated from the *M. sexta* PPO1 plasmid (DIG-PPO1) in Section 4.2.2.1, was prepared for incubation with the membranes. DIG-PPO1 was chosen as the probe for use as its parent DNA, a clone of the *M. sexta* PPO1 gene, showed slightly higher identity than the *M. sexta* PPO2 clone, to the overall amino acid sequences of eight other Lepidoptera phenoloxidases (SwissProt/TrEMBL database accession numbers: Q9GU89, Q9GU90, Q964D5, Q6UEH6, O77002, O76208, Q9Y0B4 and Q9Y0B3). The DNA concentration of the probe was estimated from the resulting mini-gel produced in section 4.2.2.1, based on the fact that the smallest quantity of DNA that can be visualized in a gel after EtBr staining is

approximately 10 ng. From this, the volume of probe required per membrane, where approximately 50 ng of DIG-labelled probe per membrane is optimal, was mixed with 0.5 ml of hybridisation solution and boiled in a water bath for 10 minutes. The denatured probe was diluted immediately in the pre-warmed hybridisation solution present in each of the hybridisation tubes. These were sealed tightly and placed back into the hybridisation oven for an overnight incubation at the desired hybridisation temperature.

#### **4.2.2.4 Post hybridisation washes.**

The probe-hybridisation solution was discarded and a moderate or high stringency wash solution (moderate - 1X SSC and 0.1 % SDS; high - 0.1X SSC and 0.1 % SDS) was pre-warmed to the hybridisation temperature used previously. Each membrane was washed twice for 5 minutes in 100 ml of a room temperature low stringency wash solution (2X SSC and 0.1 % SDS), followed by three 15 minute washes in 80 ml of pre-warmed moderate or high stringency wash solution at the hybridisation temperature.

Detection of membrane bound DIG-labelled probe was performed using either the BCIP/NBT colourimetric or CDP-Star chemilluminiscent method. In preparation for the former, each membrane was submerged for 2 minutes in 100 ml of 0.3 % Tween-20 in Malate buffer (0.1 M Maleic Acid; 0.15 M NaCl; pH 7.5 - sterile) then incubated for 1 hour in 50 ml of 1% Blocking solution (Blocking reagent (Roche Cat #1 096 176) in Malate buffer). Alternatively, for the CDP-Star method, each membrane was transferred into 100 ml of Malate buffer for 5 minutes and finally incubated for 1 hour in 50ml of 1 % Blocking solution.

#### **4.2.2.5 Incubating probe hybridized membranes with an Anti-DIG-Alkaline phosphatase antibody.**

Blocking solution was recovered from section 4.2.2.4 in 50 ml aliquots. 2 µl of Anti-DIG-AP antibody (Roche Cat# 1 093 274) was added to each and inverted a number of times to ensure dispersal. Each membrane was incubated in one of these antibody solutions at room temperature for 30 minutes. The membranes were then transferred to and washed two (NBT/BCIP colourimetric detection) or three times (CDP-Star chemilluminiscent detection) in 50 ml of 0.2 % Tween-20 in Malate buffer.

#### **4.2.2.6 Detection of membrane bound DIG-labelled DNA probe.**

When applying the NBT/BCIP colourimetric detection method, each membrane was transferred into 50 ml of Detection buffer (0.1 M Tris-HCl; 0.1 M NaCl; pH 9.5) for 3 minutes to equilibrate at room temperature. 2 ml per membrane of NBT/BCIP solution was prepared as described in the product data sheets (NBT – Roche Cat# 1 383 221; BCIP – Roche Cat# 1 383 213). The solution was wrapped in tinfoil to protect it from light exposure. Each membrane was removed from the Detection buffer and placed DNA side up onto the inside leaf of a cut open A4 clear plastic poly-file. 2 ml of NBT/BCIP solution was quickly dispensed over the entire surface of each membrane. The poly-file was closed over and wrapped in tinfoil before gently smoothing over the membranes to disperse the colourimetric detection solution and displace any air bubbles. The membranes were incubated at room temperature for 16 hours. To stop the reaction, the membranes were rinsed in 50 ml of TE buffer for 5 minutes at room temperature, and the staining pattern recorded by scanning the wet membranes.

Application of the CDP-Star chemilluminiscent detection method required the following modifications: firstly, each membrane was transferred into 50 ml of Equilibration buffer (0.1 M Tris-HCl; 0.1 M NaCl; 0.05 M MgCl<sub>2</sub>; pH 9.5) for 10 minutes to equilibrate at room temperature. For each membrane, 497.5 µl of Equilibration buffer and 2.5 µl of the CDP-Star detection mix (Roche Cat# 1 685 627) was transferred onto the inside leaf of a cut open clear A4 poly-file. The Equilibration buffer was drained and each membrane placed DNA-side up onto the detection solution in the poly-file. The poly-file was closed over and wrapped in tinfoil, before gently smoothing over the membranes to disperse the chemilluminiscent detection solution and displace any air bubbles. The membranes were incubated for 5 minutes and then heat sealed DNA-side up in a fresh clear plastic poly-file. In a dark room, each membrane was placed DNA-side up under a sheet of x-ray film for 30 - 60 minutes. The film was developed and fixed.

#### **4.2.3 Screening a *Spodoptera littoralis* cDNA library for a prophenoloxidase cDNA.**

##### **4.2.3.1 Preparation of *E. coli* Y1090 viable working and glycerol stocks.**

*E. coli* Y1090 cells were kindly gifted by the Institute of Aquaculture, University of Stirling. They had been stored in glycerol at -40°C. The original glycerol stock was thawed on ice and a loop-full of the cells spread onto each of two LB ampicillin agar plates. The glycerol stock was quickly refrozen and the agar plates inverted and incubated at 37°C overnight. After approximately 16 hours, the plates were checked for colony formation. To build a viable working cell stock, a core of agar containing a single colony of cells was picked from one of the overnight agar plates and added to each of two 5 ml aliquots of LB broth containing 50

µg/ml ampicillin. The cultures were sealed and placed in a 37°C orbital incubator overnight. A sterile colony spreader was used to spread one loop-full of each overnight culture onto each of four LB 50 µg/ml ampicillin agar plates. The plates were inverted and placed in a static incubator overnight at 37°C. Each plate was checked for colony formation before being sealed and stored inverted at 4°C.

Fresh glycerol stocks of the *E. coli* Y1090 cells were prepared by inoculating two 5 ml aliquots of LB 50 µg/ml ampicillin broth with a viable colony grown on an LB ampicillin plate in the final step above. These inoculums were incubated at 37°C overnight in an orbital incubator. 350 µl of cells from these overnight cultures was mixed with 150 µl of sterile glycerol in 5 separate 1.5 ml Eppendorf tubes. To ensure the culture cells and glycerol were mixed thoroughly, each was repeatedly vortexed and chilled, then stored at -40°C.

#### **4.2.3.2 cDNA library titration.**

Gifted cDNA libraries L5p and XL6 had been cloned into the Lambda gt11 phage vector and subsequently packaged into competent *E. coli* Y1090r<sup>-</sup> cells. Both were generated from homogenised whole *S. littoralis* larvae parasitized by either non-irradiated (L5p) or X-ray irradiated (XL6) female brachonid parasitoid wasps, of the species *Chelonus inanitus* (Johner and Lanzrein, 2002). A series of dilutions (1:100 – 1:10 million) of both cDNA libraries were prepared in chilled SM buffer (0.1 M NaCl, 8.0 mM MgSO<sub>4</sub>, 0.05 M Tris-HCl pH 7.5, 0.01 % gelatin). Dilutions of the libraries proved to be rather unstable and therefore fresh dilutions were prepared for each titer or screening procedure.

Prior to incubation with either of the Lambda gt11 packaged cDNA libraries, two centrifuge tubes containing 10 ml of sterile LB broth with final concentrations of 50 µg/ml ampicillin, 10 mM sterile MgSO<sub>4</sub> and 0.2 % filter sterilized maltose, were inoculated with an *E. coli* Y1090 colony from the viable stock plates prepared in Section 4.2.3.1 . These cells were placed in an orbital incubator overnight at 30°C and allowed to grow to an OD<sub>600</sub> of no more than 1.0. The overnight cultures were centrifuged at 2000 rpm and 4°C for 10 minutes to pellet the bacteria. The pellets were re-suspended with half the original volume of filter sterile 10 mM MgSO<sub>4</sub>. 1 ml of one of these re-suspended pellets was transferred to a fresh centrifuge tube and diluted with filter sterile 10 mM MgSO<sub>4</sub> to a final OD<sub>600</sub> of 0.5. These diluted cells were used immediately in the following steps, whilst the remaining undiluted cells were placed in an orbital incubator at 37°C for 1 hour. These cells were then stored at 4°C and were regarded as viable for titering and screening for up to 2 weeks after preparation.

Nine 10 ml culture tubes were prepared (1 control and 4 for each dilution of both Lambda gt11 phage packaged cDNA libraries), as were nine room temperature LB 50 µg/ml ampicillin agar plates. 200 µl of *E. coli* cells diluted in 10 mM MgSO<sub>4</sub> were transferred into each culture tube followed by 1 µl of the relevant cDNA library dilution. For the control, 1 µl of SM buffer was used instead. All nine culture tubes were incubated at 37°C for 20 minutes to allow the phage to adsorb to the bacteria surface. After incubation, 4.5 ml of molten LB top agar containing 50 µg/ml ampicillin was added to each tube one at a time, swirled gently and immediately poured onto the surface of the corresponding room temperature agar plate. The plates were allowed to dry for 5 minutes before being inverted and incubated at 37°C for 12 - 16 hours (Plaques first became visible after approximately 7 hours). The following

morning plaque counts were performed where feasible and the average titer of each library was calculated.

#### **4.2.3.3 Plaque lifts for screening.**

Prior to screening, the required number of 95 mm squares of positively charged nylon membrane (Roche Cat# 1 417 240) were cut. Each membrane was soaked in sterile distilled water for 2 minutes, and then placed on top of one another alternating with slightly larger pieces of Whatmann filter paper. The membrane stack was wrapped loosely in tinfoil and autoclaved.

*E. coli* cell cultures were prepared overnight for incubation with the Lambda gt11 phage packaged L5p cDNA library as described in Section 4.2.3.2. This library was chosen for its greater stability when diluted and its higher plaque forming unit count. The overnight cultures were centrifuged, resuspended and diluted as outlined in section 4.2.3.2. Seven 100 mm LB ampicillin agar plates were brought to room temperature and a fresh 1:10000 dilution of the L5p cDNA library was prepared in chilled SM buffer and kept on ice for 1 hour before storing at -20°C.

Seven plastic 10 ml culture tubes and seven 100 mm LB agar plates were labelled '1' – '6' and one a 'control'. To the bottom of tube '1', 1200 µl of the diluted *E. coli* cells and 60 µl of the fresh 1:10000 cDNA dilution was pipetted whilst 200 µl of cells and 10 µl of SM buffer was pipetted into the control tube. Both were swirled gently and incubated at 37°C for 20 minutes. Whilst incubating, ampicillin was added to liquified LB top agar to a final concentration of 50 µg/ml.

After 20 minutes, the 1260  $\mu$ l incubation volume was split 6 x 210  $\mu$ l between the six labelled culture tubes. 4.5 ml of LB top agar was added to each tube (including the control) one at a time, swirled and poured evenly over each corresponding plate. Once dry, the plates were inverted and incubated at 37°C until plaques had formed which were no larger than 1 mm in diameter (approximately 4 hours). The plates were then stored inverted overnight at 4°C to ensure full hardening of the top agar for performing plaque lifts.

Each sterile nylon membrane square prepared earlier was labelled using lead pencil at one corner. A labelling system of 1A, 1B, 2A, 2B, 3A etc. was employed as replica lifts were to be taken from each of the six numbered plates. One at a time, each plate prepared the previous day was removed from the fridge and subjected to the duplicate plaque lifts. The first membrane was left for 2 minutes, during which time a needle was used to stab through the membrane into the agar below in a 3 corner asymmetrical pattern. These points were also marked on the base of the plate using a permanent marker. Blunt ended forceps were used to carefully peel back the membrane from the agar. The membrane was transferred plaque-side up onto a wad of Whatmann filter paper soaked in denaturing solution (1.5 M NaCl and 0.5 M NaOH), ensuring that no solution flooded over the membrane, and left for 5 minutes. It was then transferred plaque-side up, to a second wad of filter paper soaked this time in neutralizing solution (1.5 M NaCl and 0.5 M TrisHCl, pH 7.5) for a further 5 minutes. Finally this membrane was transferred to another wad of filter paper soaked in sterile 2X SSC (20X SSC = 3.0 M NaCl and 0.3 M sodium citrate, pH 7.0) and retained there until all membranes were ready for DNA fixing. The replica plaque lift membrane was left on the agar surface for 4 minutes and soaked in denaturing solution, neutralising solution and 2X

SSC as above. The agar plate was immediately returned to 4°C. This process was repeated for all other plates; with membranes 2A and 2B being replica lifts of plate 2 and so on.

Following completion of all plaque lifts, the membranes were allowed to air dry on a fresh sheet of filter paper for 20 minutes. Each was placed plaque-side down onto a UV light box and exposed to UV light for approximately 2 minutes to fix the DNA. The membranes were then stacked between alternating squares of filter paper and stored dry at room temperature wrapped in tin foil.

#### **4.2.3.4 DIG-labelled PPO1 DNA probe hybridisation of cDNA library plaque lifts.**

Each plaque lift membrane was subjected to hybridisation with the DIG-PPO1 probe and subsequent washing, antibody incubation and bound probe colourimetric detection steps as outlined in Sections 4.2.2.3 to 4.2.2.6. As a control for the hybridisation procedure, a dot blot was prepared as described in Section 4.2.2.2, and probed alongside the plaque lift membranes.

#### **4.2.4 Restriction digest of *Spodoptera littoralis* genomic DNA.**

##### **4.2.4.1 Restriction digest.**

Genomic DNA had been isolated and purified from *S. littoralis* hemocytes by Nairn (2003, unpublished work), and stored at -40°C. To check the DNA was still intact, 4 µl of each of the three isolated samples, 1A, 2A and 2B, was mixed with 2 µl of 6X Type-2 loading buffer and electrophoresed at 50 V for 2 – 3 hours in a 20 cm, 1X TBE, 0.8 % agarose, 0.2 µg/ml EtBr gel. Reference DNA bands were provided by 1 µl of 1 kb DNA Ladder (New England

Biolabs Cat# N32325) mixed with 2 µl of the above loading buffer. The sample with the highest yield of good quality genomic DNA was used in each subsequent restriction digest.

For each restriction enzyme used (*EcoRI* and *HindIII* separately, and also in combination), a fresh 0.2 ml PCR tube was labelled and placed on ice. 10 µl of 50 ng/µl *S. littoralis* genomic DNA was added to each tube along with 2.3 µl of the relevant restriction enzyme buffer. The mixture was stirred gently, and then left to stand on ice for approximately 3 hours. Keeping all on ice, 1 µl of each restriction enzyme was added to the appropriately labelled PCR tube and the mixture stirred gently on ice for 2-3 minutes. The digests were warmed slowly to 37°C in a water bath, left at 37°C for 30 minutes, then placed back on ice, and a second 1 µl aliquot of the appropriate restriction enzyme was added and stirred on ice as before. Once again each digest was warmed slowly to 37°C in a water bath, and then left at that temperature for 12 - 18 hours.

The overnight digest reactions along with a sample of non-digested genomic DNA, the clone *Manduca sexta* PPO1 plasmid and Lambda HindIII markers (ABgene, Cat# AB-0200), were prepared and loaded onto a 20 cm, 1 X TBE, 0.8 % agarose, 0.2 µg/ml EtBr gel, and separated by electrophoresis at 50 V for approximately 2 hours. The gel was visualized under UV light exposure and used for subsequent Southern Blotting.

#### **4.2.4.2 Southern blotting via the capillary method.**

Southern blotting was performed to transfer the digest fragments and control DNA onto a sterile nylon membrane as described in Section 4.2.1.4.

#### **4.2.4.3 DIG-labeled PPO1 DNA probe hybridisation of restriction digest membrane.**

The DNA fixed southern blot membrane was subjected to hybridisation with the DIG-PPO1 probe and subsequent washing, antibody incubation and bound probe detection steps as outlined in Sections 4.2.2.3 to 4.2.2.6. The clone *Manduca sexta* PPO1 plasmid sample loaded onto the blotted restriction digest gel acted as the control for these steps.

#### **4.2.5 Comparing the sensitivity of DIG-labelled PPO1 and DIG-labelled PPO2 DNA probes.**

To compare the specificity of two DIG-labelled DNA PPO probes in the recognition and binding of a heterologous PPO DNA sequence, a number of duplicate gels were prepared.. The first two gels (Gel 1-PPO1 and Gel 1-PPO2) each contained 10 µl of the products of two PCRs which used CuA3-F and Cys2-R primers and a 1:10 dilution of either the *M. sexta* PPO1 or *M. sexta* PPO2 clone plasmid as the template DNA. PCR conditions were 95°C for 2 minutes, followed by 30 cycles of 30 seconds at 95°C, 45 seconds at 52°C and 1 minute at 72°C. An annealing touchdown ramp of 1°C/second was employed. All components were at final concentrations as described in section 4.2.1.3. The second pair of gels (Gel 2-PPO1 and Gel 2-PPO2) both contained 0.5 µl of a 1:10 dilution of the *M. sexta* PPO1 and *M. sexta* PPO2 clone plasmids, and 5 µl of the products of a further two PCR reactions. These were prepared as before, with one containing MsextaPPO1-F and MsextaPPO1-R primers and a 1:10 dilution of the *M. sexta* PPO1 clone plasmid as the template DNA, and the other containing the MsextaPPO2-F and MsextaPPO2-R primers and a 1:10 dilution of the *M. sexta* PPO2 clone plasmid as the template DNA. PCR conditions for these reactions were as

above with the exception that the annealing temperature and touchdown ramp used were 55°C and 5°C/second respectively. The gels were run at 50 V for 1.5 hours, and photographed under UV light exposure.

The gels were subjected to Southern blotting, membrane hybridisation and probe detection protocols as described in sections 4.2.1.4 and 4.2.2.3 to 4.2.2.6, with the exception that the membranes resulting from the blotting of Gel 1-PPO1 and Gel 2-PPO1 were hybridised with the DIG-PPO1 probe and those membranes generated from Gel 1-PPO2 and Gel 2-PPO2 were hybridised with the DIG-PPO2 probe.

## **4.3 Results**

### **4.3.1 Gradient PCRs using degenerate primers generated numerous products of varying size.**

Prior to conducting PCR reactions for the amplification of a PPO cDNA from the L5p and XL6 cDNA libraries, the viability of each *Spodoptera littoralis* cDNA library was determined. Primers designed for the amplification of actin were used in control PCR reactions which contained either the L5p or XL6 library. As can be seen from Figure 20, the 400 bp actin product bands are approximately 50-fold brighter in reactions containing library L5p as compared to library XL6, where reaction and staining conditions were constant. Two repeats of these control PCRs produced similar outcomes. It was therefore assumed that cDNA library L5p was the more viable of the two libraries, and was used in all further PCRs.

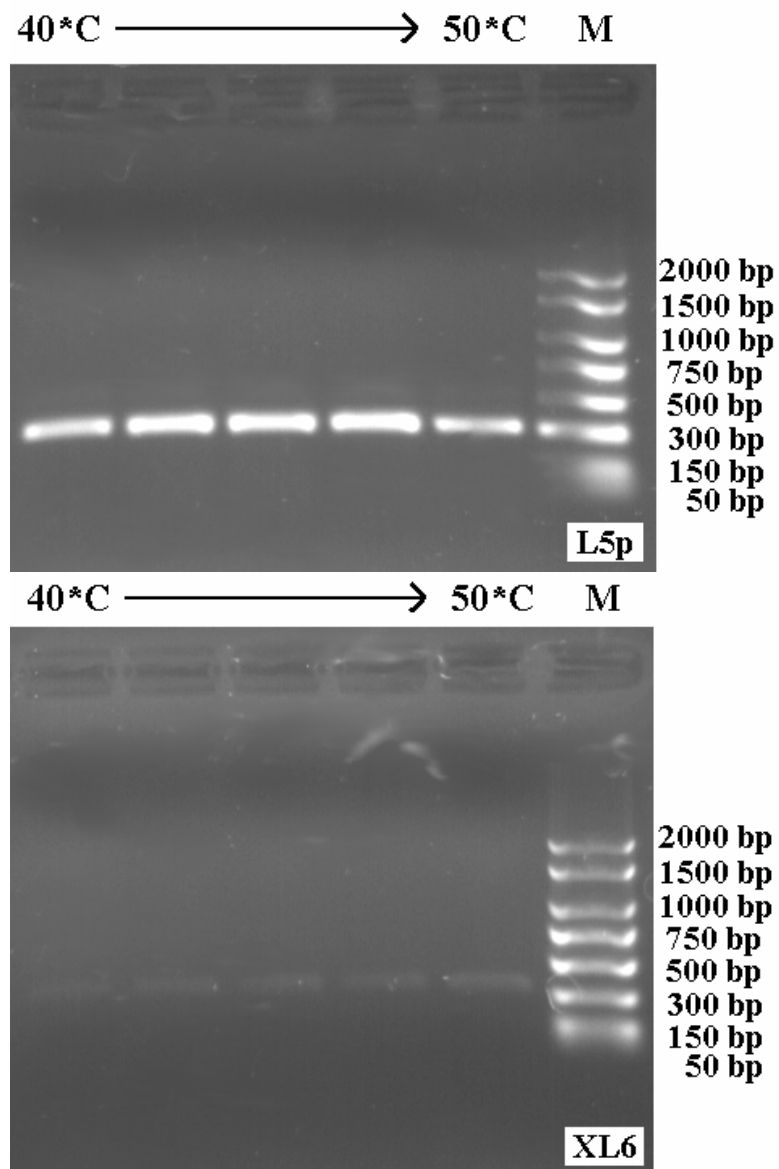


Figure 20: Amplification of actin cDNA from *Spodoptera littoralis* L5p and XL6 cDNA libraries. A DNA fragment of approximately 400 bp was generated across the full temperature gradient indicated, although the product band was approximately 50-fold brighter when the L5p library was the template DNA. This suggested that the L5p library was more viable and thus more suitable for use in PCR reactions aimed at amplifying a phenoloxidase cDNA. Two further repeat reactions produced the same results.

For the amplification of a *S. littoralis* PPO cDNA, a series of forward and reverse degenerate primers were designed based on the highly conserved regions of previously sequenced arthropod PPO gene sequences (Section 9.1 - Appendix A). To determine which combinations of these primers could successfully amplify Lepidoptera PPO DNA, a series of PCR reactions were conducted using the *M. sexta* PPO1 clone as the template DNA. Four primers with varying degrees of degeneracy had been designed on the basis of the sequence HHWHWHLVYP from the CuA binding site of PPO (CuA-F, CuA2-F, CuA3-F and CuA4-F). To conserve reaction components and reduce the required time, only one of these – CuA4-F – was tested in the control PCRs in combination with all possible reverse primers. It was chosen as it was the shortest of the four primers, with the sequence 5'-CA(CT)-CA(CT)-T(AG)(GCT)-CA(CT)-TGG-CA-3' (HHWHWH), which is completely conserved throughout all known Lepidoptera PPOs. The remaining three contained some or all of the latter part of this CuA binding region sequence – LVYP – which occasionally shows variation amongst species, and therefore were each used only once in combination with a single selected reverse primer. The nucleotide sequences of these other primers can be found in Chapter 9 - Appendix A.

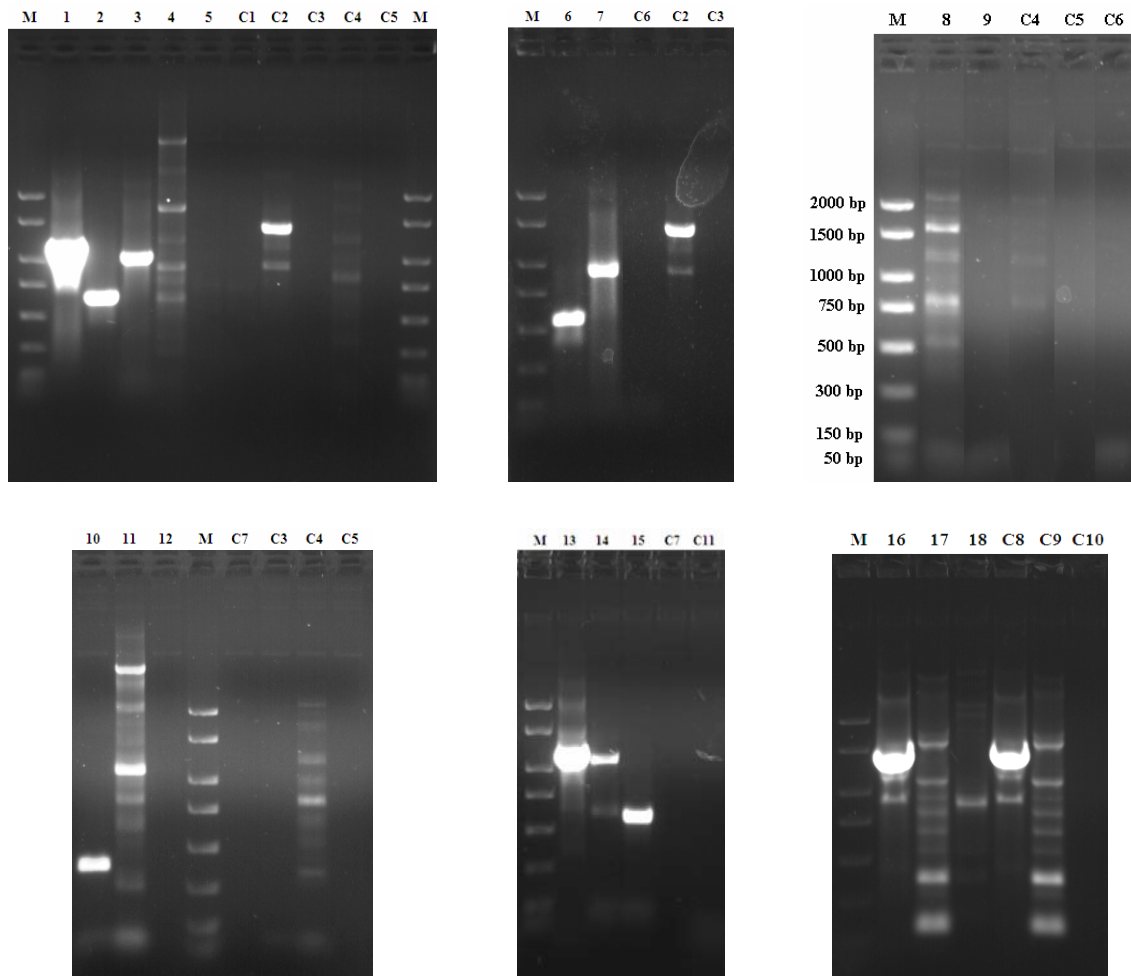


Figure 21: Determining the suitability of various degenerate primer pair combinations for the amplification of an *S. littoralis* PPO DNA fragment. Each lane shows products formed in PCR reactions which contained the *M. sexta* PPO1 clone as the template DNA and one pair of degenerate primers. Lanes marked 'M' contained PCR markers with sizes as detailed in the top right image. Primer combinations and expected fragment size (in brackets), as determined from the known sequence of the *M. sexta* PPO1 clone, were as follows: Lane 1 – MsextaPPO1-F and MsextaPPO1-R (1155 bp); Lane 2 – CuA4-F and CuB2-R (606 bp); Lane 3 – CuA4-F and MIELD-R (969 bp); Lane 4 – CuA4-F and Cys2-R (1131 bp); Lane 5 – CuA4-F and Cterm-R (1317 bp); Lane 6 – GELF-F and CuB2-R (534 bp); Lane 7 – GELF-F and MIELD-R (897 bp); Lane 8 – GELF-F and Cys2-R (1059 bp); Lane 9 – GELF-F and Cterm-R (1245 bp); Lane 10 – CuB2-F and MIELD-R (387 bp); Lane 11 – CuB2-F and Cys2-R (549 bp); Lane 12 – CuB2-F and Cterm-R (735 bp); Lane 13 – CuA4-F and Cys-R (1131 bp); Lane 14 – GELF-F and Cys-R (1065 bp); Lane 15 – CuB2-F and Cys-R (555 bp); Lane 16 – CuA-F and Cterm-R (1317 bp); Lane 17 – CuA2-F and Cterm-R (1317 bp); Lane 18 – CuA3-F and Cterm-R (1317 bp). Control PCR reactions were performed to ensure primers could not generate products alone. Lanes C1 – C11 contained only CuA4-F, CuB2-R, MIELD-R, Cys2-R, Cterm-R, GELF-F, CuB2-F, CuA-F, CuA2-F, CuA3-F or Cys-R respectively. Reactions containing no template DNA generated no products (data not shown).

The outcomes of the various control PCRs, shown in Figure 21, demonstrated firstly that not all primer combinations resulted in successful amplification of fragments of the *M. sexta* PPO1 clone. Also evident was that some reactions generated a range of non-specific products, either in addition to or not including the band of expected size. The absence of template DNA resulted in no products being formed (data not shown). Furthermore, it appeared that a number of the degenerate primers were capable of acting alone in the amplification of DNA fragments from the template DNA. These results have been summarised in Table 4, where the primer combinations have been arranged into categories according to the products formed.

Table 4: Primer pairs categorized according to the DNA products formed during PCRs in which each primer pair was used to amplify a particular stretch of a *M. sexta* PPO clone. Those which were successful in the amplification of a DNA fragment of the expected size, as well as those generating non-specific products in addition to this expected fragment, were utilized as primer pairs in subsequent rounds of PCR designed to amplify a PPO gene fragment from an *S. littoralis* L5p cDNA library. The number in brackets alongside each primer pair indicates the lane number in Figure 21 which illustrates the products formed.

| Successful Amplification of Desired Product Size | Non-specific product Amplification | Unsuccessful Amplification of Desired Product Size |
|--|------------------------------------|--|
| CuA4-F & CuB2-R (2)                              | CuA4-F & Cys2-R (4)                | CuA4-F & Cterm-R (5)                               |
| CuA4-F & MIELD-R (3)                             | GELF-F & Cys2-R (8)                | CuB2-F & Cterm-R (12)                              |
| CuA4-F & Cys-R (13)                              | GELF-F & Cterm-R (9)               |  |
| GELF-F & CuB2-R (6)                              | CuB2-F & Cys2-R (11)               |  |
| GELF-F & MIELD-R (7)                             | CuA-F & Cterm-R (16)               |  |
| GELF-F & Cys-R (14)                              | CuA2-F & Cterm-R (17)              |  |
| CuB2-F & MIELD-R (10)                            | CuA3-F & Cterm-R (18)              |  |
| CuB2-F & Cys-R (15)                              |                                    |  |
| MsextaPPO1-F & MsextaPPO1-R (1)                  |                                    |  |

Primer pairs which generated non-specific products were still considered as potential combinations for the amplification of an *S. littoralis* PPO, as modifications to reaction and PCR cycle conditions could potentially resolve this issue. Therefore, those primer pairs

which were found to successfully amplify the expected size of DNA fragment (with or without additional non-specific products) during PCR, were used in a series of PCR reactions for the amplification of a PPO cDNA, using the L5p cDNA library as the template DNA. To optimise amplification of any PPO cDNA present within this library, and to reduce non-specific product formation, a number of variations in the reaction conditions were tested. These included the use of (a) different Taq polymerase enzymes, (b) PCR reaction pre-mixes or separate components, (c) various annealing temperature gradients, (d) various annealing touchdown rates, (e) differing concentrations of the cDNA template and (f) PCR extension phases of differing lengths. Ultimately, using a standard Taq DNA polymerase (QIAGEN Cat# 201205) in PCR reactions prepared using separate buffer and dNTP components, resulted in more successful product formation. Also, using an annealing touchdown ramp of 2.5°C/second increased the specificity of primer pairs.

A number of selected PCR reactions, which generated product bands of the expected size, were repeated to ensure reproducibility, before the DNA products were transferred to nylon membranes via Southern blotting. It was apparent that whilst product bands were formed which approximated the expected size there were many other non-specific products. Although reaction conditions were modified in attempts to eliminate this non-specific cDNA amplification, no particular set of conditions could eliminate the problem. By performing blotting and DIG-labelled probing of the membranes, it was predicted that any PPO DNA amplified during the PCRs could be identified amongst these multiple product bands. The gel images shown in Figure 22 - Figure 29, show those selected PCR reactions which potentially contained a fragment of DNA with the sequence of a PPO. Following Southern blotting of these gels, each membrane was hybridised with the DIG-labelled PPO1 probe, washed,

incubated with the Anti-DIG AP alkaline phosphatase antibody and subjected to NBT/BCIP colourimetric detection protocols, generating the membrane probe-binding patterns discussed in section 4.3.2.

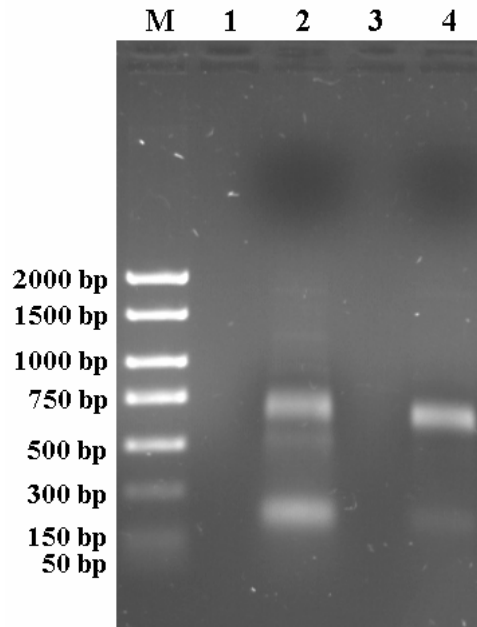


Figure 22: PCR reaction products selected for Southern blotting and subsequent membrane probing. All reactions used the *Spodoptera littoralis* L5p cDNA library as the template DNA. The reaction products in each numbered lane are the result of the following primer pair combinations (reaction annealing temperature and expected product size are shown in brackets): Lane 2 – CuA4-F and Cterm-R (45°C, 1341 bp); Lane 4 – CuA4-F and Cterm-R (49.4°C, 1341 bp). PCR marker sizes in Lane M are indicated to the left. Each PCR reaction used a 2.5°C/sec annealing touchdown ramp to increase primer annealing specificity. Southern blotting of this gel and subsequent membrane manipulation resulted in the membrane found in Panel A, Figure 32.

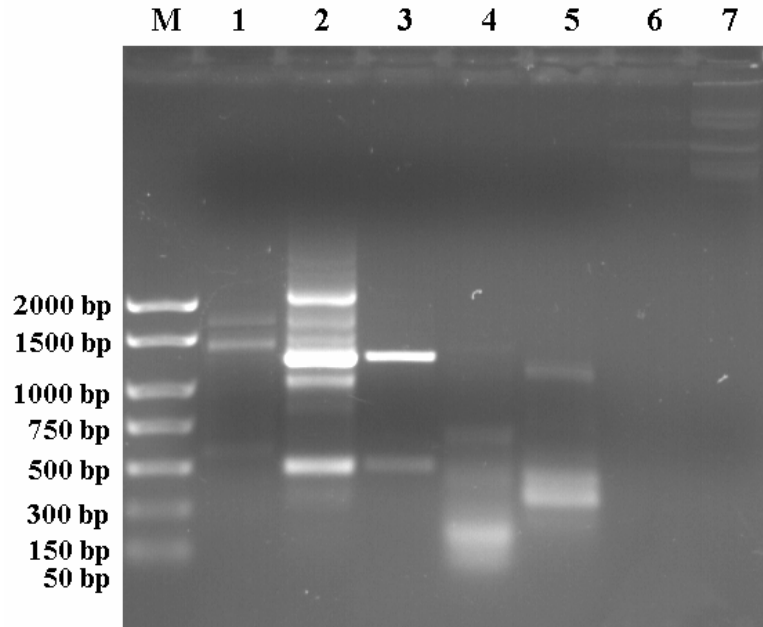


Figure 23: PCR reaction products selected for Southern blotting and subsequent membrane probing. All reactions used the *Spodoptera littoralis* L5p cDNA library as the template DNA. The reaction products in each numbered lane are the result of the following primer pair combinations (reaction annealing temperature and expected product size are shown in brackets): Lane 1 – CuA4-F and Cterm-R (55°C, 1341 bp); Lane 2 – GELF-F and Cys2-R (55°C, 1044 bp); Lane 3 – GELF-F and Cys2-R (59.4°C, 1044 bp) Lane 4 - CuA-F and Cys-R (40°C, 1155 bp); Lane 5 – CuA-F and MIELD-R (40°C, 987 bp); Lane 6 – 1  $\mu$ l of a 1:10 dilution of the *M. sexta* clone plasmid; Lane 7 – 5  $\mu$ l of a 1:10 dilution of the *M. sexta* clone plasmid. PCR marker sizes in Lane M are indicated to the left. Each PCR reaction used a 2.5°C/sec annealing touchdown ramp to increase primer annealing specificity. Southern blotting of this gel and subsequent membrane manipulation resulted in the membrane found in Panel B, Figure 32.

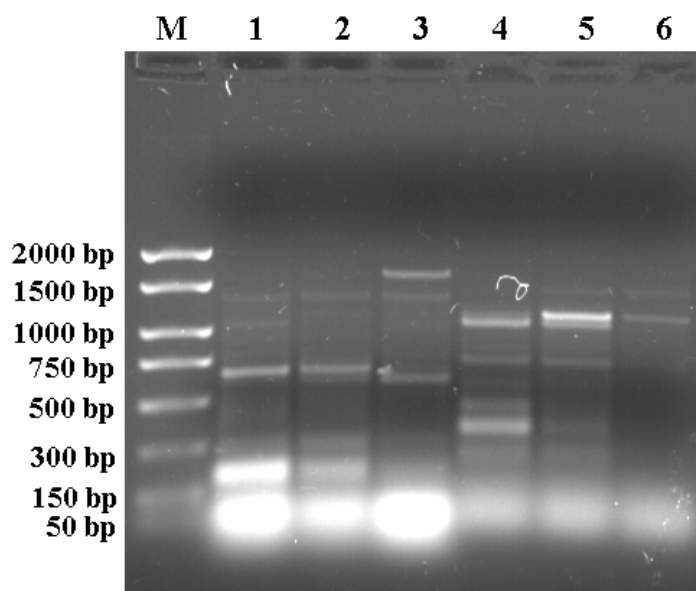


Figure 24: PCR reaction products selected for Southern blotting and subsequent membrane probing. All reactions used the *Spodoptera littoralis* L5p cDNA library as the template DNA. The reaction products in each numbered lane are the result of the following primer pair combinations (reaction annealing temperature and expected product size are shown in brackets): Lane 1 – CuA-F and Cys-R (40°C, 1155 bp); Lane 2 – CuA-F and Cys-R (44.4°C, 1155 bp); Lane 3 – CuA-F and Cys-R (50°C, 1155 bp); Lane 4 – CuA-F and MIELD-R (40°C, 987 bp); Lane 5 – CuA-F and MIELD-R (44.4°C, 987 bp); Lane 6 – CuA-F and MIELD-R (50°C, 987 bp). PCR marker sizes in Lane M are indicated to the left. Each PCR reaction used a 2.5°C/sec annealing touchdown ramp to increase primer annealing specificity. Southern blotting of this gel and subsequent membrane manipulation resulted in the membrane found in Panel A, Figure 33.

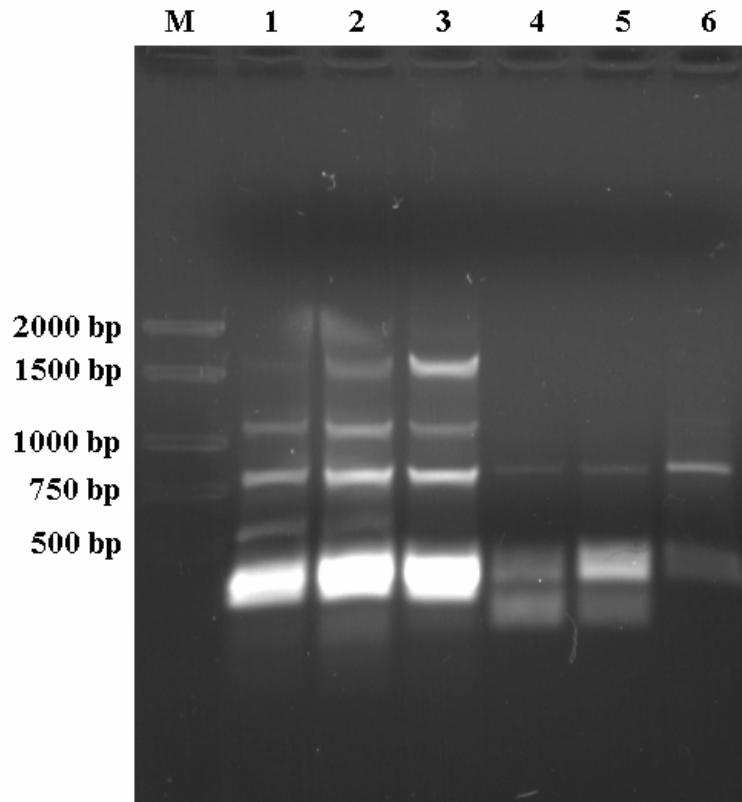


Figure 25: PCR reaction products selected for Southern blotting and subsequent membrane probing. All reactions used the *Spodoptera littoralis* L5p cDNA library as the template DNA. The reaction products in each numbered lane are the result of the following primer pair combinations (reaction annealing temperature and expected product size are shown in brackets): Lane 1 – CuA2-F and CuB2-R (40°C, 606 bp); Lane 2 – CuA2 and CuB2-R (44.4°C, 606 bp); Lane 3 – CuA2-F and CuB2-R (50°C, 606 bp); Lane 4 – CuA2-F and MIELD-R (40°C, 987 bp); Lane 5 – CuA2-F and CuB2-R (44.4°C, 987 bp) Lane 6 – CuA2-F and MIELD-R (50°C, 987 bp). PCR marker sizes in Lane M are indicated to the left. Each PCR reaction used a 2.5°C/sec annealing touchdown ramp to increase primer annealing specificity. Southern blotting of this gel and subsequent membrane manipulation resulted in the membrane found in Panel B, Figure 33.

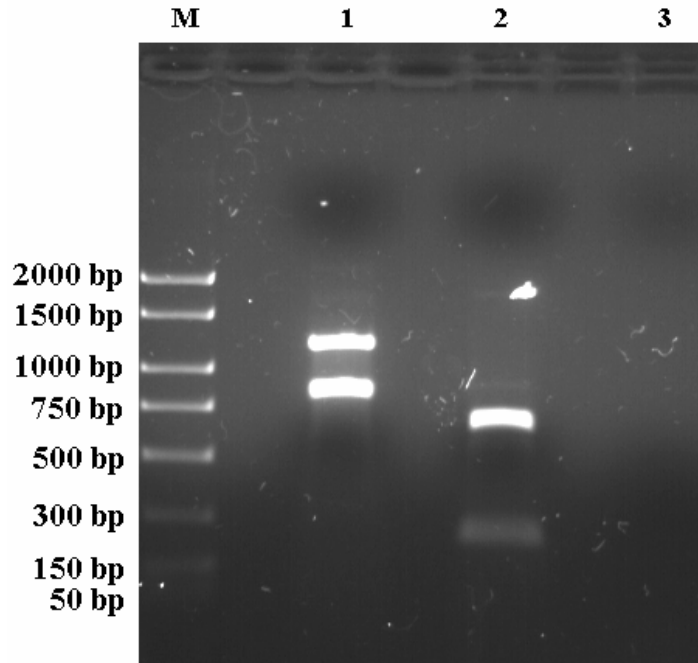


Figure 26: PCR reaction products selected for Southern blotting and subsequent membrane probing. All reactions used the *Spodoptera littoralis* L5p cDNA library as the template DNA. The reaction products in each numbered lane are the result of the following primer pair combinations (reaction annealing temperature and expected product size are shown in brackets): Lane 1 – GELF-F and Cys-R (55°C, 1044 bp); Lane 2 – CuA4-F and Cterm-R (49.4°C, 1341 bp) and Lane 3 – contains 1  $\mu$ l of a 1:10 dilution of the *M. sexta* PPO1 clone plasmid as a control for subsequent hybridisation steps. PCR marker sizes in Lane M are indicated to the left. Each PCR reaction used a 2.5°C/sec annealing touchdown ramp to increase primer annealing specificity. Southern blotting of this gel and subsequent membrane manipulation resulted in the membrane found in Panel C, Figure 33.

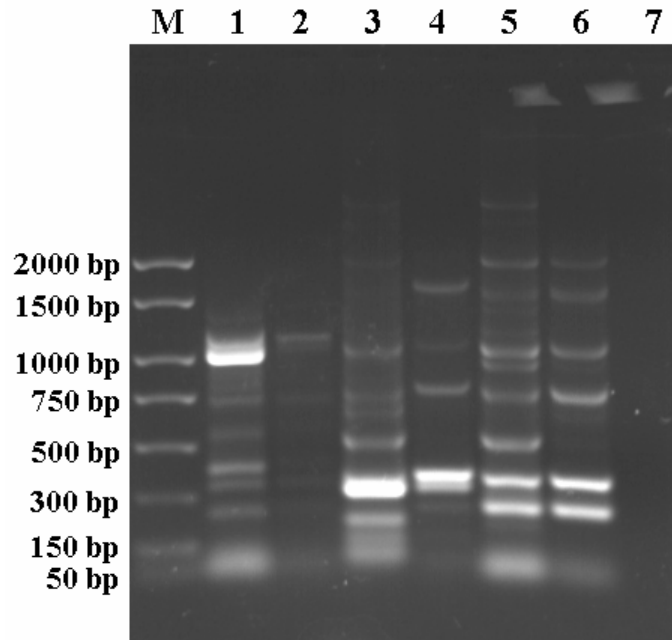


Figure 27: PCR reaction products selected for Southern blotting and subsequent membrane probing. All reactions used the *Spodoptera littoralis* L5p cDNA library as the template DNA. The reaction products in each numbered lane are the result of the following primer pair combinations (reaction annealing temperature and expected product size are shown in brackets): Lane 1 – CuA-F and MIELD-R (40°C, 987 bp); Lane 2 – CuA-F and MIELD-R (44.4°C, 987 bp); Lane 3 – CuA2-F and CuB2-R (40°C, 606 bp); Lane 4 – CuA2-F and CuB2-R (50°C, 606 bp); Lane 5 – CuA2-F and MIELD-R (40°C, 987 bp); Lane 6 – CuA2-F and MIELD-R (50°C, 987 bp); and Lane 7 – contains 1  $\mu$ l of a 1:10 dilution of the *M. sexta* PPO1 clone plasmid as a control for subsequent hybridisation steps. PCR marker sizes in Lane M are indicated to the left. Each PCR reaction used a 2.5°C/sec annealing touchdown ramp to increase primer annealing specificity. Southern blotting of this gel and subsequent membrane manipulation resulted in the membrane found in Panel A, Figure 34.

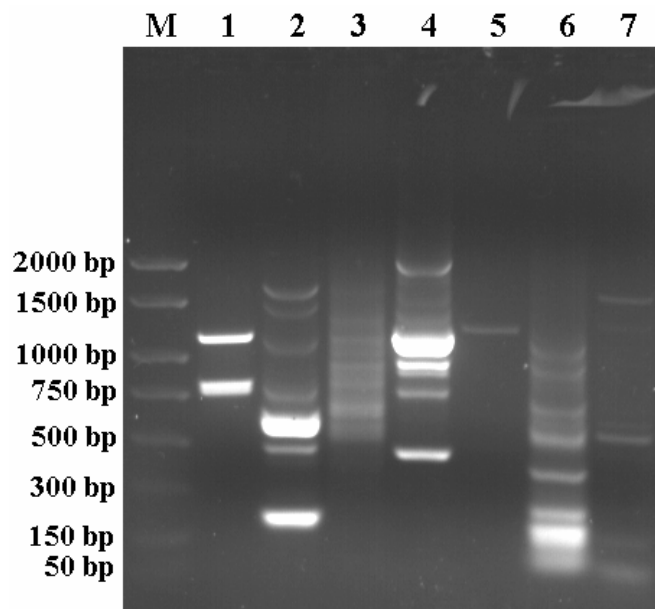


Figure 28: PCR reaction products selected for Southern blotting and subsequent membrane probing. All reactions used the *Spodoptera littoralis* L5p cDNA library as the template DNA. The reaction products in each numbered lane are the result of the following primer pair combinations (reaction annealing temperature and expected product size are shown in brackets): Lane 1 – GELF-F and Cys-R (55°C, 1044 bp); Lane 2 – CuA4-F and Cterm-R (49.4°C, 1341 bp); Lane 3 – CuA4-F and Cterm-R (45°C, 1341 bp); Lane 4 – GELF-F and Cys2-R (55°C, 1044 bp); Lane 5 – GELF-F and Cys2-R (60.9°C, 1044 bp); Lane 6 – CuA-F and Cys-R (40°C, 1155 bp); and Lane 7 – CuA-F and Cys-R (50°C, 1155 bp). PCR marker sizes in Lane M are indicated to the left. Each PCR reaction used a 2.5°C/sec annealing touchdown ramp to increase primer annealing specificity. Southern blotting of this gel and subsequent membrane manipulation resulted in the membrane found in Panel B, Figure 34.

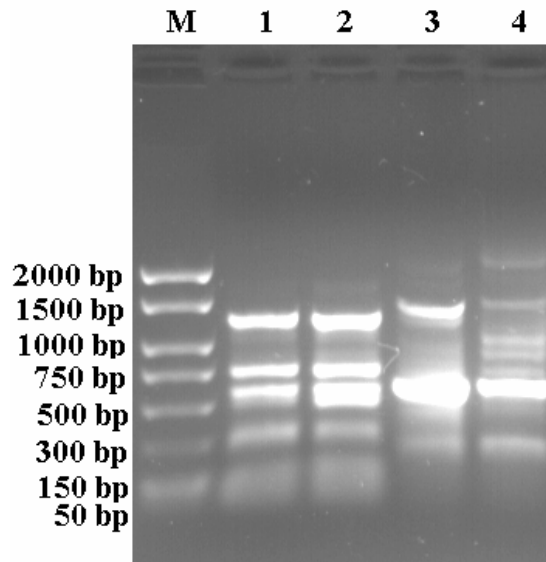


Figure 29: PCR reaction products selected for Southern blotting and subsequent membrane probing. All reactions used the *Spodoptera littoralis* L5p cDNA library as the template DNA. The reaction products in each numbered lane are the result of the following primer pair combinations (reaction annealing temperature and expected product size are shown in brackets): Lane 1 – MsextaPPO1-F and MsextaPPO1-R (35°C, 1158 bp); Lane 2 – MsextaPPO1-F and MsextaPPO1-R (40.6°C, 1158 bp); Lane 3 – MsextaPPO2-F and MsextaPPO2-R (35°C, 1179 bp); Lane 4 - MsextaPPO2-F and MsextaPPO2-R (45°C, 1179 bp). PCR marker sizes in Lane M are indicated to the left. Each PCR reaction used a 1°C/sec annealing touchdown ramp to increase primer annealing specificity. Southern blotting of this gel and subsequent membrane manipulation resulted in the membrane found in Figure 35.

#### **4.3.2 DIG-labelled PPO1 probe hybridisation to membrane bound PCR product DNA could not conclusively identify any prophenoloxidase DNA.**

Whilst a single, PCR amplified DNA band on an agarose gel may appear to have the approximate base pair size predicted from the primer combination used, one cannot assume it represents the desired DNA fragment. Furthermore, as was the outcome of section 4.3.1, PCRs may generate multiple products of varying size as a result of non-specific primer annealing and strand amplification. Southern blotting of DNA gels and membrane hybridisation using a labelled probe, heterologous to the gene of interest, enables more confident identification of DNA fragments amplified during PCR which represent the target DNA. Two heterologous DIG-labelled PPO probes were successfully generated, from a clone of either *M. sexta* PPO1 or PPO2, during PCRs in which some TTP was replaced with DIG-11-UTPs. Successfully labelled probes were identified on the basis of their apparent slower electrophoretic mobility compared to the corresponding non-labelled probe reactions (Figure 30).

The DIG-labelled PPO1 probe was initially used in hybridisation of a dot blot, spotted with serial dilutions of the *M. sexta* PPO1 clone plasmid. This procedure allowed determination of the probes sensitivity and also demonstrated whether the colorimetric system was effective enough for bound probe detection. The resulting membrane (Figure 31) indicated that the DIG-PPO1 probe was capable of detecting PPO DNA at concentrations as low as 2 pg and was therefore suitable for use in probing for PPO DNA. Similarly, the NBT/BCIP

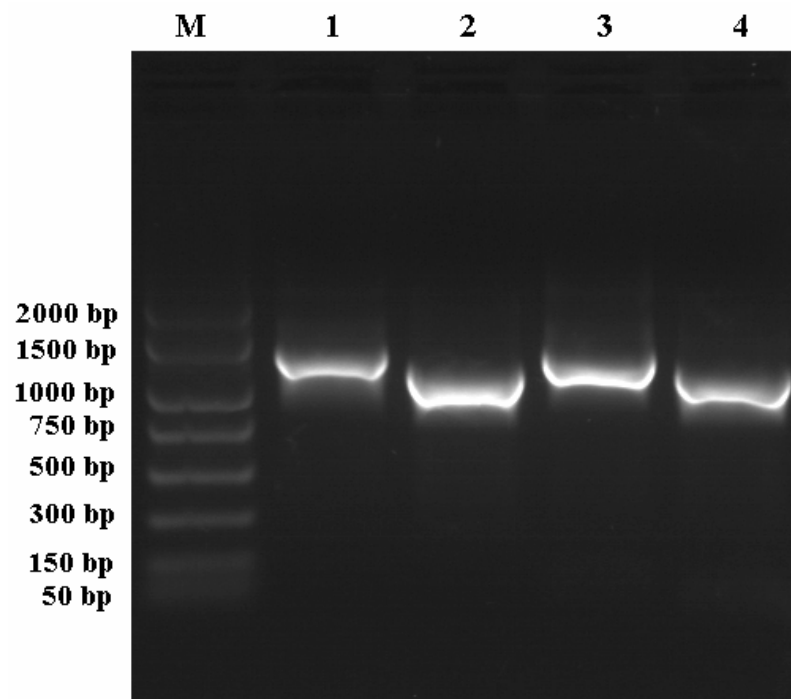


Figure 30: DIG-labelled heterologous prophenoloxidase probe synthesis. The successful incorporation of DIG-11-UTP into amplified *M. sexta* PPO1 and PPO2 clones during PCR is determined by electrophoresis. The resulting DIG-labelled PPO1 and PPO2 probes (Lanes 1 and 3 respectively) show an apparent increase in their base pair size compared to the corresponding non-labelling reactions (Lanes 2 and 4 respectively).

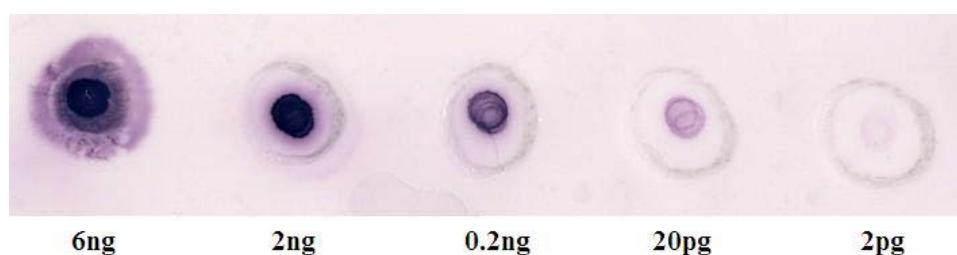


Figure 31: DIG-labelled PPO-1 probe hybridised dot blot spotted with a series of dilutions of the *M. sexta* PPO1 clone plasmid. This method provides a control to test the sensitivity of the DIG-labelled PPO1 probe, and also to determine whether the NBT/BCIP colourimetric detection method is suitable. 2  $\mu$ l of each of the dilutions of the *M. sexta* PPO1 clone plasmid was spotted onto the membrane as detailed.

colourimetric system was suitable for the detection of membrane bound probe, with no evidence of background staining or non-staining at low probe binding levels.

The PCR product-bound membranes, generated by Southern blotting of the gels shown in Figure 22 to Figure 29, were subjected to hybridisation and colourimetric detection protocols like those used in production of the dot blot above, producing the membranes shown in Figure 32 to Figure 35. The precise hybridisation conditions are detailed within each figure caption. Upon first glance it was immediately evident that probe binding to membrane-bound DNA was highly non-specific. Whilst, as expected, the DIG-PPO1 probe bound strongly to bands in the lanes containing its own parent DNA (the *M. sexta* PPO1 clone), DNA marker and multiple PCR product band binding also occurred, even under high stringency conditions. Ultimately, the non-specificity of the DIG-PPO1 probe binding presented the problem that any DNA bands which may have contained PPO DNA could not be identified conclusively.

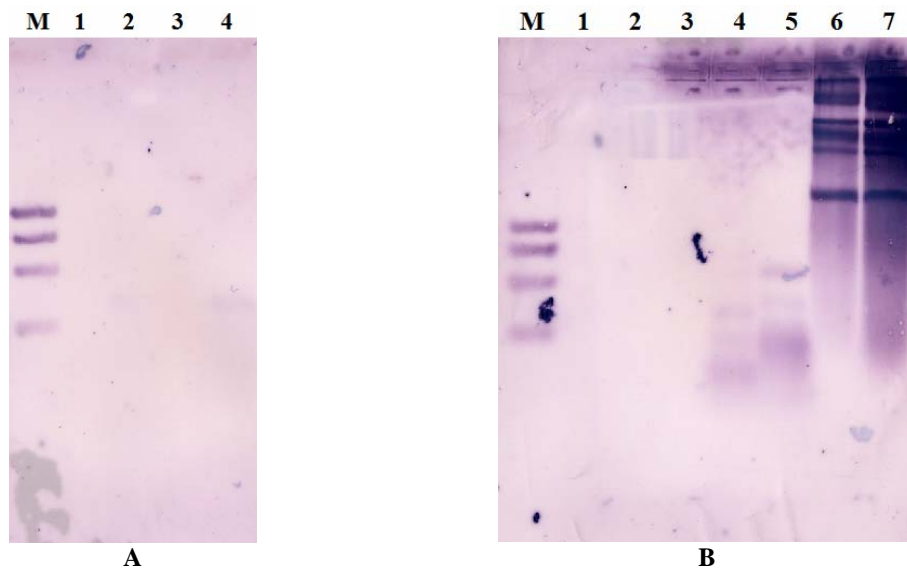


Figure 32: DIG-labelled PPO1 probe hybridized membranes. Membranes were subjected to 60°C hybridisation and low and moderate stringency washes prior to Anti-DIG-AP antibody incubation and BCIP/NBT colorimetric detection protocols. Membranes A and B contain bound DNA transferred by Southern blotting from the gels shown in Figure 22 and Figure 23 respectively.

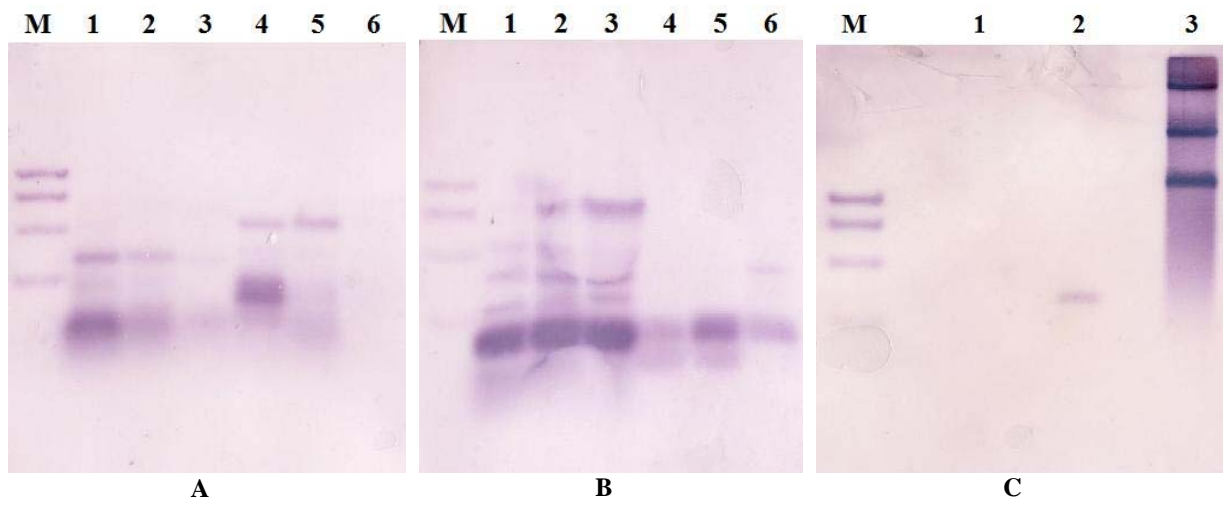


Figure 33: DIG-labelled PPO1 probe hybridized membranes. Membranes were subjected to a 65°C hybridisation step and low and moderate stringency washes prior to Anti-DIG-AP antibody incubation and BCIP/NBT colorimetric detection protocols. Membranes A, B and C contain bound DNA transferred by Southern blotting from the gels shown in Figure 24, Figure 25 and Figure 26 respectively.

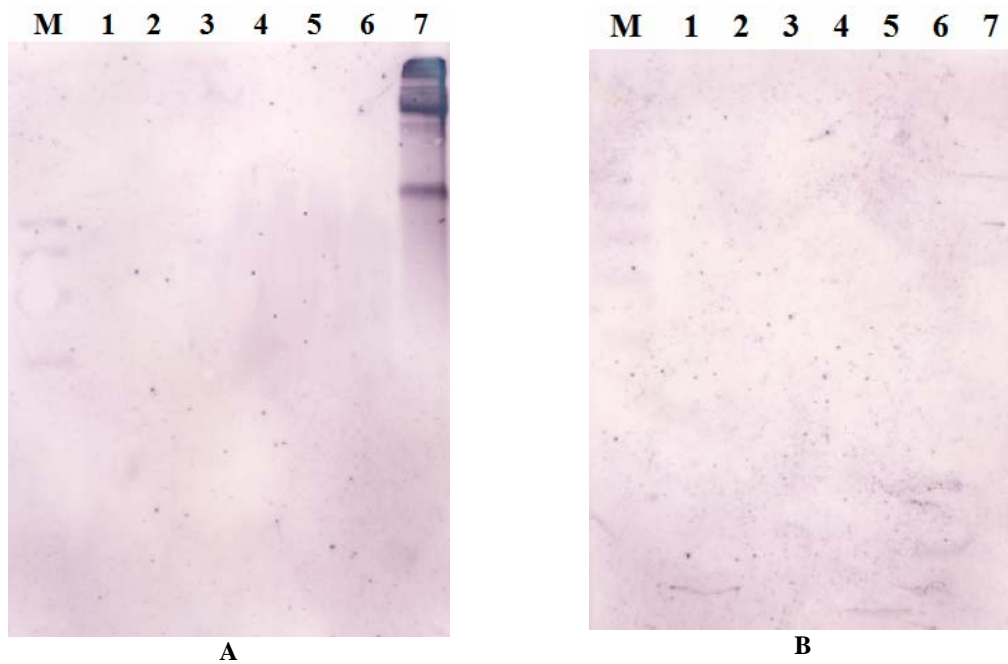


Figure 34: DIG-labelled PPO1 probe hybridized membranes. Membranes were subjected to a 65°C hybridisation step and low and high stringency washes prior to Anti-DIG-AP antibody incubation and BCIP/NBT colorimetric detection protocols. Membranes A and B contain bound DNA transferred by Southern blotting from the gels shown in Figure 27 and Figure 28 respectively.



Figure 35: DIG-labelled PPO1 probe hybridized membrane. Membranes were subjected to a 65°C hybridisation step and low and high stringency washes prior to Anti-DIG-AP antibody incubation and BCIP/NBT colorimetric detection protocols. Membrane contains bound DNA transferred by Southern blotting from the gel shown in Figure 29.

### **4.3.3 cDNA library screening and genomic DNA digests, initially suggest *Spodoptera littoralis* does not contain a prophenoloxidase gene.**

Southern blot analysis of attempts to amplify the *S. littoralis* PPO gene, using specifically designed degenerate primers, failed to reveal whether any PPO cDNA had been amplified from the *S. littoralis* L5p cDNA library. This was despite control experiments demonstrating that particular combinations of degenerate primers successfully amplified a PPO DNA fragment from *M. sexta*.

To further test whether or not the cDNA library contained any PPO cDNA, a library screen was performed as described in methods section 4.2.3. Assuming a fully intact cDNA library, it was hypothesised that DIG-labelled probe hybridisation of the resulting plaque lift membranes, would result in membranes with small regions of staining representing those plaques on the original plates which contained PPO cDNA. As can be seen in Figure 36, the cDNA library screening process produced no evidence of staining suggesting no PPO cDNA was present.

In a bid to rule out the possibility that *S. littoralis* has no PPO gene in the first instance, a restriction digest of *S. littoralis* hemocyte genomic DNA was performed. As discussed in Chapter 2, hemocytes are believed to be the source of PPO in insects. Prior to conducting the digest reactions, the integrity of the isolated genomic DNA was tested by electrophoresis of a small aliquot of each sample (1A, 2A and 2B) in an agarose gel. This gel (Figure 37)

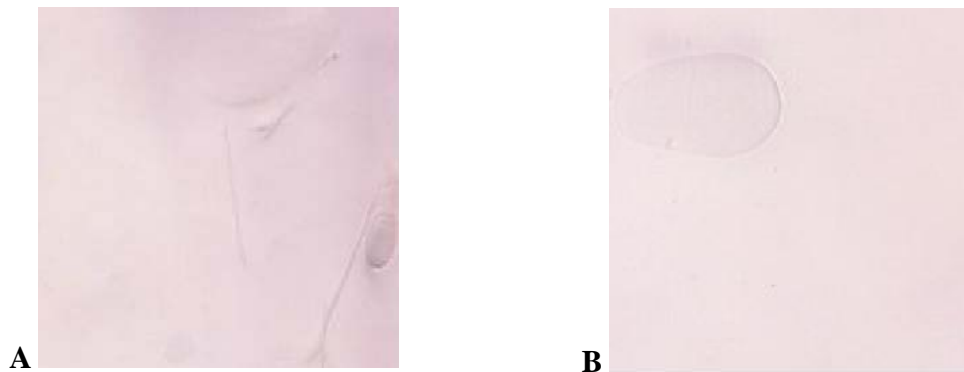


Figure 36: Plaque lift membranes from a screen of the *S. littoralis* L5p cDNA library. Plaque lifts were conducted on each of six plates in duplicate. All were hybridised with the DIG-labelled PPO1 probe at 65°C and washed under low and moderate stringency conditions. The duplicate membranes above are representative of all the membrane pairs resulting from screening of the cDNA library. They show no small dots of staining representing DIG-labelled PPO1 probe binding, suggesting perhaps that the cDNA library was of poor quality and therefore did not contain any representative PPO cDNA or that *S. littoralis* does not contain a PPO gene.

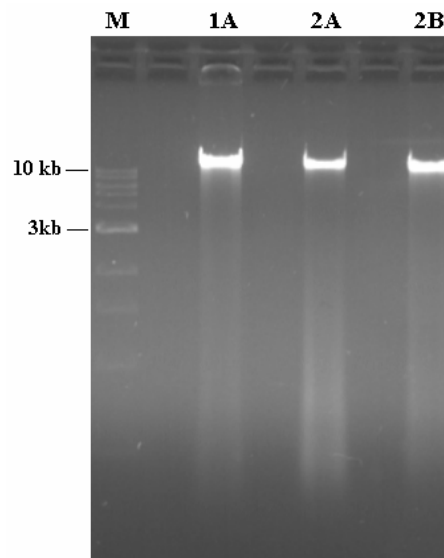


Figure 37: Check of *S. littoralis* genomic DNA integrity. Genomic DNA was isolated from *S. littoralis* hemocytes by Nairn (2003, unpublished work). Prior to its use in restriction digest reactions, 4µl of each DNA sample (1A, 2A and 2B) was electrophoresed on a 0.8% agarose 1X TBE 0.2 µg/ml EtBr gel to check its integrity. Lane 'M' contains the 1kb DNA ladder markers (New England BioLabs Cat# N32325). The resulting gel shows that each sample had remained intact during storage, but DNA sample 1A has a higher yield.

confirmed that the genomic DNA in all three samples was intact; although sample 1A appeared to have a higher yield, so was that used for subsequent restriction digests.

The restriction enzymes *EcoRI* and *HindIII* were used separately and in combination during both first and second attempt genomic DNA digest reactions, the products of which were separated by electrophoresis and transferred to the surface of a nylon membrane by Southern blotting. DIG-labelled probe hybridisation, washing, antibody incubation and bound probe detection produced the membranes shown in Figure 38. During both the first and second attempts at probing the digest products, the DIG-labelled PPO1 probe bound only to those regions of the membranes which contained the *M. sexta* clone PPO1 plasmid DNA – that is, the probes parent DNA which was used as a control for the hybridisation and detection steps. No genomic DNA digest fragments showed any evidence of probe binding, which suggests that *S. littoralis* hemocyte genomic DNA contains no stretch of sequence with identity to the *M. sexta* PPO probe.

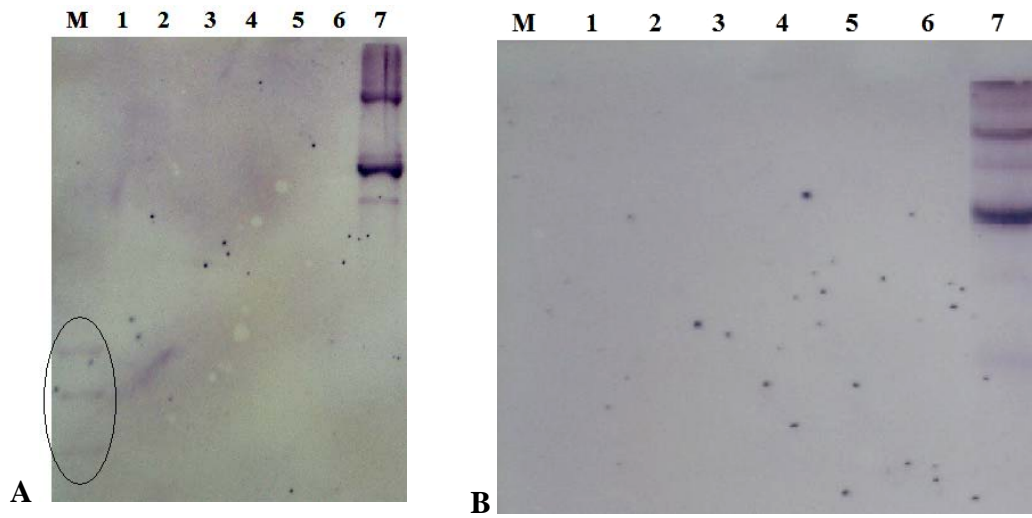


Figure 38: DIG-labelled PPO1 probe incubated nylon membranes generated by Southern blotting of agarose gels containing the separated products of a series of *S. littoralis* genomic DNA restriction digest reactions. Membranes A and B were generated by repeats of the methods. Membranes were hybridised at 65°C and washed using low and high stringency wash conditions. The lane contents are as follows: EcoR1 digest products (Lane 1), HindIII digest products (Lane 2), EcoR1/HindIII digest products (Lane 3), non-digested *S. littoralis* hemocyte genomic DNA (Lane 4), and the *M. sexta* PPO1 clone plasmid from which the DIG-labelled probe used was synthesised (Lane 7). DIG-PPO1 probe binding could only be detected in that lane (Lane 7) which contained the *M. sexta* clone PPO1 plasmid DNA – the template DNA of the probe. Binding of the DIG-PPO1 probe to the marker DNA is visible in Lane M of membrane A (circled).

Analogous to the non-specificity of the probe highlighted in section 4.3.2, there is evidence of probe binding to the DNA marker bands. Once again this suggests non-specificity in the binding of the DIG-labelled PPO1 probe to DNA. Whilst a dot blot had been conducted (Methods 4.2.2.2 and Results 4.3.2) which demonstrated that the DIG-PPO1 probe was sensitive enough for its designed use, continued speculation over its specificity deemed it necessary to perform much more rigorous control experiments in an attempt to establish whether either of the probes synthesised in section 4.2.2.1 (DIG-PPO1 or DIG-PPO2) had suitable specificity in the recognition and binding of heterologous PPO sequences. The results of these controls form the basis of the following section.

#### **4.3.4 Neither DIG-labelled probe is suitably sensitive or specific enough for its intended use.**

An alignment of the amino acid sequence of either *M. sexta* PPO1 or *M. sexta* PPO2 with the sequences of eight different Lepidoptera PPOs, showed that *M. sexta* PPO1 shared a slightly higher percentage identity to these other PPO sequences than *M. sexta* PPO2. It was hypothesised that the probe generated from the clone of *M. sexta* PPO1, would therefore have a sequence with a higher percentage identity to a PPO from *S. littoralis*. Numerous rounds of *M. sexta* PPO1 probe hybridisation and detection were performed to identify any PPO DNA present amongst: (i) the products of PCR reactions using an *S. littoralis* cDNA library and different combinations of specifically designed degenerate primers for PPO amplification; (ii) *S. littoralis* cDNA library plaque lifts and; (iii) the products of *S. littoralis* genomic DNA digests. Consequently, no *S. littoralis* PPO DNA was identified, as noted in sections 4.3.2

and 4.3.3, and suspicions were raised over the probes' ability to detect and specifically bind to PPO sequences heterologous to its own sequence.

Results are presented (Figure 39 and Figure 40) of a control experiment, performed to elucidate which of the two DIG-labelled probes was the more specific, and therefore which was the most suited to its designed purpose. Duplicate membranes were probed with one or the other of the DIG-labelled probes (DIG-PPO1 or DIG-PPO2), and compared on the basis of their bound probes' sensitivity and specificity towards PPO DNA. The membranes indicated that the DIG-PPO2 probe was more sensitive for detecting PPO DNA heterologous to its own sequence, and not the DIG-PPO1 probe as initially hypothesised. This was surmised on the basis that the DIG-PPO2 probe shows the ability to recognise both *M. sexta* PPO1 and PPO2 DNA at suitably high levels at both 65°C and 68°C hybridisation temperatures, whilst the DIG-PPO1 probe shows strong recognition of *M. sexta* PPO1 DNA but only very weak recognition of *M. sexta* PPO2 DNA. More importantly however both the DIG-PPO1 and DIG-PPO2 probes demonstrated high levels of non-specificity in their binding to PPO DNA. In both cases, the probes bound to the DNA markers and non-specific PCR products, as well as the probes parent DNA. Ultimately, these results revealed that the DIG-PPO2 probe was the more sensitive of the two probes for the detection of heterologous PPO DNA sequences, however, the demonstration of persistent non-specificity by both probes, under high stringency conditions, made it clear that neither was suitable for its intended use.

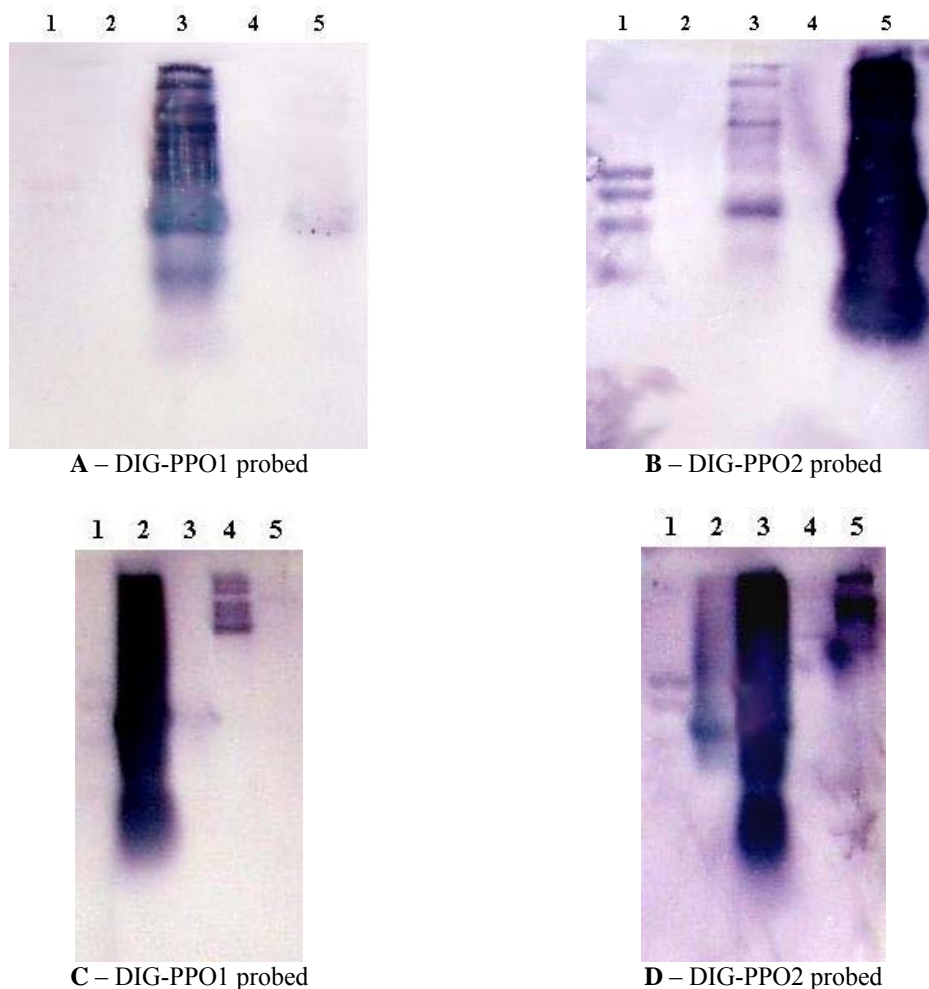


Figure 39: Probing of duplicate membranes with the DIG-PPO1 or DIG-PPO2 DNA probe to determine which was the more sensitive and specific in the recognition and binding of a PPO sequence heterologous to its own. Replica membranes A and B contain PCR markers (Lane 1), products of a PCR reaction amplifying the *M. sexta* PPO1 clone using CuA3-F and Cys-R primers (Lane 3) and products of a PCR reaction amplifying the *M. sexta* PPO2 clone using CuA3-F and Cys-R primers (Lane 5). In replica membranes C and D the lane contents are 1 – PCR markers, 2 – products of a PCR reaction amplifying the *M. sexta* PPO1 clone using *M. sexta* PPO1-specific forward and reverse primers, 3 – products of a PCR reaction amplifying the *M. sexta* PPO2 clone using *M. sexta* PPO2-specific forward and reverse primers, 4 – a 1:10 dilution of the *M. sexta* PPO1 clone, and 5 – a 1:10 dilution of the *M. sexta* PPO2 clone. All four membranes were hybridised at 65°C and washed under low and moderate stringency washes. Ultimately the DIG-PPO2 probe was the most sensitive of the two probes however neither probe demonstrated any specificity solely for PPO DNA, evidenced by their binding to marker and non-specific PCR product DNA bands

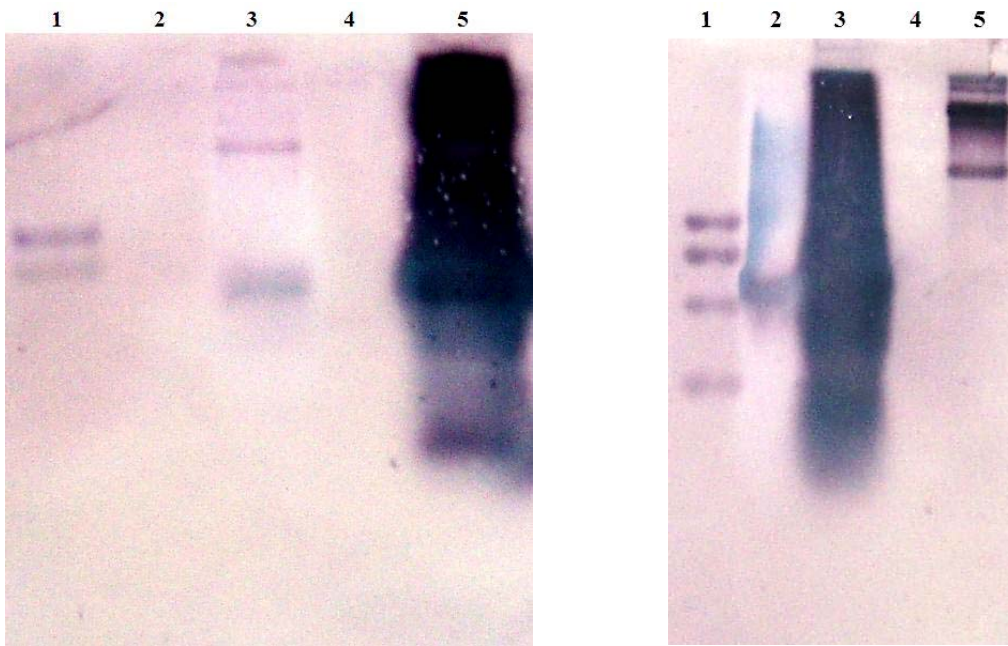


Figure 40: Probing of duplicate membranes using the DIG-PPO2 probe at 68°C hybridisation and using low and high stringency washes. Probing and bound probe detection methods were also identical. Lane contents of membranes A and B above are as described in Figure 39 for membranes A and B respectively. The conditions used here included a higher hybridisation temperature and higher wash stringency than was used in probing of the membranes in Figure 39, in an attempt to eliminate binding of the DIG-PPO2 probe to marker DNA and other non-PPO DNA PCR products. Unfortunately these efforts failed to reduce the non-specificity of the DIG-PPO2 probe, and as is evident, probe binding to markers and other DNA bands remains an issue even under these higher stringency conditions.

## **4.4 Discussion**

The results presented within the current chapter were the outcome of experiments designed for the purpose of isolating, amplifying and characterising a PPO gene from the Lepidoptera insect *S. littoralis*. A range of molecular methods were employed, each generating DNA-bound membranes which were subsequently hybridised with a heterologous DIG-labelled PPO DNA probe. Despite numerous efforts, no PPO gene fragment could be conclusively identified amongst multiple PCR products or during library screening and genomic DNA digests. The following sections discuss the results and offer possible explanations, considered during the progress of the research, as to why no PPO gene could be identified.

### **4.4.1 PPO gene transcription may be inhibited in Braconid wasp parasitised Lepidoptera larvae.**

The larval cDNA library utilised during PCR and library screening procedures had been generated from whole *S. littoralis* larvae, parasitized by the Braconid wasp, *C. inanitus*. It was initially proposed that this cDNA library would be enriched with PPO cDNA, and therefore suited to its intended use. Following analysis of the results from PCR product probing and cDNA library screens (presented in sections 4.3.2 and 4.3.3), it seemed, however, that the *S. littoralis* cDNA library contained no identifiable PPO cDNA.

Consideration was given to the possibility that parasitisation of *S. littoralis* larvae by *C. inanitus*, may cause temporary cessation of transcription of the insects PPO gene(s). Reports have provided evidence for the negative effects of parasitisation on immune response

mechanisms (Lavine and Beckage, 1995; Amaya et al., 2005) and although there is evidence that the effects of parasitisation on other immune response and development-associated proteins are at some post-transcriptional step (Shelby et al., 1998), it was deemed feasible that host biological pathways could be controlled at various gene expression steps, to optimise conditions for the growth and development of the parasitoid wasp egg.

A recent publication (Schlenke et al., 2007) has provided new evidence to suggest that control of PO activity in parasitoid wasp infected *Drosophila melanogaster* larvae can vary depending on the parasitoid species involved. Furthermore, Schlenke et al, 2007 report that the normal upregulation of PPO gene expression resulting during immune response can be blocked by an as yet unidentified pathway, upon parasitisation of *D. melanogaster* by *Leptopilina boulardi*. This implies a transcriptional level of control over the action of PO in this particular host-parasitoid system.

At this time there is no conclusive evidence to suggest that PPO gene transcription in Lepidoptera is affected by parasitisation. However amongst the different host-parasitoid systems thus far studied, the hosts immune response and physiology have been shown to be impaired to various extents and at different transcriptional, translational and protein levels. The molecular mechanisms underlying the effect of PDVs, ovarian and venom proteins on Lepidoptera host immune systems and physiology, nonetheless remain largely undetermined (Zhang et al., 2004). Subsequently, before any confident conclusion can be made as to whether or not the parasitized larvae cDNA library used here would have contained any PPO cDNA, a greater understanding of these mechanisms is necessary.

#### **4.4.2 The cDNA library may have been synthesised from a low PPO transcript copy number or degraded RNA source.**

Research using *Spodoptera litura* has demonstrated that PPO mRNA transcripts vary in abundance in native non-immune challenged hemocytes during the course of larval development (Rajagopal et al., 2005). Larvae used in those experiments were only large enough to bleed during the 4<sup>th</sup>, 5<sup>th</sup> and 6<sup>th</sup> instars, but it was noted that PPO transcript levels increased at the start of the 4<sup>th</sup> instar, peaked during the 5<sup>th</sup>, and fell during the 6<sup>th</sup>. Therefore, it may be proposed that hemocyte PPO mRNA is present at its maximal concentration during the active feeding stage of all *Spodoptera* spp. larvae. The cDNA library utilised (L5p) was from 5<sup>th</sup> instar *S. littoralis* larvae, so provided parasitisation does not affect PPO gene transcription, PPO mRNA was hypothesised to have been abundantly present for isolation prior to the synthesis of the cDNA library.

RNA isolation and cDNA synthesis are, however, very difficult tasks to achieve successfully unless the laboratory environment is free from RNase contamination. RNase enzymes act to degrade RNA molecules, and therefore any cDNA synthesised from a degraded mRNA source will not be a complete representation of all the transcripts present in the tissue or organism at the time of RNA isolation. Consequently, despite confidence that the cDNA library was viable (as demonstrated in section 4.3.1 during amplification of actin) and had been synthesised from a PPO mRNA rich source, it cannot be dismissed that the isolated RNA was partially degraded during any of the preparative steps of cDNA library synthesis, leading to a reduction in, or complete loss of, intact PPO mRNA.

#### **4.4.3 No PPO DNA could be identified due to the low sensitivity and high non-specificity of the DIG-labelled probe.**

The next phase of experiments addressed the persistent problem of DIG-labelled PPO1 probe non-specificity. The DIG-PPO1 probe was chosen for use in all membrane hybridisation steps, as *M. sexta* PPO1 demonstrated slightly higher identity than *M. sexta* PPO2 to a number of other Lepidoptera PPO sequences. It was thought this would increase the likelihood of specifically identifying an *S. littoralis* DNA fragment. However, following numerous attempts to hybridise a probe to a PCR product or DNA digest band, it became apparent that this was not the case. It was evident that the DIG-PPO1 probe lacked the specificity required of a probe used for identification of a particular DNA. A control experiment was conducted to evaluate the nature of each DIG-labelled probes sensitivity and specificity towards heterologous PPO DNA. These control membranes (Figure 39, section 4.3.4) demonstrated that the DIG labelled PPO2 probe was in fact the more sensitive of the two probes, binding substantially to both a heterologous PPO DNA (*M. sexta* PPO1 clone) as well as its own parent DNA (*M. sexta* PPO2 clone). Nonetheless, neither of the probes possessed any kind of specificity solely towards PPO DNA, binding also to marker and non-specific PCR product DNA, even under high stringency hybridisation and membrane wash conditions. It therefore cannot be dismissed that PPO DNA fragments were present amongst the cDNA library screening plaques, PCR or restriction digest products. Based on the evidence provided from these control experiments, the poor specificity displayed by the DIG-PPO1 probe was deemed the most feasible explanation for the unsuccessful attempts to identify an *S. littoralis* PPO DNA.

#### 4.4.4 Summary of conclusions.

Despite efforts to identify a PPO gene fragment from the parasitized *S. littoralis* cDNA library, none were identified by either cDNA library screening or Southern blotting of gel separated PCR or restriction digest products. A number of possible explanations have been offered including the possibility that parasitisation blocks the normal upregulation of PPO gene transcription in *S. littoralis*, as has been shown to be the case with the *Drosophila melanogaster*-*Leptopilina boulardi* host-parasitoid system. It is highly unlikely that *S. littoralis* lacks any PPO gene as previous research has demonstrated that the hemolymph of this insect species possesses PO activity (Cotter and Wilson, 2002; Lee and Anstee, 1995; Cotter et al., 2004). In addition, PPO has previously been purified from *S. littoralis* and identified by peptide mass fingerprinting (Nairn, 2003, unpublished data). However, evidence suggests the most likely reason was that neither of the DIG-labelled PPO probes used during hybridisation possessed sufficient specificity to identify heterologous PPO DNA. On the basis of sequence identity amongst a number of Lepidoptera PPOs, it was proposed that *S. littoralis* PPO would share approximately 30 - 40% identity with *M. sexta* PPO. *Manduca sexta* PPO1 and PPO2 are approximately 50% identical in amino acid sequence. Given that, under high stringency conditions, the DIG-labelled probe generated from one could not recognise the other with high specificity, and both still bound to the DNA markers, it became clear these probes would be unlikely to recognise and bind heterologous PPO sequences from any closely related species. Ultimately, even if the cDNA library screening plaque lift, restriction digest or PCR gel membranes had contained PPO DNA bound at their surfaces, using the currently discussed DIG-labelled probes would not have enabled confident identification of a PPO DNA.

## **Chapter 5 : Steps towards isolating a Prophenoloxidase Gene from *Spodoptera littoralis* hemocytes.**

### **5.1 Introduction**

Current research suggests that PPO is synthesised solely in insect hemocytes, or more specifically, the oenocytes (Müller et al., 1999). Subsequently PPO gene transcripts can be found only in this cell type. In Chapter 4, the cDNA library used to screen for a PPO gene had been generated from whole larvae preparations, and consideration was given to the possibility that PPO mRNA was in low abundance relative to the transcripts of the genes in other insect tissues. This may have contributed to the difficulties encountered during attempts to isolate a PPO gene. Also discussed in Chapter 4 was the possibility that Brachonid wasp parasitized *S. littoralis* larvae, such as those used for synthesis of the cDNA library, experience a reduction in the transcription of a number of immune system and physiologically important genes, including PPO. Evidence suggests that the effects of parasitisation on the host can occur at multiple points during the steps from gene to DNA to protein in order to disrupt host immune function and physiology. These effects also appear to vary between host-parasitoid systems. It is therefore possible that *C. inanitus* parasitized *S. littoralis* may display reduce PPO mRNA levels. This would increase the technical difficulties associated with PPO gene isolation from such a source.

*Spodoptera* sp. exhibit a trait known as density dependent phase polyphenism, where larvae reared under conditions of low population density (LD) during development appear pale

brown/green in colour with light brown head capsules, and those which develop under high population density (HD) have very dark brown cuticles and head capsules (see Figure 41).



Figure 41: *Spodoptera littoralis* larvae display a characteristic known as density dependant phase polyphenism. Individuals reared in high density populations have darker cuticles and head capsules due to enhanced cuticular melanisation (left), compared to those reared in low density populations, which are usually pale brown/green with pale brown head capsules. Scale shown is in centimetres.

Research has directly correlated these phenotypes to the level of PO activity detectable in the hemolymph of representatives of each population density (Cotter et al., 2004). HD larvae are proposed to invest more in immune function as they are more likely to encounter infection. Enhanced immune function results in higher levels of PO activity and the subsequent deposition of melanin leading to the darkening of the insects' cuticle. LD larvae experience the opposite.

The aim of the following research was to generate first strand cDNA from RNA isolated from the hemocytes of non-parasitised *S. littoralis* larvae. This cDNA was intended to act as the template DNA for real time PCR experiments designed to amplify a PPO gene. It was

hypothesised that using hemocytes from a non-parasitised larval source would eliminate the possible difficulties mentioned above. Problems encountered during attempts to isolate intact total RNA from *S. littoralis* hemocytes, and time constraints on the project limited the progress of these experiments.

## **5.2 Methods**

### **5.2.1 *Spodoptera littoralis* larvae culture.**

3 - 4 day old *S. littoralis* larvae were initially derived from a laboratory colony held by Dr. Kenneth Wilson at the University of Lancaster. Individuals were selected at random for solitary rearing (representing low density population, *solitaria* phase) whilst 5 larvae from the same family were used to recreate a high density scenario (*gregaria* phase). Larvae were reared in 50 ml culture pots on a semi-artificial wheatgerm-based diet (Reeson et al., 1998). Up to 4 days old, larvae were maintained under a 14 hours of light: 10 hours of dark regime at a constant temperature of 25°C. From day 5 onwards, larvae were reared to a suitable size for hemolymph collection at 22 ± 2°C under an approximately 12/12 hour light/dark cycle.

### **5.2.2 Hemolymph collection and isolation of hemocytes.**

Larvae were sedated by chilling at 4°C for approximately 1 hour. 800 µl of RNase-free sterile de-coagulation buffer (10 mM NaCac, 20 mM CaCl<sub>2</sub>, pH 6.5 - 0.1 % DEPC treated) was pipetted into RNase-free sterile 1.5 ml Eppendorf tubes, then placed on ice. Wearing gloves and handling carefully between the thumb and forefinger, a sterile syringe needle was used to puncture the sedated larvas' pro-leg. Any hemolymph which bled from the wound was collected into one of the Eppendorf tubes containing cold de-coagulation buffer. Bled larvae

were returned to their respective diet pots and gloves were rinsed with ethanol prior to handling the next larvae. The hemolymph from a number of larvae was pooled (solitary pale, solitary dark and gregarious larval hemolymph were pooled separately) so that 200  $\mu$ l was collected into each 800  $\mu$ l of de-coagulation buffer. The diluted hemolymph was gently mixed by inverting the Eppendorf tube and then stored on ice.

Following hemolymph collection from all of the larvae, hemolymph samples were centrifuged at 3,500 rpm and 4°C for 5 minutes. Inspection of a sample of the pellet and supernatant under 40X magnification revealed that this method suitably removed hemocytes from suspension without damage. All of the supernatant was removed and the remaining hemocyte pellet was re-suspended, using gentle fingertip agitation, in 200  $\mu$ l of de-coagulation buffer (equal to the volume of hemolymph they originated from).

For storage, the re-suspended hemocytes were pooled into 1 ml batches and centrifuged again at 3500 rpm, 4°C for 5 minutes. Most of the supernatant was aspirated, leaving approximately 200  $\mu$ l above the pellet. The pellet was re-suspended up to 1 ml in RNALater (Ambion Cat# 7020) to stabilise the hemocyte RNA prior to its isolation. The hemocyte samples were then stored at -70°C until use.

### **5.2.3 Total RNA isolation from hemocytes.**

As the presence of RNase results in unwanted degradation of isolated RNA, all solutions, plastic ware, glassware, work surfaces and equipment to be used during RNA isolation were treated appropriately to eliminate ribonuclease (RNase) contamination using detergent,

ethanol, 0.1% DEPC and/or an autoclave. Guaranteed RNase free plastic-ware and solutions were used where possible.

Total RNA was isolated from hemocytes of *S. littoralis* larvae using Ambions' RiboPure™ Kit (Cat# 1924). A minimum of  $5 \times 10^6$  hemocytes were required for each RNA isolation (considered necessary to yield sufficient RNA), therefore isolated RNALater re-suspended *S. littoralis* hemocytes were pooled on the basis that 1 ml of hemolymph contains approximately  $4 \times 10^6$  hemocytes. Due to the viscous nature of RNALater, the sample was centrifuged at 10,000 rpm and 4°C for 5 minutes to pellet the hemocytes. The protocol provided with the RiboPure™ Kit was conducted as outlined from Part B, Step 1b for cells in suspension, with the following modifications: (i) the additional centrifugation step in Part B, Step 3 was conducted to remove insoluble material from the homogenate, (ii) 200  $\mu$ l of chloroform (without isoamyl alcohol) was used in Part C, Step 1 instead of the preferred 100  $\mu$ l of bromochloropropane (BCP), and (iii) the repeat application of 100  $\mu$ l of Elution Buffer suggested in Part D, Step 4 was not conducted to prevent any further dilution of the RNA.

A sample of the eluted RNA was diluted 1:50 with ddH<sub>2</sub>O (0.1 % DEPC-treated and autoclaved) and the A<sub>260</sub> recorded. 40  $\mu$ g/ml of pure ssRNA in water has an A<sub>260</sub> = 1, and from this the approximate concentration of RNA was calculated. To estimate the purity of the isolated RNA, A<sub>280</sub> measurements were recorded. The A<sub>260</sub>:A<sub>280</sub> ratio of suitably purified isolated RNA should be between 1.8 and 2.1. To determine the integrity of the isolated RNA, a volume of the sample containing approximately 2  $\mu$ g of RNA was mixed with Type-II 6X Loading Buffer and loaded onto a native, 1X TBE, 1 % agarose, 0.2  $\mu$ g/ml EtBr gel. Alongside 5  $\mu$ l of Lambda HindIII Markers (ABGene, Cat# AB-0200), the RNA samples

were electrophoresed in 1X TBE at 5 V/cm until the bromophenol blue had migrated approximately two thirds through the length of the gel. The gel was visualized under UV light and its image captured. Any RNA sample identified as being intact and pure, had its remaining volume divided into 10 µl aliquots and stored at -20°C (short term) or -80°C (long term) until use.

## **5.3 Results**

### **5.3.1 Larvae culture.**

*Spodoptera littoralis* larvae were gifted at 4 days old, from which time they were reared to a suitable size for hemolymph collection (approximately 14 - 15 days old). Isolated larvae (phase *solitaria*) and groups of 5 larvae (phase *gregaria*) were reared, and an example of the development of one of the solitary larvae is shown in Figure 42. Whilst the environmental conditions were not optimal, most solitary larvae and some of the gregarious larvae developed successfully and, once ready, were bled once each day for 2 days until pupation. On average each healthy larva provided between 50 and 200 µl of hemolymph, where approximately 1.25 ml was required for each total RNA isolation attempt.



5 days



6 days



7 days



10 days



12 days



14 days

Figure 42: A photographic record of the growth phases of solitary *Spodoptera littoralis* larva over a 14 day period. By day 14/15 larvae were ready for bleeding (3 – 4 cm length), and depending on health, were bled once each day for two days. The scale shown is in centimetres.

However, a number of points were noted during the rearing and bleeding of these *S. littoralis* larvae. All solitary larvae developed successfully with no fatalities recorded. Most exhibited the pale brown/white cuticular colouration expected, although approximately one third displayed evidence of enhanced cuticular melanisation and darkened head capsules. Their appearance was therefore more similar to that of gregarious larvae. None of the gregarious larvae, however, exhibited pale colouration – all possessed very dark cuticular pigmentation and head capsules as expected. Unlike the solitary larvae, in general, most of the gregarious larvae exhibited slower rates of development and an overall smaller final instar larval size. Within each high density culture pot, a drastic variation in the growth rate between gregarious individuals became apparent and was most notable by the final instar/14 days old (Figure 43).



Figure 43: *Spodoptera littoralis* larvae reared under conditions designed to recreate high density population, had slower development rates and smaller larval size than those reared in solitary conditions. A typical example of a high population density (*gregaria* phase) culture pot from this experiment is shown above, and illustrates the great difference in size between individuals by the age of 14 days. Whilst the larva nearest the scale bar is of expected size, that to the centre left is equivalent in size to that of a 10 day old larva. 1 in 4 fatalities occurred in gregarious larvae and many of the surviving gregarious larvae had melanised hemolymph indicative of active PO. The fatalities were generally among the smaller larvae and appeared to be a result of cannibalistic behaviour. The scale shown is in centimetres.

The smaller individuals in each high density culture pot appeared to become victims of cannibalism; however the cannibals could not be identified. It was estimated, assuming that the 'missing' larvae had not died from another cause before their bodies were consumed, that 25 % of the gregarious larvae were lost as a result of cannibalistic behaviour. The surviving group reared larvae were bled in a manner similar to the solitary larvae; however, approximately 50 % of these survivors had hemolymph which appeared blackened and grainy. This suggests that these particular larvae had activated hemolymph PO making their hemolymph unsuitable for collection. These larvae tended to have almost completely black cuticles and were not as active as those gregarious larvae which possessed 'normal' non-PO-activated pale blue hemolymph. The combination of cannibalistic behaviour, and survivors with melanised hemolymph, consequently had a large impact on the total volume of hemolymph which could be pooled from the gregarious larvae. It was therefore necessary to repeat larval culture.

### **5.3.2 Total RNA isolation.**

The first step towards generating first strand cDNA is the isolation of total RNA from the selected tissue or cell type, which in this instance was the hemocyte from *S. littoralis* larvae. Achieving the expected yield of total RNA from the isolation process, initially presented a problem. Using the protocol accompanying the Ambion RNA isolation kit as a guide, it was predicted that approximately 125 µg of total RNA could be yielded from the estimated number of hemocytes pooled for total RNA isolation ( $5 \times 10^6$  cells). The calculated quantity of RNA in each of the first three RNA isolation attempts was, however, never any greater than 74 µg. This problem was overcome in later attempts by using a more rigorous mechanical shearing method to disrupt the hemocytes and release the RNA.

A persistently encountered problem however, was retaining total RNA integrity during isolation. Completely intact mRNA is paramount for the synthesis of first strand cDNA or cDNA libraries, as experiments using degraded sources are unlikely to be fruitful. Five attempts were made to isolate total RNA from *S. littoralis* hemocytes (photographs of attempts 2 - 5 can be found in Section 9.3 - Appendix C); however, none resulted in completely intact total RNA. Figure 44 Panel A shows a native agarose gel electrophoresed sample from the first total RNA isolation attempt. Whilst the 28S and 18S ribosomal RNA bands (rRNAs) are identifiable, smearing indicates degradation of the RNA sample. rRNA from completely intact total RNA appears as two sharp, clear bands (example in Figure 44 Panel B), which was clearly not the case with this, or any of the other four, isolated samples. None of the isolated hemocyte total RNA samples were therefore suitable for use in the synthesis of first strand cDNA.

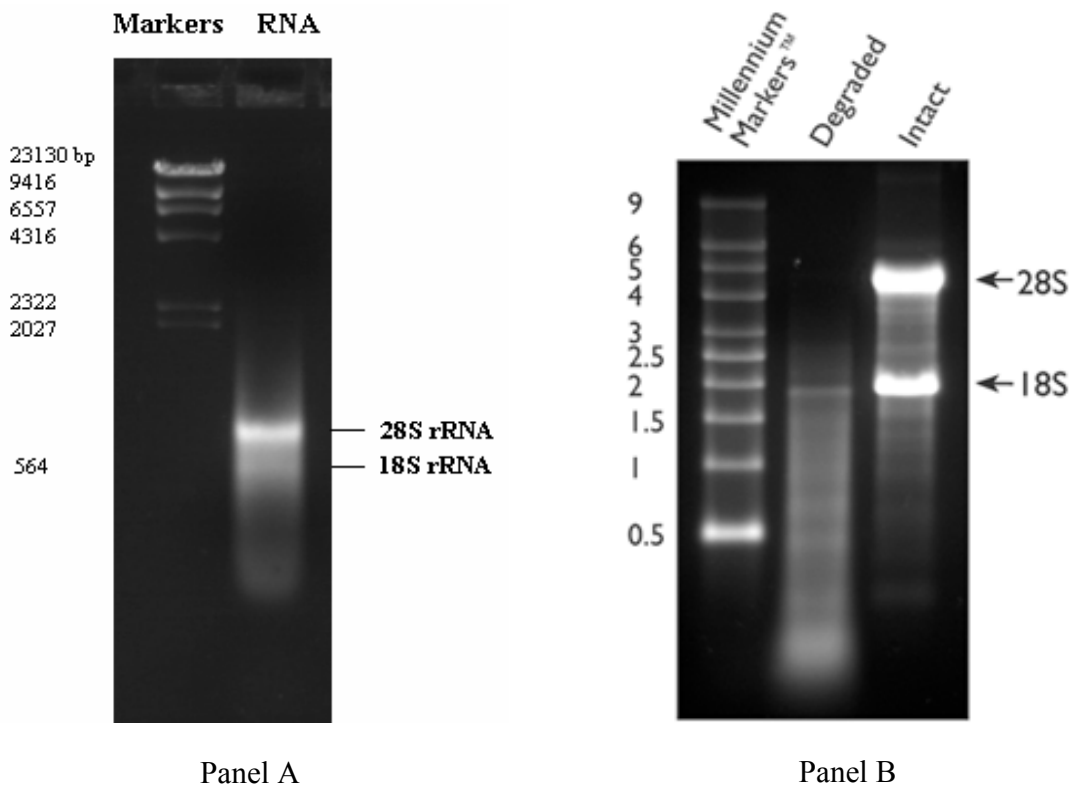


Figure 44: Total RNA integrity check. The sample in Panel A was the most successful of five RNA isolation attempts. The sample was separated in a native 1% agarose gel. In panel B, examples of fully degraded and intact total RNA samples are shown in a 1.5 % denaturing agarose gel (Taken from (Ambion, Accessed: 2006.)). These illustrate that the 28S and 18S ribosomal RNA (rRNA) bands in panel A are not as sharp and clear as is desirable, although they can still be identified. The sample is therefore too degraded to provide a reliable source of mRNAs for synthesis of a complete *S. littoralis* hemocyte first strand cDNA mix.

## 5.4 Discussion

Research conducted in this chapter was designed with the aim of isolating a PPO gene from *S. littoralis* hemocytes, using molecular methods including RNA isolation, first strand cDNA synthesis, and reverse transcription and real time PCR. The second, longer term aim was to identify, by 2D-gel electrophoresis, any variations between proteins present in the hemolymph of low and high density reared *S. littoralis* larvae.

In Chapter 4, the *S. littoralis* cDNA library used throughout the experiments had been generated from preparations of whole larvae, earlier parasitized by the Braconid parasitoid wasp *Chelonus inanitus*. Subsequent discussions suggested that such a source may have been low in PPO cDNA and so not ideal for its intended purpose. The approach described here involved rearing *S. littoralis* larvae, which had not been exposed to parasitoids, viruses or microorganisms, and bleeding them for isolation of their hemocytes. By removing the ‘infection’ variable from the experiment, and isolating the cell type believed to be the site of synthesis of all PPOs, this approach was considered to present greater opportunity for the isolation of a PPO gene.

However, problems encountered during the rearing of larvae and total RNA isolation from their hemocytes, along with time limitations on the project, resulted in neither of the above aims being achieved. These points are discussed in the following sections.

#### **5.4.1 Solitary larvae display variation in their level of cuticular melanisation.**

Solitary larvae presented no significant problems during their growth and development, and all reached a suitable size for bleeding at around 14 days old. Whilst some solitary larvae bled smaller volumes of hemolymph than others, all of their hemolymph was opaque pale blue in colour indicating no PO activation and thus that the larvae were not experiencing any infection.

It was however noted that approximately one third of the solitary larvae developed melanised cuticles and blackened head capsules, akin to the phenotype of gregarious larvae. As described in section 5.1, *S. littoralis* exhibits a trait known as density dependent phase polyphenism. Under constant optimal environmental conditions, individuals have either light or dark cuticular pigmentation depending on whether they are reared in low or high population density respectively. It was therefore considered unusual that some of the solitary larvae should have the dark pigmentation expected of gregarious larvae. There is evidence, however, that rearing temperature can have a notable effect on the level of cuticular melanisation amongst larvae of another Noctuidae moth, *Spodoptera exempta* (Gunn, 1998). In these experiments, larvae were subjected to either a lower (20°C) or higher (35°C) temperature than their optimal rearing temperature ( $27 \pm 1^\circ\text{C}$ ) from the second instar onwards. Amongst their observations, Gunn (1998) recorded that solitary larvae reared at the lower temperature had enhanced cuticular melanisation and black head capsules, resulting in their resemblance to gregarious larvae. Gregarious *S. exempta* larvae were found to show no real change in colour at this lower rearing temperature. This may perhaps explain the observation made during the experiment conducted here, as both the solitary and group

reared larvae experienced rearing temperatures, from day 4 onwards, between 20 - 24°C, which is lower than the optimal 25°C at which they had been previously reared.

Also noted from this same published research using *S. exempta* (Gunn, 1998) was the tendency for larvae to adopt and retain the colouration typical of gregarious larvae, rather than that of solitary larvae, even following alterations to their rearing conditions. The *S. littoralis* larvae used in the experiments conducted here were exposed to high density rearing conditions until they were 4 days old. It may be suggested, therefore, that a number of the larvae which were randomly selected for solitary rearing had already begun to adopt the gregarious cuticular colouration by the time they were transferred into solitary conditions. These individuals subsequently retained the gregarious characteristics during their solitary development.

#### **5.4.2 Slowed development, cannibalism and hemolymph melanisation in gregarious *Spodoptera littoralis* larvae.**

Whilst the solitary larvae displayed two obvious phenotypes, all of the gregarious larvae possessed very dark cuticular pigmentation and head capsules, as expected. Unlike the solitary larvae, the gregarious larvae in general exhibited slower rates of development and an overall smaller final instar larval size. Furthermore, variation in the growth rate between gregarious individuals from the same culture pot became apparent and was most notable by the final instar/14 days old (Figure 43). The smaller individuals in each high density culture pot seemed to fall victim to cannibalistic behaviour by the larger larvae. It was estimated, assuming that the cannibalized larvae did not die from another cause before their bodies were consumed, that 25% of the gregarious larvae were lost as a result of this behaviour. Further

reading has revealed that cannibalism is a frequent, well documented behaviour in larval Lepidoptera (Chapman et al., 1999b; Chapman et al., 2000). It may be speculated that cannibalism confers direct and/or indirect nutritional benefits by increasing survival and development rates whilst reducing predation and competition for food sources. There can also be assumed to be disadvantages for the cannibal such as the risk of injury or death from the defensive responses of victims, or the transmission of pathogens during consumption of the victim. Indeed the latter of these potential 'costs' has already been demonstrated as a possibility with respect to transmission of nuclear polyhedrosis virus (Chapman et al., 1999a). However, the exact benefits and costs of cannibalism remain to be elucidated (Chapman et al., 1999b).

The surviving group reared larvae were bled as the solitary larvae; however, approximately 50% of these survivors had hemolymph with a grainy black appearance. This suggested that these particular larvae had activated hemolymph PO, indicative of infection, rendering their hemolymph unsuitable for collection. These larvae generally had almost completely black cuticles and were not as active as those gregarious larvae which possessed non-PO activated pale blue hemolymph. It is possible that pathogens may be transmitted from victim to cannibal. Whilst no steps were taken to determine whether the remaining larvae with melanised blood were carrying pathogens, it may be the case that the smaller, less well developed larvae, which became victims of cannibalistic behaviour, were weakened by infection. Their subsequent consumption by any of the remaining larger larvae may have led to spread of the infection to these cannibals.

### **5.4.3 RNA degradation**

Hemolymph pooled from *S. littoralis* larvae, was used to isolate hemocytes from which attempts were made to isolate total RNA. The aim was to use the mRNA from this total RNA for the synthesis of first strand cDNA, and perform real time PCR using specifically designed degenerate primers for the amplification of a PPO cDNA. Unfortunately, the process of RNA isolation was unsuccessful.

Synthesis of first strand cDNA requires RNA of extremely high integrity, which in turn requires that the sample should never become contaminated with RNases. RNases are ubiquitously present in the environment, and it is therefore essential that all laboratory work surfaces, equipment and materials are treated to remove such RNA degrading enzymes. To reduce RNA degradation prior to isolation, hemocytes were stored in RNALater at -70°C. During the RNA isolation steps, all the recommended precautions outlined in the protocol accompanying the RiboPure™ total RNA isolation kit were taken, in order to eliminate RNase contamination. Furthermore, thorough sample homogenisation was performed to reduce RNA degradation whilst maximising the recovery of RNA.

Despite these efforts, all five attempts to isolate fully intact total RNA were unsuccessful. RNase contamination was clearly an issue during these experiments and whilst all possible steps to eliminate RNases were taken, the equipment and laboratory environment where the experiments were conducted were perhaps not suitable for conducting RNA based research.

## **Chapter 6 : Arthropod Hemocyanin – An introduction to structure and function.**

### **6.1 Introduction**

Arthropod hemocyanins (Hcs) are members of the non-haem metallo-enzyme protein subclass known as the Type-3 copper containing proteins (Maddaluno and Faull, 1999; Decker and Tucek, 2000; Bak et al., 1986). Further examples from this group include tyrosinase and arthropod phenoloxidase (PO) (see Table 5). All Type-3 copper proteins contain a highly conserved binuclear copper active-site, in which each copper is coordinated and tightly bound by three histidine residues (Decker and Tucek, 2000; Lee et al., 2004). However, their physiological functions can vary widely as demonstrated in Table 5. The primary biological function of Hc is as a respiratory protein, and it is found in molluscs and the arthropod classes Crustacea, Chelicerata and more recently Insecta (Decker et al., 2001; Möller and Decker, 2004; Zlateva et al., 1996; Hagner-Holler et al., 2004). They are important for efficient aerobic metabolism, just as haemoglobins are important oxygen carrier proteins in many species, including humans (Lee et al., 2004). It should be noted that an arthropod-type Hc has been identified out-with the Arthropoda and Mollusca, in the phyla Onychophora – the velvet worms. Despite conserved sequence and structural characteristics important for oxygen binding function, analyses have shown that this member of the Hc superfamily acts more like a PO (Kusche et al., 2002; Decker, 2005). In recent decades, however, arthropod and mollusc Hcs have demonstrated they can be irreversibly transformed, under physiological conditions, to function as a PO

Table 5: Examples of proteins containing the Type-3 copper centre, and their location, activity and function within biological systems. Phenoloxidase (Ashida and Brey, 1997; Decker and Tuzcek, 2000; Sugumaran et al., 2000b; Sugumaran and Nellaiappan, 2000), tyrosinase (Sugumaran et al., 2000a; Decker and Jaenicke, 2004) and catecholoxidase (Greving et al., ) possess the Type-3 copper centre only, whereas ceruloplasmin (Maltais et al., 2003) and laccase (Garcia-Pineda et al., 2004; Santagostini et al., 2004) also contain the Type-2 copper centre.

| E.C. Number and Name   | Location  | Activity   | Function  |
|--|---|--|---|
| E.C. 1.10.3.1<br>Phenoloxidase<br>(insect/arthropod)                   | Synthesised in hemocytes and released into hemolymph.<br><br>May also be transported to cuticle via epidermal cells.      | Hydroxylation of monophenols to <i>o</i> -diphenols<br><br>Oxidation of <i>o</i> -diphenols to <i>o</i> -quinones  | Initiates pigment (e.g. melanin) and other polyphenolic compound formation<br><br>Roles in insects include sclerotisation, wound healing and primary immune response. |
| E.C. 1.14.18.1<br>Tyrosinase<br><br>Also referred to as phenoloxidase. | Mammalian equivalent of phenoloxidase. Confined to specialised cells called melanocytes. Also found in bacteria and fungi | Hydroxylation of monophenols to <i>o</i> -diphenols<br><br>Oxidation of <i>o</i> -diphenols to <i>o</i> -quinones  | Initiates pigment (e.g. melanin) and other polyphenolic compound formation.<br><br>Melanin involved in browning of hair and skin in mammals.                          |
| E.C. 1.10.3.1<br>Catecholoxidase                                       | Found in higher plant tissues.<br><br>Membrane bound until cellular damage causes its release.                            | Oxidation of <i>o</i> -diphenols to <i>o</i> -quinones   | A role in photosynthesis proposed<br><br>Plant defence against insects and disease.   |
| E.C. 1.16.3.1<br>Ceruloplasmin   | Secreted by hepatocytes into mammalian blood serum.<br><br>Also expressed in the mammalian nervous system.                | Possesses ferroxidase activity, catalysing the oxidation of Fe <sup>2+</sup> to Fe <sup>3+</sup> .<br><br>Also possesses antioxidant capacities.                               | Exact function uncertain. Roles in inflammation, angiogenesis, iron homeostasis, neuronal development and protection against oxidative stress have been implied.      |
| E.C. 1.10.3.2<br>Laccase   | Plants, fungi and more recently found in bacteria.  | Usually phenolic in nature, substrates are oxidised to provide electrons for the co-occurring reduction of O <sub>2</sub> → H <sub>2</sub> O.                                  | Exact function uncertain. Implicated in the synthesis and/or degradation of lignin, wound response mechanisms and the morphogenesis of microorganisms.                |
| E.C. 1.10.3.3<br>Ascorbate oxidase                                     | Cell walls and cytoplasm of higher plants   | Catalyses the aerobic oxidation of L-ascorbate to dehydroascorbate with the simultaneous reduction of O <sub>2</sub> → H <sub>2</sub> O via a single electron transfer system. | Biological function unknown, although activity is known to increase during plant stress conditions.   |

(Zlateva et al., 1996; Decker and Rimke, 1998; Decker et al., 2001; Decker and Jaenicke, 2004; Nagai et al., 2001), and also be processed to produce antimicrobial peptides (Lee et al., 2004). This intrinsic PO activity can also be elicited *in vitro* by incubation with substances such as detergents, salts and lipids (Nagai et al., 2001). It has therefore been speculated that Hc may have a second role in humoral immunity, being converted from Hc to a PO-type enzyme when the animal is wounded or subject to infection (Lee et al., 2004). There are however currently no conclusive lines of evidence for the activation of Hc PO activity *in vivo*, although one recent report claims that, together, beta-1,3-glucans and hemocyte components can elicit PO activity in Hc from the crustacean *Penaeus japonicus* (Kuruma prawn). Further experiments to corroborate this could indicate that Hc is involved in the melanisation of microorganisms (Cerenius and Söderhäll, 2004; Adachi et al., 2003). Whilst both arthropod and mollusc Hcs possess inducible PO activity, sequence comparisons show arthropod POs share greater sequence similarity to arthropod Hcs than mollusc Hcs (Lee et al., 2004), and, unless otherwise stated, arthropod Hcs will be the focus of the remaining discussion.

## **6.2 A History of the Studies of Hemocyanin**

Hcs have been identified in a number of arthropod subphyla, including the Myriapoda and Hexapoda, however they have been studied most extensively only in the Chelicerata, where they are found widespread, and the malacostacan Crustacea (Burmester, 2001). These studies form attempts to understand the mechanism involved during molecular dioxygen activation of non-haem systems (Maddaluno and Faull, 1999). However, for some time, the structure of Hc (arthropod and mollusc) remained elusive as a result of the great length of its polypeptide chains, heterogeneity of subunits and complex quaternary structure. Despite these factors, the

1970s and 80s saw the chemical and spectroscopic characterisation of the nature of the Hc active site (Tamburro et al., 1976; Kuiper et al., 1980; Volbeda et al., 1989; Hwang and Solomon, 1982). Furthermore, since c1980 amino acid sequences have been elucidated, a great deal of primary structure information has become available, and the three dimensional structures of a number of Hc types have been proposed (Mangum et al., 1985; Bak et al., 1986; Voit et al., 2000; Decker, 2005). The earliest recognizable images of Hc, captured in 1964 by Van Bruggen, were electron microscope images of Hc from the ancient chelicerate *Limulus polyphemus* (the Atlantic horseshoe crab) (Taveau et al., 1997). Pioneering studies by Sullivan et al (Sullivan et al., 1974; Sullivan et al., 1976) were however the first step towards resolving the structure of Hc. Sullivan fractionated *L. polyphemus* Hc on a DEAE-Sephadex column after EDTA treatment, and concluded that it consisted of at least five different subunit types, termed I to V. Later work by Lamy et al (1979) used immunological techniques to show that some of these fractions were heterogeneous and that *L. polyphemus* Hc in fact consisted of eight subunit types (Taveau et al., 1997). It was not until the early eighties that qualitative data about the three dimensional arrangement of these subunits was discovered by Van Heel and Frank using multivariate statistical analysis of negatively stained half-molecules (Taveau et al., 1997). At the same time, X-ray crystallography provided the first three dimensional reconstruction of a hexameric Hc (from the lobster *Panulirus interruptus*), a structure which was readily accepted as the building block of all arthropod hemocyanins and provided an understanding of their general organization (Taveau et al., 1997). Between the early 1990's and the present day, high resolution 3-D structures have become available, including that of the hexameric subunit LpII from *L. polyphemus* Hc, resolved at atomic resolution (Hazes et al., 1993; Decker, 2005). The most recent focus of research is in the area of characterising Hcs function, and has demonstrated unarguably that

this protein has an intrinsic inducible phenoloxidase-type activity with which there are proposed associated conformational changes taking place (Decker, 2005).

Although there has been a rapid enhancement in our understanding of the structure and function of arthropod Hcs, the very complex nature of this protein means there is still much for us to learn before we can confidently state its physiological role. The ensuing discussion reviews our current understanding of Hcs structure and function.

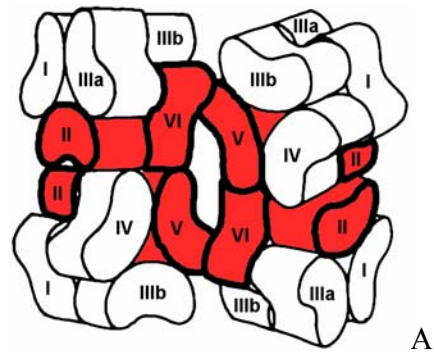
## **6.3 The Structure of Hemocyanin**

### **6.3.1 Quaternary Structure**

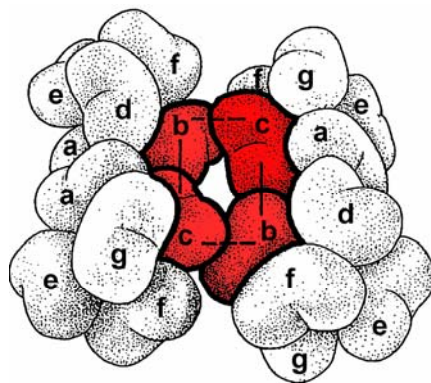
Hcs are high molecular weight, extracellular, copper-containing glycoproteins composed of multiple subunits of differing types (Decker and Jaenicke, 2004; Decker et al., 2001; Ali et al., 1995). With regards to quaternary structure, subunit size and composition, arthropod and mollusc Hcs differ considerably (Voit et al., 2000), and are in fact now considered as two distinct proteins, originally given the same name because of similarities in oxygen binding (Cuff et al., 1998; van Holde et al., 2001). At the quaternary level arthropod (chelicerate and crustacean) Hcs are composed of 3-15 heterogeneous, kidney shaped subunits (Ali et al., 1995; Decker and Tuzek, 2000), which combine to form a regular cubic hexamer with dimensions of approximately 10 x 10 x 10 nm (Möller and Decker, 2004). Depending on species or physiological conditions, multiples of these hexamers (1x6-mer to 8x6-mers) are formed, with total molecular weights ranging between  $4 \times 10^5$  and  $4 \times 10^6$  Da (Voit et al., 2000; Maddaluno and Faull, 1999; Meissner et al., 2004). Typically, crustacean Hcs are composed

of 1x or 2x6-mers (although there are exceptions), whilst chelicerate Hcs form larger assemblages of 4x, 6x or 8x6-mers (Ali et al., 1995; Meissner et al., 2004).

*Limulus polyphemus* has the largest and most complex of the known arthropod Hcs (Hazes et al., 1993). It is composed of eight immunologically distinct subunit types, arranged into two superimposed 4x6-meric structures to form the 8x6-mer Hc particle, which has a molecular weight of approximately  $3.6 \times 10^6$  Da (Voit et al., 2000; Taveau et al., 1997; Liu and Magnus, 2002). Each of the eight subunit types exists at particular locations within the quaternary structure of the hemocyanin molecule (van Holde et al., 2001; Hazes et al., 1993), as a result of the considerable specificity of inter-subunit interactions (van Bruggen et al., 1980). This specific arrangement is a necessity for full biological activity (Voit et al., 2000), and the non-covalent interactions between the subunits are key elements in maintaining the overall Hc fold (Gatto et al., 2004). Figure 45A shows the quaternary arrangement of the different subunit types within the *L. polyphemus* Hc 4x6-mer half-molecule. The eight subunit types have been termed LpI, II, IIA, IIIA, IIIB, IV, V and VI, and are present in a ratio of 3:4:1:4:4:4:2:2 (Decker et al., 2001). The 4x6-meric structures make contact and connect via subunit LpIV on each half molecule (Taveau et al., 1997).



A



B

Figure 45: Quaternary structures of the 4x6-meric hemocyanin subunits from *Limulus polyphemus* (Panel A) and *Eurytelma californicum* (Panel B). The subunits shown in red are those known to possess phenoloxidase activity. The complete native *L. polyphemus* hemocyanin is composed of two superimposed 4 x 6-mers (Adapted from (Decker et al., 2001)).

Another well studied arthropod Hc is that from the North American tarantula *Eurypelma californicum*. This 4x6-meric Hc (Figure 45B) has a molecular weight of approximately  $1.8 \times 10^6$  Da, and comparable structure to that of the *L. polyphemus* Hc half-molecule (Decker et al., 2001). However, *E. californicum* Hc is composed of only seven immunologically distinct subunit types, which have been assigned as a, b, c, d, e, f and g, and formation of the 24-mer complex requires the aggregation of these seven subunits in a constant stoichiometric ratio of 4:2:2:4:4:4:4 respectively (Voit et al., 2000). The assembled 24-meric subunit of *E. californicum* has its 4 hexamers bound together tightly by two non-covalent bonds which form between the linker subunits b and c of each 2x6-meric half molecule (Adachi et al., 2003; Decker, 2005)

### **6.3.2 Tertiary Structure**

Arthropod Hc subunit structure was first suggested during studies using *L. polyphemus* subunit LpII (Taveau et al., 1997; Sullivan et al., 1974). Arthropod subunits range from 70 – 75 kDa (Möller and Decker, 2004; Decker et al., 2001), and possess three domains (Lee et al., 2004) arranged to form the subunit's characteristic 'kidney' shape (Figure 46). Domain I (residues 1 - 154) in LpII lies at the N-terminus and contains between 7 and 8  $\alpha$ -helices. Domain II (residues 155 - 380) is also highly helical and holds the dicopper centre copper pair buried within its core. This domain is also important structurally as it dominates the inter-subunit contacts within each Hc hexamer. Finally, domain III (residues 381 - 628), which lies at the C-terminus, has a seven stranded antiparallel Greek key  $\beta$ -barrel topology, with two loops extending from its centre. These later structures appear to function as arms

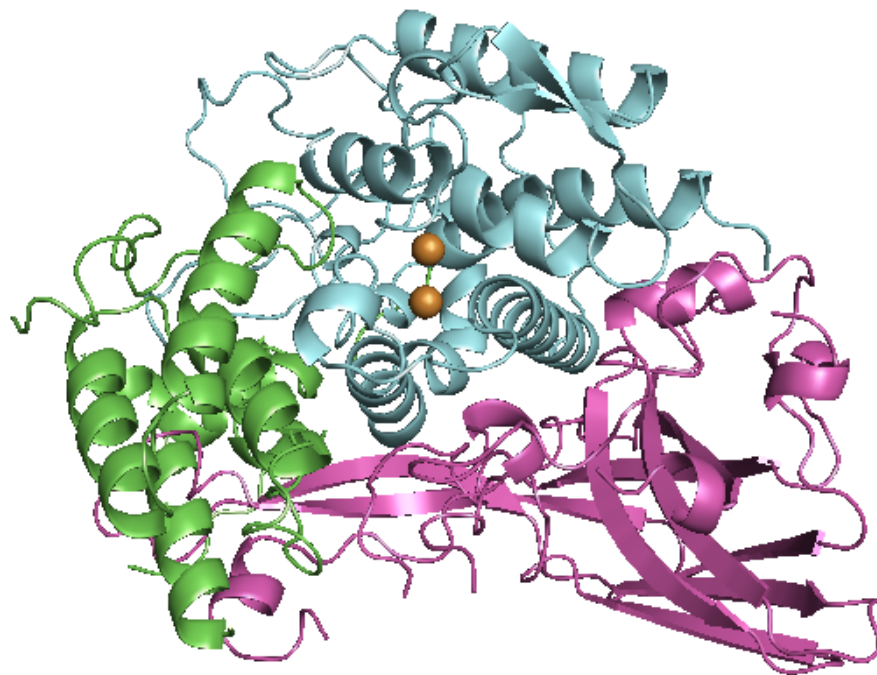


Figure 46: Tertiary structure of subunit II of *Limulus polyphemus* hemocyanin. The three domains are coloured green (domain I), cyan (domain II) and magenta (domain III). CuA and CuB are shown as orange spheres. Image generated using PDB file 1LLA and Pymol molecular graphics software.

holding the three domains together (Decker and Jaenicke, 2004; Bak et al., 1986; Voit et al., 2000; Ali et al., 1995; Cuff et al., 1998; Hazes et al., 1993).

As discussed earlier, arthropod Hc subunits are heterogeneous, and this property is thought to be important for establishing the proper aggregation state of the molecule and ensuring the subunits cooperative binding properties (Decker and Jaenicke, 2004). Despite their heterogeneous nature, the polypeptide sequences are sufficiently similar that all arthropod Hc subunits probably have a tertiary structure similar to the LpII subunit of *L. polyphemus* Hc (Decker and Jaenicke, 2004).

### **6.3.3 Active Site Structure**

Arthropod Hcs are Type 3 copper proteins, and as such contain a highly conserved dicopper centre, with each copper (CuA and CuB) having an approximate trigonal planar coordination by the N $\epsilon$  atom of three histidine residues (Decker and Tuzek, 2000; Hazes et al., 1993). These coordinating histidines are provided by a four  $\alpha$ -helical bundle, with the four structural elements locating to different regions of the protein fold of domain II (Gatto et al., 2004; van Holde et al., 2001). In arthropod Hc (Figure 47), two histidines binding CuB are provided by successive turns of one  $\alpha$ -helix and the third by a second helix. CuA histidines are provided in a similar fashion, but by alpha helices which run antiparallel to those providing the CuB coordinating histidines (Decker and Tuzek, 2000).

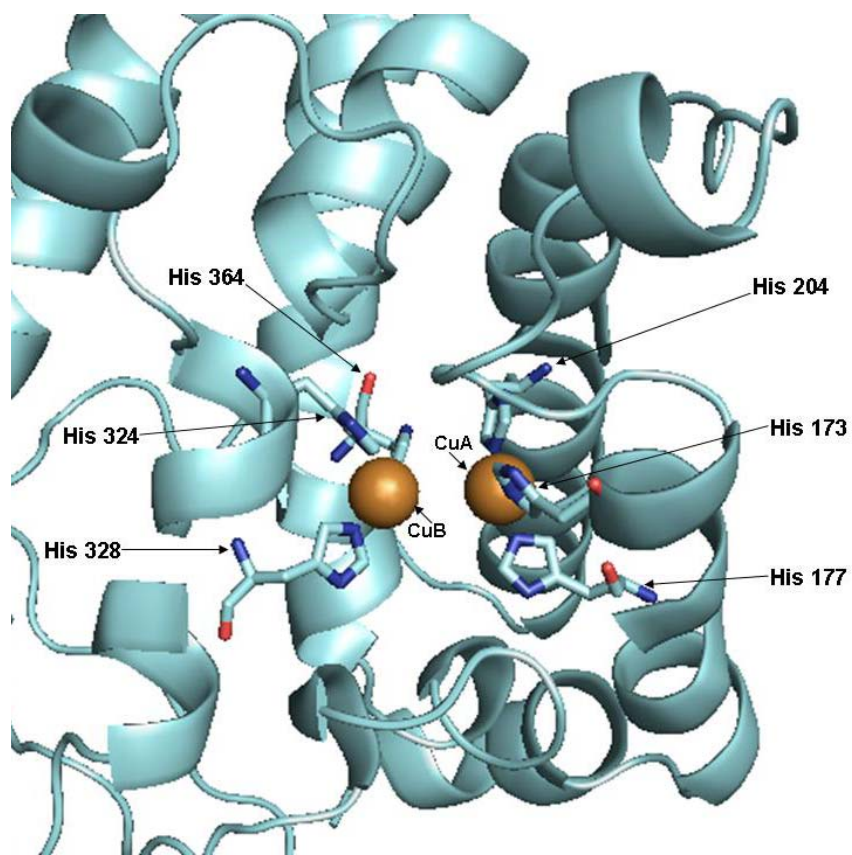


Figure 47: The binuclear copper site of *Limulus polyphemus* hemocyanin subunit II. CuA and CuB (orange) and their coordinating His (shown in stick format) are highlighted. View shown is perpendicular to the Cu-Cu axis. Image produced as in Figure 46.

Another feature of arthropod Hcs is the presence of a 'placeholder' amino acid situated in the entrance, at a distance of 4.9Å, to the dicopper centre (Decker and Tuzcek, 2000) (Figure 48). This placeholder originates from domain I, and is a phenylalanine residue in *L. polyphemus* (Phe49) and *Tachypleus tridentatus* (Japanese Horseshoe crab) (Decker and Rimke, 1998; Nagai et al., 2001). Placeholder amino acids are believed to function to block the entry of larger substrates to the dicopper centre whilst the Hc is functioning solely as an oxygen transporter. Under particular conditions, this placeholder can be pulled out of the dicopper centre to elicit a secondary function.

The two copper ions of the Hc dicopper centre have great importance in the function of the Hc molecule; however they are also important from a structural perspective. As the copper ions of each subunit are coordinated by ligands (histidines) provided by structural elements from various regions of the protein fold, it can be expected that they will have a role as a tertiary structural element. Recent experiments using a number of biophysical and biochemical techniques and Hc from the crustacean *Carcinus aestuarii* (Mediterranean Shore crab), have in fact shown that the copper ions play a stabilizing role on the proteins tertiary structure. Removal of these coppers results in the loss of some domain-domain interactions whilst secondary structure remains essentially unchanged (Gatto et al., 2004).

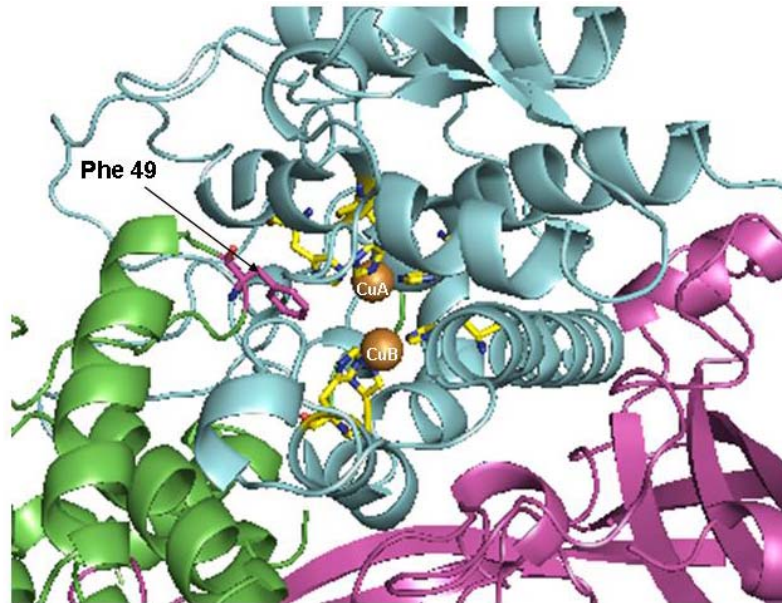


Figure 48: Active site of *Limulus polyphemus* subunit II hemocyanin showing the orientation of the 'placeholder' amino acid, phenylalanine-49 (magenta coloured residue shown in stick format in domain I), in the entrance to the dicopper centre. Domains are highlighted in green (domain I), cyan (domain II) and magenta (domain III). Copper ions are shown as orange spheres and their coordinating histidine residues in yellow stick format. Note the differing domain location of the dicopper centre and Phe-49 residue. Image produced as in Figure 46.

### 6.3.4 Ion Binding Sites

As well as possessing a functionally and structurally important dicopper centre, arthropod Hcs also possess a binding site for a chloride ion and a putative binding site for a calcium ion (Figure 49). Such sites have been identified in *L. polyphemus* Hc subunit II. Chloride and calcium are known to be important heterotropic allosteric effectors of cooperative oxygen binding by the *L. polyphemus* Hc complex (Hazes et al., 1993).

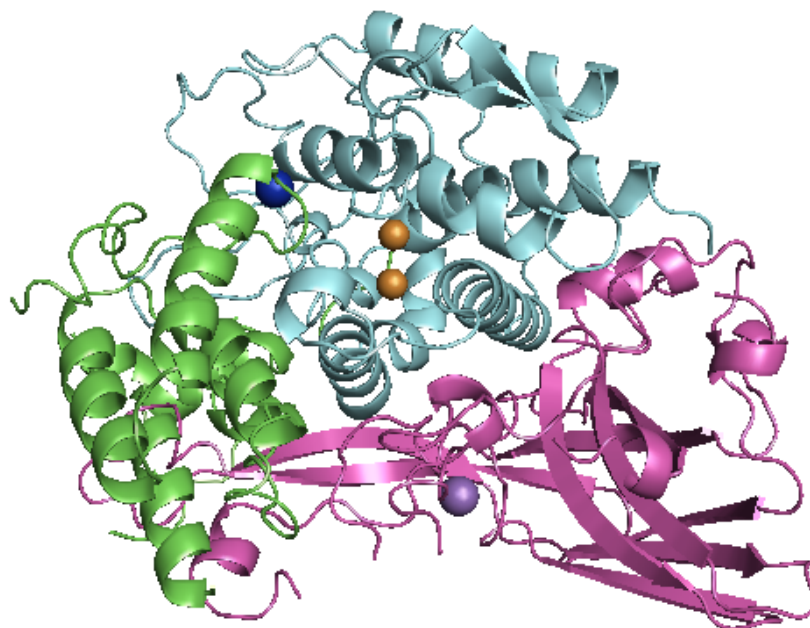


Figure 49: Ion binding sites in *Limulus polyphemus* hemocyanin subunit II. The chloride ion (blue sphere) binding site is positioned at the interface of domain I (green) and II (cyan), whilst the putative calcium ion (purple sphere) binding site is located at the subunit surface near two flexible regions of domain III (magenta). Both chloride and calcium ions are known to be important effectors of cooperative oxygen binding by the *L. polyphemus* hemocyanin complex (Sullivan et al., 1974; Hazes et al., 1993). The copper ions of the dicopper centre are represented by orange spheres at the core of domain II. Image produced as in Figure 46.

The chloride site binds one chloride ion and is located at the interface of the first and second domains of the LpII subunit. Chloride ions are allosteric effectors of O<sub>2</sub> binding in Hc. It has been proposed that chloride ions reduce the affinity of Hc for O<sub>2</sub> via differential binding to the oxy- and deoxy- forms of Hc, or by causing a change in the ligand-linked aggregation state, or both (Sullivan et al., 1974; Hazes et al., 1993). Chloride ions have also been shown to reduce O<sub>2</sub> affinity by binding more tightly to Hc in the low affinity state than the high affinity state. This is proposed to be as a result of a structural change in the chloride binding site at the tertiary level during the transition between low and high oxygen affinity states (Sullivan et al., 1974; Hazes et al., 1993). An important point to note however is the non-uniform effect of chloride ions on different subunits within one Hc type. For example, only subunits II, IIA, IIIA and IIIB exhibit the chloride effect in *L. polyphemus* Hc (Sullivan et al., 1974).

The putative calcium site binds one metal ion and is located at the subunit surface, near two flexible regions in domain III of the LpII subunit type. It has both a regulatory and structural role in *L. polyphemus* Hc. Given that calcium binding is important for stability, and along with the two disulphide bridges present in each subunit, it is thought that this ion acts to stabilise the structure of both the hexamer and the native multi-hexamer (Hazes et al., 1993). Calcium also acts to decrease the O<sub>2</sub> affinity whilst increasing the cooperativity of the Hc multi-hexameric complex (Hazes et al., 1993).

### **6.3.5 Primary Structure**

At the primary structural level each arthropod Hc subunit is composed of approximately 660 amino acids per polypeptide chain (Ali et al., 1995). Except for a region of 42 amino acids that is involved in CuB coordination, there is little sequence similarity between arthropod and mollusc Hcs (Cuff et al., 1998). Amongst arthropod Hcs there are greater sequence identities, most notably in domain II which carries the dicopper centre (Decker, 2005). When the known sequences of all seven *E. californicum* subunits are compared, 52-65% sequence similarity is observed, with 32% being strictly conserved throughout (Voit et al., 2000).

Although arthropod Hcs are extra-cellular, no signal peptides have ever been identified in chelicerate Hcs. The available amino acid sequences from the N-terminal ends of the native polypeptides of *E. californicum* Hc corroborate this result and show only the removal of the first (initiator) methionine (Voit et al., 2000). This is consistent with the fact that in chelicerates, Hcs are synthesised by free ribosomes and released via cell rupture (Voit et al., 2000). A signal peptide sequence has however been identified in Hc from the crustacean *Penaeus vannamei* (a penaeid shrimp) (Sellos et al., 1997). Once again, this is consistent with the site of synthesis of crustacean Hc and its proposed method of release into the hemolymph, as is discussed in section 6.4.1.

## **6.4 Arthropod Hemocyanin – a multifunctional protein?**

### **6.4.1 Site of Hemocyanin Synthesis**

The site of synthesis of Hc appears to vary amongst the arthropod subphyla, as was noted in section 6.3.5. In the chelicerate *E. californicum* for example, Hc is synthesised by free

ribosomes in hemocytes which are attached to the inner wall of the heart (Voit et al., 2000). On the other hand, studies using the crustaceans *Penaeus monodon* (Black Tiger shrimp) and *Cancer magister* (Dungeness crab) define the site of biosynthesis of Hc as the hepatopancreas. More specifically in *P. monodon*, the F-cells, or epithelium, lining the hepatopancreas tubules, were shown by studying the expression of mRNAs for Hc, to be the only tissue/cell type in the shrimp to synthesise this protein. Furthermore the synthesis of this protein appears to be the F-cells' main function (Lehnert and Johnson, 2002). Immunofluorescence experiments using *C. magister* also convincingly demonstrated the presence of Hc in the stomach wall, reticular connective tissues and eye stalks (Durstewitz and Terwilliger, 1997). It remains unclear whether these are sites of Hc synthesis, storage or degradation, or represent tissue types containing cells filled with Hc transported there from other tissues. It is also possible however that these immunofluorescence results are the result of cross-reactivity of the antibody with cryptocyanin (Durstewitz and Terwilliger, 1997), a closely related non-respiratory Type-3 copper protein involved in crustacean moulting. This protein has lost the ability to bind oxygen, lacking three of the six highly conserved histidine residues present in Hc, and is present in the hemolymph of arthropods at higher concentrations than Hc during pre-moult (Terwilliger et al., 1999). Therefore the generally accepted site of synthesis of crustacean Hc is the F-cells of the hepatopancreas. Further studies are required to elucidate the exact mechanism by which Hc synthesised in the F-cells, accumulates in the hemolymph. Lehnert and Johnson, 2002, proposed that crustacean Hc synthesised by the F-cells' rough endoplasmic reticulum, is processed by the Golgi apparatus and released from secretory vesicles into the hepatopancreas lumen. It would then, by some unknown process, be translocated to the hemolymph via the hepatopancreas tubule type cells.

Ultimately, Hc is found freely dissolved in hemolymph (Cuff et al., 1998) and forms the predominant protein component of the hemolymph of most arthropods (Lehnert and Johnson, 2002). For example Hc is typically present at 5 – 120 mg/ml in the chelicerate *E. californicum* (Decker and Rimke, 1998) and approximately 6 – 38 mg/ml in the crustacean *Cancer magister* (Dungeness crab) (Brown and Terwilliger, 1998; Decker, 2005). This figure may reflect the importance of Hc in arthropods as an oxygen transporter protein, and also, as will be discussed, as a potential immune system component. Hc has a very important function in oxygen transport, and is capable of achieving 100% saturation during periods of higher oxygen demand by respiring tissues (Brown and Terwilliger, 1998). More recently, research has demonstrated that this protein may have additional roles in immune defence and wound healing (Cerenius and Söderhäll, 2004).

#### **6.4.2 Primary Function – Oxygen Transporter**

In arthropods, Hc functions primarily as an oxygen transporter, a role based on its capability to reversibly bind molecular dioxygen at its dicopper centre (Zlateva et al., 1996). One molecule of oxygen binds to the deoxygenated protein at the respiratory surfaces. It binds in a side on conformation ( $\mu - \eta^2: \eta^2$ ) forming a peroxide ion ( $O_2^{2-}$ ) bridge between the two Cu (I) ions, oxidizing them to the valence state Cu (II) (Dainese et al., 1998; Maddaluno and Faull, 1999; Durstewitz and Terwilliger, 1997; Cuff et al., 1998; Decker, 2005). The oxygen is then transported to respiring tissues via the circulatory system, a process essential for efficient aerobic metabolism (van Holde et al., 2001).

As discussed in Section 6.3.2, the dicopper centre is at the core of domain II of each arthropod Hc subunit. In *L. polyphemus* subunit II, there appears to be a solvent tunnel which

extends from the protein surface to the dicopper centre. A glutamic acid residue (Glu-309) obstructs this tunnel, and may potentially function as a gate, controlling entry of O<sub>2</sub> to the dicopper centre (Hazes et al., 1993). Therefore the oxygenation step may require a structural change to occur before O<sub>2</sub> can reach the copper centre (Hazes et al., 1993). Small angle x-ray scattering (SAXS) has in fact suggested that all structural levels are involved during the conformational change upon oxygen binding in Hc (Möller and Decker, 2004).

### **6.4.3 Secondary Function – Defensive Protein**

In most instances, a single protein performs a single well defined biological function with high specificity and efficiency (Decker and Rimke, 1998). However, arthropod Hc contrasts this theme by appearing to exhibit a secondary function as a PO-type enzyme *in vitro* (Decker et al., 2001). PO is an enzyme widely distributed amongst fauna and flora (although it may be referred to as tyrosinase, catecholoxidase or polyphenol oxidase depending on its source), and is involved in many physiologically important functions including melanisation, sclerotisation (cuticular hardening) and host defence (Decker et al., 2001; Decker and Jaenicke, 2004; Lee et al., 2004). Native PO is found only in insects and crustaceans. It possesses both tyrosinase and *o*-diphenoloxidase activity and catalyses a two-step reaction (Figure 50) which results in the

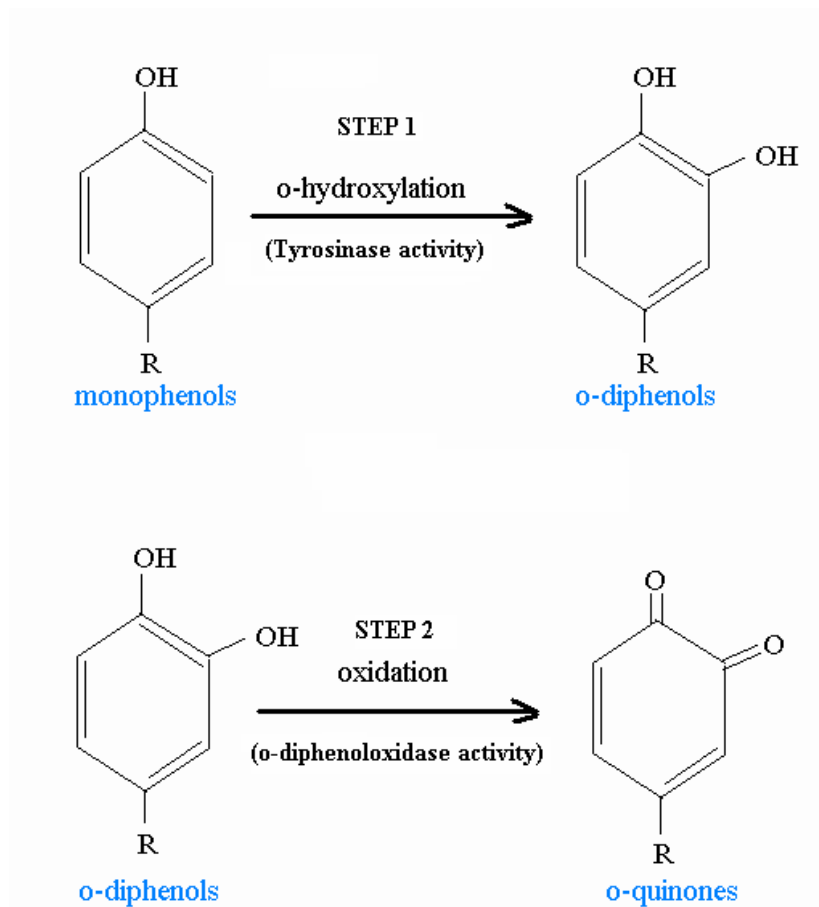


Figure 50: Phenoloxidase catalyses a two-step reaction which incorporates molecular oxygen into phenolic molecules at its dicopper centre. Crustacean Hcs are thought only to possess *o*-diphenoloxidase activity (only one exception has been found), whilst chelicerate hemocyanins have been shown to exhibit both tyrosinase and *o*-diphenoloxidase activity (Decker and Jaenicke, 2004).

incorporation of oxygen into phenolic molecules (Hall et al., 1995a; Decker and Tuczec, 2000; Ashida and Brey, 1997; Decker and Terwilliger, 2000). Arthropod Hc (found in crustaceans and chelicerates and more recently in one insect species (Hagner-Holler et al., 2004)) displays this same ability once its PO-type activity is elicited, although crustacean Hcs generally appear to exhibit only *o*-diphenoloxidase activity (Decker and Jaenicke, 2004). *In vitro* activation of Hc PO activity has been achieved via two methods: proteolytic cleavage and incubation with detergents, lipids or antimicrobial peptides (Decker et al., 2001; Nellaiappan and Sugumaran, 1996; Nagai et al., 2001). Initially it was thought that chelicerates possessed a distinct native PO protein, however further investigation revealed that this PO activity was the result of a detergent activated Hc (Nellaiappan and Sugumaran, 1996; Decker and Tuczec, 2000).

Limited proteolysis by the serine proteases trypsin and chymotrypsin induces PO activity in most Hcs (Decker et al., 2001; Decker and Rimke, 1998; Lee et al., 2004). Proteolytic cleavage of *E. californicum* and *L. polyphemus* Hc is known to remove an N-terminal fragment from those subunits which possess inducible PO activity – for example subunits II, V and VI in *L. polyphemus* Hc and the linker subunits b and c in *E. californicum* Hc (Decker et al., 2001; Adachi et al., 2003). This fragment includes the conserved ‘placeholder’ amino acid, Phe-49, and thus its removal is believed to open the dicopper centre for the entrance of larger phenolic substrates (Decker and Rimke, 1998; Decker and Tuczec, 2000; Lee et al., 2004). *L. polyphemus* and *E. californicum* are ancient chelicerates with no, as yet identified, native PO, and their Hcs display strong PO activity in comparison to crustaceans (Decker, 2005). Therefore if proteolysis is used *in vivo*, for example during an important vulnerable

stage in arthropod development, Hcs native function may switch to a serve as a PO. Although the activity may be low, this would be compensated for by the high concentration of Hc in the hemolymph as discussed in section 6.4.1 (Decker and Rimke, 1998). Recent research has indicated that cysteine proteases are potential candidates for Hc activation *in vivo*, as components of a system somewhat analogous to the insect PPO serine protease cascade (Adachi et al., 2003). Since removal of the conserved placeholder amino acid appears to be all that is necessary to elicit PO activity in arthropod Hc, this implies that no rearrangement of the dicopper centre is necessary to develop the proteins secondary catalytic function (Decker and Rimke, 1998; Decker and Tuzek, 2000; Decker and Jaenicke, 2004).

It must be emphasized however that *in vitro* proteolysis can only elicit low levels of PO activity in comparison with that achieved upon incubation of Hc with detergents such as sodium dodecyl sulphate (SDS) or cetylpyridinium chloride (CPC) (Decker et al., 2001; Decker and Tuzek, 2000; Nellaiappan and Sugumaran, 1996). Although, there are instances, e.g. the Hc of the crustacean *Pacifastacus leniusculus* (crayfish), where no detectable PO activity arises after treatment with such substances; only proteolysis can trigger PO activity in this Hc species (Lee et al., 2004). As with proteolytic cleavage, PO activation by detergents appears to be limited to only a few of the various subunit types of each Hc (Decker et al., 2001). Unlike proteolysis however, detergent activation does not involve cleavage of a part of the protein structure. Research using Hc from *L. polyphemus* and *E. californicum*, suggest instead that SDS may induce a conformational change, a distortion or slight unfolding of the protein (Decker and Tuzek, 2000). SDS is a known denaturant and acts at mid to high concentrations (a range which includes CMC and above) to cause protein unfolding. However, at lower concentrations, SDS may perform a much more selective

action, causing protein folding, superactivation and/or conformational change. It must be noted that the actual concentration range for each of the definitions 'low', 'mid' and 'high' is dependant on a number of factors including the chemical and physical interactions between SDS and the protein in question (Moosavi-Movahedi, 2005). In arthropod Hc, SDS perhaps induces a conformational change which may pull the conserved placeholder amino acid out of the dicopper centre entrance, opening the dicopper centre to larger phenolic substrates for hours, without complete unfolding (Decker and Jaenicke, 2004).

The structural changes taking place during this detergent induced activation step have not yet been characterized. The presented research which follows in Chapter 7 addresses this issue, and discusses the results of a number of biophysical methods used in a bid to provide insight into the structural changes taking place in three chelicerate Hcs upon incubation with submicellar and micellar concentrations of SDS.

## **Chapter 7 : Biophysical Characterisation of the Mode of Activation of Phenoloxidase Activity in Arthropod Hemocyanin**

### **7.1 Introduction**

#### **7.1.1 Overview**

Characterising the structure and function of arthropod hemocyanin (Hc) has been the focus of a number of research groups since the late 1970's. An oxygen transport protein under native conditions, Hc has been identified as possessing an intrinsic phenoloxidase (PO)-type activity upon *in vitro* incubation with denaturing agents such as perchlorate (Zlateva et al., 1996), proteolytic enzymes (Decker and Rimke, 1998; Lee et al., 2004; Nellaiappan and Sugumaran, 1996), detergents such as sodium dodecyl sulphate (SDS) and cetylpyridium chloride (CPC) (Decker et al., 2001; Jaenicke and Decker, 2004; Nellaiappan and Sugumaran, 1996), phospholipids and fatty acids (Nellaiappan and Sugumaran, 1996; Nagai and Kawabata, 2000), and antimicrobial peptides (Nagai et al., 2001). There are currently no conclusive lines of evidence for the activation of Hc PO activity *in vivo* (Cerenius and Söderhäll, 2004), however recently, it has been demonstrated that the PO activity of Hc from the Kumura prawn, *Peneaus japonicus*, can be elicited *in vitro* by  $\beta$ -1,3-glucans and hemocyte components (Adachi et al., 2003). Further experiments are required to confirm these findings, but if found to be true, could indicate a role for arthropod Hc in the melanisation of invading micro-organisms (Cerenius and Söderhäll, 2004).

Reports on the PO activity of arthropod Hcs have concentrated on a number of key areas; these include determining the level of PO activity which can be triggered by various

treatments, identifying the specific subunits which display inducible PO activity, and attempting to identify possible components involved in conversion of Hc to PO *in vivo*. There are however no published reports, at the molecular level, of the conformational changes associated with activation of arthropod Hc PO activity by artificial activators such as SDS.

### **7.1.2 Current Knowledge of the Activation of Arthropod Hemocyanin**

#### **Phenoloxidase Activity.**

Arthropod Hcs appear to vary in terms of the level of PO activity which can be elicited in response to a range of activating treatments. Chelicerate Hcs, such as Hc from *Limulus polyphemus* (Atlantic Horseshoe crab) or *Eurypelma californicum* (North American tarantula), appear to exhibit only very minimal levels of PO activity following limited proteolysis by trypsin. In comparison, upon incubation with the detergents SDS or CPC, these Hcs show very high levels of PO activity (Decker et al., 2001; Decker and Tuczec, 2000). The PO activity of Hc from the Freshwater crayfish, *Pacifasticus leniusculus* (Crustacea), in contrast, cannot be elicited by treatment with detergents; only proteolytic cleavage can perform this function (Lee et al., 2004). This latter finding was unusual as SDS leads to activation of PO activity in a range of Hcs from arthropods (chelicerata and crustacea) and molluscs, as well as PPOs from plants and animals (Decker and Tuczec, 2000). Perchlorate and hemocyte lysate supernatant components have been found to elicit some level of PO activity in crustacean Hc whereas they have no effect on chelicerate Hc PO activity (Zlateva et al., 1996; Adachi et al., 2003). Likewise, studies of chelicerate Hc identified the non-proteolytic activation of PO activity by phospholipids and antimicrobial peptides (Nellaiappan and Sugumaran, 1996; Nagai et al., 2001).

In terms of the subunits of arthropod Hc which display inducible PO activity, a number of studies by Heinz Decker and his colleagues (Decker et al., 2001; Decker and Rimke, 1998; Jaenicke and Decker, 2004) have demonstrated that chelicerate Hcs show PO activity which is restricted to certain subunit types. Subunits II, V and VI show PO activity in *L. polyphemus* Hc, and of these V and VI bridge the four hexamers of each half molecule of this 8 x 6-meric protein. *E. californicum* Hc subunits b and c share the same topological positions within this 4 x 6-meric molecule, and are in fact the two subunit types which were identified as demonstrating inducible PO activity (See Figure 45, Chapter 6 for illustration of subunit topology). Crustacean Hcs conversely appear to show no localisation of PO activity, but rather display weak enzymatic activity in all subunit types.

Since the turn of the century, preliminary studies have provided some clues to the potential pathway for the activation of Hc PO activity *in vivo* (Nagai et al., 2001; Adachi et al., 2003). Experiments conducted *in vitro* by Adachi et al (2003) have demonstrated that the PO activity of Hc from the Kumura prawn, *Penaeus japonicus* (Crustacea) can be induced by hemocyte components in the presence of the elicitor  $\beta$ -1,3-glucan. The absence of hemocyte lysate from the reactions resulted in no significant PO activity implying no direct interaction between Hc and elicitor molecules. Serine/cysteine proteases were implied in the activation mechanism of crustacean Hc PO activity, though not directly. Rather than cleavage of the peptide chain, cleavage of the reductive bonds (such as disulphide bonds) within certain subunits of this crustacean Hc appeared necessary for induction of Hc PO activity, perhaps resulting in a conformational change which opens the Hc dicopper center (Adachi et al., 2003). Hemocyte component activated Hc demonstrated the ability to catalyse the oxidation

of tyrosine and DOPA to dopaquinone – an early step in the melanogenic pathway. More recently, SDS activated Hc from the same species was found also to catalyse a later step in melanin synthesis; the oxidation of 5,6-dihydroxyindole (DHI) to DHI-quinone which produces black melanin pigment (Adachi et al., 2005). Further work is required in this area; however, it is very tempting to speculate that these results suggest a dual role for Hc in arthropods; both as an oxygen carrier and as a defence protein involved in the defensive immune reactions.

### **7.1.3 Hypotheses on the Structural Changes Required to Elicit Phenoloxidase Activity in Arthropod Hemocyanin.**

To date, there have been no reports describing experiments designed to characterise the artificially induced conformational changes taking place in the Hc molecule upon incubation with SDS. Decker and Rimke (1998) and Decker and Jaenicke (2004) have proposed that, regardless of the activating agent used, triggering of Hc PO activity requires removal of the placeholder amino acid from the entrance to the dicopper centre (Phe-49 in *L. polyphemus* and *E. californicum*), thus allowing entry of larger phenolic substrates. A few years prior to this it was suggested that a conformational change was associated with percholate and SDS induced activation of arthropod Hc (Zlateva et al., 1996; Nellaiappan and Sugumaran, 1996), and so it appears likely that non-proteolytic activation (by detergents, phospholipids, denaturants and antimicrobial peptides) involves a structural shift which pulls the placeholder amino acid out of the proteins dicopper centre.

The aim of the investigation presented in the following chapter is to characterise the conformational changes associated with non-proteolytic activation of PO activity in

arthropod Hc. The results of this biophysical study provide some preliminary indications of the structural changes associated with SDS induced activation of PO activity, in Hc from the ancient chelicerates *L. polyphemus* and *E. californicum*, and the more modern chelicerate *Pandinus imperator* (Emperor scorpion). SDS is routinely used as the activating agent during assays of PO activity of native PO enzymes. Due to the structural and physiochemical characteristics shared between Hc and PO, it is proposed that the conformational changes identified in this current investigation will provide clues for the activation mechanism of native PO.

## **7.2 Methods**

### **7.2.1 Phenoloxidase Activity Assays.**

The PO activity of arthropod Hc was measured in 1 ml assay reactions. Firstly, SDS was mixed with 100 mM sodium phosphate buffer (Stock: 200 mM Na<sub>2</sub>HPO<sub>4</sub>, 200 mM NaH<sub>2</sub>PO<sub>4</sub>) to final concentrations of between 0.25 mM and 40 mM SDS, covering the sub-micellar and micellar range of this detergent in the above buffer. *Limulus polyphemus* (Merck-Calbiochem, No. 374804), *Eurypelma californicum* or *Pandinus imperator* Hc (purified protein gifted by Heinz Decker, (Nillius, 2002)) was added to the SDS/buffer mix at a final concentration of 1, 0.3 or 0.16 mg/ml respectively and incubated at room temperature for 5 minutes. The reaction was initiated by the addition of dopamine substrate to a final excess of 2 mM. PO activity was monitored by recording the increase in A<sub>475</sub> (resulting from the formation of dopachrome and its derivatives) every 20 seconds for 3 minutes using an Ultrospec 2100pro UV/Visible spectrophotometer, from which the specific activity of each Hc was derived. Activity was expressed in units where 1 unit equates to the formation of 1

$\mu\text{mol}$  dopachrome per minute, assuming the molar absorption coefficient for dopachrome is  $3600 \text{ M}^{-1}\text{cm}^{-1}$ . Control assays were performed to ensure that neither Hc alone or free copper, could catalyse the conversion of dopamine to dopachrome under the assay conditions used.

To investigate whether the induced PO activity of Hc could be reversed, 1 ml assay reactions were prepared as above, using only *L. polyphemus* or *P. imperator* Hcs, containing SDS at a final concentration of 1.1 mM (micellar concentration). Each reaction was incubated for 5 minutes at room temperature before monitoring PO activity again as above. 300  $\mu\text{l}$  of this reaction was then diluted 3-fold in 100 mM sodium phosphate pH 7.5, and a further 300  $\mu\text{l}$  diluted 3-fold in 100 mM sodium phosphate pH 7.5 containing additional excess dopamine substrate. The PO activity of these diluted reactions was recorded following 5 minutes incubation at room temperature.

To determine whether free phospholipids and small unilamellar phospholipid vesicles (SUVs) could exert an effect similar to SDS on *L. polyphemus* and *P. imperator* Hc, standard assays were conducted as detailed previously, with the exception that SDS was replaced with either free phospholipids (a 50:50 mixture of phosphatidylcholine (PC) and phosphatidylethanolamine (PE)) at final concentrations of 0.5 mM or 1.0 mM, or SUVs (composed of a 50:50 ratio of PC and PE) containing a total phospholipid concentration of 0.5 mM or 1.0 mM. Preparation of these phospholipids and SUVs is described in section 7.2.8 below. Phenoloxidase activity was recorded as outlined previously.

### 7.2.2 Isothermal Titration Calorimetry.

Hc from *L. polyphemus*, *P. imperator* and *E. californicum* was prepared to approximately 0.7 mg/ml (giving a monomer concentration of 10  $\mu$ M, assuming the molecular weight of a single Hc monomer is 72,600 Da) in 100 mM sodium phosphate pH 7.5 and dialysed for 24 hours, against the same buffer, at 4°C. SDS solutions of 75 mM and 30 mM were prepared in the remaining dialysis buffer and loaded into the 250  $\mu$ l syringe of a MicroCal VP-ITC titration calorimeter. Immediately prior to use, the Hc solutions were degassed. Each binding experiment was conducted at 25°C, and involved an initial injection of 1  $\mu$ l, followed by 25 x 10  $\mu$ l injections of SDS (30 mM for *L. polyphemus* and *P. imperator* Hc and 75 mM for *E. californicum*) into a stirred ITC cell (1.4 ml volume) containing the Hc/buffer solution. Control experiments were conducted under identical conditions to estimate the CMC of SDS in 100 mM sodium phosphate pH 7.5, and also to correct for the heat of dilution of SDS and the protein. The integrated heat effects of binding of SDS to Hc were corrected for heats of dilution where necessary and analysed using a standard MicroCal Origin software package. The data was analysed in terms of simple single binding-site and sequential binding-site models.

For the purposes of the ICP-OES experiments detailed in section 7.2.7, ITC was also utilised to gauge an accurate value for the CMC of SDS in 100 mM TrisHCl pH 7.5. This involved recording the heat of dilution during injection of 25 x 10  $\mu$ l aliquots of 20 mM SDS into an ITC cell containing 100 mM TrisHCl pH 7.5 only.

### **7.2.3 Circular Dichroism Spectroscopy.**

1 ml reactions containing 100 mM sodium phosphate buffer pH 7.5 and increasing concentrations of SDS were prepared before adding Hc to a final concentration of 0.3 mg/ml. *L. polyphemus*, *P. imperator* and *E. californicum* Hc were incubated at room temperature in the presence of 0 – 3.5 mM, 0 – 2.0 mM and 0 or 5.0 mM SDS, respectively, for 5 minutes (16 hours additional incubation for *E. californicum* Hc). Near UV CD spectra were recorded using a Jasco J600 spectropolarimeter over the range 250 – 400 nm in a rectangular 0.5 cm pathlength cell, whilst far UV spectra were recorded in a Jasco J-810 spectropolarimeter over 180 – 260 nm in a cylindrical 0.02 cm pathlength cell. 1S-(+)-10-camphorsulphonic acid was used to calibrate the spectropolarimeters. Each spectrum was an average of 4 scans, recorded at a scan rate of 10 nm/min with a time constant of 2 seconds, corrected by subtraction of a spectrum of buffer alone.

### **7.2.4 Fluorescence Spectroscopy.**

A series of 1 ml reactions containing SDS at final concentrations of up to 2.7 mM (*L. polyphemus*), 2.0 mM (*P. imperator*) or 5.0 mM (*E. californicum*) were prepared in 100 mM sodium phosphate buffer pH 7.5. Hc was added to a final concentration of 0.1 mg/ml and the reaction incubated until there were no further structural changes with time; generally 5 minutes was required. Fluorescence measurements were recorded at room temperature in a Perkin Elmer Luminescence Spectrometer (Model: LS 50B) using a 1 ml/1 cm pathlength quartz cuvette. Intrinsic tryptophan fluorescence emission spectra from 300 – 510 nm were obtained using an excitation wavelength of 290 nm, whilst the emission fluorescence spectra of copper (II) quenching of the dicopper centre bound peroxide from 400 – 510 nm, were

obtained by excitation at 330 nm. All spectra were recorded at a scan rate of 50 nm/min with excitation and emission band widths set at 5 nm. A control to eliminate the possibility that a direct interaction between tryptophan residues and SDS could cause changes in fluorescence was performed. All spectra were corrected by subtracting a spectrum of buffer alone. SDS had no influence on the fluorescence spectra under the conditions described.

Similar reactions were prepared to determine the effect of SUVs and free phospholipids on the tryptophan environment of arthropod Hc. Free phospholipids (a 50:50 mixture of phosphatidylcholine (PC) and phosphatidylethanolamine (PE)) at final concentrations of 0.5, 1.0 or 4.0 mM, or SUVs (composed of a 50:50 ratio of PC and PE) containing a total phospholipid concentration of 0.5 mM or 1.0 mM, were added instead of SDS. Preparation of these phospholipids and SUVs is described in section 7.2.8 below. Intrinsic tryptophan fluorescence emission spectra were recorded as detailed earlier.

### **7.2.5 Dynamic Light Scattering.**

All dynamic light scattering (DLS) measurements were recorded using a Malvern, Nano ZS (Red Badge) Differential Light Scatterer (633 nm red He-Ne laser). Particle size (diameter) was determined for *P. imperator* and *E. californicum* Hc in the presence of varying concentrations of SDS. 200 µl reactions containing Hc at a final concentration of 1 mg/ml, were prepared in 100 mM sodium phosphate buffer, pH 7.5 containing SDS at a final submicellar concentration (0.5 mM for both Hc types) or micellar concentration (2.0 mM and 5.0 mM in the case of *P. imperator* and *E. californicum*, respectively). A control reaction containing no SDS was prepared for each Hc type. All measurements were performed in a 100 µl DTS2145 low volume glass cuvette. Particle size measurements were recorded using

15 scans of 10 s duration, at 10 minute intervals over a total period of 40 min. A further 15 scans of 10 second duration were recorded 24 h after the initial preparation of the reactions. All measurements were recorded at 20 °C.

Dynamic light scattering was also used to confirm the CMC of SDS in 100 mM sodium phosphate buffer, pH 7.5. A series of SDS solutions (0.5 mM - 5.0 mM) were prepared in 100 mM sodium phosphate buffer, pH 7.5. Particle size measurements were recorded as detailed above except no measurements were made after 24 hours.

#### **7.2.6 Absorbance Spectroscopy.**

Absorbance spectra of Hc were recorded at room temperature from 240 - 400 nm, in the presence of increasing concentrations of SDS (0 - 2.7 mM for *L. polyphemus*; 0 - 2.0 mM for *P. imperator*; 0 and 5.0 mM for *E. californicum*). 1 ml reactions containing 100 mM sodium phosphate pH 7.5 and SDS were prepared, and Hc added to a final concentration of 0.3 mg/ml. Following 5 minutes incubation at room temperature (16 hours additional incubation was required for *E. californicum* Hc), spectra were recorded using a Jasco V-550 UV/Visible spectrophotometer. Changes in the binuclear copper centre were recorded by observing any changes in the 340 nm absorbance peak characteristic of Type-3 copper proteins. Protein concentrations were accurately determined by recording the absorbance at 280 nm, and using a value of 1.39 for the absorbance of a 1 mg/ml solution of LimHc in a cell of 1 cm pathlength cell, and a value of 1.10 for EuryHc and PanHc.

### 7.2.7 Inductively Coupled Plasma Optical Emission Spectroscopy.

Due to the formation of insoluble copper phosphate upon addition of  $\text{CuSO}_4$  to the 100 mM sodium phosphate pH 7.5 buffer used in all other experiments, for ICP-OES analysis, 1 mg/ml *L. polyphemus* Hc samples were prepared in 100 mM TrisHCl pH 7.5. Hc was incubated at room temperature for 5 minutes in the presence of no SDS, sub-micellar concentrations (1.0 mM) or micellar concentrations (2.0 mM) of SDS (the CMC of SDS in this buffer was determined by ITC). The protein concentration of each reaction was recorded before it was applied to a NAP-5 desalting column (GE Healthcare Cat# 17085301) equilibrated with 10 ml of 100 mM TrisHCl pH 7.5 buffer or buffer/SDS solution. 10 x 0.3 ml fractions of eluant were collected in 0.5 ml Eppendorf tubes. The  $A_{280}$  of each fraction was recorded in a 0.5 ml quartz cuvette to determine the elution point of the protein. Protein peak and wash fractions were pooled to a final volume of 1 ml. Wash fractions are those which would contain copper were it released from the protein into solution. The elution point of free copper was determined from a control column to which a solution of  $\text{CuSO}_4$  in 100 mM TrisHCl pH 7.5 was applied (contained 1000-fold more Cu (II) than 1 mg/ml *L. polyphemus* Hc, for spectroscopic detection purposes).

ICP-OES measurements were recorded using a Perkin Elmer Optima DV4300 instrument. The machine was calibrated, and a standard curve of copper concentration constructed, using a series of dilutions of a  $\text{CuSO}_4$  solution, each of which was prepared in 100 mM TrisHCl, pH 7.5. Standards and pooled samples were diluted 5-fold with 5% Nitric acid prior to loading into the ICP-OES machine. Copper in each standard and sample was detected at the

characteristic copper emission wavelength 327.393 nm, which experienced the least interference from contaminating elements.

### **7.2.8 Phospholipid and Small Unilamellar Vesicle Preparation.**

A solution of small unilamellar vesicles (SUVs) containing 5 mM phospholipids with a 50:50 ratio of L- $\alpha$ -phosphatidylcholine (PC) (Sigma Cat # P-7443) and L- $\alpha$ -phosphatidylethanolamine (PE) (Sigma Cat # P-8193), was prepared in 100 mM sodium phosphate pH 7.5 buffer using the Morrissey Lab protocol available online via Avanti Polar Lipids (Morrissey, Accessed: 2005.). The final product was a suspension of SUVs with diameters typically in the range of 15-50 nm (Avanti Polar Lipids Inc., Accessed: 2005.). A 5 mM solution of phospholipids at a ratio of 50:50 PE:PC was also prepared using a similar protocol, with the exception that the final sonication step was not required. These SUV and phospholipid mixtures were used for activity assays and fluorescence spectroscopy as outlined in sections 7.2.1 and 7.2.4 respectively.

## **7.3 Results**

### **7.3.1 SDS Induced Phenoloxidase Activity of Arthropod Hemocyanins.**

The SDS-induced PO activity of three arthropod Hcs was measured spectrophotometrically by recording the rate of formation of dopachrome and its derivatives at 475 nm. Two ancient chelicerate Hcs (*Limulus polyphemus* and *Eurypelma californicum*) and one more modern chelicerate Hc (*Pandinus imperator*) were used, and are referred to as LimHc, EuryHc and PanHc from hereon in. The CMC of SDS under the conditions used (100 mM sodium phosphate pH 7.5) was determined by isothermal titration calorimetry ( $1.085 \pm 0.035$  mM),

and verified by dynamic light scattering measurements of particle size (1.00 – 1.05  $\mu\text{m}$ ). For future purposes, CMC was taken to be 1.05  $\text{mM}$  where the buffer used was 100  $\text{mM}$  sodium phosphate pH 7.5. Each Hc was incubated for 5 minutes in the presence of SDS at a range of submicellar (0 – 1.05  $\text{mM}$ ) and micellar concentrations (1.05 – 40.0  $\text{mM}$ ).

The results from these assays (Figure 51) indicate that for all three Hc types, SDS concentrations lower than approximately 0.7  $\text{mM}$  do not elicit any significant increase in the detectable PO activity. At concentrations of 0.7 to 1.0  $\text{mM}$  SDS, however, where monomeric SDS is assumed to predominate, PO activity is exhibited and increases to 70%, 89.2% and 57.1% of the maximum activity in LimHc, PanHc and EuryHc respectively.

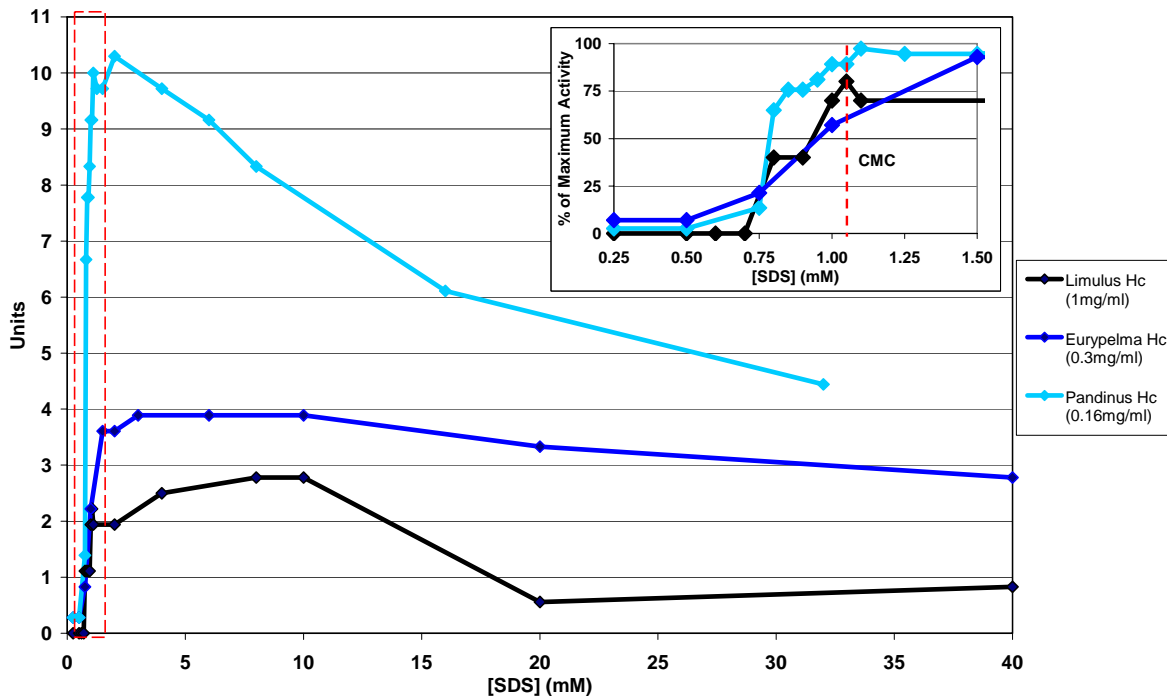


Figure 51: Induced phenoloxidase activity of hemocyanin from *Limulus polyphemus*, *Pandinus imperator* and *Eurypelma californicum*. Typical assays included 2 mM dopamine hydrochloride plus hemocyanin (concentrations in legend) in 1 ml of 100 mM sodium phosphate buffer, pH 7.5. Phenoloxidase activity (expressed in units where 1 unit = formation of 1  $\mu$ mol of dopachrome per minute) was initiated by the addition of SDS, and after 5 minutes, followed by monitoring an increase in absorbance at 475 nm resulting from the formation of dopachrome and its derivatives. Inset provides clearer detail of the region of the main plot contained within the red box, and shows PO activity expressed as a percentage of the maximum activity achieved by each hemocyanin. A full version of the inset plot including data for SDS up to 40 mM can be found in Section 9.4 – Appendix D.

Above 1.0 mM SDS, micelles are present, and increasing SDS concentrations above 1 mM SDS results in the PO activity continuing to increase to a maximum activity of 2.78 units/mg for LimHc (at 8 – 10 mM SDS), 64.25 units/mg for PanHc (at 2 mM SDS) and 12.9 units/mg for EuryHc (at 3 – 10 mM SDS), where 1 unit is equal to 1  $\mu\text{mol}$  of dopachrome formed per minute. The data demonstrates an apparent plateau of PO activity upon reaching the maximum activity in LimHc and EuryHc. At SDS concentrations higher than 10 mM, the PO activity of these Hcs decreases. The activity of PanHc, however, does not plateau but instead starts to decrease almost linearly at SDS concentrations above 2 mM. The activity plots of each Hc nonetheless take the form of a bell-shaped curve. Fewer data points are available for the EuryHc around the CMC of SDS due to a limited availability of stock protein.

Control assays demonstrated that the conversion of dopamine to dopachrome could not be catalysed by (a) LimHc, PanHc or EuryHc in the absence of SDS and also (b) the presence of free copper in the assay solution (were it the case that copper ions were released from the Hc dicopper centre upon interaction with SDS). Further controls showed that the PO activity was directly related to the quantity of Hc present.

### **7.3.2 The Binding of SDS to Arthropod Hemocyanin.**

Isothermal titration calorimetry (ITC) was used in the first instance to estimate the CMC of SDS in the two buffer systems used during experiments: 100 mM sodium phosphate pH 7.5 and 100 mM TrisHCl pH 7.5. CMC was taken as the point at which no further significant endothermic heat changes (due to micelle dissociation) were apparent from the raw data of injections of micellar SDS into buffer (CMC is indicated by a blue arrow in Figure 52, Figure 53, Figure 54 and Figure 55).

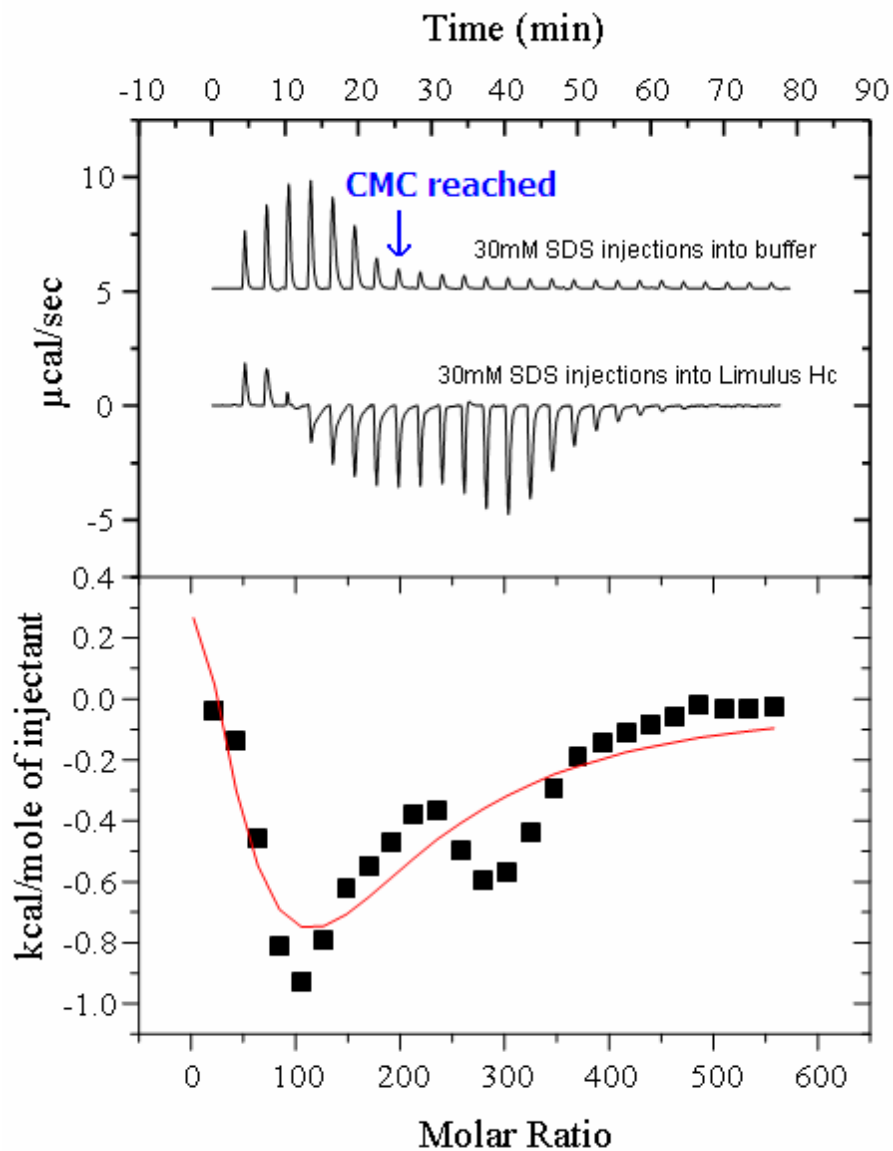


Figure 52: ITC data for binding of SDS to *Limulus polyphemus* hemocyanin. Upper trace in top panel shows a control in which SDS was injected into buffer alone to determine the CMC of SDS in 100 mM sodium phosphate buffer, pH 7.5, and also to correct for heat of dilution of the ligand. Lower trace in upper panel presents the data for injection of 30 mM SDS (0.15 mM per injection) into  $0.77 \pm 0.015$  mg/ml (10  $\mu$ M) *L. polyphemus* hemocyanin monomers (equivalent to 210 nM of the 8 x 6-meric unit). The lower panel shows the calculated binding isotherm (integrated heat data), corresponding to the lower trace in the upper panel, and the best-fitted curve of the data. The calorimetry data shown were analysed by nonlinear regression in terms of a sequential binding site model using the MicroCal ORIGIN software package.

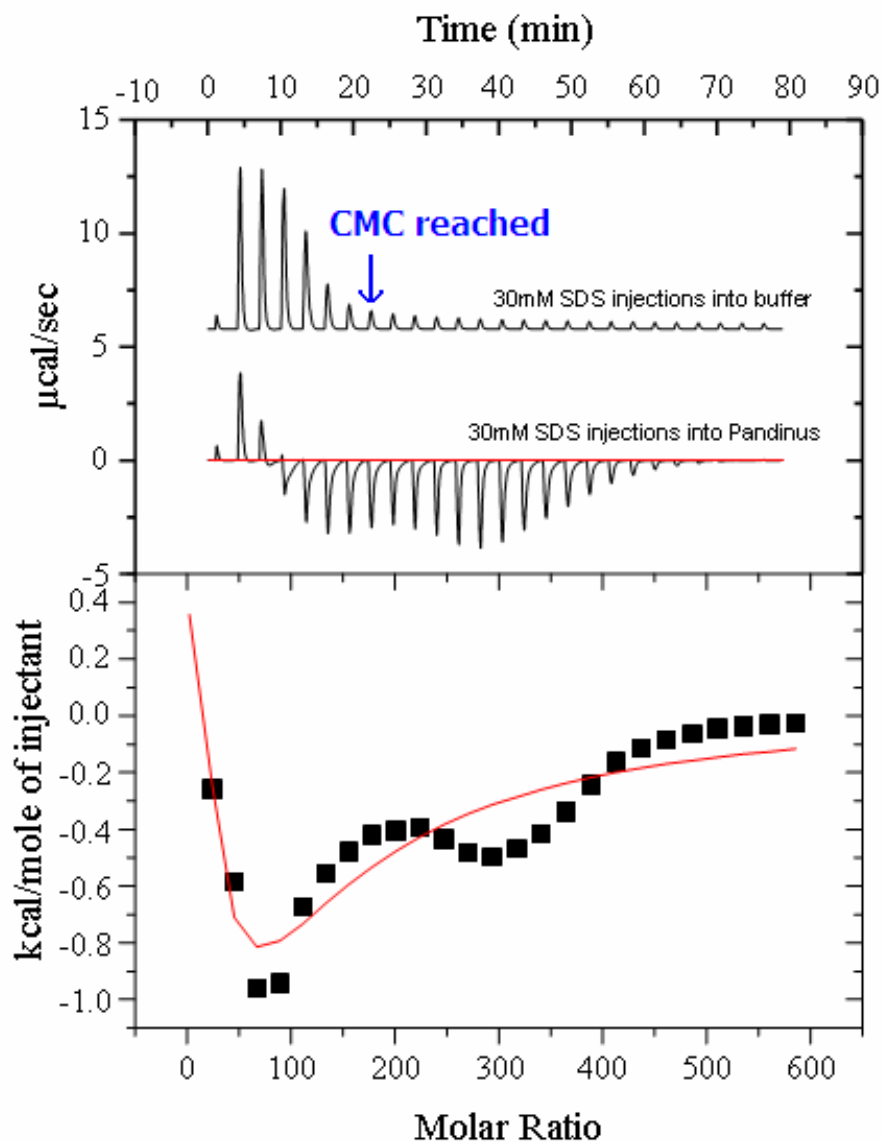


Figure 53: ITC data for binding of SDS to *Pandinus imperator* hemocyanin. Upper trace in top panel shows a control in which SDS was injected into buffer alone to determine the CMC of SDS in 100 mM sodium phosphate buffer, pH 7.5, and also to correct for heat of dilution of the ligand. Lower trace in upper panel presents the data for injection of 30mM SDS (0.15 mM per injection) into  $0.77 \pm 0.015$  mg/ml (10  $\mu$ M) *P. imperator* hemocyanin monomers (equivalent to 420 nM of the 4 x 6-meric unit). The lower panel shows the calculated binding isotherm (integrated heat data), corresponding to the lower trace in the upper panel, and the best-fitted curve of the data. The calorimetry data shown were analysed by nonlinear regression in terms of a sequential binding site model using the MicroCal ORIGIN software package.

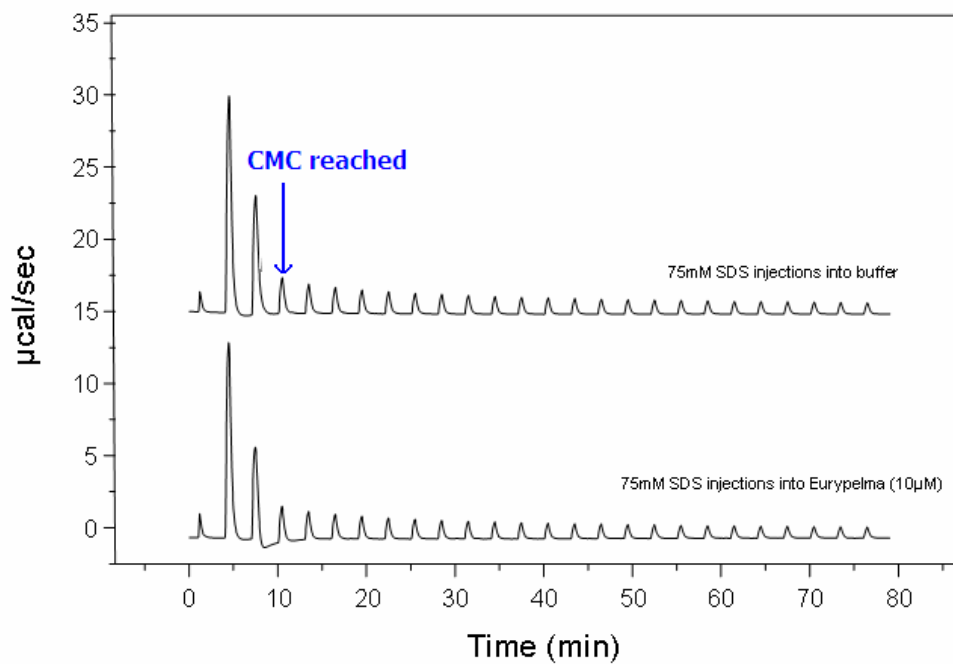


Figure 54: ITC data for binding of SDS to *Eurypelma californicum* hemocyanin. Upper trace shows the control in which SDS was injected into buffer alone to determine the CMC of SDS in 100 mM sodium phosphate buffer, pH 7.5, and also to correct for heat of dilution of the ligand. Lower trace presents the data for injection of 75mM (0.375 mM per injection) SDS into  $0.77 \pm 0.015$  mg/ml (10  $\mu\text{M}$ ) *E. californicum* hemocyanin monomers (equivalent to 420 nM of the 4 x 6-meric unit). As is evident from this lower trace, no heat changes occurred as a result of SDS injection into the protein, therefore no data was available for analysis.

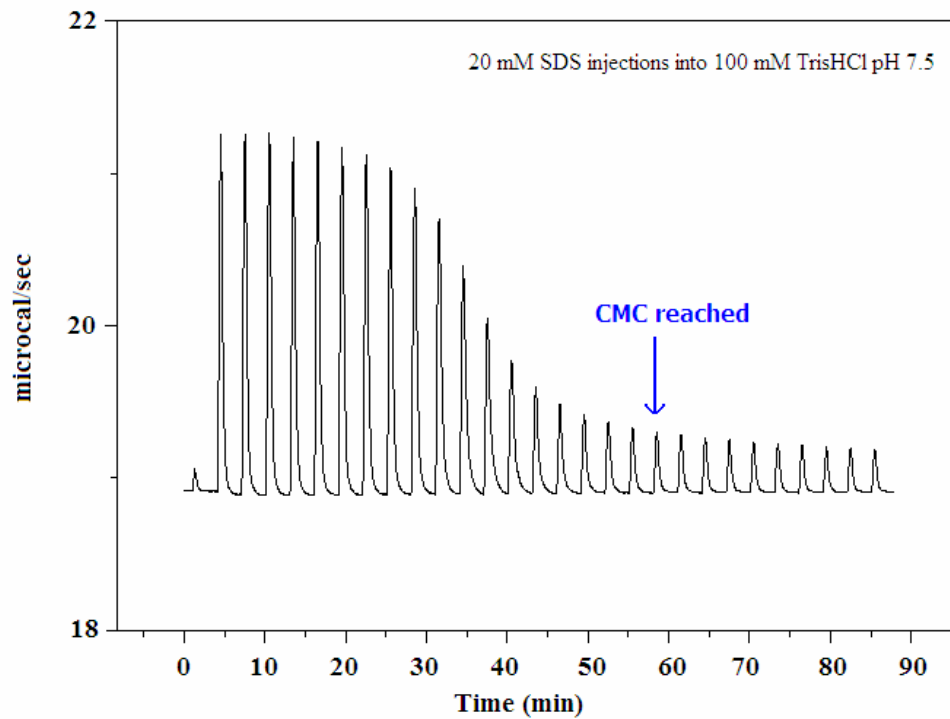


Figure 55: Determination of the critical micelle concentration of SDS in 100 mM TrisHCl pH 7.5 buffer, which was used in ICP OES experiments. The trace shows data for the injection of 20 mM SDS (0.1 mM per injection) into 100 mM TrisHCl pH 7.5 buffer alone.

On this basis, the CMC of SDS under all experimental conditions (which used the buffer 100 mM sodium phosphate pH 7.5, except those for ICP-OES) was  $1.085 \pm 0.035$  mM, whilst for ICP-OES (in which the buffer 100 mM TrisHCl pH 7.5 was used) the CMC was taken as 1.9 mM.

The binding of SDS monomers/micelles to LimHc, PanHc and EuryHc was also examined using ITC. Hc was titrated with SDS so that the calculated binding isotherm for each Hc was representative of binding of SDS to protein at concentrations ranging from below to above the CMC. Analyses of the data were performed by Margaret Nutley of the University of Glasgow Calorimetry Facility, by non-linear regression in terms of either a simple single or sequential binding site model, using the MicroCal ORIGIN software package.

The ITC data for each Hc is presented in Figure 52, Figure 53 and Figure 54, and shows the binding isotherm analysed, where applicable, in terms of a sequential binding site model. Data analysed in terms of a single binding site model can be found in Section 9.5 – Appendix E. With the exception of EuryHc which produced no thermal response, binding of SDS to Hc at submicellar concentrations is initially mildly endothermic as a result of system perturbations during initial titration steps. Increasing SDS concentrations resulted in a biphasic exothermic response suggesting initial binding of SDS monomers to Hc followed by protein-micelle interactions. However due to the nature of the complexity of the binding isotherms no standard binding model could be used for their analysis and subsequently no thermodynamic data could be gleaned for the binding of SDS to Hc.

### 7.3.3 The Effect of SDS on Arthropod Hemocyanin Secondary Structure.

Far-UV circular dichroism spectra of each Hc, in the presence of SDS at submicellar and micellar concentrations, were recorded to give an indication of the secondary structural changes elicited in Hc by monomers and micelles of this detergent (Figure 56, Figure 57 and Figure 58). Spectra show small yet significant changes in the secondary structure of all three Hcs. Changes in the molecular ellipticity at 208 nm and 220 – 222 nm are typically associated with alterations to a proteins  $\alpha$ -helical content (Georgieva et al., 1998). In the present data, these wavelengths indicated an increase in total  $\alpha$ -helical content of all three Hcs with increasing SDS concentration. This was confirmed upon analysis of the data with the secondary structure prediction tool DICHROWEB using SELCON 3 and reference set 3 (kindly performed by Thomas Jess, formerly of the University of Glasgow BBSRC funded Circular Dichroism Facility) (Table 6). These analyses also revealed a concurrent significant decrease in  $\beta$ -sheet content, a slight increase in turns and a slight decrease in unordered structures for all three Hcs. Low monomeric SDS concentrations (0.4 mM) could elicit only minimal structural change. Upon incubation with higher monomeric SDS concentrations (0.7 mM) 20.7 % and 42 % of the total observed change was recorded respectively. At around the CMC of SDS, LimHc had undergone 56.3 % of the total secondary structural change observed, whilst PanHc had shown between 42.0 – 69.0 % change. Only at higher micellar concentrations of SDS (3.5 mM for LimHc and 2.0 mM for PanHc) were there no further significant secondary structural changes recorded. Unlike LimHc and PanHc, EuryHc required a much longer incubation period with SDS in order to display similar secondary structural changes. Denaturation of EuryHc in the presence of SDS for 16 hours was not observed.

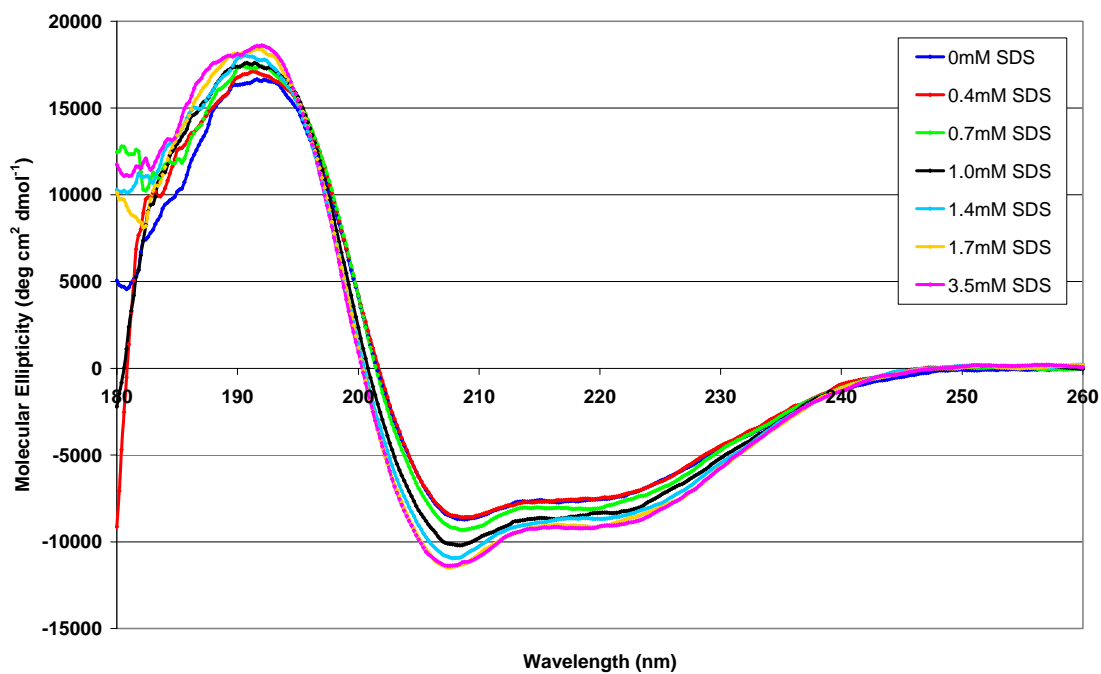


Figure 56: Far UV CD spectra of 0.3 mg/ml *Limulus polyphemus* hemocyanin following 5 minute incubations with SDS across the range 0 – 3.5 mM.

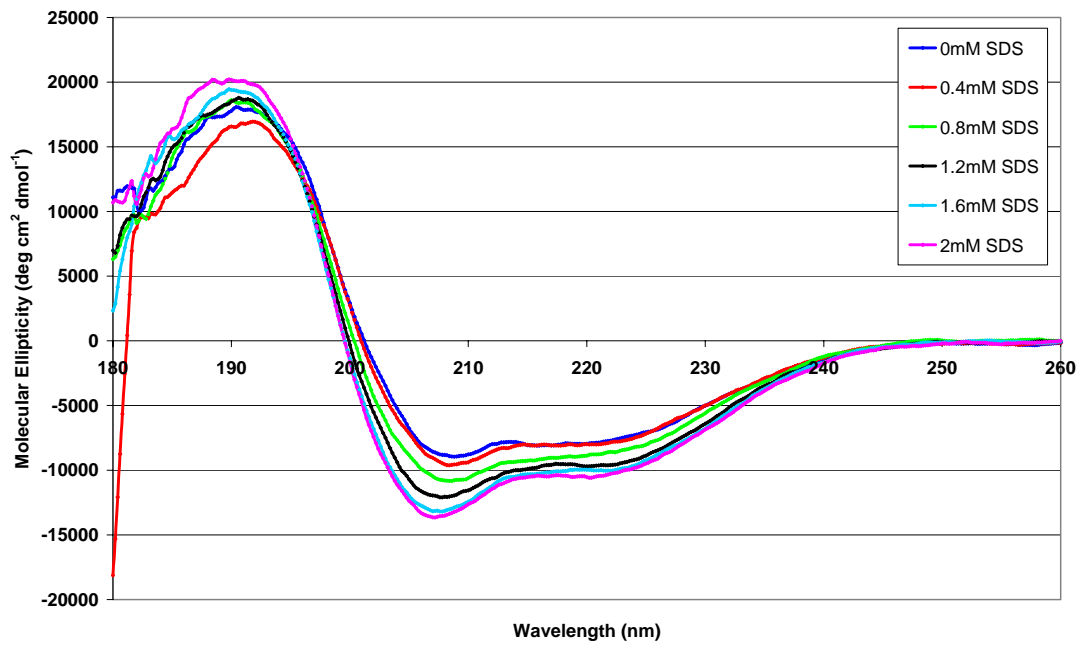


Figure 57: Far UV CD spectra of 0.3 mg/ml *Pandinus imperator* hemocyanin following 5 minute incubations in SDS across the range 0 – 2.0 mM.

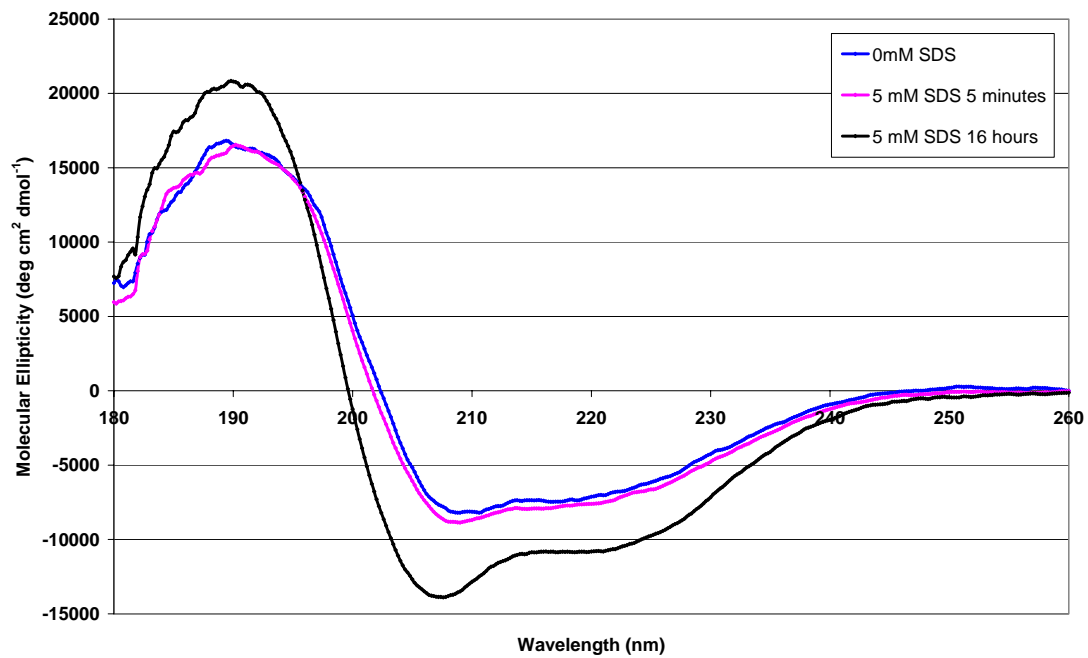


Figure 58: Far UV CD spectra of 0.3 mg/ml *Eurypelma californicum* hemocyanin in the absence of SDS and following a 5 minute and 16 hour incubation in 5.0 mM SDS.

Table 6: Percentage change in secondary structure content of each hemocyanin following incubation in SDS as detailed within the table. Secondary structure predictions were conducted on DICHROWEB, using SELCON 3 and reference set 3.

| Hemocyanin Strain      | Experimental Conditions            | Helix | Sheet | Turns | Unordered |
|------------------------|------------------------------------|-------|-------|-------|-----------|
| Limulus polyphemus     | 0mM SDS                            | 22.3% | 25.0% | 20.5% | 29.2%     |
| Limulus polyphemus     | 3.5mM SDS<br>– 5 minute incubation | 30.9% | 17.3% | 22.2% | 28.8%     |
| Pandinus imperator     | 0mM SDS                            | 26.5% | 20.6% | 22.6% | 28.6%     |
| Pandinus imperator     | 2mM SDS<br>– 5 minute incubation   | 36.4% | 14.6% | 23.1% | 26.9%     |
| Eurypelma californicum | 0mM SDS                            | 25.2% | 21.6% | 22.4% | 28.5%     |
| Eurypelma californicum | 5mM SDS<br>–16 hours incubation    | 37.5% | 12.9% | 23.1% | 27.2%     |

### **7.3.4 The Effect of SDS on Arthropod Hemocyanin Tertiary and Quaternary Structure.**

Tertiary structural changes occurring in Hc upon activation of PO activity by SDS were investigated by recording the intrinsic tryptophan (Trp) fluorescence and near UV circular dichroism spectra of each Hc at sub-micellar and micellar SDS concentrations. Dynamic light scattering was also used to determine any changes in the particle size of PanHc and EuryHc under similar SDS conditions.

#### **7.3.4.1 Intrinsic Tryptophan Fluorescence.**

Increasing concentrations of SDS resulted in a marked 4 to 5-fold increase in the intensity of intrinsic Trp fluorescence of LimHc and PanHc and a 3-fold increase in EuryHc, although the latter required 16 hours additional incubation before displaying these spectral changes (Figure 59, Figure 60 and Figure 61). At low monomeric concentrations of SDS (0.4 mM) PanHc exhibits an increase in Trp fluorescence of 14.5% of the maximum change observed. LimHc is predicted to exhibit a similar increase although no data was collected at 0.4 mM SDS for this Hc. Upon incubation with 0.7 mM SDS, PanHc and LimHc display an increase in Trp fluorescence intensity of 53 % and 57.2 % of the maximum respectively. At and just above CMC (1.0 – 1.4 mM), the fluorescence intensity increase had almost reached the maximum, with LimHc showing 87.9 – 93.1% change and PanHc 91.8%. No further increase in Trp fluorescence intensity was observed in LimHc and PanHc upon reaching SDS concentrations of 2.7 mM and 2 mM respectively.

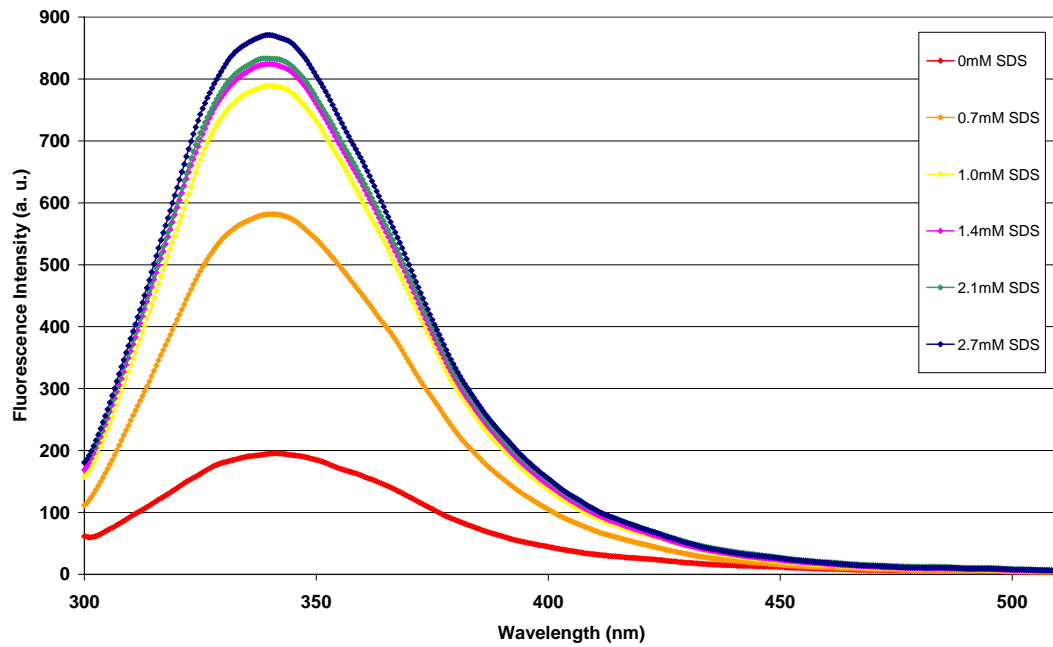


Figure 59: Fluorescence emission spectra of 0.1 mg/ml *Limulus polyphemus* hemocyanin in 100 mM sodium phosphate buffer pH 7.5, excited at 290 nm, following 5 minutes incubation in SDS across the range 0 – 2.7 mM.

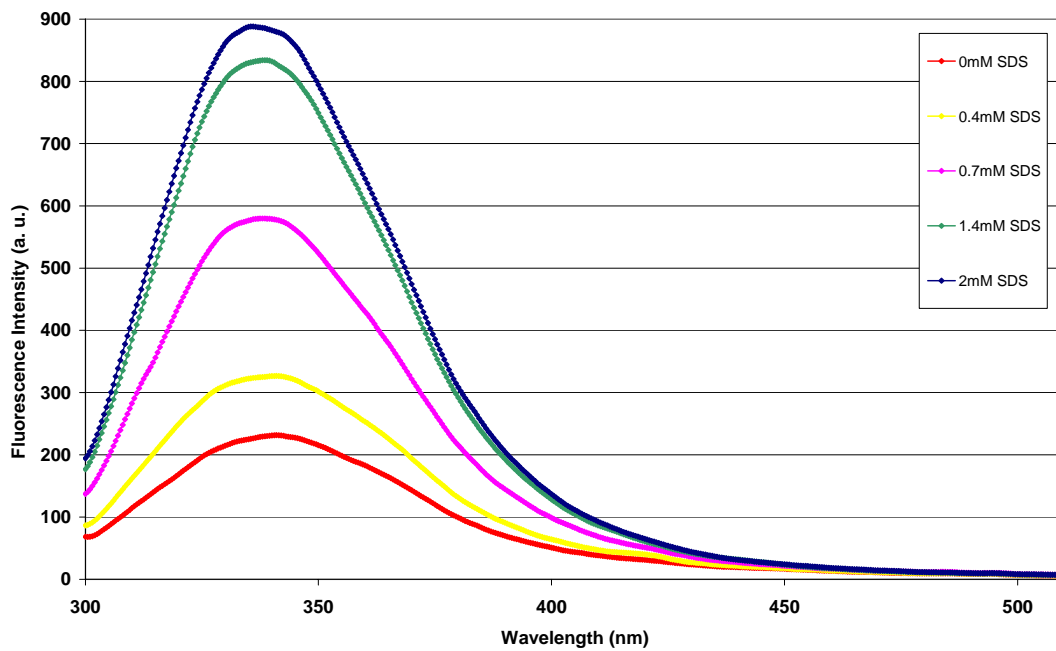


Figure 60: Fluorescence emission spectra of 0.1 mg/ml *Pandinus imperator* hemocyanin in 100 mM sodium phosphate buffer pH 7.5, excited at 290 nm, following 5 minutes incubation in SDS across the range 0 – 2.0 mM.

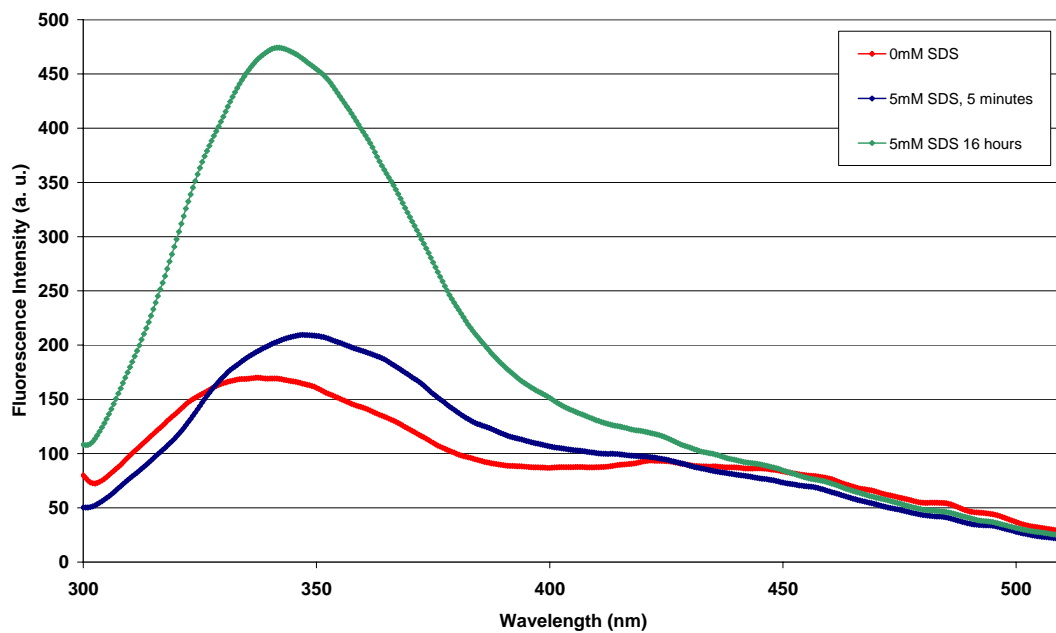


Figure 61: Fluorescence emission spectra of 0.1 mg/ml *Eurypelma californicum* hemocyanin in 100 mM sodium phosphate buffer pH 7.5, excited at 290nm, in the absence of SDS and following 5 minutes or 16 hours incubation in 5.0 mM SDS.

Eury Hc displayed only a minimal increase (13.0%) in Trp fluorescence intensity following 5 minutes in the presence of 5 mM SDS, however a further incubation of 16 hours at room temperature resulted in an increase similar to that exhibited by LimHc and PanHc incubated for 5 minutes in 0.4 – 0.7 mM SDS.

A blue shift was observed in the Trp fluorescence peak of both LimHc and PanHc upon incubation with SDS at concentrations of 0.7 mM and above (Table 7). The maximum blue shift recorded in each Hc was from 341 to 339 nm (0 – 2.1 mM SDS) in LimHc and from 341 to 335.5 nm (0 – 2.0 mM SDS) in PanHc. Conversely EuryHc initially underwent a red shift in the Trp fluorescence peak from 337.5 nm to 347 nm following 5 minutes in the presence of 5 mM SDS. The peak subsequently exhibited a blue shift to 342 nm following a further 16 hours under these conditions.

To eliminate the possibility that the changes in intrinsic Trp fluorescence intensity were due to local effects of SDS monomers/micelles on Trp residues, rather than conformational change, a control experiment was conducted in which the model compound *N*-acetyl-L-tryptophan amide was incubated with SDS. The spectra recorded (Figure 62) illustrate that SDS had no significant effect on the fluorescence intensity or peak wavelength of this compound. Any change in Trp fluorescence exhibited upon incubation of Hc with SDS could therefore be confidently attributed to structural change.

Table 7: Upon excitation at 290 nm, the tryptophan fluorescence peak wavelength of *Limulus polyphemus* and *Pandinus imperator* hemocyanin in 100 mM sodium phosphate buffer pH 7.5, exhibits a blue-shift in the presence of increasing concentrations of SDS. *Eurypelma californicum* hemocyanin on the other hand exhibits a red-shift after 5 minutes incubation. Following 16 hours incubation however, the latter displays a blue shift in the tryptophan fluorescence peak wavelength.

| SDS concentration (mM)    | Limulus Hc Trp Fluorescence Peak (nm) | Pandinus Hc Trp Fluorescence Peak (nm) | Eurypelma Hc Trp Fluorescence Peak (nm) |
|---------------------------|---------------------------------------|--|---|
| 0                         | 341.0                                 | 341.0                                  | 337.5                                   |
| 0.4                       | -----                                 | 341.0                                  | -----                                   |
| 0.7                       | 340.5                                 | 338.0                                  | -----                                   |
| 1.0                       | 340.0                                 | -----                                  | -----                                   |
| 1.4                       | 340.0                                 | 338.5                                  | -----                                   |
| 2.0                       | -----                                 | 335.5                                  | -----                                   |
| 2.1                       | 339.0                                 | -----                                  | -----                                   |
| 2.7                       | 340.0                                 | -----                                  | -----                                   |
| 5.0                       | -----                                 | -----                                  | 347.0                                   |
| 5.0 (16 hours incubation) | -----                                 | -----                                  | 342.0                                   |

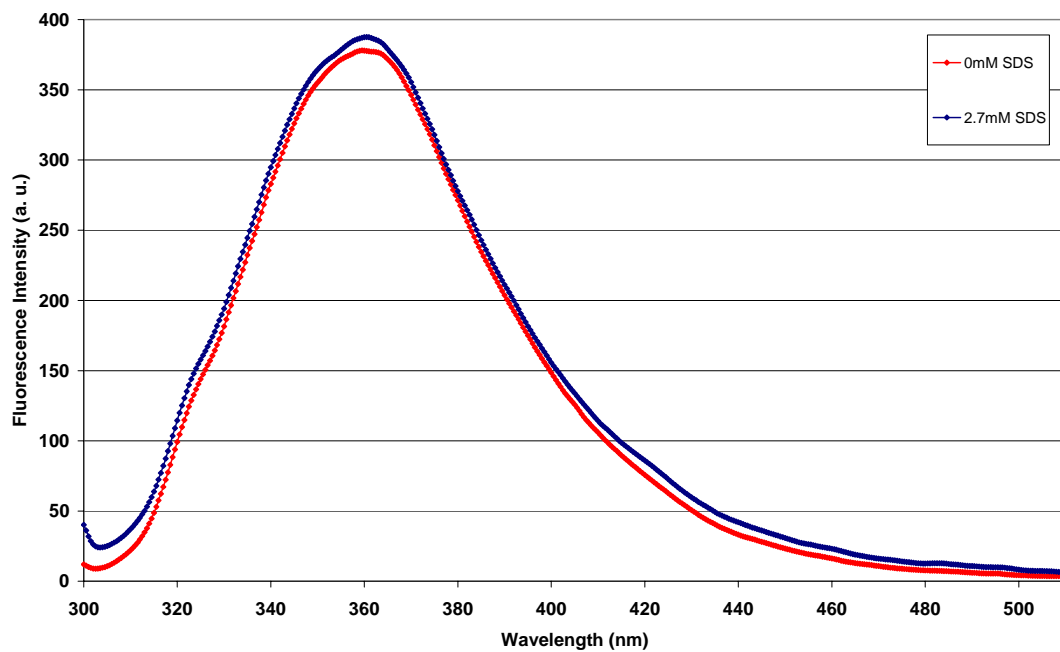


Figure 62: Fluorescence emission spectra of 2 μM *N*-acetyl tryptophan amide in 100 mM sodium phosphate buffer pH 7.5 at 290nm, in the absence of SDS and following 5 minutes incubation in 2.7 mM SDS.

#### **7.3.4.2 Aromatic Amino Acid Near UV Circular Dichroism Spectra.**

Near UV circular dichroism spectra recorded at 260 - 305 nm provided information on the effects of increasing concentrations of SDS on the microenvironment of the aromatic residues, and thus the tertiary structure, of each Hc. This technique was also used to ensure that the observed effects of SDS on Hc fluorescence were related to conformational changes.

The spectra of EuryHc (Figure 63) indicated no significant tertiary structural changes in this protein after 5 minutes incubation in 5 mM SDS. Only following a further 16 hours under these conditions were there significant spectral changes, particularly at wavelengths associated with tryptophan (290 – 305 nm) and to a lesser extent phenylalanine (260 - 270 nm). The overall shape of the EuryHc near UV aromatic amino acid spectrum changes following 16 hours incubation in 5 mM SDS, whereas following 5 minutes incubation the spectra of LimHc and PanHc retain their general shape undergoing only a change in intensity. The spectra of LimHc and PanHc (Figure 64 and Figure 65 respectively) indicated that SDS has an almost immediate effect on the tertiary structure of these Hcs.

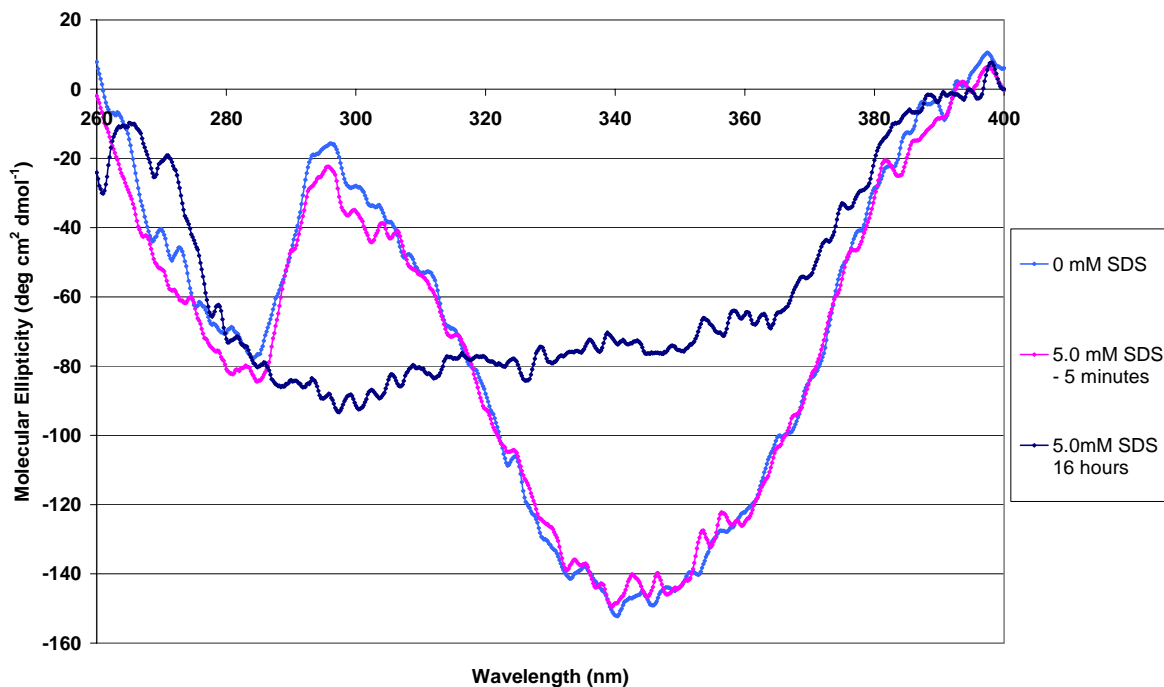


Figure 63: Near UV circular dichroism spectra of 0.3 mg/ml *Eurytelma californicum* hemocyanin in 100 mM sodium phosphate buffer pH 7.5, in the absence of SDS and following either 5 minutes or 16 hours incubation in 5.0 mM SDS. Molecular ellipticity at 260 - 305 nm is associated with the microenvironment of protein aromatic residues. The 340 nm peak is a characteristic near UV signal of the Type-3 copper centre.

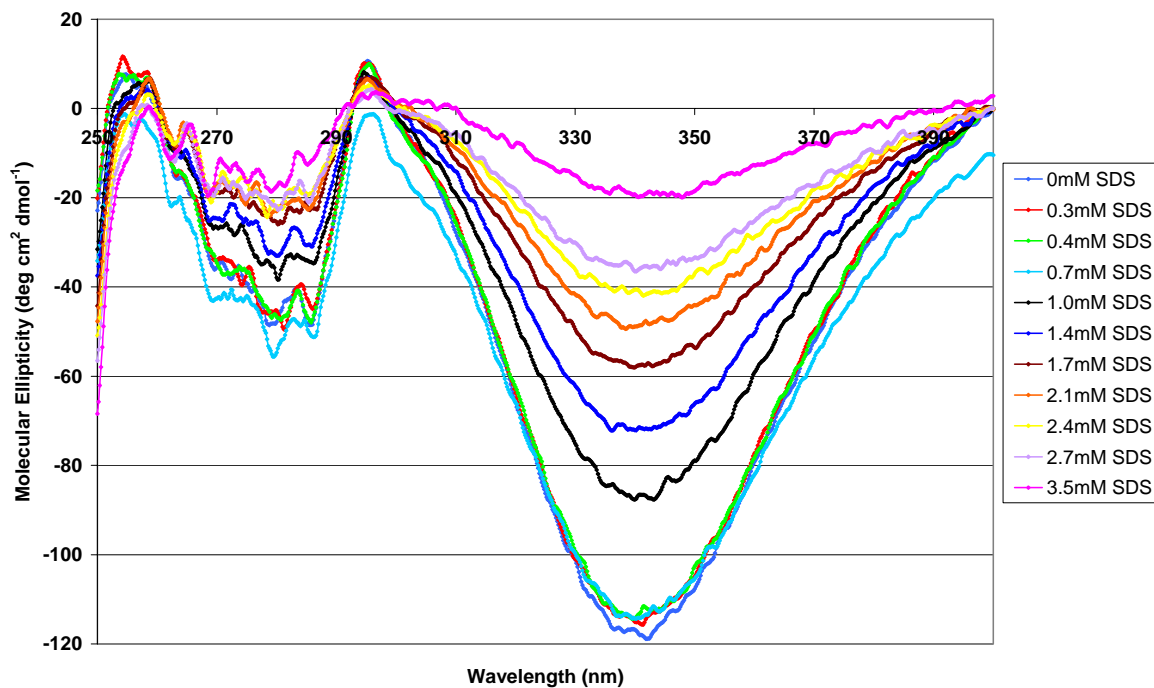


Figure 64: Near UV circular dichroism spectra of 0.3 mg/ml *Limulus polyphemus* hemocyanin in 100 mM sodium phosphate buffer pH 7.5 following 5 minutes incubation in SDS across the range 0 – 3.5 mM. Molecular ellipticity between 260 - 305 nm is associated with the microenvironment of protein aromatic residues. The 340 nm peak is a characteristic near UV signal of the Type-3 copper centre.

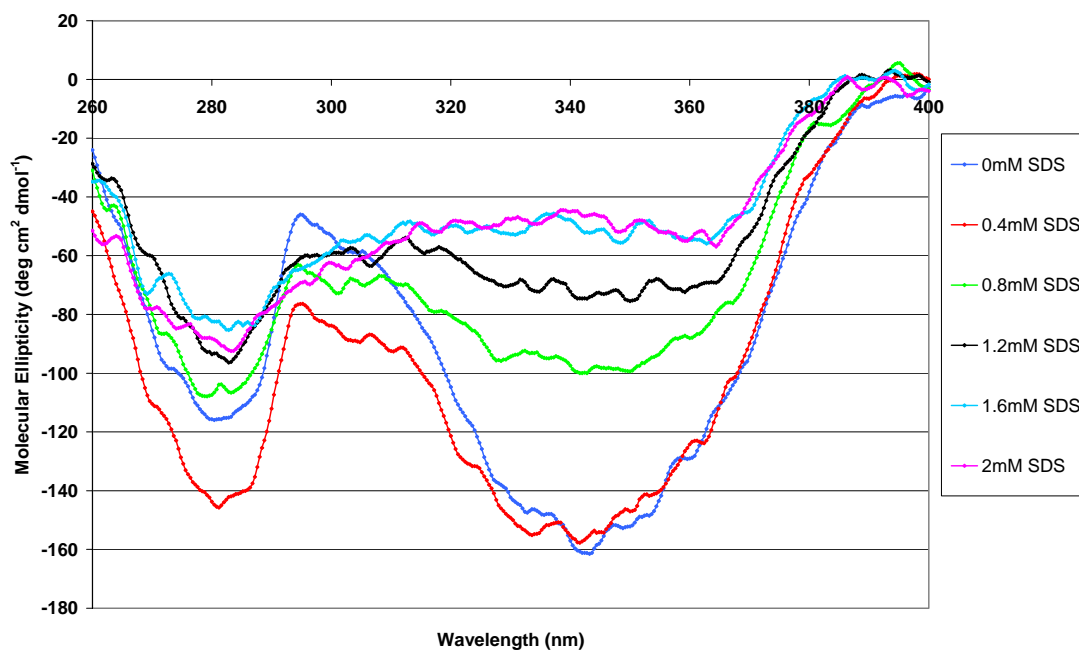


Figure 65: Near UV circular dichroism spectra of 0.3 mg/ml *Pandinus imperator* hemocyanin in 100 mM sodium phosphate buffer pH 7.5 following 5 minutes incubation in SDS across the range 0 – 2.0 mM. Molecular ellipticity at 260 - 305 nm is associated with the microenvironment of protein aromatic residues. The 340 nm peak is a characteristic near UV signal of the Type-3 copper centre.

The presence of low monomeric SDS concentrations (0 – 0.7 mM) elicits small increases in the intensity of the negative aromatic residue signal of LimHc, whilst PanHc appears to experience a more significant increase by only 0.4 mM SDS. However, at concentrations approaching CMC (0.8 – 1.0 mM) and higher, SDS causes rather significant tertiary structural changes in both Hc types. The effect of SDS on Hc at these concentrations is the reverse of the lower submicellar concentrations. Micellar concentrations of SDS result in a reduction in the intensity of the negative spectral peaks in all regions of the near-UV circular dichroism spectra between 260 and 305 nm. No further change in the aromatic residue spectral peaks was evident in LimHc and PanHc upon incubation with 3.5 and 2.0 mM SDS respectively.

Control experiments were performed to ensure that protein concentration did not have any effect on the near-UV circular dichroism spectra. Spectra were recorded of LimHc at a final concentration of 0.3, 0.6 or 0.9 mg/ml, each in the presence of 0, 1.4 and 3.5 mM SDS. When all nine spectra were overlaid (Figure 66) it was clear that the spectra were almost super-imposable indicating no influence of protein concentration of the spectral measurements.

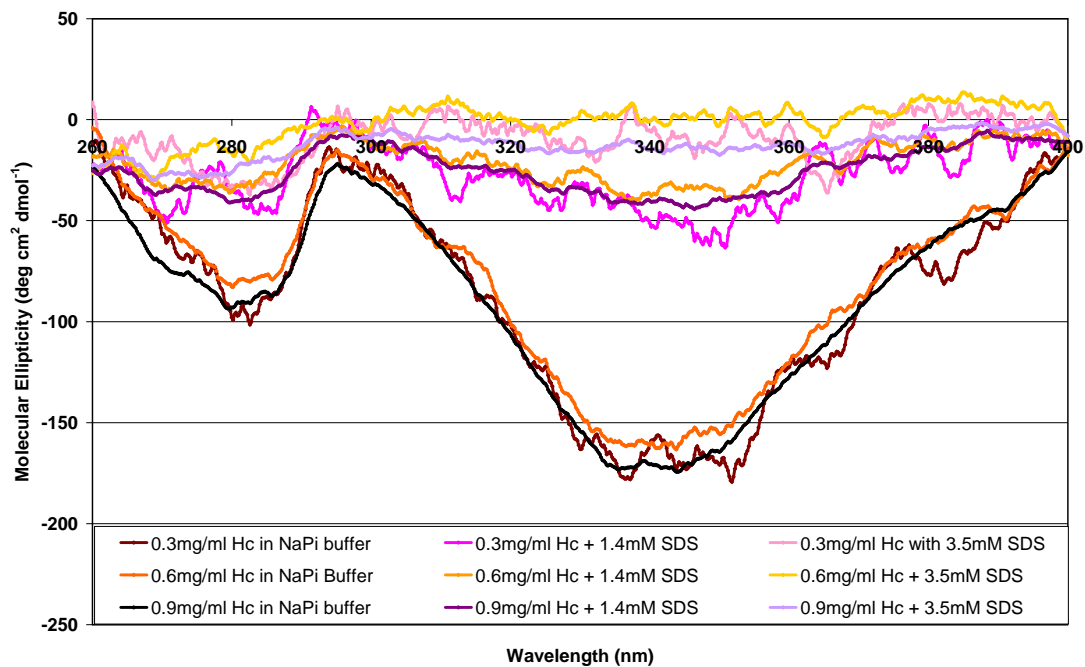


Figure 66: Near UV circular dichroism spectra of 0.3, 0.6 and 0.9 mg/ml *Limulus polyphemus* hemocyanin in 100 mM sodium phosphate buffer pH 7.5 following 5 minutes incubation is SDS at 0, 1.4 and 3.5 mM. Molecular ellipticity at 260 - 305 nm is associated with the microenvironment of protein aromatic residues. The 340 nm peak is a characteristic near UV signal of the Type-3 copper centre. The spectra indicate that protein concentration had no effect on the circular dichroism spectra at the wavelengths and SDS concentrations concerned.

#### **7.3.4.3 Dynamic Light Scattering.**

Dynamic light scattering was used to determine the effect of submicellar and micellar concentrations of SDS on the particle size of PanHc and EuryHc over a 24 hour period (1440 minutes). Measurements of Hc particle size were recorded in the presence of 0.5 mM (both Hcs), 2 mM (PanHc) and 5 mM (EuryHc) over 24 hours. Figure 67 illustrates the change in particle diameter with time. The plots indicate that these Hcs retain a diameter of approximately 20 nm during the first 40 minutes incubation in either sub-micellar or micellar SDS, which is the time period within which most other technique measurements were recorded. Following a 24 hour (1440 mins) incubation period however, whilst EuryHc continues to retain its quaternary structure, PanHc appears to have experienced a reduction in particle size to approximately 10 nm diameter.

DLS was used to verify the results of ITC data which were used to determine the CMC of SDS in 100 mM sodium phosphate, pH 7.5. ITC suggested the CMC of SDS was  $1.085 \pm 0.035$  mM. Figure 68 illustrates the formation of SDS micelle particles between 1.0 and 1.05 mM. On the combined basis of ITC and DLS data, the CMC of SDS for all future experiments was taken as 1.05 mM.

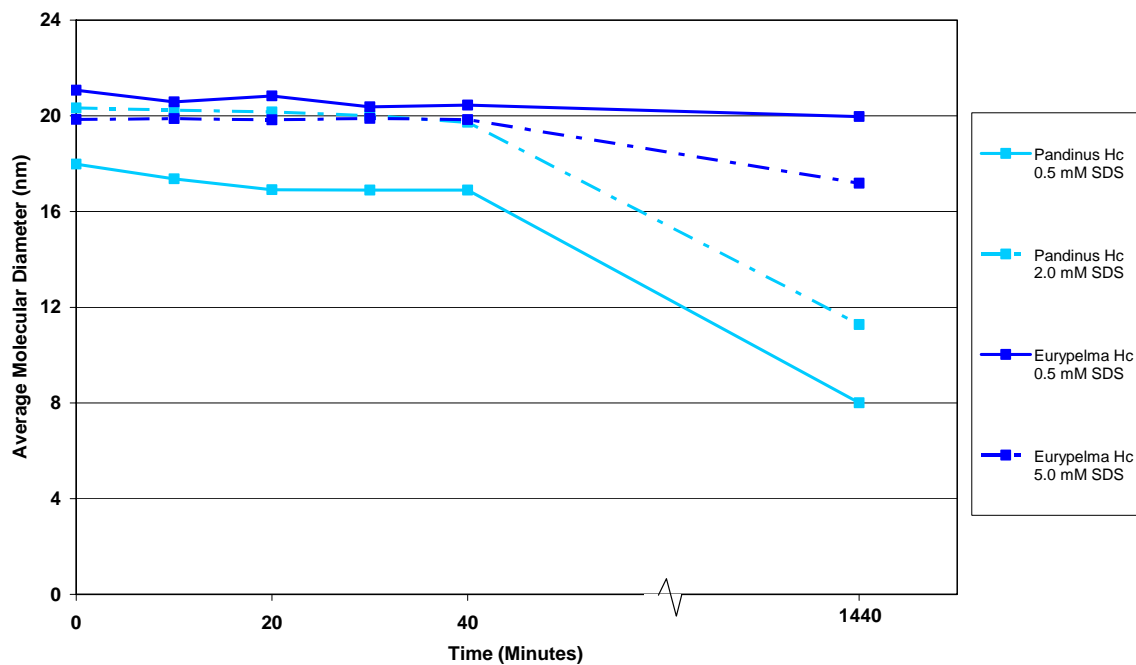


Figure 67: Determination of the stability of *Pandinus imperator* and *Eurypelma californicum* hemocyanin upon incubation with sub-micellar and micellar concentrations of SDS. Dynamic light scattering was used to monitor changes in particle size (diameter) over 24 hours, of 1 mg/ml hemocyanin samples in 100 mM sodium phosphate buffer pH 7.5, incubated with 0.5 mM SDS, 2.0 mM (*P. imperator* Hc only) or 5.0 mM (*E. californicum* Hc only) SDS.

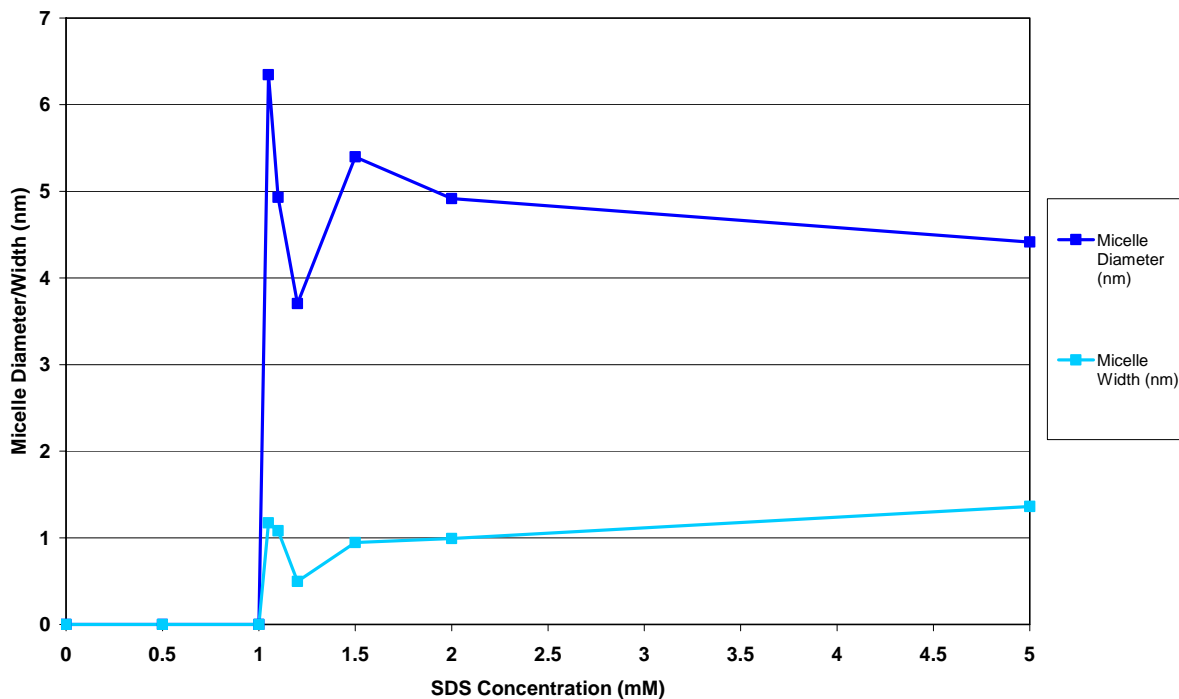


Figure 68: Determination of SDS critical micelle concentration (CMC) in 100 mM sodium phosphate buffer pH 7.5. Dynamic light scattering was used to record changes in particle size (diameter and width) of SDS when present at increasing concentrations in this buffer. The results show that the CMC of SDS in this buffer lies between 1.00 and 1.05 mM.

### **7.3.5 The Effect of SDS on the Arthropod Hemocyanin Type-III Dicopper Centre.**

#### **7.3.5.1 Absorption spectra.**

When molecular dioxygen is bound at the dicopper centre of Hc, a unique absorption peak arises at ~ 340 nm as a result of the  $O_2^{2-} \rightarrow Cu(II)$  charge transfer transitions (Solomon et al., 1990). The band at 280 nm is due to the presence of aromatic amino acid residues (Georgieva et al., 1998). Following a 5 minute incubation of either LimHc or PanHc with increasing concentrations of SDS, the intensity of the 340 nm peak of LimHc and PanHc decreased with increasing concentrations of SDS following a 5 minute incubation period (Figure 69 and Figure 70 respectively). At concentrations of SDS around the CMC (0.8 – 1.2 mM) the 340 nm absorbance peak is reduced by 47.2% in LimHc and 28.7 - 56% in PanHc, whilst the signal becomes completely absent upon incubation with 2.7 mM and 2.0 mM SDS respectively. As in all earlier described results, EuryHc demonstrated no significant change in the intensity of its 340 nm absorption peak upon 5 minute incubation with either submicellar or micellar concentrations of SDS (Figure 71). Only following 16 hours incubation in SDS were comparable changes in the absorption spectra detected (Figure 72).

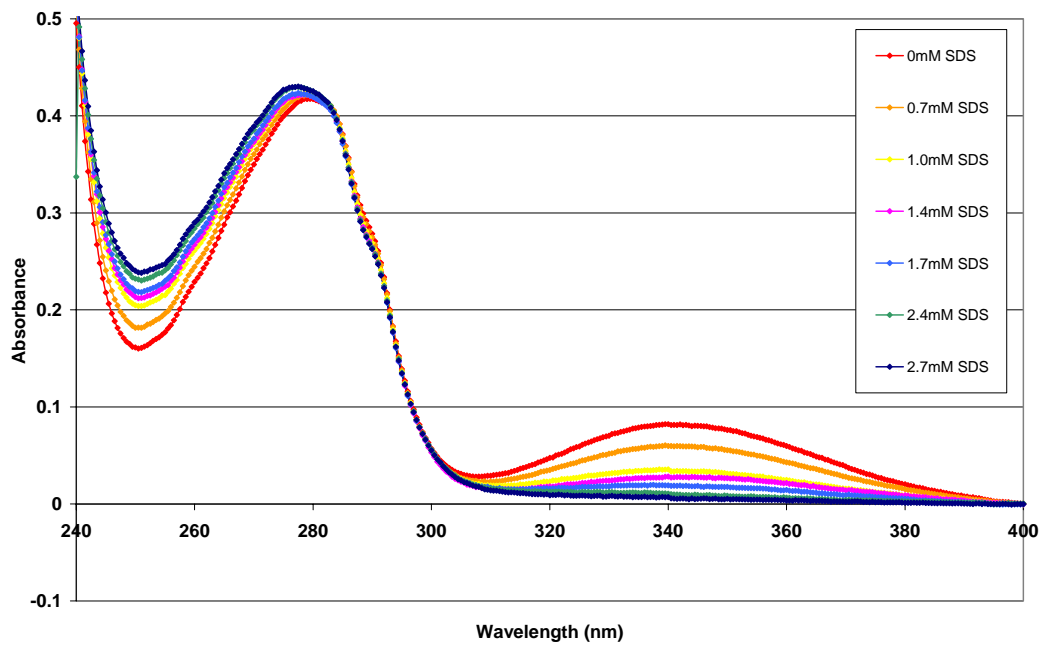


Figure 69: Absorbance spectra of 0.3 mg/ml *Limulus polyphemus* hemocyanin in 100 mM sodium phosphate buffer pH 7.5 following 5 minutes incubation in SDS across the range 0 – 2.7 mM.

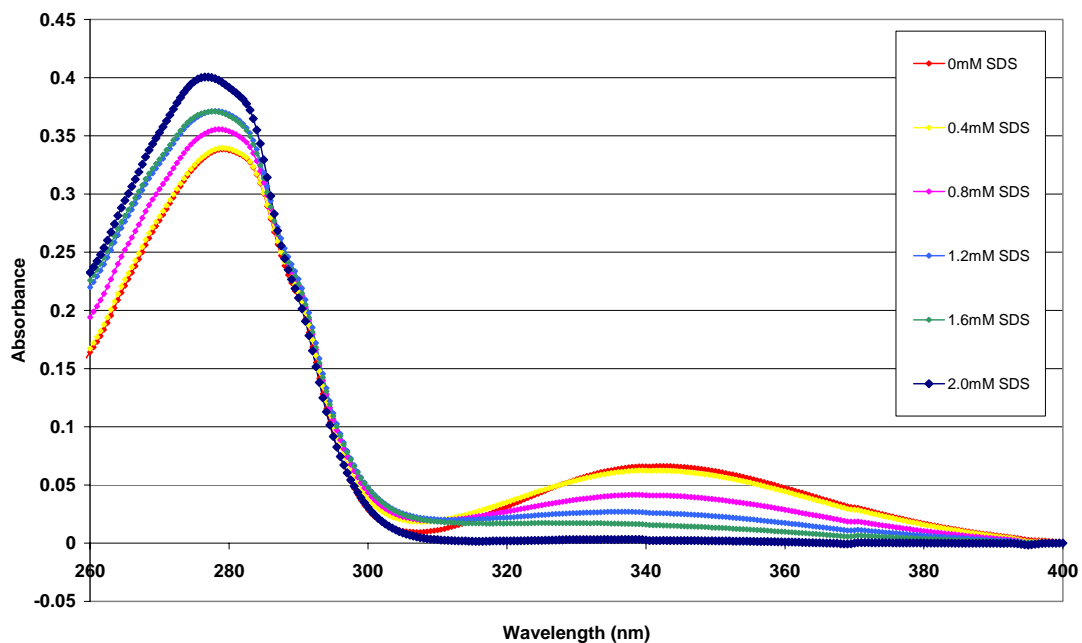


Figure 70: Absorption spectra of 0.3 mg/ml *Pandinus imperator* hemocyanin in 100 mM sodium phosphate buffer pH 7.5 following 5 minutes incubation in SDS across the range 0 – 2.0 mM.

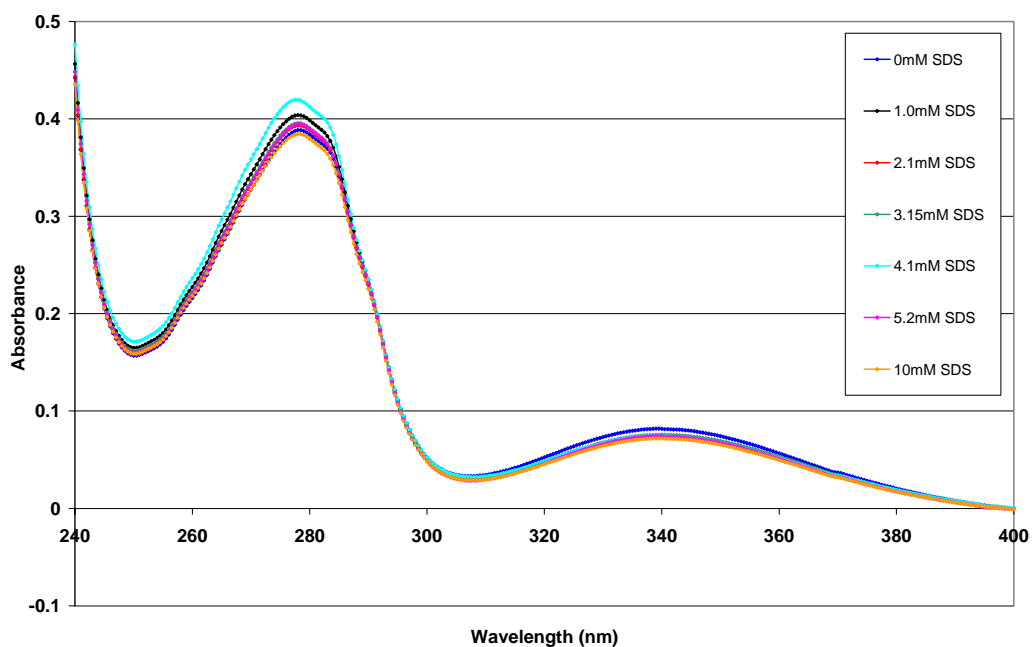


Figure 71: Absorption spectra of 0.3 mg/ml *Eurypelma californicum* hemocyanin in 100 mM sodium phosphate buffer pH 7.5 following 5 minutes incubation in SDS across the range 0 – 10 mM.

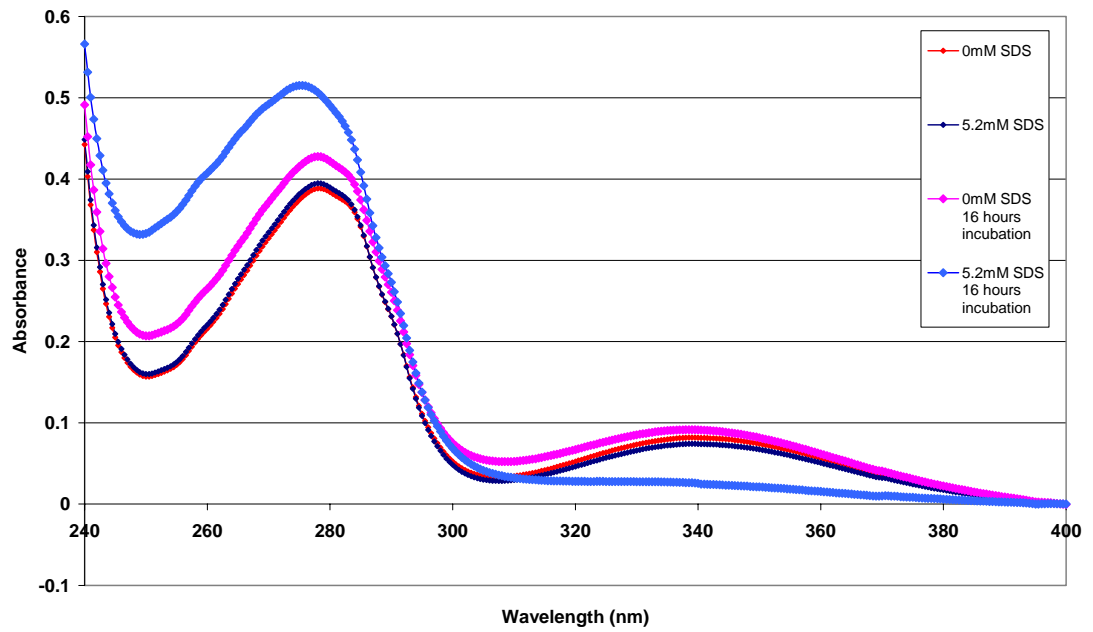


Figure 72: Absorption spectra of 0.3 mg/ml *Eurypelma californicum* hemocyanin in 100 mM sodium phosphate buffer pH 7.5 following 5 minutes or 16 hours incubation in the absence or presence of 5.2 mM SDS.

### **7.3.5.2 Type-3 Copper Centre Near UV Circular Dichroism Spectra.**

The near UV circular dichroism (CD) spectra of arthropod Hc not only provided information about the tertiary structure of the protein (discussed in section 7.3.4.2), but also clues as to changes in the nature of the copper-dioxygen charge transfer at the dicopper centre. Oxy-Hc results in a very large distinct negative ellipticity at  $\sim 340$  nm.

From Figure 64 and Figure 65 in section 7.3.4.2, which show the near UV CD spectra of LimHc and PanHc respectively, it is evident that increasing concentrations of SDS have the effect of reducing the intensity of the 340 nm signal, similar to the effect on the 340 nm absorption band for these Hcs. LimHc and PanHc show no, or a minimal, reduction in the intensity of this peak when the concentration of SDS is below 0.7 and 0.8 mM respectively. Both at and above these concentrations, SDS causes a significant reduction in the intensity of the 340 nm near UV CD spectral peak of both Hcs. Concentrations within range of the CMC (0.8 – 1.2 mM) caused a 53.3 – 75.8 % reduction in the PanHc peak and a 30.0% reduction in the LimHc peak. No further significant reduction in the 340 nm CD signal was evident at concentrations above 1.6 and 3.5 mM in PanHc and LimHc respectively. The 340 nm near UV CD spectral peak of EuryHc (Figure 63) was not significantly affected by 5 minute incubations in SDS at either submicellar or micellar concentrations. However, following 16 hours incubation in 5.0 mM SDS, a significant reduction in the signal at this wavelength was recorded, although the spectral pattern between 300 and 330 nm showed differences in shape in comparison to that of LimHc and PanHc. This may, however, have been as a result of increased signal contributions from the aromatic amino acids, especially tryptophan.

### **7.3.5.3 Fluorescence Spectra at 330nm Excitation.**

Type-3 copper proteins exhibit a characteristic fluorescence emission peak at 415 – 445 nm when excited between 325 and 345 nm. This fluorescence is in addition to the 340 nm intrinsic tryptophan emission peak observed when these proteins are excited at 280 -295 nm. Indications are that histidine carboxyl groups are responsible for the intense 415 – 445 nm fluorescence peak, however the close proximity or bonding of Cu (II) to these fluorophores in Type-3 copper proteins, results in the quenching of this fluorescence (Bacci et al., 1983).

This method was used to provide preliminary indications as to whether the copper ions at the Hc dicopper centre were remaining bound upon incubation with SDS, since the absence of a 340 nm absorption peak is a characteristic of apo-Hc (Georgieva et al., 1998). Upon excitation at 330 nm, were the histidine coordinated copper ions in Hc being lost from the dicopper centre, it was expected that there would be a significant increase in the intensity of the 415 – 445 nm fluorescence emission band with increasing SDS concentrations. However, neither LimHc, PanHc nor EuryHc (Figure 73, Figure 74 and Figure 75 respectively) demonstrated such an increase following either 5 minutes or 16 hours (EuryHc only) incubation in submicellar and micellar concentrations of SDS.

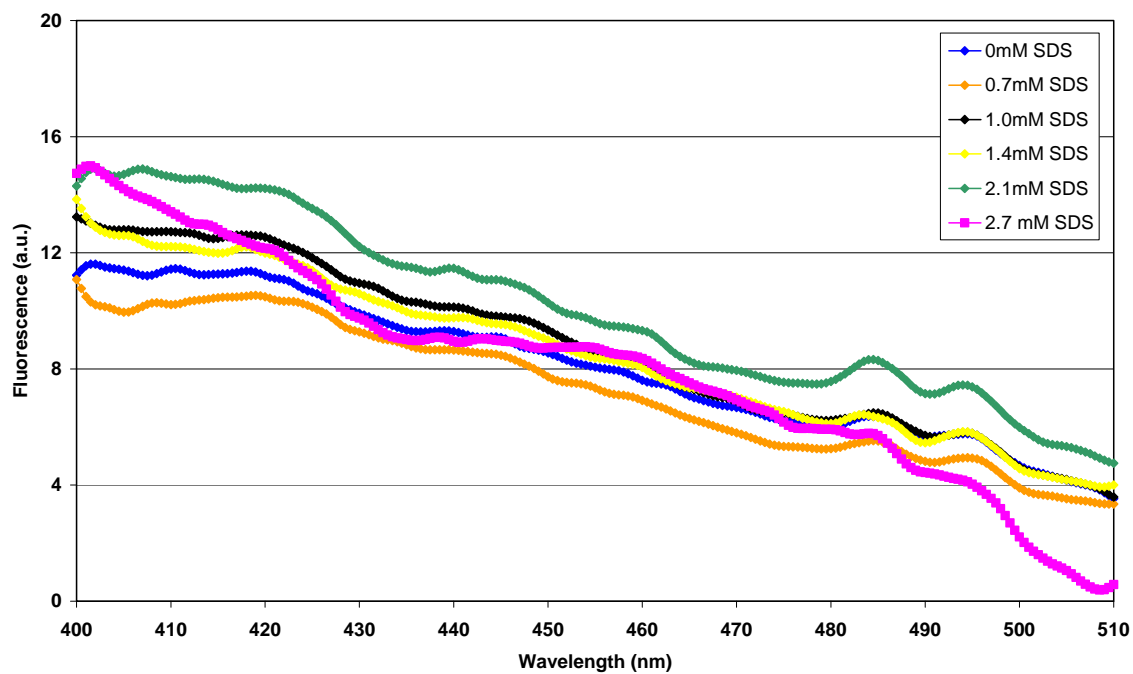


Figure 73: Fluorescence spectra of 0.1 mg/ml *Limulus polyphemus* hemocyanin in 100 mM sodium phosphate buffer pH 7.5 excited at 330 nm following 5 minutes incubation with 0 – 2.7 mM SDS.

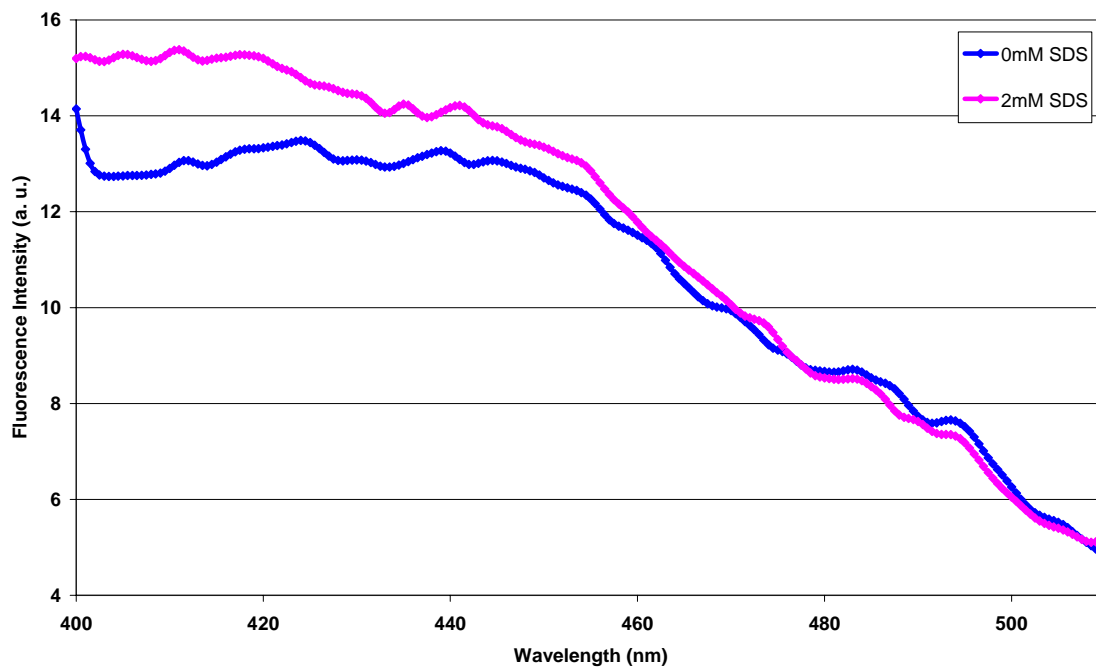


Figure 74: Fluorescence spectra of 0.1 mg/ml *Pandinus imperator* hemocyanin in 100 mM sodium phosphate buffer pH 7.5 excited at 330 nm following 5 minutes incubation with 0 or 2 mM SDS.

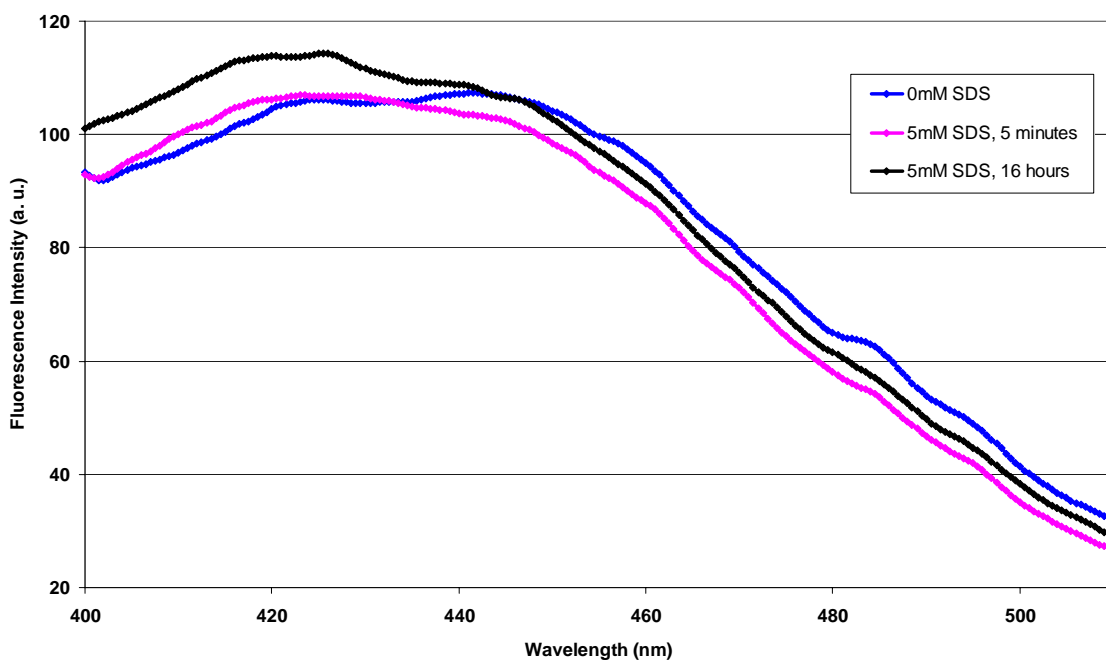


Figure 75: Fluorescence spectra of 0.1 mg/ml *Eurytelma californicum* hemocyanin in 100 mM sodium phosphate buffer pH 7.5 excited at 330 nm following 5 minutes or 16 hours incubation with 5 mM SDS.



#### **7.3.5.4 ICP OES.**

Inductively coupled plasma optical emission spectroscopy (ICP OES) is a very sensitive technique which provides quantitative data on the concentration of selected ions within a sample. Following on from the results of fluorescence measurements presented in section 7.3.5.3, this method was used to more confidently determine whether the dicopper centre copper ions remained associated with Hc during incubation with SDS. LimHc was incubated in either 1.0 or 2.0 mM SDS before the sample was applied to a desalting column. Fractions which contained the protein and those which would contain copper were it released into solution, were pooled separately and subjected to ICP OES analysis.

The results presented in Table 8 support the results from fluorescence measurements in section 7.3.5.3. The actual copper concentration in each protein fraction sample was in good agreement with the expected concentration, which was calculated on the basis that both copper ions remained associated with the LimHc dicopper centre whether sub-micellar or micellar concentrations of SDS were present. Those fractions which would be expected to contain copper were it released from LimHc upon SDS incubation, generated negative values of copper concentration, essentially indicating that no copper was present in these fractions.

Table 8: ICP-OES analysis of *Limulus polyphemus* hemocyanin in the absence and presence of SDS. Hemocyanin in 100 mM sodium phosphate buffer, pH 7.5, was incubated with no SDS, sub-micellar or micellar concentrations of SDS, then applied to a NAP-5 desalting column equilibrated with respective concentrations of SDS. Protein peak and wash eluant were pooled separately and diluted 5-fold in 5% nitric acid prior to ICP-OES analysis. The ‘Expected’ copper concentrations shown were calculated for the diluted samples, and on the basis that both copper ions remained associated with each hemocyanin subunit upon incubation with SDS. Protein concentration was determined from UV absorbance measurements at 280nm using a value of 1.39 for a 1 mg/ml *L. polyphemus* hemocyanin solution, which in turn contained 1.7 mg/L Cu<sup>2+</sup>. The negative values of the ‘Actual’ wash eluant are due to the copper concentrations being lower than those in the 0 µg/L standard used for calibration of the ICP-OES equipment. Effectively there was no Cu in these washes.

| Sample Analysed          | Copper concentration of protein peak eluant (µg/L) |            | Copper concentration of wash eluant (µg/L) |              |
|--------------------------|--|------------|--|--------------|
|                          | Expected   | Actual     | Expected                                   | Actual       |
| Hemocyanin + buffer only | 46.2   | 51.0 ± 1.9 | 0  | -5.54 ± 0.11 |
| Hemocyanin + 1.0 mM SDS  | 51.0   | 55.4 ± 0.9 | 0  | -4.07 ± 0.47 |
| Hemocyanin + 2.0 mM SDS  | 45.2   | 48.7 ± 0.8 | 0  | -2.80 ± 0.18 |

For the purposes of ICP OES, it was necessary to use a 100 mM TrisHCl pH 7.5 buffer due to the formation of insoluble copper carbonate upon addition of copper sulphate to the 100 mM sodium phosphate pH 7.5 buffer used in all other experiments. An assay of both LimHc and PanHc PO activity, in the presence of sub-micellar and micellar concentrations of SDS, was performed in 100 mM TrisHCl, pH 7.5 buffer to ensure equivalent activity could be elicited to that recorded in sodium phosphate buffer, which it could. ITC was used to determine the CMC of SDS in 100 mM TrisHCl pH 7.5 buffer (~1.9 mM) as detailed in section 7.3.2.

### **7.3.6 Correlation of Data from PO Activity Assays and Fluorescence and Far UV Circular Dichroism Spectroscopy.**

The relationship between the data from Hc PO activity assays versus data from Trp fluorescence and far UV CD spectroscopic measurements with increasing concentrations of SDS (Figure 76), suggested that tertiary structural changes preceded secondary structural changes in relation to SDS concentration in both LimHc and PanHc. The plot also highlights the necessity for the presence of SDS micelles to induce the optimal structural change required to elicit the maximum PO activity in these Hc molecules.

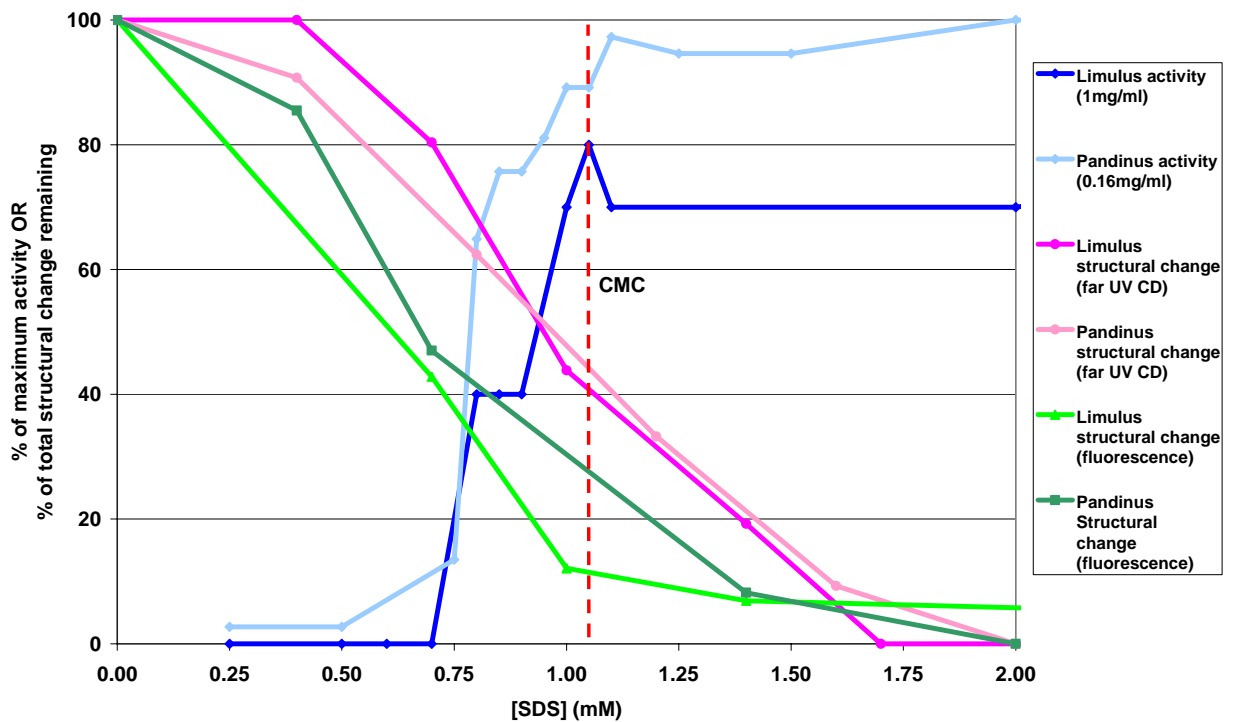


Figure 76: Relationship between the phenoloxidase activity data, far UV circular dichroism spectroscopic data and tryptophan fluorescence data of *L. polyphemus* and *P. imperator* hemocyanin following incubation with submicellar and micellar concentrations of SDS. *E. californicum* hemocyanin data was not included due to a lack of any spectroscopic change in this hemocyanin over the 5 minute time period during which most data was collected. The percentage of maximum activity and the percentage of total structural change remaining are plotted against increasing SDS concentration. For both hemocyanin types, phenoloxidase activity was correlated with the far UV circular dichroism measurements made at 207 nm and the tryptophan fluorescence measurements made at  $\lambda_{\text{max}}$ .

### **7.3.7 The Effect of Non-ionic Detergents on the Secondary and Tertiary Structure of *Limulus polyphemus* Hemocyanin Subunit II.**

The effect of the non-ionic detergent n-Nonyl- $\beta$ -D-glucopyranoside (NBDG) on Hc structure, selected on the basis that it has a similar CMC value to SDS, was investigated by recording the near and far UV spectra of *Limulus polyphemus* Hc subunit II (LpII). These experiments were conducted using a single subunit species of this Hc (supplied from Sigma as a lyophilised powder rather than a blue liquid) which did not give rise to the 340 nm near UV signal typical of the oxy-Hc Type-3 copper centre. Nonetheless, the effects of NBDG on the secondary and tertiary structure of LpII in comparison to SDS could still be investigated. Preliminary indications were that the secondary structure of Hc was unaffected by the non-ionic detergent NBDG (Figure 77), whilst SDS at the same concentration caused similar secondary structural change to that described for the whole *L. polyphemus* Hc molecule (LimHc) in section 7.3.3. NBDG was also unable to induce similar changes to SDS in the tertiary structure of LpII, indicated by no decrease in the intensity of the 260 – 305 nm signals of the near UV CD spectra (Figure 78).

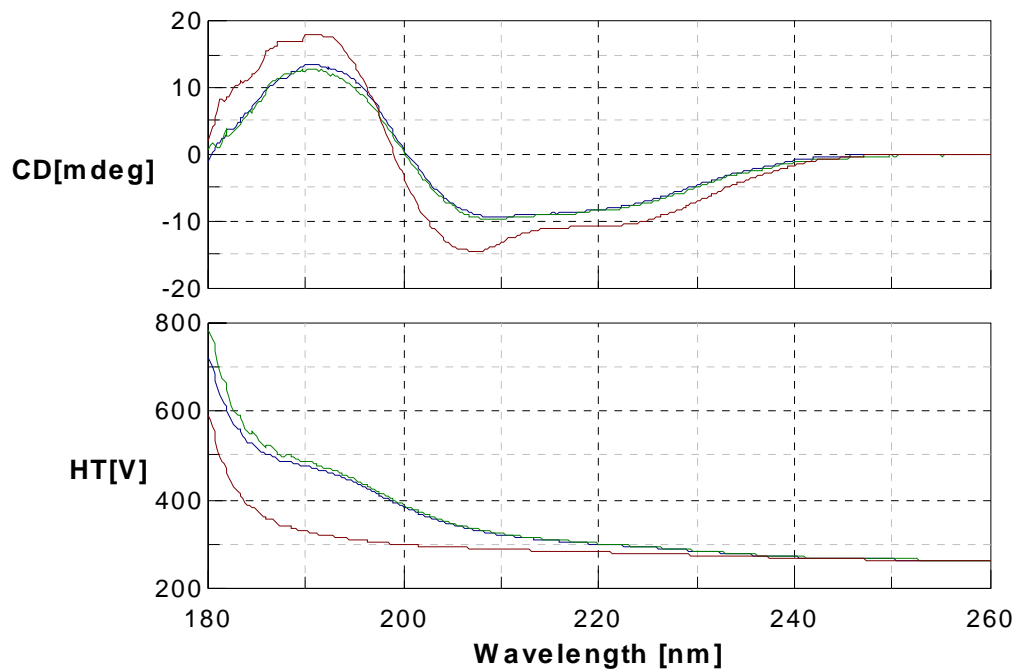


Figure 77: Far UV circular dichroism spectra (top panel) of *Limulus polyphemus* hemocyanin subunit II in 100 mM sodium phosphate buffer, pH 7.5 (green) and following 5 minutes incubation in the presence of 2.7 mM SDS (maroon) or 2.7 mM NBDG (dark blue) .

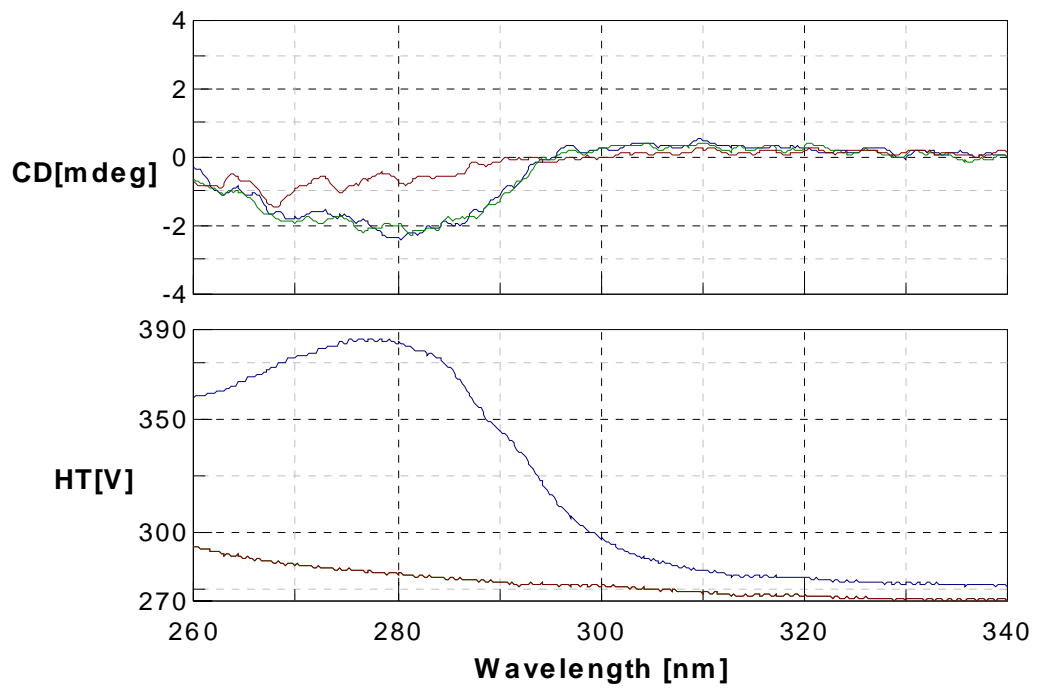


Figure 78: Near UV circular dichroism spectra (top panel) of *Limulus polyphemus* hemocyanin subunit II in 100 mM sodium phosphate buffer, pH 7.5 (green) and following 5 minutes incubation in the presence of 2.7 mM SDS (maroon) or 2.7 mM NBDG (dark blue).

### **7.3.8 Reversibility of the Effects of SDS on Arthropod Hemocyanin.**

The results presented thus far have provided an indication of the functional and structural changes which take place in arthropod Hc upon incubation of the protein with the ionic detergent SDS at both sub-micellar and micellar concentrations. Here activity assay and CD experiments were conducted to evaluate the reversibility of the observed changes in Hc, i.e. will removal of micellar SDS result in a reduction in PO activity with a concurrent reversal of the structural change.

SDS cannot be removed from solution by simple dialysis. Therefore reactions containing SDS at a concentration above CMC were prepared as normal and then diluted in 100 mM sodium phosphate pH 7.5 buffer to reduce the SDS concentration to below CMC. Whilst this would also dilute the protein, earlier experiments indicated that CD spectra were unaffected by protein concentration and PO activity was directly related to protein concentration.

Upon incubation with micellar concentrations of SDS (1.1 mM), LimHc and PanHc demonstrated activities of 1.11 and 59 Units/mg of protein respectively (where 1 unit = the formation of 1  $\mu$ mol of dopachrome per minute). A 3-fold dilution of these reactions in 100 mM sodium phosphate pH 7.5 buffer exhibited no measurable PO activity. These steps were repeated with the exception that an additional excess of dopamine substrate was included in the buffer used for dilution of the reactions, to ensure that substrate was not limiting. Once again there was no detectable PO activity in the diluted LimHc reaction; however the diluted PanHc reaction exhibited an activity of 15.6 Units/mg protein, which is comparable with the

activity of the non-diluted reaction allowing for errors during dilution. Whilst it may be the case that the induction of LimHc PO activity is reversible, it is plausible that LimHc did possess PO activity when additional substrate was included during dilution. Poor spectrophotometer sensitivity may, however, have resulted in failure to detect any very low levels of activity present.

Near UV CD spectra were recorded for LimHc and PanHc (Figure 79 and Figure 80), whilst only LimHc was subjected to far UV CD (Figure 81) measurements due to a limited supply of PanHc. In all instances, the spectra were recorded for Hc (i) in the absence of SDS, (ii) in the presence of 1.1 mM SDS, following a 5 minute incubation, and (iii) 5 minutes after diluting reaction '(ii)' 3-fold in 100 mM sodium phosphate pH 7.5 buffer. In the presence of 0 and 1.1 mM SDS, far UV and near UV spectra were consistent with the CD data presented in sections 7.3.4.2 and 7.3.5.2 for these Hc types.

Together the results suggested that the SDS induced PO activity and dicopper centre perturbations of LimHc and PanHc could not be reversed; not at least by simple dilution of the reaction. However the structural changes which occurred at the secondary level apparently could be reversed by diluting the SDS present, back to concentrations which were below the CMC.

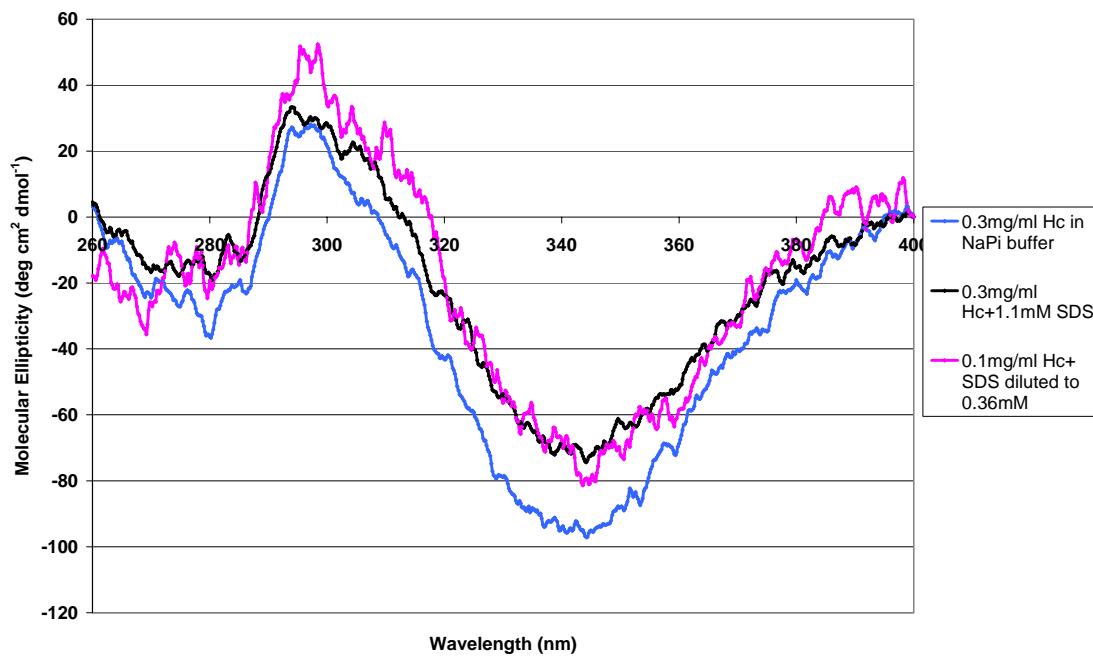


Figure 79: Near UV CD spectra of 0.9 mg/ml *Limulus polyphemus* hemocyanin in 100 mM sodium phosphate buffer, pH 7.5, before and after 5 minutes incubation with 1.1 mM SDS, then 5 minutes after the solution was diluted by a third to bring the SDS concentration to below CMC (0.36 mM), subsequently also diluting the hemocyanin to 0.3 mg/ml.

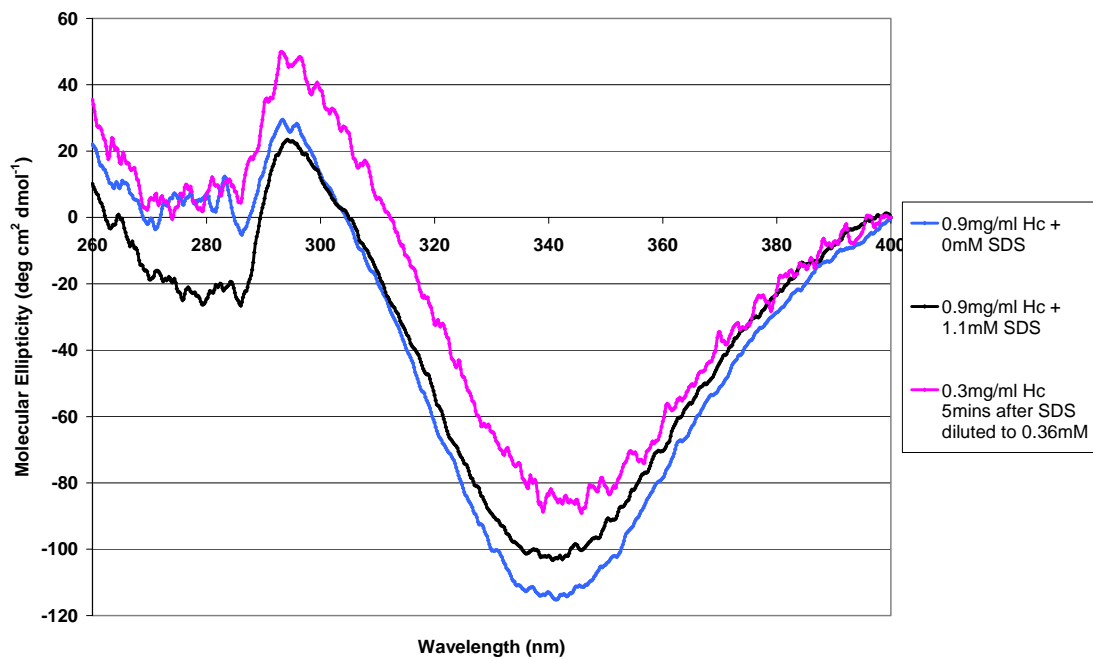


Figure 80: Near UV CD spectra of 0.9 mg/ml *Pandinus imperator* hemocyanin in 100 mM sodium phosphate buffer, pH 7.5 before and after 5 minutes incubation with 1.1 mM SDS, then also 5 minutes after the solution was diluted by a third to bring the SDS concentration to below CMC (0.36 mM), subsequently also diluting the hemocyanin to 0.3 mg/ml.

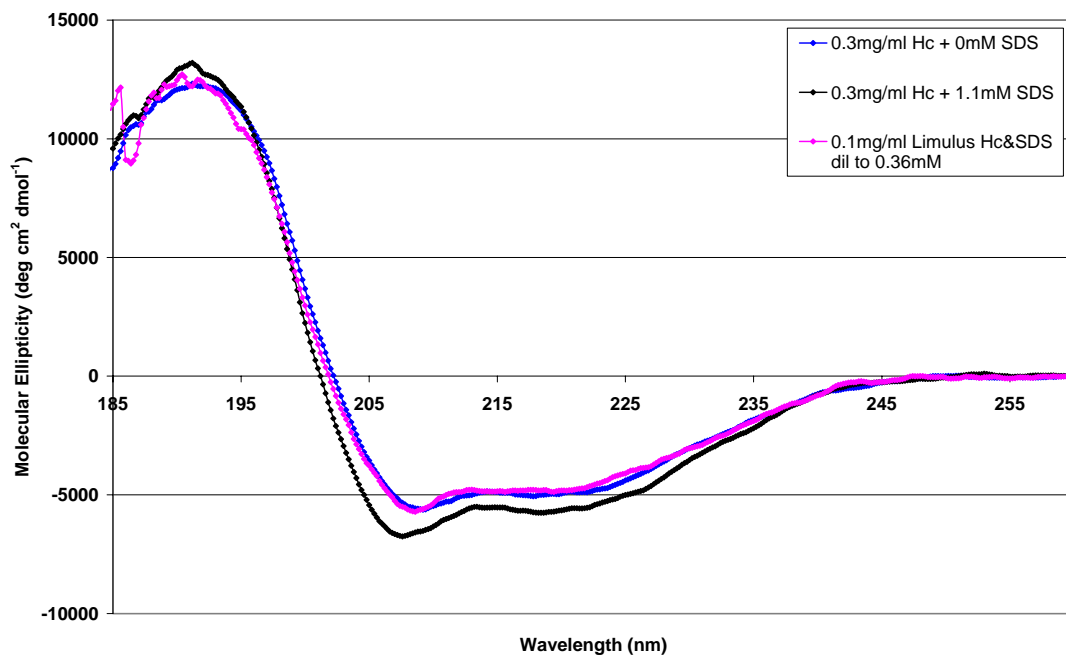


Figure 81: Far UV CD spectra of 0.3 mg/ml *Limulus polyphemus* hemocyanin in 100 mM sodium phosphate buffer, pH 7.5, before and after 5 minutes incubation with 1.1 mM SDS then once SDS was diluted out to 0.36 mM, below CMC.

### **7.3.9 The Effect of Phospholipids and Liposomes on Arthropod Hemocyanin.**

Phospholipids and SDS share common structural features. The monomers of each have a hydrophobic tail and hydrophilic head region, and can aggregate to form larger spherical multimeric structures known as liposomes or micelles respectively. They are also both amphiphilic in nature. Therefore, given the effects that monomeric and micellar SDS have been shown to have on Hc structure and function, phospholipids and liposomes were considered as potential *in vivo* elicitors of Hc PO activity. To investigate this possibility, phospholipids and liposomes were incubated with LimHc and PanHc in activity assays and fluorescence spectroscopy experiments. The resulting preliminary data was compared with that from equivalent experiments using SDS monomers and micelles, to determine whether phospholipids/liposomes could induce comparable activity levels and changes in the tryptophan fluorescence in these Hc types. A 50:50 mixture of the phospholipids phosphatidylcholine (PC) and phosphatidylethanolamine (PE) was used in all the experiments, either as monomers or in the form of small unilamellar vesicles (SUVs). The activity assays demonstrated that no measurable PO activity could be elicited in either LimHc or PanHc upon 5 minute incubation with either lipids or liposomes at either 0.5 or 1.0 mM total phospholipid.

Fluorescence spectra of LimHc and PanHc indicated that, despite no induction of PO activity, there are small changes in the environment of at least some of the tryptophan residues of both Hc types in the presence of either phospholipids (Figure 82 and Figure 83) or SUVs (Figure 84 and Figure 85).

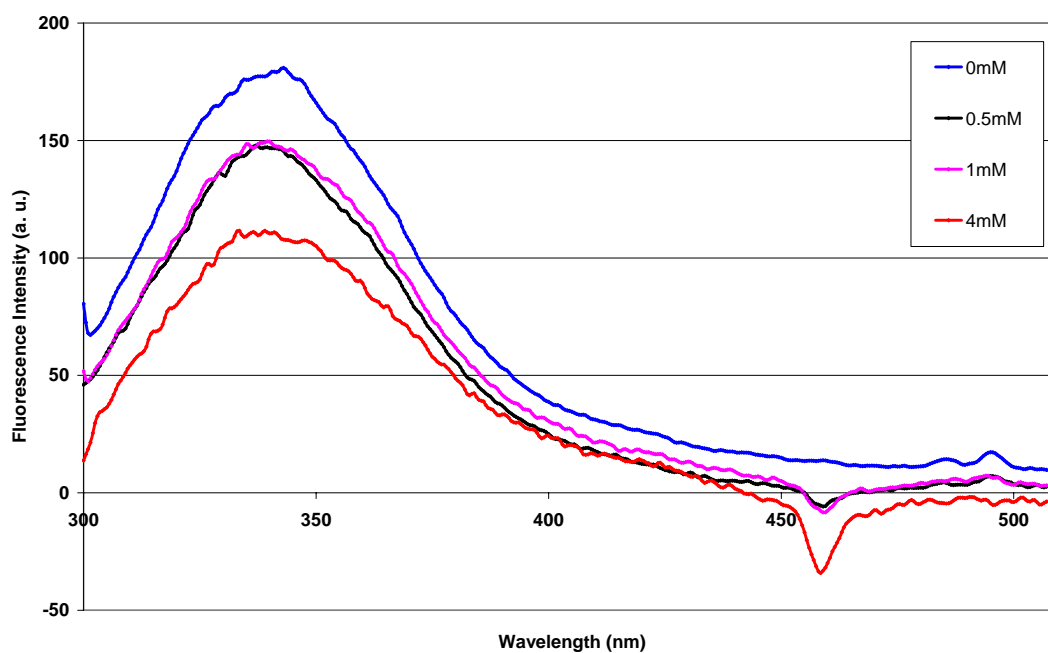


Figure 82: Fluorescence spectra of 0.1 mg/ml *Limulus polyphemus* hemocyanin in 100 mM sodium phosphate buffer, pH 7.5 following 5 minutes incubation with a 50:50 mixture of the phospholipids phosphatidylethanolamine and phosphatidylcholine at final concentrations between 0 and 4 mM as indicated in the legend.

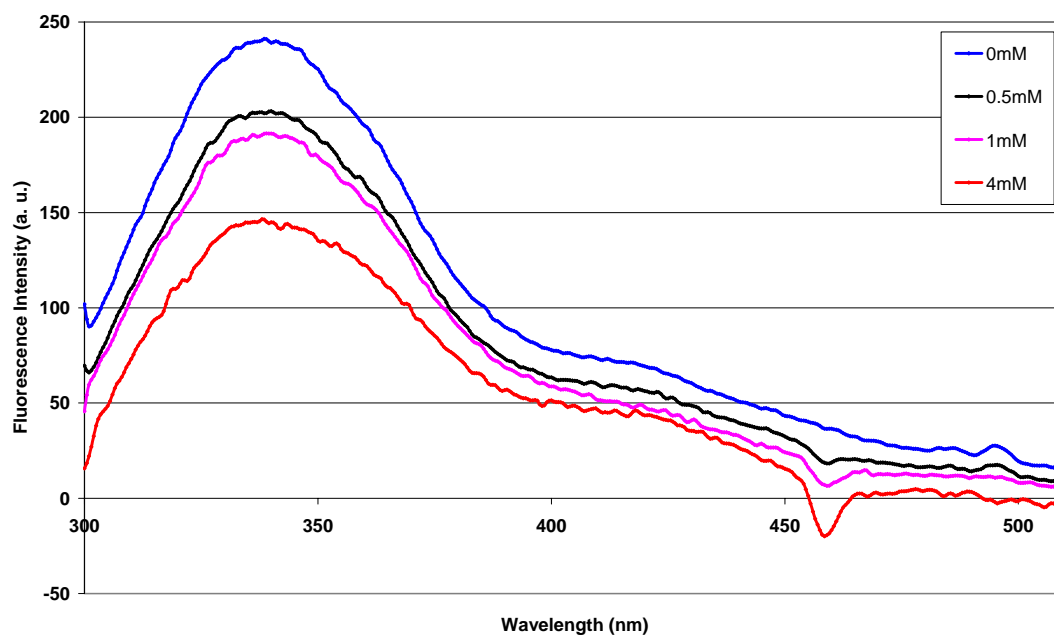


Figure 83: Fluorescence spectra of 0.1 mg/ml *Pandinus imperator* hemocyanin in 100 mM sodium phosphate buffer, pH 7.5 following 5 minutes incubation with a 50:50 mixture of the phospholipids phosphatidylethanolamine and phosphatidylcholine at final concentrations between 0 and 4 mM as indicated in the legend.

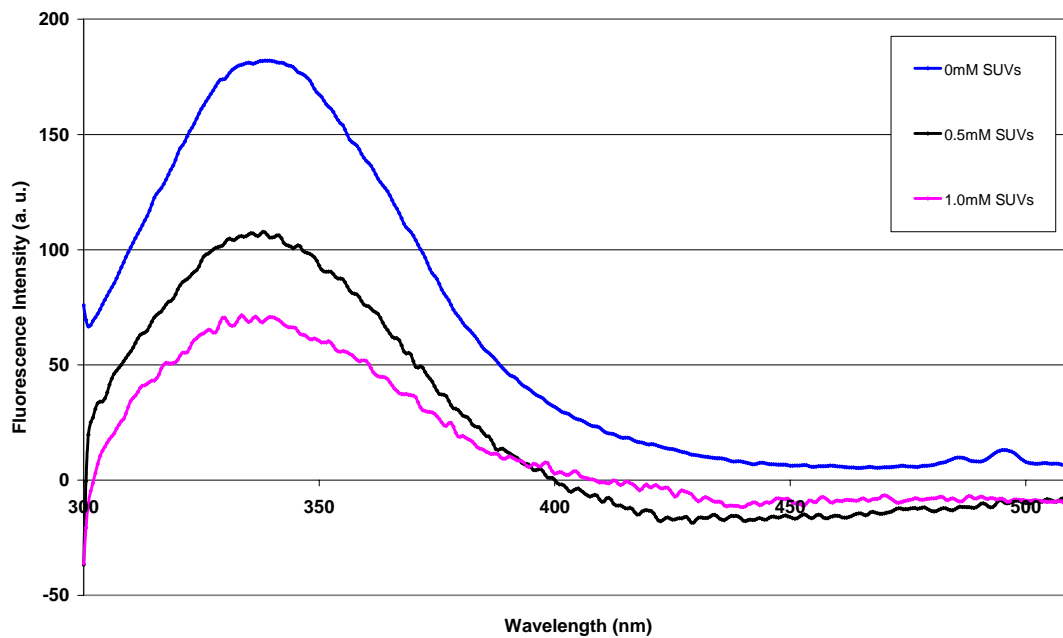


Figure 84: Fluorescence spectra of 0.1 mg/ml *Limulus polyphemus* hemocyanin in 100 mM sodium phosphate buffer, pH 7.5 following 5 minutes incubation with 0, 0.5 or 1.0 mM small unilamellar vesicles, composed of a 50:50 ratio of the phospholipids phosphatidylethanolamine and phosphatidylcholine.

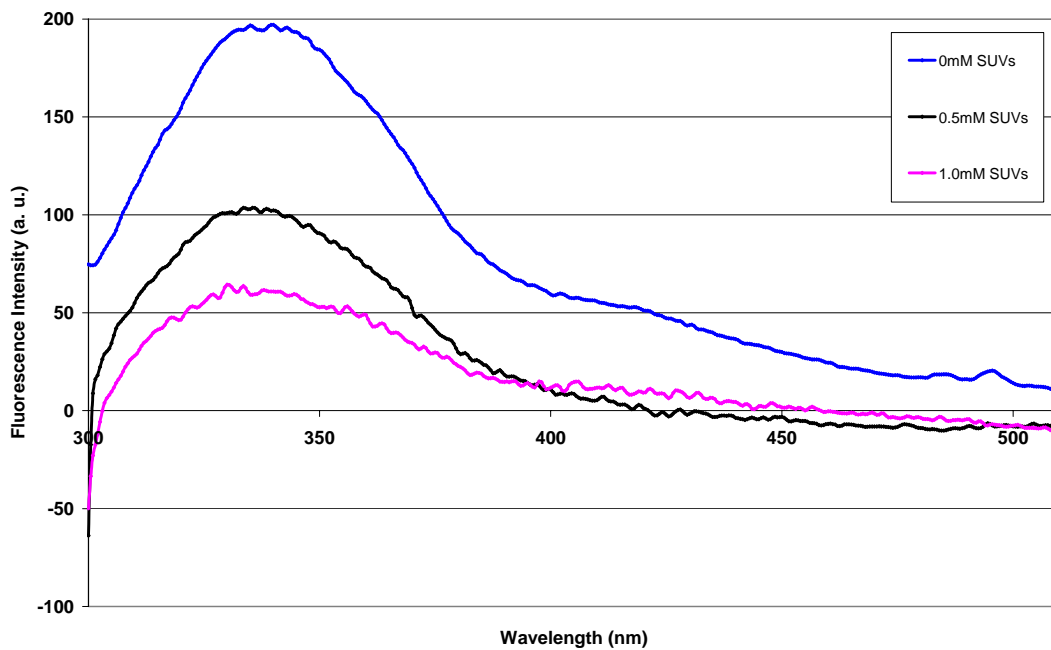


Figure 85: Fluorescence spectra of 0.1 mg/ml *Pandinus imperator* hemocyanin in 100 mM sodium phosphate buffer, pH 7.5 following 5 minutes incubation with 0, 0.5 or 1.0 mM small unilamellar vesicles, composed of a 50:50 ratio of the phospholipids phosphatidylethanolamine and phosphatidylcholine.

The effect was however different to that exhibited upon incubation of these Hc types with SDS which, as detailed in section 7.3.4.1, caused a significant increase in the intensity of the 340 nm tryptophan fluorescence emission peak with a blue-shift in the emission maximum. Instead the presence of increasing concentrations of phospholipids or SUVs caused a slight decrease in the intensity of the 340 nm emission peak, with a similar concurrent blue-shift in the wavelength of the emission peak maximum. Incubation of LimHc or PanHc with phospholipids at final concentrations of 0.5 or 1.0 mM causes a similar reduction in the peak intensity of approximately 50% of the maximum change seen upon incubation with 4.0 mM phospholipids. When similar concentrations of phospholipids in the form of SUVs were incubated with LimHc and PanHc, a greater reduction in the 340 nm peak intensity was apparent. The presence of SUVs containing 0.5 mM total phospholipid caused a peak intensity reduction of 67.3% for LimHc and 70.4% for PanHc respectively, where the change caused by 1.0 mM was taken as 100%. Similarly, the blue shift of the emission maximum is more profound in the presence of SUVs (Table 9) in comparison to that elicited by the phospholipids (Table 10). Between 0 and 1.0 mM total phospholipid, SUVs cause a 5 and 10 nm blue shift of the peak wavelength compared to a 3 and 0.5 nm blue shift caused by the presence of phospholipids, in LimHc and PanHc respectively.

Table 9: Upon excitation at 290 nm, the emission fluorescence peak of *Limulus polyphemus* and *Pandinus imperator* hemocyanin exhibits a blue-shift in the presence of increasing concentrations of SUVs.

| SUV concentration (mM) | Limulus Hc Trp Fluorescence Peak (nm) | Pandinus Hc Trp Fluorescence Peak (nm) |
|------------------------|---------------------------------------|--|
| 0                      | 338.5                                 | 340.0                                  |
| 0.5                    | 338.0                                 | 333.5                                  |
| 1.0                    | 333.5                                 | 330.0                                  |

Table 10: Upon excitation at 290 nm, the emission fluorescence peak of *Limulus polyphemus* and *Pandinus imperator* hemocyanin exhibits a blue-shift in the presence of increasing concentrations of phospholipids.

| Phospholipid concentration (mM) | Limulus Hc Trp Fluorescence Peak (nm) | Pandinus Hc Trp Fluorescence Peak (nm) |
|---------------------------------|---------------------------------------|--|
| 0                               | 342.0                                 | 338.5                                  |
| 0.5                             | 339.5                                 | 340.0                                  |
| 1.0                             | 339.5                                 | 339.0                                  |
| 4.0                             | 339.0                                 | 338.0                                  |

Controls demonstrated that the differences in the fluorescence spectra were not a result of a local quenching effect of Trp residues by phospholipids or SUVs. In summary, fluorescence intensity changes induced by the presence of phospholipids/SUVs are the opposite of those reported when adding SDS to the Hc. However, akin to the effect of SDS on these Hc types, phospholipids and SUVs cause a blue-shift in the position of the fluorescence peak. The blue-shift in the presence of SUVs is greater than in the presence of phospholipids in both Hcs.

## **7.4 Discussion**

### **7.4.1 Introduction**

The structural and functional changes taking place in arthropod Hc upon incubation with the anionic detergent SDS were investigated using a number of biophysical techniques. The primary aim was to characterise changes associated with the presence of SDS monomers and micelles, in Hc from the ancient chelicerates *L. polyphemus* and *E. californicum* and the more modern chelicerate *P. imperator*. Some additional experiments were also conducted to provide preliminary indications of the reversibility of the effects of SDS, and the effect of non-ionic detergents and phospholipids on the structure and function of arthropod Hc.

### **7.4.2 The SDS Induced PO Activity of Arthropod Hemocyanin Suggests Enzyme-Micelle Interaction.**

The effect of increasing concentrations of SDS on induction of arthropod Hc PO activity was investigated spectroscopically by following the formation of dopachrome at 475 nm. SDS at

concentrations exceeding the CMC was required to induce the maximum possible activity in all three Hc types. Beyond the optimal SDS concentration, activity was found to decline yielding a bell-shaped activity plot indicating an interaction between the protein and SDS micelles and/or the sequestering of substrate within micelles, during which the enzymatic activity reacts with free substrate (Celej et al., 2004). This was the first report of such a relationship between SDS concentration and the PO activity which it elicits in arthropod Hc *in vitro*.

There have been a number of studies and models proposed for the mechanism of enzyme denaturation by surfactants such as SDS. However more recently, several papers have been published which report surfactant enhanced activity of some enzymes (Spreti et al., 2001; Spreti et al., 1999; Celej et al., 2004; Kanade et al., 2006; Chen et al., 2006; Viparelli et al., 2003). The PO activity of arthropod Hc induced by increasing SDS concentrations, revealed a similar pattern to that detailed in the above papers for different enzymes in the presence of different surfactants. Celej *et al* (2004) described the superactivation of  $\alpha$ -chymotrypsin activity by the cationic detergent CTABr (hexadecyltrimethylammonium bromide). Whilst  $\alpha$ -chymotrypsin activity increased only in the presence of CTABr micelles, the activity plot was nonetheless a bell-shaped curve akin to that described for the current SDS induced Hc PO activity. A more recent paper by Kanade et al (2006) found that the activity of field bean (*Dolichos lablab*) polyphenol oxidase is superactivated by the anionic detergent SDS. Again the activity measurements yielded a bell-shaped curve with activity increasing and decreasing almost linearly to and from the activity maximum, which was achieved at the CMC of SDS under the conditions used (1.19 mM). A further similarity to the present research was that at low monomeric concentrations, bean polyphenol oxidase demonstrated

only very minimal activity, which rapidly increased upon reaching a particular SDS concentration. In Section 6.4.3, Chapter 6, discussions comparing the proteolytic and SDS induced activation of chelicerate Hc have already noted that the level of activity induced by SDS was higher than that elicited by proteolytic cleavage of the polypeptide chain. With this knowledge and on the basis of the similarity between the activity plots of arthropod Hc,  $\alpha$ -chymotrypsin and bean polyphenol oxidase, it may therefore be proposed that SDS causes the superactivation of arthropod Hc intrinsic PO activity as a result of enzyme-micelle interactions.

As mentioned above, the decrease in PO activity at higher SDS concentrations suggested a situation where enzyme-micelle interactions were taking place, during which the enzyme reacts with free substrate. The resulting bell shaped activity plot resembled the model in which free substrate becomes increasingly unfavourably segregated by the surfactant. In this model, as surfactant concentration and therefore the number of micelles in solution increases, substrate trapping reduces the available free substrate for the micelle bound enzyme, and so there is a reduction in the enzymes activity (Celej et al., 2004; Viparelli et al., 1999). Whilst substrate partitioning was a plausible explanation for the reduction in the PO activity of arthropod Hc at higher micellar SDS concentrations, as none of the structural investigations recorded data for Hc in the presence of higher than 2 (PanHc), 3.5 (Lim Hc) or 5 mM (EuryHc) SDS, the possibility could not be dismissed that the reduction in Hc PO activity was as a result of Hc denaturation and/or micelle substrate partitioning; at least for PanHc and LimHc. SAXS data presented in an upcoming collaborative paper (inserted after section 9.5 - Appendix E) detailing the results of this present research (Baird et al., 2007), along with

the DLS data in section 7.3.4.3, indicates that denaturation of EuryHc is not the likely cause for loss of PO activity at high micellar SDS concentrations in this Hc type.

Despite all three Hc types showing a reduction in induced PO activity at higher micellar concentrations of SDS, the concentration from which the decrease occurred and the level of decrease varied. PanHc PO activity decreased above 2 mM SDS, whilst LimHc and EuryHc began to show a decrease only upon reaching concentrations greater than 10 mM SDS. Furthermore, Eury Hc showed only a modest decrease in activity to 71.4% of the maximum activity upon incubation with 40 mM SDS. In comparison, LimHc and PanHc PO activity decreased to 30 and 43.2% of their maximum activity in the presence of 40 and 32 mM SDS respectively. Taking these points into consideration, as well as the optimal activities recorded for each Hc type, it appeared that EuryHc and LimHc had more restricted substrate access to their dicopper centres, whilst the PanHc dicopper centre was more open allowing for higher specific activity. The EuryHc data also suggested, that compared to LimHc and PanHc, this protein was more stable and resistant to any structural effects of higher (>10 mM) micellar concentrations of SDS. Variations in the flexibility of the dicopper centre and overall structural stability of these three Hc types were also revealed during structural studies, the results of which are discussed in section 7.4.4.

### **7.4.3 The Interaction Between SDS and Arthropod Hemocyanin Demonstrates Very Complex Thermodynamics.**

The thermodynamics of SDS binding to each arthropod Hc type was studied using ITC. The resulting binding isotherm calculated for each Hc was representative of SDS binding to Hc when SDS was present at initially monomeric concentrations, gradually increasing to

micellar concentrations. However, no interpretable thermodynamic data was obtained for any of the three Hc types.

Following incubation of EuryHc with increasing concentrations of SDS, there were no detectable heat changes and thus no isotherm could be calculated for this protein. It was considered a possibility that EuryHc may have required a longer incubation in SDS before any heat changes would be detectable. In fact, this was further corroborated by structural studies of this protein, the results of which are discussed in section 7.4.4. The nature of the ITC method meant it was not possible to include a longer incubation as a variable in the experiment.

Despite heat change data being recorded for LimHc and PanHc, the biphasic binding isotherms obtained were too complex to be analysed in terms of either a simple single or sequential binding site model. Our data was kindly further analysed by Dr Alan Cooper from the University of Glasgow using more complex models, however still no suitable model for analysis of the binding of SDS to Hc could be identified.

The complex nature of the thermodynamics of protein-micelle interactions has been reported previously (Moosavi-Movahedi, 2005), however a general schematic of the isotherm of the binding of ionic surfactants to proteins has been described (Valstar, 2000). This isotherm (Figure 86) displays four characteristic regions with increasing

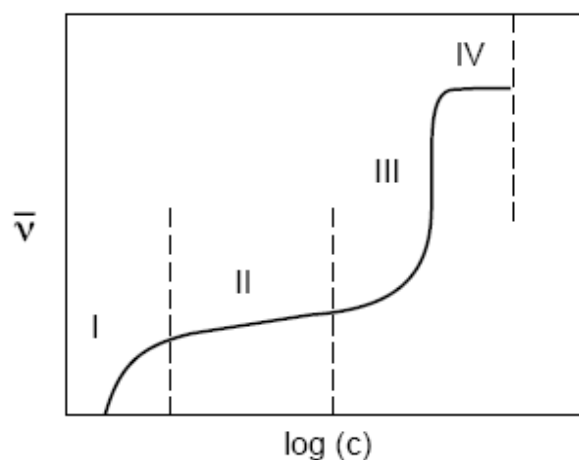


Figure 86: Schematic binding isotherm of protein-surfactant interactions. In general, the isotherm of the binding of ionic surfactants to proteins displays four characteristic regions (with increasing surfactant concentration): (I) specific binding, (II) non-cooperative binding, (III) cooperative binding, and (IV) saturation. Taken from Valstar, 2000.

surfactant concentration: (I) specific binding, (II) non-cooperative binding, (III) cooperative binding and (IV) saturation. The isotherm of SDS binding to either LimHc or PanHc exhibits little similarity to this generalised isotherm, perhaps as a result of the large number of potential concurrent interactions, as well as other factors, which may have had an influence on the heat changes recorded. As a consequence the isotherm could not be dissected into distinct phases for analysis. Possible factors influencing the ITC data included heat changes associated with (i) any structural changes taking place within the Hc molecule in the presence of SDS, (ii) changes in the interaction between protein and monomers/micelles as the protein structure changes, (iii) the interaction of SDS monomers and micelles with each other as well as the protein, (iv) the presence of both monomers and micelles above CMC – both may bind Hc at the same time and (iv) as the number of injections of SDS into the protein increased, so had the length of time the protein had been in the presence of SDS. Additional complexities may have arisen due to the large size of the arthropod Hc molecule and also because only

certain subunits within the complete multimeric chelicerate Hc molecule appear to exhibit inducible PO activity (as reported in Section 6.4.3, Chapter 6).

#### **7.4.4 SDS Causes Significant Structural Changes in Arthropod Hemocyanin, Particularly in the Region of the Dicopper centre.**

A number of biophysical techniques were employed in an attempt to identify any structural changes in arthropod Hc upon incubation with a range of submicellar and micellar concentrations of SDS. In brief, the data collected demonstrated that Hc retains its overall quaternary structure throughout the duration of the experiments in the presence of SDS either above or below its CMC. There are however significant changes in the tertiary structure and smaller changes in the secondary structure of the Hc molecule in the presence of increasing concentrations of SDS, most probably in the region of the dicopper centre, which were not as a result of the loss of the coordinated copper ions. The results gleaned from each technique applied are discussed more extensively in the following subsections, in terms of the structural level at which they provided information.

##### **7.4.4.1 Changes in Arthropod Hemocyanin Quaternary Structure.**

Dynamic light scattering is a method which measures the Brownian motion of particles suspended in liquid, and then relates this to the size of the particles. PanHc and EuryHc share similar quaternary structure, both molecules having a 4x6-meric subunit arrangement (see Figure 45, Chapter 6). EuryHc is stated as having approximate dimensions of 20 x 20 x 10 nm, therefore PanHc can be assumed to have similar dimensions. DLS data for these Hcs indicated that the diameter of each Hc type remained at 20 nm for at least 40 minutes in the presence of SDS at concentrations either below or above CMC, confirming that each Hc

retained its full quaternary arrangement during this time. DLS provided evidence of the greater structural stability of EuryHc, as this Hc type could retain its native quaternary structure for at least 1440 minutes in the presence of submicellar and micellar concentrations of SDS. By comparison, after 24 hours incubation in SDS, the molecular diameter of PanHc decreased to approximately 10 nm, indicating that this Hc had disassociated into its 1x6-meric form, suggesting this was a less stable protein.

#### **7.4.4.2 Changes in Arthropod Hemocyanin Tertiary Structure.**

Tertiary structural change in arthropod Hc upon incubation with increasing concentrations of SDS was investigated using a combination of two methods: intrinsic Trp fluorescence spectroscopy and near UV CD spectroscopy. Intrinsic Trp fluorescence was measured by exciting the protein at 290 nm then recording the fluorescence emission spectra between 300 and 510 nm. Near UV CD spectra were recorded between 260 and 305 nm, which provided information on the microenvironment of all the aromatic residues in the Hc molecule.

In reactions containing either LimHc or PanHc, increasing concentrations of SDS caused an increase in the Trp fluorescence intensity and a decrease in the intensity of the near UV CD aromatic residue spectral peaks. The non-ionic detergent NBDG was unable to elicit such changes in the near UV CD spectral region of LimHc. The extent of the changes in the fluorescence and near UV CD spectra were dependant on SDS concentration with high monomeric SDS concentrations (0.7 – 1.0 mM) resulting in the largest spectral changes, however only at concentrations above CMC were the maximum changes observed. EuryHc required 16 hours incubation in SDS before exhibiting equivalent changes in Trp fluorescence intensity.

LimHc subunit II and EuryHc subunits a – g, have between 5 and 8 Trp residues per subunit, as determined from the sequence information available for these subunits. In each subunit type, more than 50% of the total Trp residues are located to the copper coordination sites and these particular Trp are at highly conserved locations within the subunit structure (Dolashka-Angelova et al., 2005). PanHc is expected to have a similar Trp content and distribution owing to the high level of conservation of copper coordination site residues between Hc species. In Lim Hc subunit II (Figure 87) five Trp are located in domain II within the CuA and CuB coordination sites. Analysis of the intrinsic Trp fluorescence spectra of multi-tryptophan proteins is very difficult because they are an average of the fluorescence contributions from Trp residues at the surface and buried in the core of the molecule. Additional complications arise with arthropod Hc as a result of the heterogeneity of subunit composition; the number and distribution of Trp

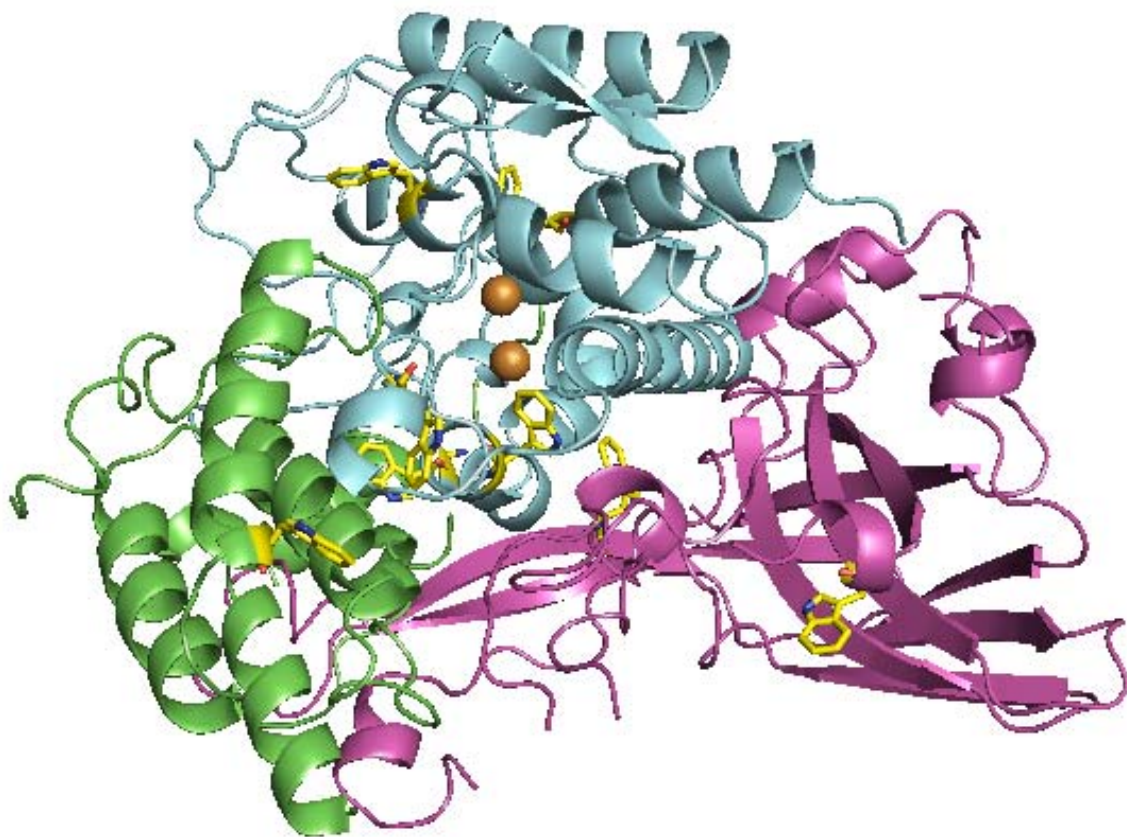


Figure 87: Location of the eight tryptophan residues (yellow) in *Limulus polyphemus* subunit II. One tryptophan (Trp65) is located in domain I (green) and two (Trp538 and 563) in domain III (magenta) whilst the remaining five (Trp174, 176, 184, 326 and 363) are located at the copper A and B binding sites of the dicopper centre in domain II (cyan). Copper ions are shown as orange spheres. Image generated using PDB file 1LLA and Pymol molecular graphics software.

residues in each subunit may vary (Muro et al., 2002) (as has been found to be the case with EuryHc (Voit et al., 2000)). However, it is reasonable to draw certain conclusions on all three Hc types based on the data obtained. The possibility that the change in Trp fluorescence was due to a local effect on these residues upon binding to SDS, rather than a conformational change, was ruled out by means of a control which demonstrated the fluorescence spectrum of the model compound *N*-acetyl-L-tryptophan amide was unaffected by the presence of SDS. Protein dissociation was disregarded as a possible explanation for the observed changes in fluorescence, as earlier DLS had shown that the Hcs retained their quaternary arrangement during the timescale of these experiments. Angelova, et al. (2005) report that the dicopper centre of subunit II from LimHc contains two Trp (Trp176 and Trp363) located within 6 Å of the CuA and CuB ions respectively, and a further two (Trp174 and Trp538) also located close to the dicopper centre. The fluorescence of these particular Trp residues is strongly quenched by the copper-dioxygen interaction in oxy-Hc. This internal quenching effect is lost upon removal of oxygen and copper (apo-Hc) from the protein. It is possible therefore that the increase in Trp fluorescence intensity, in conjunction with the small blue shift in fluorescence peak wavelength, of the Hc types studied here, is a result of a conformational change in the molecules upon incubation with SDS. This conformational change perhaps shifted the environment of the dicopper centre Trp residues, placing them in a less solvent exposed, polar yet rigid environment where they experienced a reduction in the effects of internal quenching by the copper-dioxygen complex. These structural changes took longer to occur in EuryHc compared to LimHc and PanHc.

Near UV CD spectra were recorded to ensure that the observed effects of SDS on the Trp fluorescence of Hc were related to conformational changes in the protein structure. In LimHc

and PanHc, the reduced intensity of the CD signals between 260 and 300 nm with increasing SDS concentrations, whilst the positive spectral peak at 305 remained essentially unchanged, suggested that the aromatic amino acids were being moved to a more flexible environment, reflecting the results of the intrinsic Trp fluorescence spectra. The change in intensity of the spectral peaks from 285 - 305 nm of EuryHc (only occurring following 16 hours incubation in SDS) suggested that the Trp residues in this protein were instead being moved into a more rigid environment, reflecting the results of the tryptophan fluorescence experiments. This considered, caution must be taken when proposing the effects of SDS on the microenvironment of the aromatic amino acids from the near UV CD data of these Hc molecules, as the spectral peaks above 290 nm may have been influenced by the strongly negative signal at 340 - 350 nm which is a characteristic contribution to the near UV CD spectra by the oxygen bound Type-3 dicopper centre of Hc.

Together, data obtained from intrinsic Trp fluorescence and near UV CD experiments indicated that the environments of at least some of the arthropod Hc tryptophan, phenylalanine and tyrosine residues are subject to change upon incubation of the protein with SDS, possibly as a result of localised conformational change in the region of the Hc dicopper centre, rather than protein subunit dissociation. Importantly, the greatest spectral changes were found to occur at SDS concentrations which closely approached and included the CMC of SDS in the buffer system used. The maximum structural changes could however only be induced upon incubation of the protein with SDS concentrations exceeding the CMC. This indicated that the presence of SDS micelles and/or high concentrations of monomers is necessary to cause the structural changes which induced maximal intrinsic Hc PO activity.

Interestingly, the tertiary structural changes in EuryHc take much longer to respond to the presence of SDS, further suggesting EuryHc is a more stable, less flexible protein.

#### **7.4.4.3 Changes in Arthropod Hemocyanin Secondary Structure.**

Far UV circular dichroism was employed to determine quantitatively the effect of increasing concentrations of SDS on the overall secondary structure content of arthropod Hc. Data collected between 195 and 240 nm was subsequently analysed using the secondary structure prediction tool DICHROWEB, using SELCON 3 and reference set 3. For LimHc and PanHc, increasing concentrations of SDS caused small yet significant changes in the secondary structure composition of these molecules. These secondary structural changes appeared to be preceded by the tertiary structural changes discussed earlier, in terms of percentage change at each SDS concentration used. The most notable changes in secondary structure were an increase in  $\alpha$ -helical and concurrent decrease in  $\beta$ -sheet content. Similar to the tertiary structural changes described earlier, SDS concentrations at CMC and above were required to induce the largest and maximum secondary structural changes respectively. The greater structural stability of EuryHc was again emphasised as this Hc type required 16 hours incubation in SDS before equivalent secondary structural changes were detected. Unlike SDS, however, the non-ionic detergent NBDG was unable to elicit such secondary structural changes in LimHc.

It has been known for some time that the presence of the detergent SDS causes proteins to display a larger than normal amount of secondary structure. Subsequently, it has also been discovered that some proteins, such as trichosanthin, the A-chain of ricin and apocytochrome c, undergo helical folding in the presence of SDS micelles, and that these micelles are the

factor inducing the folding (Parker and Song, 1992). An investigation by Parker and Song (1992) demonstrated that a number of other proteins, namely pepsin, carbonic anhydrase and alcohol dehydrogenase, also respond to the presence of SDS by exhibiting an increase in their ordered  $\alpha$ -helical secondary structure content in comparison to the native molecule. They proposed that in order to respond in such a way to the presence of SDS, it is necessary for a protein to contain regions of amphiphilic sequence within its primary sequence, which have the potential to form amphiphilic  $\alpha$ -helices. These amphiphilic sequences should exceed the amount of sequence which is already involved in the formation of  $\alpha$ -helices in the native structure. In such scenarios it is expected that the presence of SDS would cause an increase in the  $\alpha$ -helical content of the protein. These proteins also demonstrate a decrease in  $\beta$ -sheet and unordered structure and an increase in turns. This pattern of secondary structural change is identical to that described in the current research for all three arthropod Hcs in the presence of SDS, therefore it may be the case that Hc contains a markedly high amount of primary sequence which has the potential to form amphiphilic  $\alpha$ -helices, which it may do upon incubation with SDS.

#### **7.4.4.4 Changes in the Arthropod Hemocyanin Type-3 Dicopper centre.**

In a bid to determine the effect of SDS on the dicopper centre of arthropod Hc, a range of biophysical methods were employed. The first of these methods were absorbance and near UV CD spectroscopy. The absorbance spectrum of native oxygenated Hc (oxy-Hc) has two distinct peaks at 280 nm and 343 nm. The former is due to the presence of aromatic amino acids and the latter connected with the copper-dioxygen system at the dicopper centre. The 343 nm peak is absent in Hc which lacks the two copper ions (apo-Hc) or bound dioxygen (deoxy-Hc) (Georgieva et al., 1998). Incubation of LimHc, PanHc or EuryHc with increasing

concentrations of SDS resulted in a gradual reduction in the intensity of the 343 nm peak, although again EuryHc required 16 hours incubation before a complete loss of the 343 nm absorbance signal was recorded.

Near UV CD spectroscopy can provide information on non-protein components which give rise to CD signals in regions of the near UV spectrum well separated from those of the aromatic amino acids (Kelly and Price, 1997). The near UV CD spectrum of oxy-Hc contains a strong negative ellipticity at around 340 - 350 nm which results from the peroxide to copper (II) charge transfer transitions at the dicopper centre (Solomon, 1983; Georgieva et al., 1998). Once again, apo-Hc does not exhibit this near UV spectral peak. As evidenced from the near UV spectra recorded in the presence of increasing concentrations of SDS, LimHc and PanHc exhibited a severe reduction of this characteristic oxy-Hc ellipticity. EuryHc again required 16 hours incubation in SDS to exhibit an equivalent loss.

Following the results of the intrinsic Trp fluorescence (discussed in section 7.4.4.2), absorbance and near UV CD spectroscopy experiments, which could have been interpreted as demonstrating that oxy-Hc was becoming apo-Hc in the presence of SDS, it was considered necessary to confirm whether the copper ions were remaining associated with Hc upon incubation with SDS.

Two techniques, fluorescence spectroscopy and ICP OES, were utilised to investigate whether the copper ions were remaining bound at the dicopper centre of Hc. Excitation of Type-3 copper proteins at a wavelength between 325 – 345 nm has been shown to result in an intense novel fluorescence band between 415 – 445 nm. This fluorescence was proposed

to be the result of interactions between the carboxyl groups of amino acids (most likely histidine residues) at, or near, the proteins dicopper centre. Importantly, however, the presence of the bound copper pair at the dicopper centre of these Type-3 copper proteins was found to significantly quench this novel fluorescence band (Bacci et al., 1983). Results of such fluorescence experiments using LimHc, PanHc and EuryHc in the presence of SDS (at concentrations which had severely reduced the 343 nm absorption and 340 - 350 nm near UV CD spectral peaks), suggested that the copper ions were in fact remaining bound at the dicopper centre of the arthropod Hc subunits in the presence of SDS, even following 16 hours incubation in the case of EuryHc.

ICP OES was used to ensure that both CuA and CuB ions were remaining bound at the LimHc dicopper centre, as it was considered a possibility that even the loss of a single copper ion may cause absorbance and near UV CD spectral changes. ICP OES results demonstrated that the actual concentration of copper was in good agreement with the estimated copper concentrations of a solution of native multimeric LimHc, which had been calculated on the basis that both copper ions remain bound at the dicopper centre of each LimHc subunit in the presence of SDS.

Taking into consideration all the data collected, it was concluded that SDS was not causing the loss of copper ions from the dicopper centre of any of the LimHc subunits. Therefore it was proposed that for all three Hc types under investigation the Trp fluorescence, absorbance and near UV CD spectral changes were not due to the formation of apo-Hc. These spectral changes are suggested to be due to the formation of de-oxy Hc, or a perturbation of the dioxygen to copper (II) charge transfer transitions at the dicopper centre, as a result of

structural conformational change in the protein in the presence of SDS. This perturbation may be in the form of a change in the orientation, or a distortion, of the bound peroxide, or a modification to the mode of coordination of the CuA and/or CuB ions. Furthermore, the EuryHc dicopper centre structure is more resilient to the effects of SDS than LimHc and PanHc, suggesting that EuryHc possesses greater overall structural stability and reduced dicopper centre flexibility.

#### **7.4.5 SDS Induced Arthropod Hemocyanin Phenoloxidase Activity and the Associated Structural Changes Appear to Vary in their Reversibility.**

To determine whether the reported effects of SDS on arthropod intrinsic PO activity and structure were reversible, a preliminary investigation was conducted using LimHc and PanHc, and activity assay and near and far UV CD spectroscopy. Upon dilution of SDS in the reactions from a concentration above CMC to one below CMC, it was predicted that reversible reactions would show (i) the detectable PO activity levels returning to zero (or at least a very minimal level) and (ii) the CD spectra demonstrating a reversal in the direction of the spectral peak intensities. It was in fact suggested by the results of these experiments that SDS induced PO activity and perturbations of the dicopper centre were irreversible. Conversely the structural changes caused by the presence of micellar SDS at the secondary level could be reversed by dilution of the SDS to submicellar concentrations.

The method of diluting the reaction in an attempt to 'remove' the presence of micellar concentrations of SDS was not ideal, as the protein and substrate were diluted also. Furthermore, SDS could not be completely prevented from interacting with the Hc molecules using this method. Controls had demonstrated that CD spectra were unaffected by protein

concentration, and Hc PO activity was directly related to protein concentration. Additional substrate was also added during the dilution step of the PO activity assays to account for substrate limitation on the reaction. However, had there been any SDS monomers and/or micelles remaining associated with the Hc molecules following dilution, this may have produced results which were not a true representation of the reversibility of the effects of higher concentrations of SDS. Laveda, et al. (2000) demonstrated that the SDS induced enzymatic activity of peach polyphenol oxidase could be fully reversed by SDS entrapment (stripping) by cyclodextrins. Cyclodextrins are low molecular weight, water-soluble oligosaccharides produced from starch, and as a result of their 'bucket-shaped' molecular structure, they can function as molecular containers to trap 'guest' molecules by forming non-covalent complexes with them (Wacker-Chemie GmbH, 2002; Laveda F. et al., 2000). SDS entrapment may have been a more suitable method for studying the reversibility of the activation of PO activity in arthropod Hc. However, the extent of the interference that cyclodextrins would have on the spectral measurements made in the current investigation, would have to be evaluated before making any assessment of their suitability for use in structural studies.

#### **7.4.6 Lipids/Liposomes and physiological relevance of SDS induced PO activity**

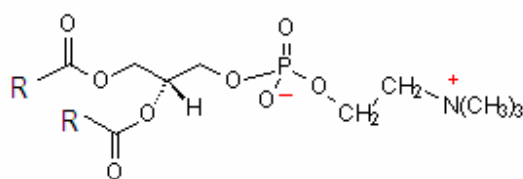
Thus far, the presented research has focused on the effect of the anionic detergent SDS on the function and structure of arthropod Hc. However, SDS is not a molecule which Hc will encounter in its native environment; the hemolymph of arthropods. Therefore consideration was given to potential candidates which could be responsible for inducing PO activity in Hc *in vivo* via a similar mechanism to that proposed for SDS. Nellaiappan and Sugumaran (1996) presented evidence for the existence of a PO-type enzyme in the hemolymph of *L.*

*polyphemus* which could be activated by phospholipids. Whilst at the time they did not realise this PO-type enzyme was in fact an activated Hc, they did note that phospholipid induced PO activity could give an additional advantage to the crab. They hypothesised that rupturing of membranes during infection would release phospholipids into the hemolymph where they could activate the PO activity of Hc for defensive melanisation and encapsulation reactions. In addition, there have been a number of other reports that suggest the PO activity of arthropod Hc can be induced by phospholipids (Nagai and Kawabata, 2000; Nagai et al., 2001; Sugumaran and Nelloiappan, 1990; Sugumaran and Nelloiappan, 1991).

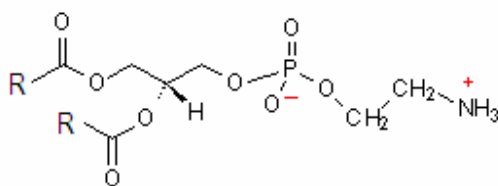
Phospholipids share a number of common features with SDS (and other detergents) which would make it reasonable to consider them as possible *in vivo* elicitors of arthropod Hc PO activity. They are both amphiphilic in nature and possess hydrophilic head and hydrophobic hydrocarbon tail regions to their structure (Figure 88). As such monomers of each can form globular aggregates called either liposomes (phospholipids) or micelles (SDS), placing the hydrophilic tails out of contact with water.

A preliminary investigation was therefore conducted, using activity assays and intrinsic Trp fluorescence, to provide initial indications as to whether phospholipids could induce similar PO activity levels and structural changes as SDS in LimHc and PanHc. Phosphatidylethanolamine (PE) and phosphatidylcholine (PC) (source: soybean) were the phospholipids utilised as they are generally the first and second most common phospholipids in animals respectively (Christie, Accessed: 2005.; Chrissie, Accessed: 2005.), and in *L. polyphemus* they predominate the total phospholipid content of the granular amoebocyte cells at 36.3 and 42.4% respectively (MacPherson et al., 1998). Furthermore, PE is frequently the

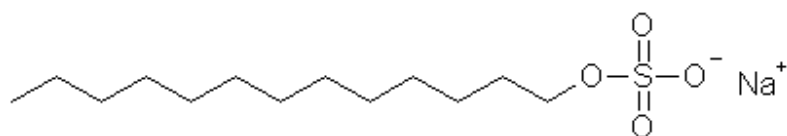
main phospholipid component of microbial membranes (Chrissie, Accessed: 2005.), and if released into the hemolymph upon infection, it could be proposed that they may activate Hc PO activity.



*L*-alpha-Phosphatidyl choline from soybean



*L*-alpha-Phosphatidyl ethanolamine from soybean



Sodium dodecyl sulphate

Figure 88: Structure of the phospholipids phosphatidylethanolamine and phosphatidylcholine (adapted from Avanti Polar Lipids, Accessed: 2007.) and the detergent sodium dodecyl sulphate (SDS) (Key Centre for Polymer Colloids, Accessed: 2007.). 'R' represents the fatty acid side chains of the phospholipids which can range in length and may be either saturated or unsaturated.

Despite indications from previous investigations, the results of the current research showed that neither free phospholipids, nor those in the form of small unilamellar vesicles (SUVs – equivalent to an SDS micelle in structure though not size), could induce PO activity in LimHc or PanHc. It is possible that differences in the reaction conditions between the experiments conducted in the earlier reports and those used in the current research are responsible for these apparently contradicting results. In the experiments conducted by Nelliappan and Sugumaran (1996), Hc PO activity assays were performed in 50 mM sodium phosphate pH 7.0 buffer and the reaction initiated by incubation of Hc with 5 µg of phospholipid which had been dissolved in ethanol. In the present investigation the assay buffer was 100 mM sodium phosphate pH 7.5 and Hc was incubated with either approximately 360 or 720 µg of phospholipid (either as monomers or SUVs) which had been re-suspended in assay buffer. The former earlier experimental reactions ultimately always contained 10% ethanol. Whilst it was reported that this had no effect on Hc PO activity, the presence of ethanol may have altered the nature of the interaction of the phospholipid molecules with each other and the protein, compared to that which would have occurred were ethanol not present. However, as it was deemed necessary to include ethanol in the assay in order to keep the phospholipids in solution, its absence from the current assays may have led to incomplete dissolution of the phospholipids.

In terms of the structural changes elicited by either phospholipids or SUVs, it appeared that their presence caused an increase in the quenching effect that the copper centre copper-dioxygen interaction had on the Trp residues at or near to the dicopper centre. As discussed in section 7.4.4.2, SDS causes a reduction in this quenching, resulting in an increase in Trp fluorescence intensity. In both instances however, there was a blue shift in the Trp

fluorescence peak wavelength, suggesting the Trp residues had been shifted to a less solvent exposed, polar yet rigid environment. It was considered a possibility that under the presently reported reaction conditions, phospholipids may instead have had a stabilising effect on the structure of LimHc and PanHc.

Under native conditions, Hc from the arthropods *Pacifastacus leniusculus* (crayfish) (Hall et al., 1995b), *Latrodectus mirabilis* (spider) (Cunningham et al., 2000), *Carcinus maenus* (crab) (Zatta, 1981) and *Polybetes pythagoricus* (spider) (Cunningham et al., 1999) has been shown to contain a small amount of bound lipid. Lipids cannot circulate freely in an aqueous medium such as the hemolymph as a result of their hydrophobic nature. Instead they are transported from sites of uptake/synthesis to sites of storage/use via proteins called lipoproteins (Cunningham et al., 2000). Hall et al. (1995) noted that whilst Hc does not contain sufficient bound lipid to be classified as a lipoprotein, it does constitute approximately 90% of the total hemolymph protein. Subsequently a substantial percentage of the total lipids in hemolymph are associated with Hc suggesting that Hc may play an important role in lipid transport, perhaps indeed functioning as an apolipoprotein (the protein component of a lipoprotein). This would be in addition to its known native respiratory and proposed immune response functions, and has been suggested to offer additional structural stability to the protein (Zatta, 1981).

An important finding was reported by Cunningham et al. (1999) which suggested that only the native hexameric form of Hc from *P. pythagorius* could bind lipids *in vitro*. This implied that native Hc multimers possessed particular characteristics which enabled them to interact with lipids, such as domains of low polarity. All earlier investigations which had reported

that arthropod Hc contained a phospholipid inducible PO activity, used monomeric forms of Hc in their experiments, whilst the currently presented research used native 4 x 6-meric or 8 x 6-meric Hc. It is therefore plausible to suggest that phospholipids interact with Hc monomers via a different mechanism to that which they do with multimeric Hc molecules. The former interaction appears to result in a change of Hc function to a PO type enzyme whilst the interaction with the native multimer may stabilise the protein structure. This would perhaps help explain the varying effects that SDS and phospholipids have been shown to have on multimeric Hcs, and also the contrasting results between the current Hc PO activity assays and previously published results from investigations studying the phospholipid mediated activation of Hc PO activity.

#### **7.4.7 Summary and Conclusions**

The present investigation was designed with the aim of characterising the mode of activation of PO activity in hemocyanin from three arthropod species. The results have been discussed in more detail in earlier sections (7.4.2 through 7.4.6), however, the main findings of the research are summarised below.

Hemocyanin from the three chelicerates *L. polyphemus*, *E. californicum* and *P. imperator* clearly possessed an intrinsic PO-type enzymatic activity which could be induced by incubating the protein with the anionic detergent SDS. This activation was concurrent with significant localised conformational changes in the protein structure most probably at, or in the vicinity of, the dicopper centre, causing either the formation of de-oxy Hc, or a perturbation of the dioxygen to copper (II) charge transfer transitions; at least in the case of LimHc and PanHc. Equivalent structural changes were detected in EuryHc following 16

hours incubation with SDS, and so it is therefore possible that the optimal PO activity of EuryHc may have been much larger, given a longer incubation in SDS. The changes in the dicopper centre were not as a result of a loss of the coordinated copper ions, but may instead have been due to a change in the orientation, or a distortion, of the bound peroxide, or a modification to the mode of coordination of the CuA and/or CuB ions. The reversibility of these functional and structural changes in Hc caused by SDS was also investigated preliminarily using LimHc and PanHc. Whilst this area needs much further work, particularly to clarify the reversibility of the effects of SDS on tertiary structure, early indications are that the induced PO activity and changes in the nature of the dicopper centre are irreversible, whilst the secondary structural changes can be reversed.

The concentration of SDS with which the Hc molecules were incubated had a significant influence on the level of PO activity elicited and the conformational changes induced. Low monomeric SDS concentrations induced minimal activity and structural change. However at high monomeric to micellar concentrations (0.7 – 1.05 mM) significant PO activity and structural changes were recorded, although secondary structural changes were preceded by tertiary structural changes. This suggested an initial increase in flexibility possibly induced by monomeric SDS, however it was the micellar form of this anionic detergent which was required to cause the conformational changes necessary for optimal PO activity. Exceeding a particular SDS concentration (dependant on Hc type), PO activity began to decrease resulting in a bell shaped activity plot. This suggested that whilst monomers of SDS can interact with the Hc molecule to cause the discussed changes in structure and function, enzyme-micelle interaction is a pre-requisite of full activation of Hc enzymatic activity and complete conformational change.

Discussions in earlier sections which were based on the results of the Hc PO activity assays and structural studies, noted that there appeared to be variation between Hc types in terms of the flexibility of the dicopper centre to entry of larger phenolic substrates, and also in terms of the overall structural stability of the molecule in the presence of SDS. The maximum specific activities achieved by LimHc and EuryHc were much lower than that displayed by PanHc. This suggested that EuryHc and LimHc had less flexible dicopper centres resulting in restricted substrate access, whilst the PanHc dicopper centre was more open allowing for the higher specific activity. There also appeared to be a hierarchy of structural stability in these three Hc types with EuryHc being the most stable, followed by LimHc then PanHc. EuryHc required at least 16 hours incubation in SDS to induce the secondary, tertiary and dicopper centre structural changes seen in the other Hc types after 5 minutes. Furthermore, at the quaternary level, EuryHc retained its native 4 x 6meric arrangement for at least 24 hours in the presence of micellar concentrations of SDS, whilst PanHc disassociated into 1 x 6mers at between 40 minutes and 24 hours incubation. Both EuryHc and LimHc exhibited stability in their maximum PO activity levels in the presence of up to approximately 10 mM SDS before a decrease was recorded, however PanHc PO activity began decreasing above 2 mM SDS. EuryHc nonetheless retained higher activity levels above 10 mM than LimHc. In conjunction, this data indicated that Hcs from the ancient chelicerates *L. polyphemus* and *E. californicum* are more structurally rigid and stable than the Hc from the more modern chelicerate *P. imperator*. The extreme stability of EuryHc and LimHc has been reported previously in terms of high temperature exposure (Sternner et al., 1995; Georgieva et al., 1998). The enhanced thermostability of EuryHc (4x6-mer) has been attributed to the extreme environmental conditions which *E. californicum* has to endure in its native habitat (high

absolute temperatures and large temperature fluctuations of more than 70°C between day and night), during which the animal still requires a maintained oxygen supply. As the organisms respiratory protein, Hc must be highly adaptable to these drastic environmental changes, and in fact can remain fully functioning and structurally intact up to 90°C, thus fulfilling its role in these extreme conditions (Sternier et al., 1995). The intrinsic stability of EuryHc may explain why this protein exhibited such a high level of stability in the presence of SDS in this study. Having a reduced maximum PO activity level is a compromise for this added stability. The extreme stability of proteins originating from thermophilic organisms has been known for many decades. Thermostable proteins are found also to be thermoactive demonstrating higher temperature optima than their mesophilic homologues. Under mesophilic conditions such thermophilic enzymes exhibit additional stability over their mesophilic counterparts; however they appear to have reduced activity. Only at higher temperatures can these thermophilic enzymes attain the flexibility in structure required to achieve optimal activity (Danson et al., 1996; Vieille and Zeikus, 2001). It may therefore be the case that the optimal temperature for eliciting PO activity in EuryHc will be somewhat higher than LimHc and PanHc. *L. polyphemus* does not inhabit such an extreme environment and therefore the enhanced thermostability of Hc from this species could not be similarly explained. Instead it has been proposed that the complex oligomeric structure of this protein (8x6-mer) was responsible for the extreme thermostability (Georgieva et al., 1998), and there have been other reports of increased stability in enzymes from thermophilic organisms being achieved by forming larger oligomeric structures than their mesophilic equivalents (Villeret et al., 1998; Vieille and Zeikus, 2001). This may also explain the lower stability in PanHc which is a 4x6-meric molecule from a mesophilic environment. Ultimately all three Hc types demonstrate similar conformational changes in the presence of SDS micelles, however the

ancient Hc types exhibit greater stability but lower PO activity levels, whilst the modern Hc type has evolved to possess higher levels of PO activity but at the cost of possessing much reduced structural stability.

Phospholipids were utilised in some final experiments to establish whether these amphiphilic molecules could potentially be candidates for the *in vivo* elicitors of arthropod Hc PO activity, due to their structural and physiochemical similarities to SDS. However, contradicting the work of earlier research, this current investigation concluded that phospholipids had no effect similar to SDS on the function or structure of the native Hc molecule from either LimHc or PanHc. It was proposed that variations in the experimental conditions used by each research group may have been the underlying cause for the contrasting results. It seemed more probable however that the differing results occurred since all earlier experiments were conducted using Hc in its monomeric form whilst the present investigation used native 4x6-meric or 8x6-meric Hc molecules. Native Hcs from the arthropod subphyla Crustacea and Araneae have been proposed to function as apolipoproteins with their bound lipid content providing a stabilising effect on the protein structure. Although further work is required, it was proposed that the results of the current research may have suggested a similar role for Hc as an apolipoprotein in chelicerates, where the bound lipids enhance the native proteins structural stability rather than induce its intrinsic PO activity.

It is important to note that due to the heterogeneity of the subunits of arthropod Hc, and because only certain subunit types have been suggested to exhibit PO activity, this may mean that the functional and structural analyses conducted in the present investigations, have

provided data which is an average of the structural changes taking place in the whole multimeric molecule, and not just in those subunits found to possess inducible PO activity. However, in LimHc it has been suggested that all LimHc subunits function cooperatively during oxygen binding, undergoing similar simultaneous structural changes which remove the dicopper centre placeholder Phe-49 allowing oxygen to enter (Hazes et al., 1993; Hartmann and Decker, 2002; Decker et al., 1996). It has also been proposed that removal of the placeholder amino acid from the dicopper centre entrance is all that is necessary to elicit PO activity in arthropod Hc (Decker and Rimke, 1998; Decker and Jaenicke, 2004). Therefore a similar cooperative structural mechanism may apply for the induction of Hc PO activity by SDS, whereby all subunit types undergo similar induced structural changes resulting in a functional change in the hemocyanin molecule.

It has become apparent that Hc is a multifunctional protein which defies the central dogma of 'one active site, one function'. This study has provided the first invaluable insights into the mode of SDS induced activation of PO activity in arthropod Hc, although it is still necessary to establish the optimal conditions for each Hc type. It is foreseen that a similar mechanism will also exist for the natural induction of PO activity in Hc. Further investigations in this field will however be required to confirm this expectation.

## **Chapter 8 : Summary of Research Findings and Future Work**

The presented thesis has detailed and discussed the results of experiments designed with the purpose of addressing the two central aims of the research. These aims were firstly to isolate and sequence a gene coding for the enzyme phenoloxidase (PO) from larvae of the crop pest insect *Spodoptera littoralis* (the Egyptian Cotton Leafworm), and secondly to use a range of biophysical techniques to characterize the mode of SDS induced activation of PO activity in arthropod hemocyanin (Hc). In this final chapter, the research findings are summarised and potential further work is described, as are reasons for the importance of continuing to study the structure and function of Type-3 copper proteins.

### **8.1 Summary of Chapters 3, 4 and 5 – Attempts to Isolate a Phenoloxidase Gene from Larvae of the Egyptian Cotton Leafworm, *Spodoptera littoralis*.**

In Chapter 3, a previously isolated and cloned 600 bp putative *S. littoralis* prophenoloxidase (PPO) gene fragment was sequenced and analysed to determine its origin. Analysis revealed that the 600 bp gene fragment shared sequence identity to arthropod PPO and Hc only in the region of the CuA binding site, which was the site the forward primer had been designed to recognize and bind during PCR amplification. The 600 bp fragment in fact demonstrated greater sequence identity to insect  $\beta$ -galactosidase. It was concluded that non-specific priming by the primers was responsible for the amplification of this product. The design of the primers was guided by multiple alignments of a number of insect PPO gene sequences. Similar primers had been used previously by other research groups to successfully amplify

PPO genes from different insect species (Müller et al., 1999; Chase et al., 2000; Lourenco et al., 2005), suggesting the design was logical and the primers were fit for purpose.

An alternative approach was adopted for the research presented in Chapter 4. In a further bid to isolate a PPO gene from *S. littoralis*, a range of molecular methods were employed, in which restricted *S.littoralis* genomic DNA, amplified *S.littoralis* DNA fragments and *S.littoralis* cDNA libraries were prepared for subsequent hybridisation with a heterologous DIG-labelled PPO DNA probe. Despite efforts to identify a PPO gene fragment from an *S. littoralis* cDNA library and genomic DNA, none were identified by either cDNA library screening, or Southern blotting of gel separated PCR or genomic DNA restriction digest products. A number of possible explanations were considered to explain this outcome. Firstly, the cDNA library which was screened and used in many of the PCR reactions originated from larvae which had been parasitized by a parasitic wasp. It was initially hypothesised that parasitisation may inhibit the transcription of the PPO gene(s) in *S. littoralis*, as previous reports provided evidence for the negative effects of parasitisation on hemocyte function and other immune response mechanisms (Lavine and Beckage, 1995; Di Venere et al., 1998). These immune suppressive effects are proposed to optimise conditions for successful development of the parasitoid wasp egg (Shelby et al., 1998). However, more recent investigations have suggested that PO activity is controlled at some post-transcriptional step by parasitisation (Zhang et al., 2004; Hartzer et al., 2005). Secondly, the possibility that the cDNA library used may have contained a low copy number of PPO cDNA was considered. Recent findings suggest that the larval stage, used for synthesis of the cDNA library, contains abundant quantities of PPO mRNA (Rajagopal et al., 2005), implying that PPO cDNA copy number was not a limiting factor. Finally, it was concluded that the most

likely explanation was the poor specificity and sensitivity of the DIG-labelled PPO DNA probes used during the hybridisation of DNA-bound membranes. Therefore, in the event that the membranes contained PPO DNA bound at their surfaces, the DIG-labelled probes used were not suitable for the confident identification of PPO DNA.

Chapter 5 reported the attempts made to generate a non-parasitized larval *S. littoralis* hemocyte cDNA library for screening for a PPO gene. Hemocytes were chosen as the tissue source as they are reported to be the site of synthesis of PPO mRNA (Müller et al., 1999). However, problems encountered during attempts to isolate intact total RNA from *S. littoralis* hemocytes, and time constraints on the project limited the progress of these experiments.

Therefore, despite the numerous efforts to isolate and sequence an *S. littoralis* PPO gene, the attempts made were unsuccessful. Continuation of this work should involve persevering with attempts to generate a fully intact cDNA library from larval hemocytes which are proposed to be an enriched source of PPO DNA. Using this cDNA library, RT-PCR experiments should be performed using specifically designed primers for insect PPO gene amplification. Successful isolation, sequencing and identification of an *S. littoralis* PPO gene fragment would allow the use of 5' and 3' RACE experiments to generate a complete PPO gene sequence. This sequence could then be used as a template for the synthesis of *S. littoralis* specific DIG-labelled PPO DNA probes to screen the hemocyte cDNA library for further PPO genes. Knowledge of the amino acid sequence of an *S. littoralis* PPO will enable protein structure prediction tools to be used to provide hypothetical models for the structure of this insect PPO. This predicted model could subsequently enable structural comparisons between insect PPO and other type-3 copper proteins known capable of catalysing similar reactions, such as

tyrosinase, and catecholoxidase. It may also be possible to clone the *S. littoralis* PPO gene into an expression vector for expression of the gene product in *E. coli*. This has already been demonstrated possible with *Spodoptera litura* PO (Rajagopal et al., 2005), and may provide the opportunity to study the structure of this protein and its activation mechanism *in vitro*.

## **8.2 Summary of Chapter 7 – Biophysical Characterisation of the Mode of SDS Induced Arthropod Hemocyanin Phenoloxidase Activity.**

Whilst the structure of arthropod PO remains elusive, another member of the Type-3 copper protein family, arthropod Hc, provides a suitable model upon which to base predictions of the structure of PO. PO and Hc contain a highly conserved sequence of amino acids at their CuA and CuB binding sites, indicating a similar three dimensional arrangement in the dicopper centre of each protein (Ashida and Brey, 1995; Decker and Terwilliger, 2000). Nonproteolytic activation of native PO using SDS is routinely performed to assay for PO activity. Since arthropod Hc possesses an intrinsic PO activity which can also be induced by SDS, amongst other *in vitro* treatments (Decker and Rimke, 1998; Decker et al., 2001; Decker and Jaenicke, 2004; Nagai et al., 2001; Zlateva et al., 1996; Lee et al., 2004; Nellaiappan and Sugumaran, 1996; Jaenicke and Decker, 2004; Nagai and Kawabata, 2000), it is proposed that Hc will also provide a suitable model for the mechanism of activation of native arthropod PO. In Chapter 7, a range of biophysical methods were employed to characterize the conformational changes in arthropod Hc associated with induction of its intrinsic PO activity by the anionic detergent SDS. Three arthropod species were used as a source of purified native Hc; the two ancient chelicerate *Limulus polyphemus* and *Eurypelma californicum* and the more modern chelicerate *Pandinus imperator*. The results indicated that the SDS induced PO activity in these Hcs is associated with localised conformational

changes in protein structure, most likely in the vicinity of the dicopper centre, enhancing access for larger phenolic substrates. These structural changes occurred at the secondary and tertiary levels without the loss of the associated copper ions. Variations in the required incubation times in the presence of SDS, optimal activities and degrees of structural change at higher monomeric and micellar concentrations of SDS, suggested Hc from the ancient chelicerate *E. californicum* possessed much greater structural stability but lower levels of PO activity, whilst that from the modern chelicerate *P. imperator*, appeared to have the greatest flexibility in its dicopper centre and subsequently exhibited the highest levels of detectable PO activity. A trade-off between activity and structural stability was proposed for *E. californicum* Hc as this protein requires enhanced structural rigidity in order to remain fully functional at the high temperatures the organisms' environment presents. Nonetheless, for all three Hc types, SDS concentrations approximating the CMC appeared critical for the induction of the necessary structural changes required for a significant increase in the detectable PO activity to be exhibited, whilst maximum PO activity was only achieved in the presence of SDS micelles. Further experiments provided early indications that these functional and structural changes in Hc cannot be fully reversed and neither can they be induced by the non-ionic detergent NBDG or phospholipids in free or small unilamellar vesicle form; the latter contradicting earlier reports.

The preliminary results on the reversibility of the activation of Hc PO activity by SDS require further investigation. As suggested in Chapter 7, the stripping of SDS from reactions containing Hc by using cyclodextrins may prove to be a more suitable method for establishing reversibility of induction of PO activity, rather than the method of 'reaction dilution' used in the current research. It would be necessary to evaluate the contributions of

cyclodextrins to any spectral measurements before confirming their suitability for use in equivalent structural studies. Demonstrating conclusively whether the PO activity and associated structural changes in native arthropod Hc are reversible or not, may provide clues concerning the mechanism and control of Hc PO activity induction *in vivo*. If the simple removal of SDS cannot fully reverse its effects on Hc, this may imply a requirement for additional components to assist the refolding of Hc to its native conformation *in vivo*. Alternatively it may suggest that once the function of native Hc has been shifted to that of a PO-type enzyme, the protein subunits involved lose their ability to function as oxygen transporters. Conversely, if it was found that the structural and functional changes in Hc were fully reversible upon removal of SDS, this may demonstrate the protein has the ability to refold by itself in the absence of activating agents, enabling a return to its primary function.

The effects of phospholipids on arthropod Hc in the current report contradicted reports by a number of earlier research groups (Nagai and Kawabata, 2000; Nagai et al., 2001; Sugumaran and Nellaiappan, 1990; Sugumaran and Nellaiappan, 1991). Phospholipids are considered a potential *in vivo* inducer of Hc PO activity and the above earlier investigations corroborated the hypothesis by demonstrating that PO activity could be induced in arthropod Hc upon incubation with phospholipids. Presently, however, this was found not to be the case. Albeit that the reaction conditions were different in each published investigation, the factor considered most prominent was that all previous work used monomeric Hc whilst the present research used native multimeric Hc. It is therefore necessary to pursue this line of work, perhaps repeating previously published research instead using multimeric Hc, to determine the reproducibility of the data when the native Hc molecule is involved. Hc from crustaceans and spiders has been suggested to function as an apolipoprotein with its bound

lipid providing additional structural stability. Exploration of the role of phospholipids in the multimeric Hcs in this study will establish whether phospholipids are candidates for *in vivo* induction of Hc PO activity and/or important in protein stability.

A further line of research on the *in vivo* activation of arthropod Hc PO activity which should be pursued is the effects of antimicrobial peptides. A recent investigation demonstrated that antimicrobial peptides can bind to and induce PO activity in the Hc  $\alpha$ -subunit from *Tachypleus tridentatus* (Japanese horseshoe crab) (Nagai et al., 2001). Like SDS, antimicrobial peptides are amphiphilic molecules. In the chelicerate these peptides are secreted from the S-granules of granular hemocytes as part of the immune systems response to microbial infection. Antimicrobial peptides recognise foreign cells and permeabilise their cell walls by incorporating themselves into the lipid bilayer, forming pores or generally disrupting membrane integrity (Tincu and Taylor, 2004). This ultimately destroys the infecting cells, protecting the host from systemic infection and damage. Nagai et al (2001) also found that *T. tridentatus* Hc could bind and be activated by antimicrobial peptide-coated chitin (a major component of fungal cell walls and arthropod exoskeletons). They proposed that antimicrobial peptide-coated chitin exposed at sites of exoskeleton damage or at the surface of infecting fungal cells may act as a scaffold to localise peptide activated Hc PO activity for wound healing and host defence against infection. These results provide very promising indications that antimicrobial peptides function to elicit Hc PO activity *in vivo*. Future investigations could involve incubating various antimicrobial peptides with native *L. polyphemus*, *E. californicum* and *P. imperator* multimeric Hc to provide indications as to whether equivalent PO activity can be induced in different species of Hc and also in the complete Hc molecule rather than a single subunit type. By performing similar structural

investigations to those reported in the present thesis, it would also be possible to evaluate whether the effects of antimicrobial peptides caused similar conformational changes to SDS.

Finally, discussions in Section 7.4.4.2, Chapter 7 outlined the problems inherent in studying the tryptophan fluorescence spectra of multi-tryptophan proteins such as Hc. In a bid to interpret the contributions of each of the Trp residues in Hc to the final spectrum, fluorescence tagging or mutation of specific residues could be performed. If also used in near UV circular dichroism experiments, these modified Hc molecules may also provide further information on those residues and thus regions of the Hc protein which have the most significant involvement in the conformational changes induced by SDS upon induction of PO activity.

### **8.3 Research into the Structure and Function of Type-3 Copper Proteins has Medical, Industrial and Agricultural Importance.**

The study of the structure and function of Type-3 copper proteins is a very important field and has already shown potential benefits to the medical, industrial and agricultural sectors. In the following discussion, the underlying reasons for the interest in this area of research are outlined, as are some examples of how current knowledge of the structure and function of such proteins has been applied to the development of therapeutic, food anti-browning and soil detoxifying agents.

Tyrosinase, like PO, catalyses reactions involved in the synthesis of melanin, and is found in animals, plants, fungi and bacteria. In the skin of humans melanin synthesis occurs in the melanocytes of the basal layers of the epidermis (Sugumaran et al., 2000b). One form of

melanin, eumelanin (black-brown melanin), offers protection to the skin from the harmful effects of solar radiation by absorbing and scattering UV light. However, chronic exposure to the sun can lead to the overproduction of eumelanin and results in discolouring of the skin from hyper-pigmentation diseases such as melasma (Jones et al., 2002). On the basis of the understanding of the function of tyrosinase, a specific inhibitor of tyrosinase activity, aloesin, has been identified with potential therapeutic applications as a depigmentation agent (Jones et al., 2002). This compound was found to be much safer than previously produced depigmentation agents which, amongst other undesirable side effects, exhibited toxicity to melanocytes.

Tyrosinase has also been considered as a potential agent for use in soil and water clean up of pollutants such as xenobiotics. Xenobiotics are man-made compounds which were designed for use as pesticides and weed killers. These compounds have been applied to terrestrial and aquatic environments over the decades in damaging quantities. Whilst they do become harmless as a result of biotic and abiotic processes, being transformed into carbon dioxide, water and mineral elements, this takes a long time and often involves the formation of highly toxic intermediates (Bollag, 1992). Tyrosinases present in soil have recently been found to be involved in the random coupling of aromatic compounds in the formation of humus (Park et al., 2000). This has led to an interest in these enzymes from an agricultural point of view as potential soil and water treatments for the cleanup of xenobiotic compounds such as fluorophenols which are environmental contaminants that have increased in use since the early 1990's (Battaini et al., 2002). Immobilised tyrosinase has in fact been described as being an excellent method of phenol removal from aqueous environments and soils, whilst reducing the costs involved by increasing the percentage recovery of the enzyme

In fruits, vegetables and mushrooms, tyrosinase is the crucial enzyme responsible for the browning process which occurs during product storage and upon bruising. Browning of cut food products is a major problem facing the food industry as it affects their appearance and nutritional quality (Iyengar and McEvily, 1992). On the basis of the current knowledge of the function of tyrosinase, this has prompted investigations into the potential use of compounds which inhibit the activity of tyrosinase as anti-browning agents. Methods such as thermal processing and exclusion of oxygen have been used to inhibit enzymatic browning, however the former was found to deteriorate nutritional quality and the latter loses its effect upon reintroduction of oxygen (Lee, 2007). A number of anti-browning agents have also been identified which target enzyme activity or the substrates/products of catalysis, thus inhibiting brown pigment formation. Examples of such anti-browning agents used in the control of browning of fruits and vegetables include sulphites, acidifiers, chelators, reducing agents and cysteine (Fu et al., 2007). However the use of such compounds has been restricted by their high cost and low effectiveness and with regards to sulphites, the increasing public awareness of their associated hazards and increased regulation of their use by the Food and Drug Administration (Eissa et al., 2006). It has therefore become necessary to develop safer alternatives which function efficiently as browning-agents. Very recently, an investigation conducted by Lee (2007) demonstrated the inhibitory effect of onion extract on banana polyphenol oxidase activity during ripening. It was found that addition of onion extract heated to 100°C for 10 minutes markedly inhibited enzymatic activity. Produced from a natural food source, onion extract therefore has the potential for use as an anti-browning agent without the undesirable risks inherent in use of the previously mention sulphites.

In Chapter 3, Chapter 4 and Chapter 5 the insect species *Spodoptera littoralis* was the insect species from which attempts were made to isolate and sequence a PO gene. This Lepidopteran insect is an economically important crop pest in many regions of Africa and Asia. Prior to 1986, the compound methyl-parathion was used extensively to control *S. littoralis*, however development of resistance to this and other compounds, meant the development of alternative pest control methods was necessary (Smith et al., 1997). By gaining a greater understanding of the insect immune system and the key stages and components involved, such as PO, this may provide scope for the development of pest control methods which disrupt the insect immune response, perhaps even in a species specific manner. By inhibiting the action of PO, all developmental stages of the pest insect would be affected by inhibiting sclerotisation of newly formed cuticle, correct wound healing and the melanisation of foreign bodies. The targeted insects would subsequently suffer increased vulnerability to disease, damage and desiccation, reducing their chances of survival. On the basis of the functions of PO in insects and the structure of a tyrosinase from *Streptomyces castaneoglobisporus* (Matoba et al., 2006), Xue et al (2007) have recently identified groups of compounds with inhibitory effects on the enzymatic activity of PO from larvae of the Lepidopteran insect *Pieris rapae* (Cabbageworm). These compounds, which belong to the benzaldehyde thiosemicarbazone, benzaldehyde, and benzoic acid families, have provided a starting point for the development of novel PO inhibitors to function as environmentally friendly insecticides (Xue et al., 2007).

Despite the present experimental successes, and hypothesised uses and targeting of Type-3 copper proteins, the field still requires much further work, particularly to obtain greater

knowledge of the structure of PO and tyrosinase enzymes, which are of major concern in medical and cosmetic research and to agriculture and the food industry.

## Chapter 9 : Appendices

### 9.1 Appendix A – Primers and binding-site map.

Table 11: Primers designed specifically for the amplification of an insect phenoloxidase sequence. Primers CuA'03-F and PO2-R were previously designed by Nairn 2002 (unpublished data) and used to amplify the putative PPO 600 bp gene fragment analysed in Chapter 3. All others were utilized during PCR protocols performed in the presented research of Chapter 4. The given name of each primer is shown along with the details of its nucleotide and amino acid sequence, and the amino acid sequence position it anneals to, as established from the alignment of six different arthropod PPO sequences found in Figure 3, Chapter 2.

| Primer Name  | Nucleotide Sequence  | Amino Acid Sequence (5' – 3') | Designed Binding Site |
|--------------|--|-------------------------------|-----------------------|
| CuA'03-F     | 5'-CAC-CAC-TGG-CAC-TGG-CAC-CT(AGCT)-GT(AGC)-TAC-CC-3'            | H-H-W-H-W-H-L-V-Y-P           | 214 - 223             |
| PO2-R        | 5'-GGC-GAT-GAC-ACC-GAA-(AG)GA-CTC-CAG-GTA-3'                     | Y-L-E-S-F-G-V-I-A             | 389 - 397             |
| MsextaPPO1-F | 5'-CAC-CAC-TGG-CAC-TGG-CAC-TTG-3'                                | H-H-W-H-W-H-L                 | 214 - 220             |
| MsextaPPO1-R | 5'-GCC-CTT-GGG-TAT-CAG-CAT-3'                                    | M-L-I-P-K-G                   | 600 - 605             |
| MsextaPPO2-F | 5'-CAC-CAT-TGG-CAT-TGG-CAT CTC-3'                                | H-H-W-H-W-H-L -               | 214 - 220             |
| MsextaPPO2-R | 5'-CGT-TCC-CTT-AGG-CAC-GAG-CAT-3'                                | M-L-V-P-K-G-T                 | 600 - 606             |
| CuA-F        | 5'-CAC-CAC-TGG-CAC-TGG-CAC-CT5-GT(AGC)-TAC-CC-3'                 | H-H-W-H-W-H-L-V-Y-P           | 214 - 223             |
| CuA2-F       | 5'-CAC-CAC-TGG-CAC-TGG-CAC-C-3'                                  | H-H-W-H-W-H-L                 | 214 - 220             |
| CuA3-F       | 5'-CAC-CA(CT)-TGG-CA(CT)-TGG-CA(CT)-C-3'                         | H-H-W-H-W-H-L                 | 214 - 219             |
| CuA4-F       | 5'-CA(CT)-CA(CT)-T(AG)(GCT)-CA(CT)-TGG-CA-3'                     | H-H-W-H-W-H                   | 214 - 219             |
| GELF-F       | 5'-GG(AGCT)-GA(AG)-(CT)T(AGCT)-TT(CT)-T(AT)(CT)-TA(CT)-ATG-CA-3' | G-E-L-F-F/Y-Y-M-H             | 238 - 245             |
| CuB2-F       | 5'-TTC-TAC-(AC)G5-TGG-CAC-GC5-TAC-AT(CT)-GA(CT)-3'               | F-Y-R-W-H-A-Y-I-D             | 408 - 416             |
| CuB2-R       | 5'-(AG)TC-(AG)AT-GTA-5GC-GTG-CCA-5C(GT)-GTA-GAA-3'               | F-Y-R-W-H-A-Y-I-D             | 408 - 416             |
| MEILD-R      | 5'-GAA-(CT)TT-(AG)TC-CA(AG)-(CT)TC-(AG)AT-CAT-3'                 | M-I-E-L-D-K-F                 | 537 - 543             |
| Cys-R        | 5'-GTG-GTG-5GG-CCA-(GT)CC-(AG)CA-(GT)CC-(AG)CA-GAA-3'            | F-C-G-C-G-W-P-H-H             | 591 - 599             |
| Cys2-R       | 5'-AC(AG)-CC(AGCT)-AC(AG)-CC(AGCT)-ACC-GG-3'                     | C-G-C-G-W-P                   | 592 - 597             |
| Cterm-R      | 5'-TAC-CC(AGCT)-A(AT)(AG)-GG(AGCT)-AA(AG)-CT-3'                  | M-G-F/Y-P-F-D                 | 656 - 661             |

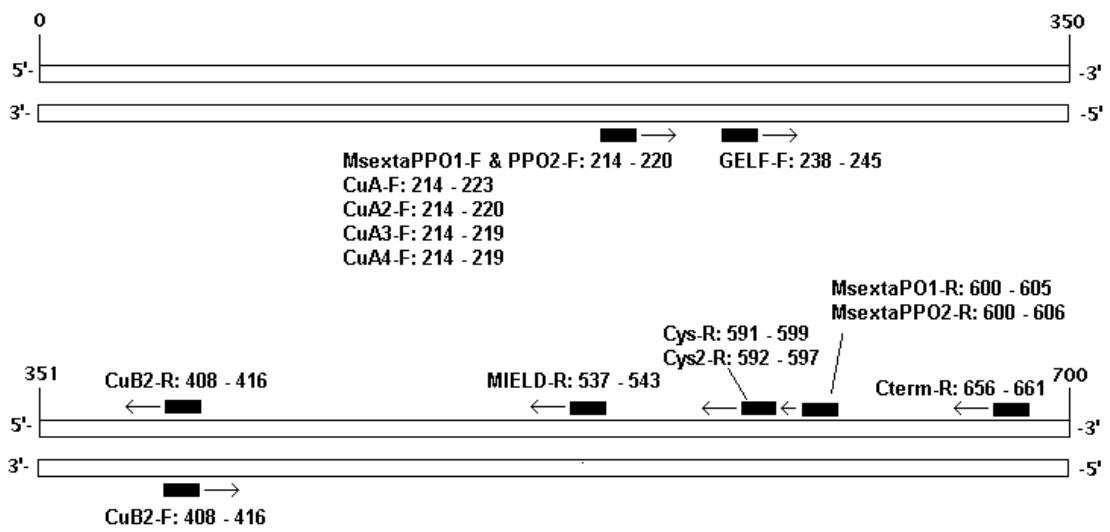


Figure 89: Primer binding-site map. Each of the degenerate primers detailed in Table 11, which were designed specifically for the amplification of a phenoloxidase sequence, are represented as labelled black rectangles positioned next to the DNA strand they are designed to anneal to. Arrows associated with each indicate the direction of strand extension once each primer has annealed to its designed sequence. The numerical values alongside each primers given name indicate the amino acids of the template PPO DNA to which the primers are designed to anneal, as estimated from the amino acid sequence alignment in Figure 3, Chapter 2.

## 9.2 Appendix B - Raw nucleotide sequence of a putative 600 bp prophenoloxidase DNA fragment as deduced in forward and reverse direction for clones 2a and 10a.

### 600 bp clone 2a (forward reaction)

GCTNCNGCNNNNGGGNNNNNNNNNGGGGTNTNGTATGANNGTTTTTAAANACNTNGAAANNNNNGGNGNNAG  
CTCGGGCCCCACACGTGTGGTCTANAGCTAGCCTANGCTCGAGAAGCTTGTGACGAATTCAGATTGGCGATG  
ACACCGAAGGANTCCAGGTNGGTATTATATTATAATTTAAGTTTTGGGGNAAAAAGTTTNNATNATTATGTTAA  
TNNATTNTTNAAAATTNTNATNNATNNATNNGGNACAAAATTNANTGTTGGTGANANTGTTAGGAACGGNACC  
ATTTNTGAANAAAANAATTCGNTTNCCTCANTAGTGTAGAGGAGAGCGTTGGTACCGACGTGGTTCTGCAGCA  
TGTTGCGGACTTGGACTCGATAGTTCATGTTGTTGCCATAGCTACCGTACTCATTTTCTANCTGGATAGCAAAC  
AAAGATTTTAAGGCCATTACAGCACTTATAATCAGATTTTGACAATTAAGTGATTNATTAATAAAATNTAA  
TGGTTTTGGTTNTAAGAANNACTNATTTAANATTNANGCCTTTTTNTNTCCCGAAGGGGGTNGACCANGGTGNC  
AGTGCCATTTGGTNGAATTNANNNAATTTNTTGGATTTCCGGANTANNTTTNANTGCNGTTTTTGGNGGNATTGN  
GTTTGGTTNNCGGAAGCCTTNTTCCNTTATTATTGNAGGTNTGGTATTTANAAANTC

### 600 bp clone 2a (reverse reaction)

GCGGCNAGGCCTNCAANNTNNACNTATAAAGCNCCTTGAAATANNACTCACTATAGGNAAAGCTCGGTACCAC  
GCATGCTGCAGACGCGTTACGTATCGGATCCAGAAATTCGTGATTACCACTGGCACTGGCACCTNGGTCTACCC  
CTTTTCGGAGATAAAAAGGCGTNATNTATATNAATNGNCTTATNACCCAANCNTTATNTTTATTTAATTAATCNC  
TAATTGNCNAATCTGATTATAAGTGCTGTGAATGGGCCTTAAAATCTTTGTTTGCTATCCAGGTAGAAAATGAG  
TACGGTAGCTATGGCAACAACATGAACATCGAGTCCAAGTCCGCAACATGCTGCAGAACCACGTCNGTACCAA  
CGCTCTCCCTNTACNATAACAGANGGAATNNGNNAATNTCTCTNTCAAAAANGGGGNNNNCGNCCCNAACNC  
CTCCCCANATCGATTTTTTGGTCCCCACTCAAGTCNGTATAATTTTTNAATAATGGTATTGTACCATAAATTNA  
TGGTNANACTTTTTTNCCTCCCAAACTTAAANTTANNAATAATAAATACCTTACCTGGGAAGTCCTTCCGGGN  
GTTTCATCCGNCCAAATCTNGAAATTTCCNGTCGACAAAGCCTTCTCCGAGCCCTTANGGCTAANCTNCTAAGAA  
CANCAACNCTNGTNGGGGGGGGGCCCCGNANCCCTCCCCGGCCGGCTGGTATTCTNTAAGNTGGTC

### 600 bp clone 10a (forward reaction)

GCNNCCNNNCTCTTGAAGCGGCCNTTGAAGTTGACCCTATAGAATACACCGGCCGCGAGCTCGGGCCCCACAC  
GTGTGGTCTAGAGCTAGCCTAGGCTCGAGAAGCTTGTGACGAATTCAGATTGGCGATGACACCGAAGGACTCC  
AGGTAGGTATTATATTATAATTTAAGTTTTGGGGAAAAAAGTCTACATAATTATGTAAATACATTATTAATAAT  
TATACTGACTTGAGTGGGGACCAAAATCGATGGTGATGAGAGTGTAGGAACGGCACCNNTTCTGAAGAAAGAA  
ATTGCATTTCCCGTCANTAGTGTAGAGGAGAGCGTTGGTACCGACGTGGTTCTGCAGCATGTTGCGGACTTGGAC  
TCGATAGTTCATGTTGTTGCCATAGCTACCGTACTCATTTTCTACCTGGATAGCAAACAAAGATTTTAAGGCC  
ATTCACAGCACTTATAATCAGATTTGACAATTAAGNTGATTAATTNAATAAATAAATATATGCTTTGGTTNTNANA  
CCACCATATAACATCNCGCCCTTTTATCNTCCAAAGGGGGTAGACCAAGGTGCCANNNGGTGAAATC  
CACNAATTCTGGNATCCNGAATACNTTAAACGCNTTNGCCANCATTGGCGTNGGTACCCGAACNNTTCCCCNATT  
ANNNGANGNCCGNCTTTTAAANCCNC

**600 bp clone 10a (reverse reaction)**

NCNNGCNNGCCTCAANNGCNTTGAAACGCCACTTCAAATACGACTCACTATAGGGAAAGCTCGGTACCACGCAT  
GCTGCAGACGCGTTACGTATCGGATCCAGAATTCGTGATTCACCACTGGCACTGGCACCTGGTCTACCCCTTCG  
GAGATAAAAGGCGTGATGTTATATGAGTGGTCTTATAACCAAAGCATTATATTTATTTAATTAATCACTTAATT  
GTCAAATCTGATTATAAGTGCTGTGAATGGGCCTTAAAATCTTTGTTTGCTATCCAGGTAGAAAATGAGTACGG  
TAGCTATGGCAACAACATGAACTATCGAGTCCAAGTCCGCAACATGCTGCAGAACCACGTCGGTACCAACGCTC  
TCCTCTACACTACTGACGGGAATGCAATTTCTTTCTTCAGAAATGGTGCCGTTCCCTAACACTCTCATCACCATC  
GATTTTGGTCCCCACTCAAGTCAGTATAATTTTAAATAATGTATTTACATAATTATGTAGACTTTTTTCCCAA  
AACTTAAATTATAATATAATACCTACCTTGGAGTCCTTCGGTGTTCATCGCCAAATCTGAATTCGGTCGACAAAG  
CTTCTCGAAGCCCTACGCTANCCTCTANACCANCACGTTGTGGGGCCCCGAGCCTCGCCGGCCGCTGTATTCT  
AATAGTTGTC

**9.3 Appendix C – Integrity checks of total RNA, isolated from *S. littoralis* hemocytes.**

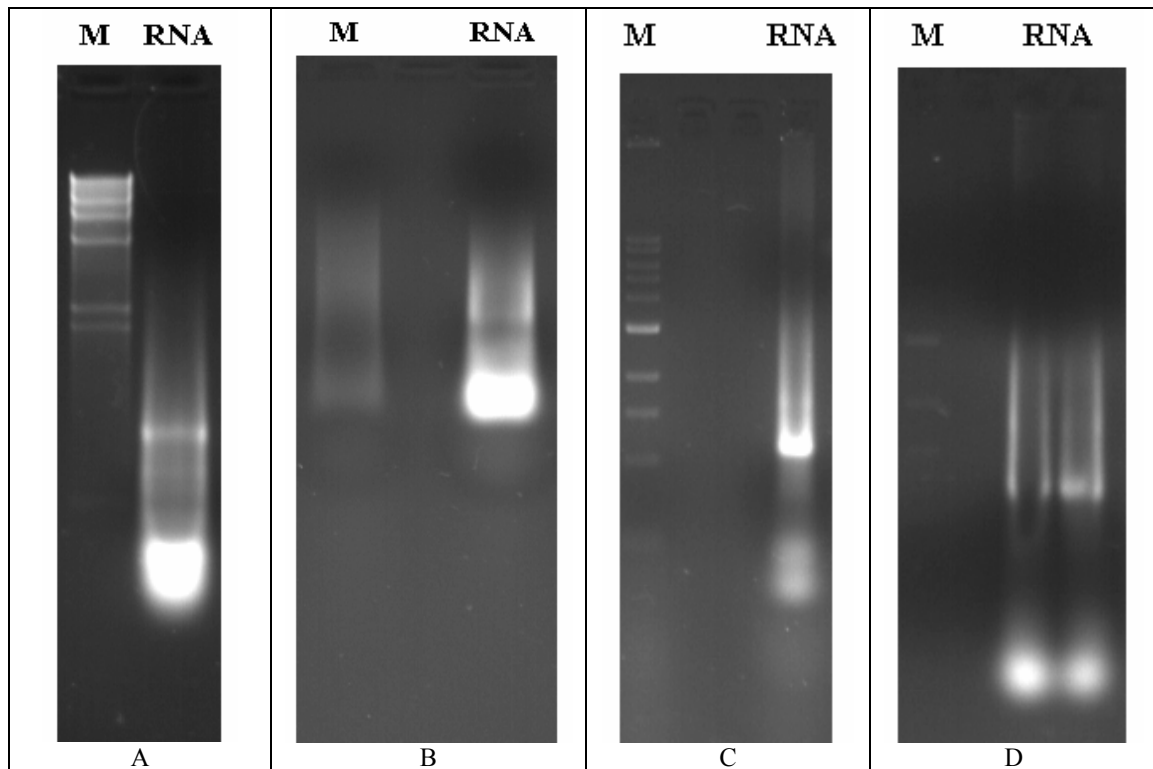


Figure 90: Isolated *Spodoptera littoralis* hemocyte total RNA integrity check. The samples shown in Panels A - D were the 2<sup>nd</sup> – 5<sup>th</sup> total RNA isolation attempts made, respectively, in Chapter 5. The samples were separated in a native 1% agarose gel. These images illustrate that the 28S and 18S ribosomal RNA (rRNA) bands are not sharp and clear as is desirable (see Figure 44 Panel B in Chapter 5), and in fact cannot be identified in most of the samples. These total RNA samples were therefore too degraded to provide a reliable source of mRNAs for synthesis of a complete *S. littoralis* hemocyte first strand cDNA mix.

#### 9.4 Appendix D – Complete activity plot of SDS induced arthropod hemocyanin phenoloxidase activity.

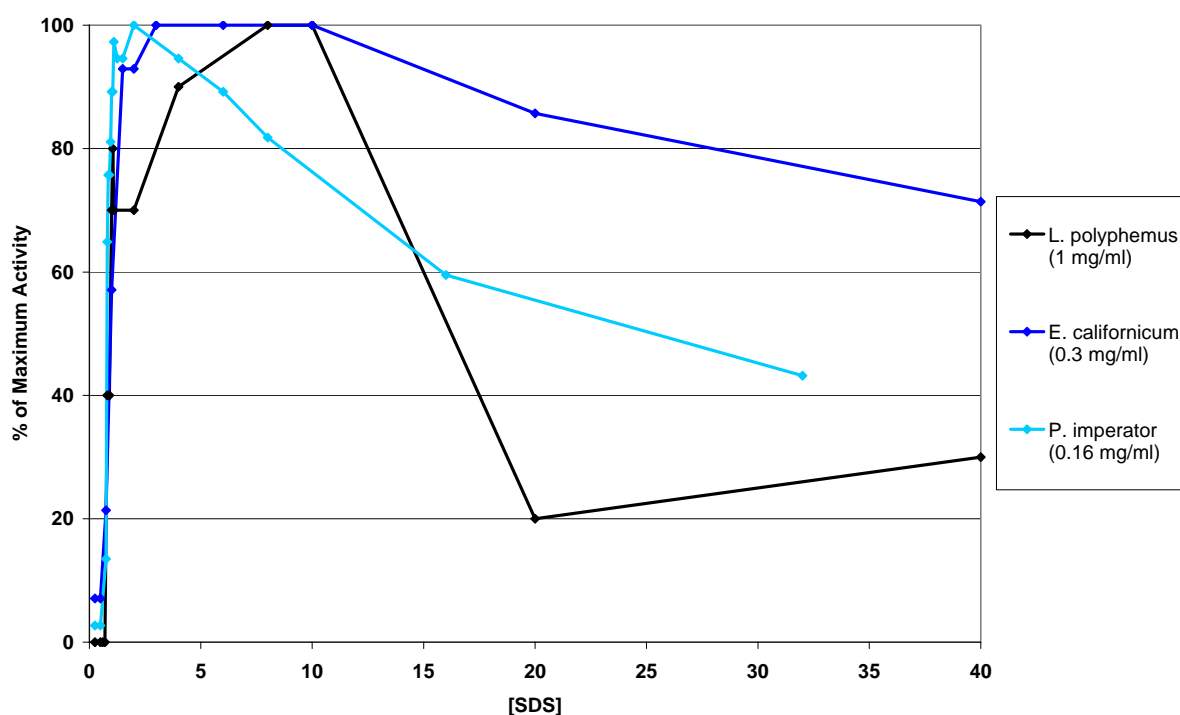


Figure 91: Induced phenoloxidase activity of hemocyanin from *Limulus polyphemus*, *Pandinus imperator* and *Eurypelma californicum*. Typical assays included 2 mM dopamine hydrochloride plus hemocyanin (concentrations in legend) in 1 ml of 100 mM sodium phosphate buffer, pH 7.5. Phenoloxidase activity (expressed as a percentage of the maximum activity achieved by each hemocyanin) was initiated by the addition of SDS, and after 5 minutes, followed by monitoring an increase in absorbance at 475 nm resulting from the formation of dopachrome and its derivatives. This plot is the complete version of the inset plot in Figure 51, Chapter 7

9.5 Appendix E – ITC data of SDS binding to arthropod hemocyanin, analysed in terms of a single binding site model.

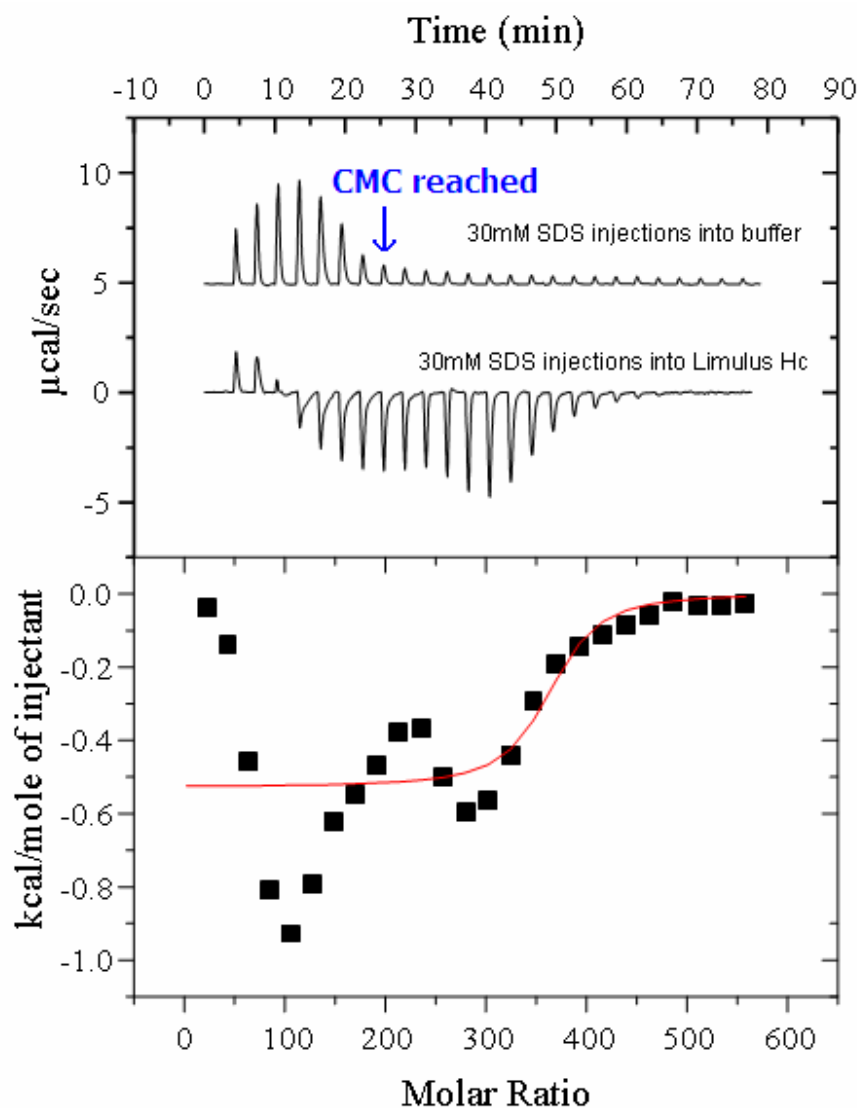


Figure 92: ITC data for binding of SDS to *Limulus polyphemus* hemocyanin. Upper trace in top panel shows a control in which SDS was injected into buffer alone to determine the CMC of SDS in 100 mM sodium phosphate buffer, pH 7.5, and also to correct for heat of dilution of the ligand. Lower trace in upper panel presents the data for injection of 30 mM SDS (0.15 mM per injection) into  $0.77 \pm 0.015$  mg/ml (10  $\mu$ M) *L. polyphemus* hemocyanin monomers (equivalent to 210 nM of the 8 x 6-meric unit). The lower panel shows the calculated binding isotherm (integrated heat data), corresponding to the lower trace in the upper panel, and the best-fitted curve of the data. The calorimetry data shown were analysed by nonlinear regression in terms of a single binding site model using the MicroCal ORIGIN software package.

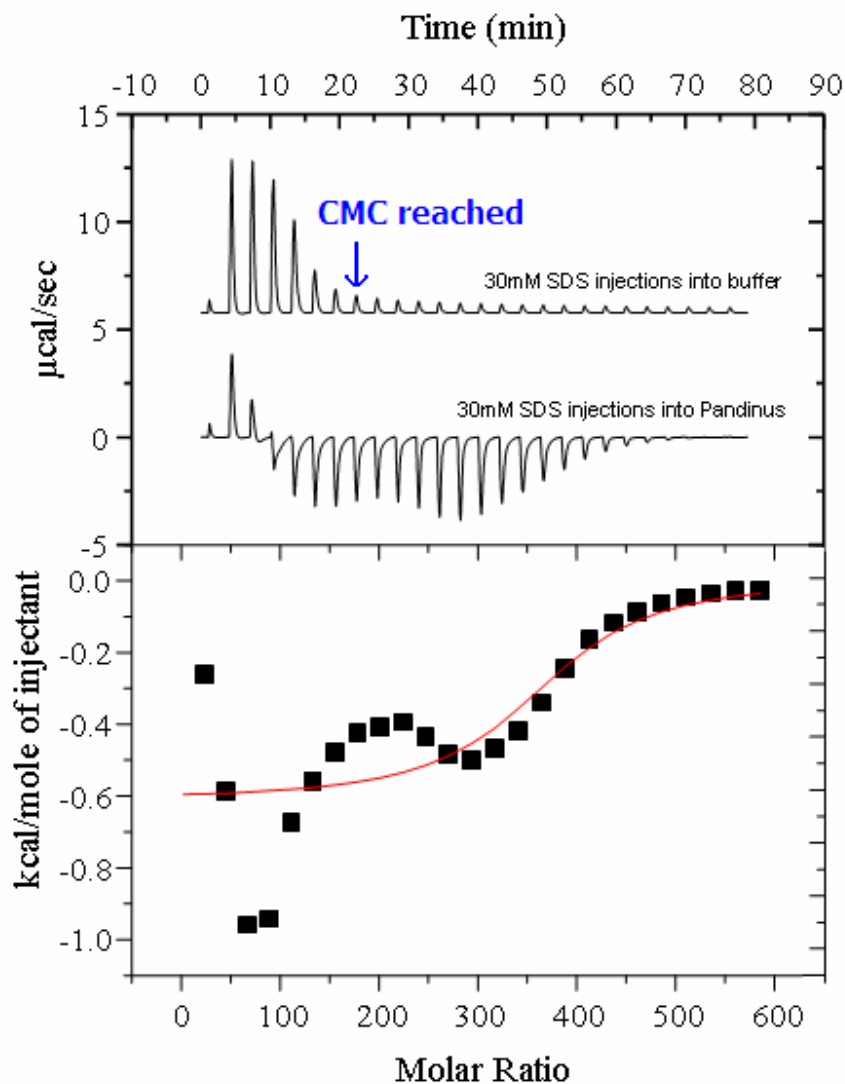


Figure 93: ITC data for binding of SDS to *Pandinus imperator* hemocyanin. Upper trace in top panel shows a control in which SDS was injected into buffer alone to determine the CMC of SDS in 100 mM sodium phosphate buffer, pH 7.5, and also to correct for heat of dilution of the ligand. Lower trace in upper panel presents the data for injection of 30mM SDS (0.15 mM per injection) into  $0.77 \pm 0.015$  mg/ml (10  $\mu$ M) *P. imperator* hemocyanin monomers (equivalent to 420 nM of the 4 x 6-meric unit). The lower panel shows the calculated binding isotherm (integrated heat data), corresponding to the lower trace in the upper panel, and the best-fitted curve of the data. The calorimetry data shown were analysed by nonlinear regression in terms of a single binding site model using the MicroCal ORIGIN software package.

## Bibliography

- Adachi, K., Wakamatsu, K., Ito, S., Miyamoto, N., Kokubo, T., Nishioka, T. and Hirata, T. (2005) An oxygen transporter hemocyanin can act on the late pathway of melanin synthesis. *Pigment Cell Research* **18** (3), pp 214-219.
- Adachi, K., Hirata, T., Nishioka, T. and Sakaguchi, M. (2003) Hemocyte components in crustaceans convert hemocyanin into a phenoloxidase-like enzyme. *Comparative Biochemistry and Physiology Part B: Biochemistry and Molecular Biology* **134** (1), pp 135-141.
- Ahmed, A., Martin, D., Manetti, A.G.O., Han, S.J., Lee, W.J., Mathiopoulos, K.D., Müller, H.M., Kafatos, F.C., Raikhal, A. and Brey, P.T. (1999) Genomic structure and ecdysone regulation of the prophenoloxidase 1 gene in the malaria vector *Anopheles gambiae*. *Proceedings of the National Academy of Science of the United States of America* **96** (26), pp 14795-14800.
- Ali, S.A., Zaidi, Z.H. and Abbasi, A. (1995) Oxygen transport proteins: I. Structure and organization of hemocyanin from scorpion (*Buthus indicus*). *Comparative Biochemistry and Physiology* **112A** (1), pp 225-232.
- Amaya, K.E., Asgari, S., Jung, R., Hongskula, M. and Beckage, N.E. (2005) Parasitization of *Manduca sexta* larvae by the parasitoid wasp *Cotesia congregata* induces an impaired host immune response. *Journal of Insect Physiology* **51** (5), pp 505-512.
- Ambion, I., TechNotes 8 (3): Is Your RNA Intact? Methods to Check RNA Integrity (online). Available: <http://www.ambion.com/techlib/tn/83/8313.html> (Accessed: 2006).
- Asano, T. and Ashida, M. (2001a) Cuticular pro-phenoloxidase of the silkworm, *Bombyx mori*. Purification and demonstration of its transport from hemolymph. *The Journal of Biological Chemistry* **276** (14), pp 11100-11112.
- Asano, T. and Ashida, M. (2001b) Transepithelially transported pro-phenoloxidase in the cuticle of the silkworm, *Bombyx mori*. Identification of its methionyl residues oxidised to methionine sulfoxides. *The Journal of Biological Chemistry* **276** (14), pp 11113-11125.

- Ashida, M. and Brey, P.T. (1995) Role of the integument in insect defense: Pro-phenol oxidase cascade in the cuticular matrix. *Proceedings of the National Academy of Science of the United States of America* **92**, pp 10698-10702.
- Ashida, M. and Brey, P.T. (1997) Recent advances in research on the insect prophenoloxidase cascade. In: Brey, P.T. and Hultmark, D., (Eds.) *Molecular mechanisms of immune responses in insects*, pp pp. 135-172. Chapman and Hall, London.
- Avanti Polar Lipids Inc., Technical information: Preparation of liposomes (online). Available: <http://www.avantilipids.com/PreparationOfLiposomes.html> (Accessed: 2005).
- Avanti Polar Lipids, I., Natural Lipids (online). Available: <http://www.avantilipids.com/index.htm> (Accessed: 2007).
- Bacci, M., Baldecchi, M.G., Fabeni, P., Linari, R. and Pazzi, G.P. (1983) Emission spectra from copper proteins containing type-3 centres. *Biophysical Chemistry* **17**, pp 125-130.
- Bae, S. and Kim, Y. (2004) Host physiological changes due to parasitism of a braconid wasp, *Cotesia plutellae*, on diamondback moth, *Plutella xylostella*. *Comparative Biochemistry and Physiology - Part A: Molecular & Integrative Physiology* **138** (1), pp 39-44.
- Baird, S., Kelly, S.M., Price, N.C., Jaenicke, E., Meesters, C., Nillius, D., Decker, H. and Nairn, J. (2007) Hemocyanin conformational changes associated with SDS-induced phenol oxidase activation. *Biochimica et Biophysica Acta: Proteins and Proteomics* **1774**, pp 1380-1394.
- Bak, H.J., Neuteboom, B., Jekel, P.A., Soeter, N.M., Vereijken, J.M. and Beintema, J.J. (1986) Structure of arthropod hemocyanin. *FEBS Letters* **204** (1), pp 141-144.
- Barnes, A.I. and Siva-Jothy, M.T. (1999) Density dependant prophylaxis in the mealworm beetle *Tenebrio molitor* L. (Coleoptera: Tenebrionidae): Cuticular melanization is an indicator of investment in immunity. *Proceedings of the Royal Society of London B, Biological Sciences* **267**, pp 177-182.
- Battaini, G., Monzani, E., Casella, L., Lonardi, E., Tepper, A.W.J.W., Canters, G.W. and Bubacco, L. (2002) Tyrosinase-catalyzed Oxidation of Fluorophenols. *Journal of*

*Biological Chemistry*. **277** (47), pp 44606-44612.

Bidla, G., Lindgren, M., Theopold, U. and Dushay, M.S. (2005) Hemolymph coagulation and phenoloxidase in *Drosophila* larvae. *Developmental & Comparative Immunology* **29** (8), pp 669-679.

Blois, M.S. (1978) The melanins: Their synthesis and structure. In: Smith, K.C., (Ed.) *Photochemical and Photobiological Reviews*, pp pp. 115-134. Plenum Press, New York.

Bollag, J.-M. (1992) Decontaminating soil with enzymes: An in situ method using phenolic and anilinic compounds. *Environmental Science and Technology* **26** (10), pp 1876.

Brown, C.A. and Terwilliger, N.B. (1998) Ontogeny of hemocyanin function in the Dungeness crab *Cancer magister*: Hemolymph modulation of hemocyanin oxygen-binding. *The Journal of Experimental Biology* **201**, pp 819-826.

Burmester, T. (2001) Molecular evolution of the arthropod hemocyanin superfamily. *Molecular Biology and Evolution* **18** (2), pp 184-195.

Celej, M.S., D'Andrea, M.G., Campana, P.T., Fidelio, G.D. and Bianconi, M.L. (2004) Superactivity and conformational changes on  $\alpha$ -chymotrypsin upon interfacial binding to cationic micelles. *Biochemical Journal* **378**, pp 1059–1066.

Cerenius, L. and Söderhäll, K. (2004) The prophenoloxidase-activating system in invertebrates. *Immunological Reviews* **198** (1), pp 116-126.

Chapman, J.W., Williams, T., Martínez, A.M., Cisneros, J., Caballero, P., D. Cave, R. and Goulson, D. (2000) Does cannibalism in *Spodoptera frugiperda* (Lepidoptera: Noctuidae) reduce the risk of predation? **48** (4), pp 321-327.

Chapman, J.W., Williams, T., Escribano, A.A., Caballero, P., Cave, R.D. and Goulson, D. (1999a) Age-related cannibalism and horizontal transmission of a nuclear polyhedrosis virus in larval *Spodoptera frugiperda*. *Ecological Entomology* **24** (3), pp 268-275.

Chapman, J.W., Williams, T., Escribano, A., Caballero, P., Cave, R.D. and Goulson, D. (1999b) Fitness consequences of cannibalism in the fall armyworm, *Spodoptera frugiperda*. *Behavioral Ecology* **10** (3), pp 298-303.

- Chase, M.R., Raina, K., Bruno, J. and Sugumaran, M. (2000) Purification, characterization and molecular cloning of prophenoloxidasases from *Sarcophaga bullata*. *Insect Biochemistry and Molecular Biology* **30**, pp 953-967.
- Chen, N., Fan, J.-B., Xiang, J., Chen, J. and Liang, Y. (2006) Enzymatic hydrolysis of microcrystalline cellulose in reverse micelles. *Biochimica et Biophysica Acta (BBA) - Proteins & Proteomics* **1764** (6), pp 1029-1035.
- Chosa, N., Fukumitsu, T., Fujimoto, K. and Ohnishi, E. (1997) Activation of prophenoloxidase A<sub>1</sub> by an activating enzyme in *Drosophila melanogaster*. *Insect Biochemistry and Molecular Biology* **27** (1), pp 61-68.
- Chrissie, W. W., The Lipid Library: Phosphatidylethanolamine and related lipids - structure, occurrence, biochemistry and analysis (online). Available: <http://www.lipidlibrary.co.uk/lipids.html> (Accessed: 2005).
- Christie, W. W., The lipid library: Phosphatidylcholine and related lipids - structure, occurrence, biochemistry and analysis (online). Available: <http://www.lipidlibrary.co.uk/lipids.html> (Accessed: 2005).
- Cotter, S.C., Hails, R.S., Cory, J.S. and Wilson, K. (2004) Density-dependent prophylaxis and condition-dependent immune function in Lepidopteran larvae: a multivariate approach. *Journal of Animal Ecology* **73** (2), pp 283-293.
- Cotter, S.C. and Wilson, K. (2002) Heritability of immune function in the caterpillar *Spodoptera littoralis*. *Heredity* **88**, pp 1-6.
- Cuff, M.E., Miller, K.I., van Holde, K.E. and Hendrickson, W.A. (1998) Crystal structure of a functional unit from Octopus hemocyanin. *Journal of Molecular Biology* **278** (4), pp 855-870.
- Cunningham, M., Gómez, C. and Pollero, R. (1999) Lipid binding capacity of spider hemocyanin. *Journal of Experimental Zoology* **284** (4), pp 368-373.
- Cunningham, M., González, A. and Pollero, R. (2000) Characterization of lipoproteins isolated from the hemolymph of the spider *Latrodectus mirabilis* (Aranae, Theridiidae). *The Journal of Arachnology* **28**, pp 49-55.
- Dainese, E., Di Muro, P., Beltramini, M., Salvato, B. and Decker, H. (1998) Subunits

- composition and allosteric control in *Carcinus aestuarii* hemocyanin. *European Journal of Biochemistry* **256**, pp 350-358.
- Danson, M.J., Hough, D.W., Russell, R.J.M., Taylor, G.L. and Pearl, L. (1996) Enzyme thermostability and thermoactivity. *Protein Engineering* **9** (8), pp 629-630.
- Decker, H. (2005) Copper proteins with dinuclear active sites. In: King, R.B., (Ed.) *Encyclopedia of Inorganic Chemistry*, 2nd Ed. pp pp. 1159-1173. John Wiley & Sons, Ltd., Chichester.
- Decker, H., Hartmann, H., Sterner, R., Schwarz, E. and Pilz, I. (1996) Small-angle X-ray scattering reveals differences between the quaternary structures of oxygenated and deoxygenated tarantula hemocyanin. *FEBS Letters* **393** (2-3), pp 226-230.
- Decker, H. and Jaenicke, E. (2004) Recent findings on phenoloxidase activity and antimicrobial activity of hemocyanins. *Developmental and Comparative Immunology* **28** (7-8), pp 673-687.
- Decker, H. and Rimke, T. (1998) Tarantula hemocyanin shows phenoloxidase activity. *The Journal of Biological Chemistry* **273** (40), pp 25889-25892.
- Decker, H., Ryan, M., Jaenicke, E. and Terwilliger, N. (2001) SDS-induced phenoloxidase activity of hemocyanins from *Limulus polyphemus*, *Eurypelma californicum*, and *Cancer magister*. *The Journal of Biological Chemistry* **276** (21), pp 17796-17799.
- Decker, H. and Terwilliger, N. (2000) Cops and Robbers: Putative evolution of copper oxygen-binding proteins. *The Journal of Experimental Biology* **203**, pp 1777-1782.
- Decker, H. and Tuczek, F. (2000) Tyrosinase/catecholoxidase activity of hemocyanins: Structural basis and molecular mechanism. *TIBS Reviews* **25**, pp 392-397.
- DEFRA, Plants and seeds - *spodoptera* species (online). Available: [www.defra.gov.uk/planth/pestnote/spod.htm](http://www.defra.gov.uk/planth/pestnote/spod.htm) (Accessed: 2003).
- Di Venere, A., Mei, G., Gilardi, G., Rosato, N., De Matteis, F., McKay, R., Gratton, E. and Finazzi Agro, A. (1998) Resolution of the heterogeneous fluorescence in multi-tryptophan proteins: ascorbate oxidase. *European Journal of Biochemistry* **257** (2), pp 337-343.

- Dolashka-Angelova, P., Dolashki, A., Stevanovic, S., Hristova, R., Atanasov, B., Nikolov, P. and Voelter, W. (2005) Structure and stability of arthropodan hemocyanin *Limulus polyphemus*. *Spectrochimica Acta Part A: Molecular and Biomolecular Spectroscopy* **61** (6), pp 1207-1217.
- Doucet, D. and Cusson, M. (1996) Role of calyx fluid in alterations of immunity in *Choristoneura fumiferana* larvae parasitized by *Tranosema rostrale*. *Comparative Biochemistry and Physiology Part A: Physiology* **114** (4), pp 311-317.
- Durstewitz, G. and Terwilliger, N.B. (1997) Developmental Changes in Hemocyanin Expression in the Dungeness Crab, *Cancer magister*. *Journal of Biological Chemistry* **272** (7), pp 4347-4350.
- Eissa, H.A., Fadel, H.H.M., Ibrahim, G.E., Hassan, I.M. and Elrashid, A.A. (2006) Thiol containing compounds as controlling agents of enzymatic browning in some apple products. *Food Research International* **39** (8), pp 855-863.
- Foukas, L.C., Katsoulas, H.L., Paraskevopoulou, N., Metheniti, A., Lambropoulou, M. and Marmaras, V.J. (1998) Phagocytosis of *Escherichia coli* by insect hemocytes requires both activation of the Ras/mitogen-activated protein kinase signal transduction pathway for attachment and beta 3 integrin for internalization. *Journal of Biological Chemistry*. **273** (24), pp 14813-14818.
- Fu, Y., Zhang, K., Wang, N. and Du, J. (2007) Effects of aqueous chlorine dioxide treatment on polyphenol oxidases from Golden Delicious apple. *LWT - Food Science and Technology* **40** (8), pp 1362-1368.
- Fujimoto, K., Okino, N., Kawabata, S., Iwanaga, S. and Ohnishi, E. (1995 ) Nucleotide sequence of the cDNA encoding the proenzyme of phenol oxidase A<sub>1</sub> of *Drosophila melanogaster*. *Proceedings of the National Academy of Science of the United States of America* **92**, pp 7769-7773.
- Garcia-Pineda, E., Castro-Mercado, E. and Lozoya-Gloria, E. (2004) Gene expression and enzyme activity of pepper (*Capsicum annum* L.) ascorbate oxidase during elicitor and wounding stress. *Plant Science* **166** (1), pp 237-243.
- Gatto, S., De Filippis, V., Spinozzi, F., Di Muro, P., Bubacco, L. and Beltramini, M. (2004) Structural role of the copper ions in the dinuclear active site of *Carcinus aestuarii* hemocyanin. *Micron* **35** (1-2), pp 43-44.

- Georgieva, D.N., Stoeva, S., Ali, S.A., Abbasi, A., Genov, N. and Voelter, W. (1998) Circular dichroism study of the hemocyanin thermostability. *Spectrochimica Acta: Part A* **54**, pp 765-771.
- Greving, J., König, D., Tucker, P. and Krebs, B. Catechol oxidase derivatives and inhibitor complexes. Web location - [http://www-hasylab.desy.de/science/annual\\_reports/2001\\_report/part2/contrib/72/5032.pdf](http://www-hasylab.desy.de/science/annual_reports/2001_report/part2/contrib/72/5032.pdf)
- Gunn, A. (1998) The determination of larval phase coloration in the African armyworm, *Spodoptera exempta* and its consequences for thermoregulation and protection from UV light. *Entomologia Experimentalis et Applicata* **86** (2), pp 125-133.
- Hagner-Holler, S., Schoen, A., Erker, W., Marden, J.H., Rupprecht, R., Decker, H. and Burmester, T. (2004) A respiratory hemocyanin from an insect. *Proceedings of the National Academy of Science of the United States of America* **101** (3), pp 871-874.
- Hall, M., Scott, T., Sugumaran, M., Söderhäll, K. and Law, J.H. (1995a) Proenzyme of *Manduca sexta* phenol oxidase: Purification, activation, substrate specificity of the active enzyme, and molecular cloning. *Proceedings of the National Academy of Science of the United States of America* **92**, pp 7764-7768.
- Hall, M., van Heusden, M.C. and Soderhall, K. (1995b) Identification of the major lipoproteins in crayfish hemolymph as proteins involved in immune recognition and clotting. *Biochemical and Biophysical Research Communications* **216** (3), pp 939-946.
- Hartmann, H. and Decker, H. (2002) All hierarchical levels are involved in conformational transitions of the 4x6-meric tarantula hemocyanin upon oxygenation. *Biochimica et Biophysica Acta - Proteins & Proteomics* **1601** (2), pp 132-137.
- Hartzer, K.L., Zhu, K.Y. and Baker, J.E. (2005) Phenoloxidase in larvae of *Plodia interpunctella* (Lepidoptera: Pyralidae): Molecular cloning of the proenzyme cDNA and enzyme activity in larvae paralyzed and parasitized by *Habrobracon hebetor* (Hymenoptera: Braconidae). *Archives of Insect Biochemistry and Physiology* **59**, pp 67-79.
- Hazes, B., Magnus, K.A., Bonaventura, C., Bonaventura, J., Dauter, Z., Kalk, K.H. and Hol, W.G.J. (1993) Crystal structure of deoxygenated *Limulus polyphemus* subunit II hemocyanin at 2.18Å resolution: Clues for a mechanism for allosteric regulation. *Protein Science* **2**, pp 597-619.

- Hwang, Y.T. and Solomon, E.I. (1982) Preparation of a spectral probe derivative of the hemocyanin biopolymer: Effects of allosteric interactions on the coupled binuclear active site. *Proceedings of the National Academy of Science of the United States of America* **79**, pp 2564-2568.
- Iyengar, R. and McEvily, A.J. (1992) Anti-browning agents: alternatives to the use of sulfites in foods. *Trends in Food Science & Technology* **3**, pp 60-64.
- Jaenicke, E. and Decker, H. (2004) Conversion of crustacean hemocyanin to catecholoxidase. *Micron* **35**, pp 89-90.
- Jiang, H., Wang, Y. and Kanost, M.R. (1998) Pro-phenol oxidase activating proteinase from an insect, *Manduca sexta*: A bacteria-inducible protein similar to *Drosophila* easter. *Proceedings of the National Academy of Science of the United States of America* **95** (21), pp 12220-12225.
- Jiang, H., Wang, Y., Korochkina, S.E., Beneš, H. and Kanost, M.R. (1997a) Molecular cloning of cDNAs for two pro-phenol oxidase subunits from the malaria vector, *Anopheles gambiae*. *Insect Biochemistry and Molecular Biology* **27** (7), pp 693-699.
- Jiang, H., Wang, Y., Ma, C. and Kanost, M.R. (1997b) Subunit composition of pro-phenol oxidase from *Manduca sexta*: Molecular cloning of subunit Pro-PO1. *Insect Biochemistry and Molecular Biology* **27** (10), pp 835-850.
- Jiang, H., Wang, Y., Yu, X.-Q. and Kanost, M.R. (2003) Prophenoloxidase-activating Proteinase-2 from Hemolymph of *Manduca sexta*. A bacteria-inducible serine proteinase containing two clip domains. *The Journal of Biological Chemistry* **278** (6), pp 3552-3561.
- Johner, A. and Lanzrein, B. (2002) Characterisation of two genes of the polydnavirus of *Chelonus inanitus* and their stage-specific expression in the host *Spodoptera littoralis*. *Journal of General Virology* **83**, pp 1075-1085.
- Jones, K., Hughes, J., Hong, M., Jia, Q. and Orndorff, S. (2002) Modulation of Melanogenesis by Aloesin: A Competitive Inhibitor of Tyrosinase. *Pigment Cell Research* **15** (5), pp 335-340.
- Kanade, S.R., Paul, B., Rao, A.G.A. and Gowda, L.R. (2006) The conformational state of polyphenoloxidase from field bean (*Dolichos lablab*) upon SDS and acid-pH activation. *Biochemical Journal* **395**, pp 551-562.

- Kawabata, T., Yasuhara, Y., Ochiai, M., Matsuura, S. and Ashida, M. (1995 ) Molecular cloning of insect pro-phenol oxidase: A copper-containing protein homologous to arthropod hemocyanin. *Proceedings of the National Academy of Science of the United States of America* **92**, pp 7774-7778.
- Kelly, S.M. and Price, N.C. (1997) The application of circular dichroism to studies of protein folding and unfolding. *Biochimica et Biophysica Acta* **1338** (2), pp 161-185.
- Key Centre for Polymer Colloids, **Polymer Chemistry Glossary** (online). Available: <http://www.kcpc.usyd.edu.au/discovery/glossary-all.html> (Accessed: 2007).
- Kopáček, P. and Sugumaran, M. (1998) Purification and characterization of insect prophenoloxidases. In: Dumphy, A.G., et al, (Eds.) *Techniques in Insect Immunology: Lab Manual*, pp pp. 179-192.
- Kopáček, P., Weise, C. and Götz, P. (1995) The prophenoloxidase from the wax moth *Galleria mellonella*: Purification and characterisation of the proenzyme. *Insect Biochemistry and Molecular Biology* **25** (10), pp 1081-1091.
- Kuiper, H.A., Agro, A.F., Antonini, E. and Brunori, M. (1980) Luminescence of carbon monoxide hemocyanins. *Proceedings of the National Academy of Science of the United States of America* **77**, pp 2387-2389.
- Kusche, K., Ruhberg, H. and Burmester, T. (2002) A hemocyanin from the Onychophora and the emergence of respiratory proteins. *Proceedings of the National Academy of Science of the United States of America* **99** (16), pp 10545-10548.
- Laveda F., Núñez-Delicado E., García-Carmona F. and Sánchez-Ferrer A. (2000) Reversible Sodium Dodecyl Sulfate Activation of Latent Peach Polyphenol Oxidase by Cyclodextrins. *Archives of Biochemistry and Biophysics* **379** (1), pp 1-6.
- Lavine, M.D. and Beckage, N.E. (1995) Polydnviruses: potent mediators of host insect immune dysfunction. *Parasitology Today* **11** (10), pp 368-378.
- Lavine, M.D. and Strand, M.R. (2002) Insect hemocytes and their role in immunity. *Insect Biochemistry and Molecular Biology* **32** (10), pp 1295-1309.
- Lee, H.S., Cho, M.Y., Lee, K.M., Kwon, T.H., Homma, K., Natori, S. and Lee, B.L. ( 1999) The pro-phenoloxidase of coleopteran insect, *Tenebrio molitor*, larvae was activated

- during cell clump/cell adhesion of insect cellular defense reactions. *FEBS Letters* **444**, pp 255-259.
- Lee, M.J. and Anstee, J.H. (1995) Phenoloxidase and its zymogen from the haemolymph of larvae of the lepidopteran *Spodoptera littoralis* (Lepidoptera: Noctuidae). *Comparative Biochemistry and Physiology* **110B** (2), pp 379-384.
- Lee, M.-K. (2007) Inhibitory effect of banana polyphenol oxidase during ripening of banana by onion extract and Maillard reaction products. *Food Chemistry* **102** (1), pp 146-149.
- Lee, S.Y., Lee, B.L. and Söderhäll, K. (2004) Processing of crayfish hemocyanin subunits into phenoloxidase. *Biochemical and Biophysical Research Communications* **322**, pp 490-496.
- Lehnert, S.A. and Johnson, S.E. (2002) Expression of hemocyanin and digestive enzyme messenger RNAs in the hepatopancreas of the Black Tiger Shrimp *Penaeus monodon*. *Comparative Biochemistry and Physiology Part B: Biochemistry and Molecular Biology* **133** (2), pp 163-171.
- Ling, E. and Yu, X.-Q. (2005) Prophenoloxidase binds to the surface of hemocytes and is involved in hemocyte melanization in *Manduca sexta*. *Insect Biochemistry and Molecular Biology* **35**, pp 1356-1366.
- Liu, S. and Magnus, K.A. (2002) Preliminary crystallographic studies of *Limulus polyphemus* hemocyanin subunits IIIa, IIIb and IV. *Biochimica et Biophysica Acta* **1596**, pp 177-181.
- Lourenco, A.P., Zufelato, M.S., Bitondi, M.M.G. and Simoes, Z.L.P. (2005) Molecular characterization of a cDNA encoding prophenoloxidase and its expression in *Apis mellifera*. *Insect Biochemistry and Molecular Biology* **35** (6), pp 541-552.
- Ma, C. and Kanost, M.R. (2000) A beta 1,3-glucan recognition protein from an insect, *Manduca sexta*, agglutinates microorganisms and activates the phenoloxidase cascade. *The Journal of Biological Chemistry* **275** (11), pp 7505-7514.
- MacPherson, J.C., Pavlovich, J.G. and Jacobs, R.S. (1998) Phospholipid composition of the granular amebocyte from the horseshoe crab, *Limulus polyphemus*. *Lipids* **99** (9), pp 931-940.

- Maddaluno, J. and Faull, K.F. (1999) Mass spectrometric characterisation of *Limulus polyphemus* hemocyanin. *Biochemical and Biophysical Research Communications* **264**, pp 883-890.
- Maltais, D., Desroches, D., Aouffen, M., Mateescu, M.A., Wang, R. and Paquin, J. (2003) The blue copper ceruloplasmin induces aggregation of newly differentiated neurons: a potential modulator of nervous system organization. *Neuroscience* **121** (1), pp 73-82.
- Mangum, C.P., Scott, J.L., Black, R.E.L., Miller, K.I. and Van Holde, K.E. (1985) Centipedal hemocyanin: Its structure and its implications for arthropod phylogeny. *Proceedings of the National Academy of Science of the United States of America* **82**, pp 3721-3725.
- Matoba, Y., Kumagai, T., Yamamoto, A., Yoshitsu, H. and Sugiyama, M. (2006) Crystallographic Evidence That the Dinuclear Copper Center of Tyrosinase Is Flexible during Catalysis. *Journal of Biological Chemistry*. **281** (13), pp 8981-8990.
- Mavrouli, M.D., Tsakas, S., Theodorou, G.L., Lampropoulou, M. and Marmaras, V.J. (2005) MAP kinases mediate phagocytosis and melanization via prophenoloxidase activation in medfly hemocytes. *Biochimica et Biophysica Acta (BBA) - Molecular Cell Research* **1744** (2), pp 145-156.
- Meissner, U., Martin, A.G., Schwarz, B.-O., Stohr, M., Gebauer, W., Harris, J.R. and Markl, J. (2004) 3-D reconstruction of hemocyanins and other invertebrate hemolymph proteins by cryo-TEM: An overview. *Micron* **35**, pp 7-9.
- Moosavi-Movahedi, A.A. (2005) Thermodynamics of protein denaturation by sodium dodecyl sulphate. *Journal of the Iranian Chemical Society* **2** (3), pp 189-196.
- Morrissey, J. H., Morrissey lab protocol for preparing phospholipid vesicles (SUV) by sonication. (online). Available: <http://www.avantilipids.com/PreparationOfLiposomes.html> (Accessed: 2005).
- Muro, P.D., Beltrammi, M., Nikolov, P., Petkova, I., Salvato, B. and Ricchelli, F. (2002) Fluorescence spectroscopy of the tryptophan microenvironment of *Carcinus aestuarii* hemocyanin. *Naturforsch* **57c**, pp 1084-1091.
- Möller, M. and Decker, H. (2004) Tarantula hemocyanins imaged by atomic force microscopy. *Micron* **35**, pp 15-16.

- Müller, H.-M., Dimopoulos, G., Blass, C. and Kafatos, F.C. (1999) A hemocyte-like cell line established from the malaria vector *Anopheles gambiae* expresses six prophenoloxidase genes. *The Journal of Biological Chemistry* **274** (17), pp 11727-11735.
- Nagai, T. and Kawabata, S. (2000) A link between blood coagulation and prophenol oxidase activation in arthropod host defense. *The Journal of Biological Chemistry* **275** (38), pp 29264-29267.
- Nagai, T., Osaki, T. and Kawabata, S. (2001) Functional conversion of hemocyanin to phenoloxidase by horseshoe crab antimicrobial peptides. *The Journal of Biological Chemistry* **276** (29), pp 27166-27170.
- Nappi, A.J. and Christensen, B.M. (2005) Melanogenesis and associated cytotoxic reactions: Applications to insect innate immunity. *Insect Biochemistry and Molecular Biology* **35** (5), pp 443-459.
- Nellaiappan, K. and Sugumaran, M. (1996) On the presence of prophenoloxidase in the hemolymph of the horseshoe crab, *Limulus*. *Comparative Biochemistry and Physiology* **113B** (1), pp 163-168.
- Nillius, S.D. (2002) Zum Immunsystem der Cheliceraten *Eurypelma californicum* und *Pandinus imperator*. University of Mainz.
- Ottaviani, E. (2005) Insect immunorecognition. *Invertebrate Survival Journal* **2** (2), pp 142-151.
- Park, J.W., Dec, J., Kim, J.-E. and Bollag, J.-M. (2000) Dehalogenation of xenobiotics as a consequence of binding to humic materials. *Archives of Environmental Contamination and Toxicology* **38** (4), pp 405-410.
- Park, S.Y., Kim, C.H., Jeong, W.H., Lee, J.H., Seo, S.J., Han, Y.S. and Lee, I.H. (2005) Effects of two hemolymph proteins on humoral defense reactions in the wax moth, *Galleria mellonella*. *Developmental & Comparative Immunology* **29** (1), pp 43-51.
- Parker, W. and Song, P.-S. (1992) Protein structures in SDS micelle-protein complexes. *Biophysical Journal* **61** (5), pp 1435-1439.
- Rajagopal, R., Thamilarasi, K., Venkatesh, G.R., Srinivas, P. and Bhatnagar, R.K. (2005)

- Immune cascade of *Spodoptera litura*: Cloning, expression, and characterization of inducible prophenol oxidase. *Biochemical and Biophysical Research Communications* **337** (1), pp 394-400.
- Reeson, A.F., Wilson, K., Gunn, A., Hails, R.S. and Goulson, D. (1998 ) Baculovirus resistance in the noctuid *Spodoptera exepsta* is phenotypically plastic and responds to population density. *Proceedings of the Royal Society of London B, Biological Sciences* **265**, pp 1787-1791.
- Richman, A. and Kafatos, F.C. (1995) Immunity to eukaryotic parasites in vector insects. *Current Opinion in Immunology* **8**, pp 14-19.
- Riley, P.A. (1997) Molecules in focus : Melanin. *International Journal of Biochemical and Cell Biology* **29**, pp 1235-1239.
- Santagostini, L., Gullotti, M., De Gioia, L., Fantucci, P., Franzini, E., Marchesini, A., Monzani, E. and Casella, L. (2004) Probing the location of the substrate binding site of ascorbate oxidase near type 1 copper: an investigation through spectroscopic, inhibition and docking studies. *The International Journal of Biochemistry & Cell Biology* **36** (5), pp 881-892.
- Saul, S. and Sugumaran, M. (1988) A novel quinone: Quinone methide isomerase generates quinone methides in insect cuticle. *FEBS Letters* **237** (1-2), pp 155-158.
- Schlenke, T.A., Morales, J., Govind, S. and Clark, A.G. (2007) Contrasting Infection Strategies in Generalist and Specialist Wasp Parasitoids of *Drosophila melanogaster*. *PLoS Pathogens* **3** (10), pp 1486-1501.
- Schmidt, O., Rahman, M.M., Ma, G., Theopold, U., Sun, Y., Sarjan, M., Fabbri, M. and Roberts, H. (2005) Mode of action of antimicrobial peptides, pore-forming toxins and biologically active peptides (Hypothesis). *Invertebrate Survival Journal* **2** (2), pp 82-90.
- Sellos, D., Lemoine, S. and Van Wormhoudt, A. (1997) Molecular cloning of hemocyanin cDNA from *Penaeus vannamei* (Crustacea, Decapoda): structure, evolution and physiological aspects. *FEBS Letters* **407** (2), pp 153-158.
- Shelby, K.S., Cui, L. and Webb, B.A. (1998) Polydnavirus-mediated inhibition of lysozyme gene expression and the antibacterial response. *Insect Molecular Biology* **7** (3), pp 265-272.

- Shelby, K.S. and Webb, B.A. (1999) Polydnavirus-mediated suppression of insect immunity. *Journal of Insect Physiology* **45** (5), pp 507-514.
- Shiao, S.H., Higgs, S., Adelman, Z., Christensen, B.M., Liu, S.H. and Chen, C.C. (2001) Effect of prophenoloxidase knockout on the melanization of microfilariae in the mosquito *Armigeres subalbatus*. *Insect Molecular Biology* **10** (4), pp 315-321.
- Smith, I. M., McNamara, D. G., Scott, P. R., and Holderness, M.(97) Quarantine pests for Europe: Data sheets on quarantine pests: *Spodoptera littoralis* and *Spodoptera litura*. CABI International, Wallingford, UK. Web location - [http://www.eppo.org/QUARANTINE/insects/Spodoptera\\_litura/PRODLI\\_ds.pdf#search=%22spodoptera%20littoralis%20damage%22](http://www.eppo.org/QUARANTINE/insects/Spodoptera_litura/PRODLI_ds.pdf#search=%22spodoptera%20littoralis%20damage%22)
- Solomon, E.I. (1983) Electronic and geometric structure-function correlations of the coupled binuclear copper active site. *Pure and Applied Chemistry* **55** (7), pp 1069-1088.
- Solomon, E.I., Cole, J.L. and Baldwin, M.J. (1990) Structure-function correlations in copper clusters in proteins. *Pure and Applied Chemistry* **62** (6), pp 1063-1066.
- Solomon, E.I., Sundaram, U.M. and Machonkin, T.E. (1996) Multicopper oxidases and oxygenases. *Chemistry Reviews* **96**, pp 2563-2605.
- Spreti, N., Alfani, F., Cantarella, M., D'Amico, F., Germani, R. and Savelli, G. (1999)  $\alpha$ -Chymotrypsin superactivity in aqueous solutions of cationic surfactants. *Journal of Molecular Catalysis B: Enzymatic* **6** (1-2), pp 99-110.
- Spreti, N., Di Profio, P., Marte, L., Bufali, S., Brinchi, L. and Savelli, G. (2001) Activation and stabilization of  $\alpha$ -chymotrypsin by cationic additives. *European Journal of Biochemistry* **268** (24), pp 6491-6497.
- Sterner, R., Vogl, T., Hinz, H.-J., Penz, F., Hoff, R., Foll, R. and Decker, H. (1995) Extreme thermostability of tarantula hemocyanin. *FEBS Letters* **364** (1), pp 9-12.
- Sugumaran, M. and Kanost, M. (1993) Regulation of insect hemolymph phenoloxidase. In: Beckage, N.E., Thompson, S.N. and Frederick, B.A., (Eds.) *Parasites and Pathogens*, pp pp. 317-342. Academic Press, San Diego.
- Sugumaran, M. (1998a) Characterization of phenoloxidase complexes. In: Dumphy, A.G., et al, (Eds.) *Techniques in Insect Immunology: Lab Manual*, pp pp. 205-215.

- Sugumaran, M. (1998b) Different modes of activation and staining of prophenoloxidase. In: Dumphy, A.G., et al, (Eds.) *Techniques in Insect Immunology: Lab Manual*, pp pp. 193-203.
- Sugumaran, M. (2001) Control mechanisms of the prophenoloxidase cascade. In: Beck, et al, (Eds.) *Phylogenetic perspectives on the invertebrate immune system*, pp pp. 289-298. Kluwer Academic/Plenum Publishers,
- Sugumaran, M. (2002) Comparative biochemistry of eumelanogenesis and the protective roles of phenoloxidase and melanin in insects. *Pigment Cell Research* **15** (1), pp 2-9.
- Sugumaran, M. and Nellaiappan, K. (1990) On the latency and nature of phenoloxidase present in the left colleterial gland of the cockroach *Periplaneta americana*. *Archives of Biochemistry and Physiology* **15** (3), pp 165-181.
- Sugumaran, M. and Nellaiappan, K. (2000) Characterization of a new phenoloxidase inhibitor from the cuticle of *Manduca sexta*. *Biochemical and Biophysical Research Communications* **268**, pp 379-383.
- Sugumaran, M., Nellaiappan, K., Amaratunga, C., Cardinale, S. and Scott, T. (2000a) Insect melanogenesis III: Metabolon formation in the melanogenic pathway - regulation of phenoloxidase activity by endogenous dopachrome isomerase (decarboxylating) from *Manduca sexta*. *Archives of Biochemistry and Biophysics* **378** (2), pp 393-403.
- Sugumaran, M., Nellaiappan, K. and Valivittan, K. (2000b) A new mechanism for the control of phenoloxidase activity: Inhibition and complex formation with quinone isomerase. *Archives of Biochemistry and Biophysics* **379** (2), pp 252-260.
- Sugumaran, M. and Nellaiappan, K. (1991) Lysolecithin - A potent activator of prophenoloxidase from the hemolymph of the lobster, *Homarus americanus*. *Biochemical and Biophysical Research Communications* **176** (3), pp 1371-1376.
- Sullivan, B., Bonaventura, J., Bonaventura, C. and Godette, G. (1976) Hemocyanin of the horseshoe crab, *Limulus polyphemus*. Structural differentiation of the isolated components. *Journal of Biological Chemistry*. **251** (23), pp 7644-7648.
- Sullivan, B., Bonaventura, J. and Bonaventura, C. (1974) Functional differences in the multiple hemocyanins of the horseshoe crab, *Limulus polyphemus* L. *Proceedings of the National Academy of Science of the United States of America* **71** (6), pp 2558-

2562.

- Söderhäll, K. and Cerenius, L. (1998) Role of the prophenoloxidase-activating system in invertebrate immunity. *Current Opinion in Immunology* **10**, pp 23-28.
- Tamburro, A.M., Salvato, B. and Zatta, P. (1976) A circular dichroism study of some hemocyanins. *Comparative Biochemistry and Physiology* **55B**, pp 347-356.
- Taveau, J.-C., Boisset, N., Lamy, J., Lambert, O. and Lamy, J.N. (1997) Three-dimensional reconstruction of *Limulus polyphemus* hemocyanin from cryoelectron microscopy. *Journal of Molecular Biology* **266** (5), pp 1002-1015.
- Terwilliger, N.B., Dangott, L. and Ryan, M. (1999) Cryptocyanin, a crustacean molting protein: Evolutionary link with arthropod hemocyanins and insect hexamerins. *Proceedings of the National Academy of Science of the United States of America* **96** (5), pp 2013-2018.
- Tincu, J.A. and Taylor, S.W. (2004) MINIREVIEW: Antimicrobial peptides from marine invertebrates. *Antimicrobial Agents and Chemotherapy* **48** (10), pp 3645-3654.
- Valstar, A. (2000) Protein-surfactant interactions. Uppsala University. Web location - [http://64.233.183.104/search?q=cache:G0zBaSkzLLYJ:www.diva-portal.org/diva/getDocument%3Furn\\_nbn\\_se\\_uu\\_diva-1070-1\\_\\_fulltext.pdf+SDS+protein+binding+isotherm&hl=en&gl=uk&ct=clnk&cd=19](http://64.233.183.104/search?q=cache:G0zBaSkzLLYJ:www.diva-portal.org/diva/getDocument%3Furn_nbn_se_uu_diva-1070-1__fulltext.pdf+SDS+protein+binding+isotherm&hl=en&gl=uk&ct=clnk&cd=19).
- van Bruggen, E.F.J., Bijlholt, M.M.C., Schutter, W.G., Wichertjes, T., Bonaventura, J., Bonaventura, C., Lamy, J., Lamy, J., Leclerc, M., Schneider, H.-J., Markl, J. and Linzen, B. (1980) The role of the structurally diverse subunits in the assembly of three cheliceratan hemocyanins. *FEBS Letters* **116** (2), pp 207-210.
- van Holde, K.E., Miller, K.I. and Decker, H. (2001) Hemocyanins and Invertebrate Evolution. *The Journal of Biological Chemistry* **276** (19), pp 15563-15566.
- Vieille, C. and Zeikus, G.J. (2001) Hyperthermophilic Enzymes: Sources, Uses, and Molecular Mechanisms for Thermostability. *Microbiology and Molecular Biology Reviews* **65** (1), pp 1-43.
- Villeret, V., Clantin, B., Tricot, C., Legrain, C., Roovers, M., Stalon, V., Glansdorff, N. and Van Beeumen, J. (1998) The crystal structure of *Pyrococcus furiosus* ornithine

carbamoyltransferase reveals a key role for oligomerization in enzyme stability at extremely high temperatures. *Proceedings of the National Academy of Science of the United States of America* **95**, pp 2801-2806.

Viparelli, P., Alfani, F. and Cantarella, M. (1999) Models for enzyme superactivity in aqueous solutions of surfactants. *Biochemical Journal* **344**, pp 765-773.

Viparelli, P., Alfani, F. and Cantarella, M. (2003) Effect of cationic and non-ionic surfactants on the hydrolysis of N-glutaryl--phenylalanine catalysed by chymotrypsin iso-enzymes. *Journal of Molecular Catalysis B: Enzymatic* **21** (4-6), pp 175-187.

Voit, R., Feldmaier-Fuchs, G., Schweikardt, T., Decker, H. and Burmester, T. (2000) Complete sequence of the 24-mer hemocyanin of the tarantula *Eurypelma californicum*: Structure and intramolecular evolution of the subunits. *The Journal of Biological Chemistry* **275** (50), pp 39339-39344.

Volbeda, A., Feiters, M.C., Vincent, M.G., Bouwman, E., Dobson, B., Kalk, K.H., Reddijk, J. and Hol, W.G.J. (1989 ) Spectroscopic investigations of *Panulirus interruptus* hemocyanin in the crystalline state. *European Journal of Biochemistry* **181**, pp 669-673.

Wacker-Chemie GmbH(2002) Technical Brochure: Cyclodextrins for pharmaceutical applications. International Speciality Products, New Jersey, USA. Web location - <http://www.ispcorp.com/products/pharma/content/forwhatsnew/cyclodex/cyclodex.pdf>

Wang, Y. and Jiang, H. (2004 ) Prophenoloxidase (proPO) activation in *Manduca sexta*: an analysis of molecular interactions among proPO, proPO-activating proteinase-3, and a cofactor. *Insect Biochemistry and Molecular Biology* **34** (8), pp 731-742.

Weeden, Shelton, Li, Y., and Hoffmann, M. P., Insect biology and ecology: A primer (online). Available: <http://www.nysaes.cornell.edu/ent/biocontrol/info/primer.html> (Accessed: 2003).

Wilson, K., Cotter, S.C., Reeson, A.F. and Pell, J.K. (2001) Melanism and disease resistance in insects. *Ecology Letters* **4**, pp 637-649.

Xue, C.-B., Zhang, L., Luo, W.-C., Xie, X.-Y., Jiang, L. and Xiao, T. (2007) 3D-QSAR and molecular docking studies of benzaldehyde thiosemicarbazone, benzaldehyde, benzoic acid, and their derivatives as phenoloxidase inhibitors. *Bioorganic &*

*Medicinal Chemistry* **15** (5), pp 2006-2015.

Yu, X.-Q., Zhu, Y.-F., Ma, C., Fabrick, J.A. and Kanost, M.R. (2002) Pattern recognition proteins in *Manduca sexta* plasma. *Insect Biochemistry and Molecular Biology* **32**, pp 1287-1293.

Yu, X.-Q., Jiang, H., Wang, Y. and Kanost, M.R. (2003) Non-proteolytic serine proteinase homologs are involved in phenoloxidase activation in the tobacco hornworm, *Manduca sexta*. *Insect Biochemistry and Molecular Biology* **33**, pp 197-208.

Yu, X.-Q., Welcome to Yu Laboratory (online). Available: <http://sbs.umkc.edu/yux/> (Accessed: 2003).

Zatta, P. (1981) Protein-lipid interactions in *Carcinus maenas* (Crustacea) hemocyanin. *Comparative Biochemistry and Physiology Part B: Biochemistry and Molecular Biology* **69** (4), pp 731-735.

Zhang, G., Lu, Z.-Q., Jiang, H. and Asgari, S. (2004) Negative regulation of prophenoloxidase (proPO) activation by a clip-domain serine proteinase homolog (SPH) from endoparasitoid venom. *Insect Biochemistry and Molecular Biology* **34** (5), pp 477-483.

Zlateva, T., Di Muro, P., Salvato, B. and Beltramini, M. (1996) The o-diphenol oxidase activity of arthropod hemocyanin. *FEBS Letters* **384**, pp 251-254.

Zou, Z., Wang, Y. and Jiang, H. (2005) *Manduca sexta* prophenoloxidase activating proteinase-1 (PAP-1) gene: Organization, expression, and regulation by immune and hormonal signals. *Insect Biochemistry and Molecular Biology* **35** (6), pp 627-636.